UNIVERSITAT DE BARCELONA

Adaptive radiations as windows to the evolution of diversity: the spider genera *Dysdera* and *Hogna* in the Madeira archipelago

Luís Carlos da Fonseca Crespo

ADAPTIVE RADIATIONS AS WINDOWS TO THE EVOLUTION OF DIVERSITY: THE SPIDER GENERA *DYSDERA* AND *HOGNA* IN THE MADEIRA ARCHIPELAGO

Luís Crespo

2021

Doctoral Thesis

UNIVERSITAT DE BARCELONA

Faculty of Biology

Department of Evolutionary Biology, Ecology and Environmental Sciences (Arthropods)

Doctorate Program of Biodiversity (H0G01)

ADAPTIVE RADIATIONS AS WINDOWS TO THE EVOLUTION OF DIVERSITY: THE SPIDER GENERA *DYSDERA* AND *HOGNA* IN THE MADEIRA ARCHIPELAGO

Thesis presented by:

Luís Carlos da Fonseca Crespo

To qualify for the title of

Doctor by the University of Barcelona

Barcelona, June 2021

DOCTORAL STUDENT   DIRECTOR AND TUTOR   CO-DIRECTOR

Luís C.da Fonseca Crespo   Dr. Miquel A. Arnedo Lombarte   Dr. Pedro M. Bondoso Cardoso

Full Professor at the Department of Evolutionary Biology,

Ecology and Environmental Sciences (Arthropods)

Curator at the Finnish Museum of

Natural History, Finland

INFORME DEL DIRECTOR

Com director de la tesis doctoral titulada "ADAPTIVE RADIATIONS AS WINDOWS TO THE EVOLUTION OF DIVERSITY: THE SPIDER GENERA DYSDERA AND HOGNA IN THE MADEIRA ARCHIPELAGO" realitzada per en Luis Carlos da Fonseca Crespo, presento el següent informe sobre la contribució del doctorand en les publicacions en coautoria que formen part de la tesis:

La tesi doctoral està elaborada com a compendi de 3 publicacions amb dades originals:

1. **Capítol 1. Luís C. Crespo, Isamberto Silva, Alba Enguídanos, Pedro Cardoso and Miquel A. Arnedo (2021) Integrative taxonomic revision of the woodlouse-hunter spider genus *Dysdera* (Araneae: Dysderidae) in the Madeira archipelago with notes on its conservation status, Zoological Journal of the Linnean Society, 192: 356–415.**

Contribució del doctorand: Disseny experimental, treball de camp, recol·lecció i curació d'espècimens, obtenció de seqüencies de DNA, dades morfològiques, realització d'il·lustracions, anàlisis, elaboració i discussió de resultats i redacció del manuscrit.

Factor d'impacte (5 Year Impact Factor): **[IF = 2.824 (2019); Q1].** Categoria *Zoology*.

2. **Capítol 2. Luís C. Crespo, Isamberto Silva, Alba Enguídanos, Pedro Cardoso and Miquel A. Arnedo (in press). The Atlantic connection: Coastal habitat favoured long distance dispersal and colonization of Azores and Madeira by *Dysdera* spiders (Araneae: Dysderidae). Systematics & Biodiversity (in press).**

Contribució del doctorand: Disseny experimental, treball de camp, recol·lecció i curació d'espècimens, obtenció de seqüencies de DNA, dades morfològiques, realització d'il·lustracions, anàlisis, elaboració i discussió de resultats i redacció del manuscrit.

Factor d'impacte (5 Year Impact Factor): **[IF = 1.953 (2019); Q2].** Categoria *Biodiversity Conservation*.

3. **Capítol 3. Luís C. Crespo, Isamberto Silva, Alba Enguídanos, Pedro Cardoso and Miquel A. Arnedo (submitted) Island hoppers: Integrative taxonomic revision of Hogna wolf spider (Araneae: Lycosidae) endemic to the Madeira islands with description of a new species. Zookeys (in review).**

Contribució del doctorand: Disseny experimental, treball de camp, recol·lecció i curació d'espècimens, obtenció de seqüencies de DNA, dades morfològiques, realització d'il·lustracions, anàlisis, elaboració i discussió de resultats i redacció del manuscrit.

Factor d'impacte (5 Year Impact Factor): **[IF = 1.137 (2019); Q3].** Categoria *Zoology*.

Digitally signed by ARNEDO LOMBARTE MIGUEL ANGEL - 46630819K
DN: c=ES, serialNumber=IDCES-46630819K, givenName=MIGUEL ANGEL, sn=ARNEDO LOMBARTE, cn=ARNEDO LOMBARTE MIGUEL ANGEL - 46630819K
Date: 2021.06.26 19:36:12 +01'00'

Barcelona, a 26 de juny de 2021

firma del director/a

Dr. Miquel A. Arnedo Lombarte (director de la Tesis)
Departamento de Biología Evolutiva, Ecología y Ciencias Ambientales
Facultad de Biología

Acknowledgements

The time I spent in the University of Barcelona, from the 1st of September of 2016 to the 3rd of July of 2020, was very remarkable. Motivated by the award of a PhD grant by FCT, I travelled to the other side of the Iberian Peninsula to learn about the contributions of molecules in shaping biodiversity.

There, I encountered an endless number of people that needs to be acknowledged in some way. I may forget to mention someone, and, for those, I apologize.

Firstly, I would like to thank my supervisor, Miquel Arnedo, for receiving me in his research group and teaching me many things about evolutionary biology. Without his support, this work would not be possible. Furthermore, adding the topics of my PhD project to his application for funding allowed for comfortable fieldwork logistics. He is also notable as great host of countless hours hanging out in his terrace or in a nearby brewery.

My co-supervisor, Pedro Cardoso, is also thanked for his support, which, due to the long distance between Barcelona and Helsinki, was sadly shorter than the ideal. The pair of visits we did served to catch up on one another, at least.

The constant flux of personnel at the Arnedo Lab in the past years resulted in a large number of friendships that cannot be detailed in so little page space. I will just mention some highlighted memories. In alphabetical order: I thank Adrià for being my fieldwork companion in the 2018 expedition to the islands, especially in the Canary Islands, which were entirely unknown to me. I thank Alba for having the patience to teach me and guide through molecular lab duties, as well as hosting during a most pleasant visit to sunny Valencia. I knew Jagoba beforehand, but it was only in Barcelona that I experienced what it was to interact closely with extroverts, and you were among the greatest of those. The creative process of a card game we made up was definitely a highlight of our time in Barcelona. Jesus, your level as extrovert is probably equal to that of Jagoba, or even greater, so please forgive this introvert for not feeling like giving a hug every time. To Marc I thank especially for the field escapades we occasionally did, as well as for countless debates on the definition of random and his humoristic impersonations. With Martina and Tin I shared many of my musical tastes and exchanged some nice dinners. Silvia was one of

Abstract

Dysdera and *Hogna* are the most speciose spider genera of the Madeira archipelago. I have extensively revised their taxonomy, describing a total of eleven new species, establishing five synonyms and revalidating one name, using illustrations, SEM and stereomicroscope imaging for descriptions. I tested their phylogenetic placement and their monophyly with a multi-locus target gene phylogeny using both mitochondrial (*cox1*, 16S+L1, ND1, 12S) and nuclear markers (28S, H3, ITS-2), while at the same time running single gene (*cox1*) based species delimitation methods, which, in turn, would be integrated with the morphological data to infer on species boundaries. In the case of *Hogna*, I have generated haplotype networks for two genes (*cox1* and ITS-2) to show the structure of haplotypes across species. I performed time-calibrated phylogenetic analyses for both genera using different frameworks.

Results indicate that Madeira was colonized by *Dysdera* at least twice, with a speciose clade represented by ten species and another represented by a single species, in both cases with Iberian or Moroccan ancestry. The single species lineage shares a common ancestor with congenerics found in the remote archipelago of Azores, being adapted to coastal habitats, which probably favoured oceanic long-distance dispersal by means of rafting. The Madeiran clade of *Hogna* appears monophyletic, although methodological support is low. Species delimitation methods did reveal geographic structure for several *Dysdera* species, but in general agreed with morphological data to assess species boundaries. In *Hogna*, however, we have uncovered a remarkable case of two species, *H. insularum* (Kulczynski, 1899) and *H. maderiana* (Walckenaer, 1837), which cannot be differentiated by either morphology or any molecular based species delimitation method. I discuss the possibility of hybridization as reported in other members of the genus, and we are developing a more thorough genomic approach to understand this pattern.

Finally, building on the extensive sampling across the archipelago for most species, I delved into conservation problems and possible protection measures for threatened species. Given the restricted range of most species in these two genera and the multiple anthropogenic threats they face, only targeted conservation programs can prevent future population extirpation and species extinctions.

Index

General Introduction

General Introduction

Islands as models to understand the drivers of diversity on Earth

Islands have long fascinated naturalists, especially after Darwin's voyage to the Galapagos, where he found seemingly related, yet different species, occupying different ecological settings (Darwin 1859). Following the publication of his theory of evolution through natural selection, islands became renowned remote places where scholars could find endemic species, occasionally with peculiar traits lacking in mainland relatives.

Later on, especially after the publication of The Theory of Island Biogeography (MacArthur and Wilson 1967), islands stood as ideal natural laboratories to study the intertwining of extinction and immigration as shapers of communities through time. Insular biotas are usually depauperated compared with the mainland, and the absence of competition and predation provides ecological opportunities for species able to successfully colonize islands to and adapt to novel ecological niches (Schluter 1988). It should bear in mind that the island concept goes beyond the prototype of oceanic islands (e.g. the Hawaiian archipelago), but to also include any area surrounded by a suboptimal border, i.e. ecological islands, such as lakes, caves or mountain tops (Cartwright 2019) as similar settings.

Insular biotas are usually depauperated compared with the mainland, and the absence of competition and predation often provides ecological opportunities for species to successfully colonize islands and adapt to novel ecological niches (Schluter 1988).

Many examples of highly proliferated and diversified endemic taxa can be found in insular systems, such as the Hawaiian honeycreepers (Lerner et al. 2011), Caribbean anoles (Losos 2009), or the cichlids of the African Rift Lakes (Irisarri et al. 2018), to cite a few. With the onset of molecular ecology, the study of these remarkable diversification events in islands in a phylogenetic framework provided us with new insights into the drivers and temporal settings of community assembly, either through processes of adaptive radiation with disruptive trait displacement, diversification through non-adaptive radiation or a combination of both.

Adaptive radiation is a widely discussed phenomenon in island evolutionary biology. As currently defined, it consists on adaptive phenotypic diversification in highly speciose monophyletic lineages, often occurring in a short time span (Losos and Ricklefs 2009, Soulebeau et al. 2015). Although traditionally all cases of species proliferation were referred as adaptive radiation, the adaptive nature of the evolution of a certain group was usually not tested against the alternative occurrence of non-adaptive speciation. This occurs when ecologically similar species are segregated by allopatry, possibly due to competitive exclusion (Rundell and Price 2009). The latter, for instance, can be predominant in *Orsonwelles* spiders of the Hawaiian archipelago (Hormiga et al. 2003), but, more often than not, a combination of both adaptive and non-adaptive processes can be observed, such as in the spider genus *Tetragnatha*, where multiple lineages show both highly differentiated sympatric species and similar allopatric species, referred as ecomorphs (Gillespie 2004). The study of the interplay between these sympatric interactions and allopatric shifts at the metapopulational level is termed landscape dynamics (Keymer et al. 2000), and model-based studies suggest that it is the interplay between these two dimensions that maximizes probability of speciation phenomena to occur (Aguilée et al. 2013, Gascuel et al. 2015).

The evolutionary progress of island lineages through time creates pockets of endemicity of high conservation concern. Due to their isolation and narrow range, endemic species are prime case-studies for extinction processes (Cardoso et al. 2010, Triantis et al. 2010, Whittaker et al. 2017, Figueiredo et al. 2019). These have always naturally occurred throughout geological time as exemplified by the fossil records, but background rates of extinction have increased by order of magnitudes with the onset of the Anthropocene, suggesting a direct implication of human activities (Wood et al. 2017). The emergent field of Conservation Biogeography attempts to understand the current state of community changes in islands and to use available knowledge to inform and minimize the loss of diversity. Although pessimism is prevalent in this field (Whittaker et al. 2005), hopeful examples of species and habitat recovery can be found (Copsey et al. 2018).

The Madeira Archipelago

Together with Azores, Selvagens, Canary Islands and Cabo Verde, the Madeira archipelago is traditionally taken as part of the biogeographic region named Macaronesia (Fig. 1). These archipelagos are situated between 15° and 39° N latitude in the Atlantic Ocean, and were historically clumped together due to the biogeographical affinities in their biota, which supports high levels of endemism (see regional checklists of the referred archipelagos in Izquierdo et al. 2004, Arechavaleta et al. 2005, Borges et al. 2008, 2010). The definition of Macaronesia was recently revised using marine taxa data, and several new eco-regions were proposed, allocating Madeira, together with the Canary Islands and Selvagens to the Webbnesia (Freitas et al. 2019).
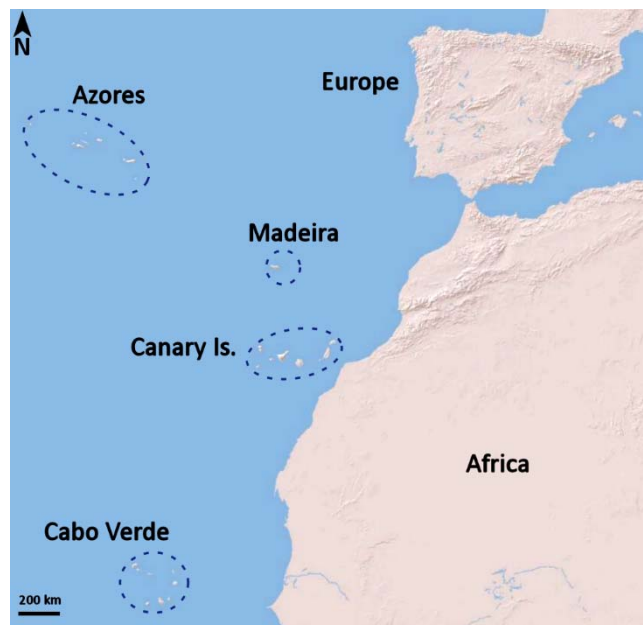
Figure 1. Map of the Macaronesia. Source: Google.

The Madeira archipelago is located approximately 900km SW of the Iberian Peninsula and 800 km W of North Africa. It is the southwestern tip of a chain of paleoislands (presently seamounts) oriented in a NE to SW direction, originating from the SW tip of the Iberian Peninsula roughly over 70 My (Geldmacher et al. 2000). The Madeira archipelago is composed of Porto Santo and adjacent islets, Madeira island and Desertas islands. The Selvagens, although politically part of Madeira, are geologically not considered as part of Madeira archipelago.

Porto Santo (43 km^2) is the oldest and more eroded island of the archipelago (14 My) (Geldmacher et al. 2000), reaching a maximum altitude of 517m at Pico do Facho. It is a predominantly flat island, with small mountain tops on its eastern half and, to a smaller extent, at the western half. Porto Santo has suffered severe extirpation of native flora since human colonization due to the conversion of land for cattle grazing and farming. Currently only the mountain tops are forested, and are so mainly with exotic species i.e. *Hesperocyparis macrocarpa* (Hartw., 1847). Several reforestation attempts were made by local authorities over the years, all with limited success. Most of the island is arid, composed by grasslands, sand banks and rocky cliffs.

Madeira (742 km^2) is the largest island of the archipelago, with a maximum altitude of 1861m at Pico Ruivo. Its aerial parts are dated as far back as 7 My (Ramalho et al. 2015). It is a rugged island, especially at its North coast, with many valleys and inaccessible mountains. A central montane plateau, Paúl da Serra, is the only flat area of the island. Due to this orography, only the SE coast of the island presents semi-arid areas, especially so at the Ponta de São Lourenço peninsula. The North coast is where the only large remains of laurel forest of the island can be found, mainly composed by woodlands of *Ocotea foetens* (Aiton) Baill., *Apollonias barbujana* (Cav.) Bornm., *Laurus novocanariensis* Rivas Mart., Lousão, Fern. Prieto, E. Dias, J.C. Costa & C. Aguiar and *Persea indica* (L.) Spreng. It was the ruggedness of Madeira that probably saved the remaining patches of laurel forest from extensive deforestation caused by human colonization. These forests are now protected through the UNESCO World Heritage program (Unesco World Heritage Committee 1999). Yet, human pressure continues to threaten this ecosystem, namely through urbanization and recreational tourism activities.

Desertas is a triad of small, barren islands SE of Madeira, dating back to 5 My (Schwarz et al. 2005). The largest of which, Deserta Grande (10 km^2), is a narrow, steep and elongate island. At the North end one small valley dominates the landscape, otherwise composed of small barren plateaus and steep slopes. No tree cover is present nowadays, due to the introduction of feral herbivores, such as rabbits and goats, during the attempts of human colonization of the island. Bugio is the second largest of this triad (3 km^2), and is even steeper than Deserta Grande, due to the practical absence of flat areas, with the exception of two small plateaus at North and South, respectively. Ilhéu Chão is the smallest (0,5 km^2) and flattest island, its landscape dominated by a single plateau. A protected area covers these islands, mostly due to the marine

biota that inhabits its surroundings, namely marine birds and a small population of the monk-seal, *Monachus monachus* (Hermann, 1779).

The subject of a land connection between Madeira and Desertas before the last glacial minimum is debatable, given that the submarine ridge between both does not exceed 140m deep. The subaerial connection of both islands was suggested by a number of authors based on biological affinities (Cook 1996, Cameron and Cook 1999, Brehm et al. 2003), but geological evidence, such as the absence of erosion on the submarine ridge (Klügel et al. 2009), argues against this possibility.

The archipelago harbours a high endemic biota (e.g. 1419 endemic terrestrial species, according to Borges et al. 2008a, including Selvagens), and several speciose arthropod taxa greatly contribute to this. The most remarkable examples of local diversification include the beetle genera *Laparocerus* Schoenherr, 1834 (Machado et al. 2017) and *Sphaericus* Wollaston, 1854 (Erber 2000) and the millipede genus *Cylindroiulus* Verhoeff, 1894 (Enghoff 1992), all with approximately 30 species. Also notable is the species proliferation of several groups of land snails (Cook 2008).

Spiders from Madeira

Before this work, the most speciose genus was the wolf spider *Hogna* Sundevall, 1833, accounting for a total of seven species (Wunderlich 1992, 1995). These are medium to large-sized generalist epigean predators with possible good ballooning and hence dispersal ability. Ballooning is the ability of some spiders to navigate air currents to become part of the aerial plankton and this way travel large distances with minimum effort.

Before our study, five *Dysdera* species were known from the Madeira archipelago, seemingly unrelated with the geographically close Canarian congenerics (Arnedo et al. 2001, Macías-Hernández et al. 2008). This genus was, for some time, suspected to harbour many endemic species due to previous sampling across islands within past projects (Crespo et al. 2013, Boieiro et al. 2018). These are preferential predators of woodlice with lower but still medium dispersal ability through rafting, i.e., using drifting wood or similar substrates to cross the ocean.

With this in my mind, it was clear that focusing on *Dysdera* and *Hogna* from Madeira could provide insights on the mechanisms of speciation in these islands. As these two genera have very different life-histories and modes of dispersal, contrasting the patterns between both groups could reveal the diversity of speciation histories occurring in Madeira.

- The *Dysdera* woodlouse hunter spiders

The Dysderidae are commonly known as six-eyed (Hormiga et al. 2020) or red-devil spiders. Historically, Dysderidae was placed in the Haplogynae, which grouped those spider families that lacked fertilization ducts in female reproductive systems. This group has received criticism due to the uncertain placement of several taxa and the lack of synapomorphies and the usually weak support in morphological phylogenetic analyses (Platnick et al. 1991, Griswold et al. 2005). More recently, the term Synspermiata was proposed to include all those families that share the presence of a synspermium, the fusion of several spermatids into one single structure (Michalik and Ramírez 2014). This lineage has been recovered as monophyletic in all molecular analyses conducted to date, including the major collaborative project of the Araneae Tree of Life (Wheeler et al. 2017) and more recently using transcriptomic data (Bond et al. 2014, Garrison et al. 2016, Fernández et al. 2018, Kallal et al. 2020, Kulkarni et al. 2021).

The type genus of Dysderidae, *Dysdera* Latreille, 1804, is the most species-rich genus (287 species, according to World Spider Catalog 2021) of its family. The genus has a western Palearctic distribution, but it is particularly diverse in the Mediterranean region, where it constitutes a relevant and highly endemic component of the forest undergrowth. The genus undergone a remarkable species diversification in the Canary Islands, where 47 endemic species have been documented so far (Wunderlich 1987, 1992, Arnedo et al. 1996, 2000, 2007, Arnedo and Ribera 1997, 1999). Canarian *Dysdera* have been shown to constitute a monophyletic lineage, with a single exception (Arnedo et al. 2001, 2007), providing one of the most extraordinary example of island diversification in oceanic islands among spiders. Phylogeographical studies conducted on the group revealed the involvement of both geological and ecological factors in shaping the current diversity of the group (Bidegaray-Batista et al. 2007, Macías-Hernández et al. 2008, 2013). On the other hand, the taxonomic study of the endemic species in an integrative

framework, combining morphological and molecular data, has been proven fundamental to unveil overlooked diversity within species complexes (Macías-Hernández et al. 2010).

The lifestyle of *Dysdera* spiders involves hiding during daytime in cryptic retreats (either in the underground or in bark) within silken cocoons and being active mostly at night, when they wander to hunt for prey. They usually favour forested areas, humid but not damp. Some species are prone to prey on woodlice, and possess unique mouthpart morphology to aid in subduing prey through specialized behaviours (Rezac et al. 2008). These mouthparts are important diagnostic characters for related species (Deeleman-Reinhold and Deeleman 1988). The occurrence of long-distance aerial dispersal, known as ballooning, is unknown in *Dysdera* (Duffey 1956, Blandenier and Fürst 1998). The low dispersal abilities of *Dysdera* has probably favoured high level of endemicity and narrow distributions that characterize most species in the genus across its distribution.

Figure 2. Two species of Madeiran endemic *Dysdera*. A: *D. dissimilis* Crespo & Arnedo, 2020. B: *D. sandrae* Crespo, 2020. Photo credits: Emídio Machado (A) & Pedro Cardoso (B).

- The *Hogna* wolf spiders

The Lycosidae, commonly known as wolf spiders, are one of the largest spider families (2430 species, according to World Spider Catalog 2021) and constitute a major component of open habitats worldwide. Most species are cursorial hunters and have abandoned any web-building behaviour. Recent phylogenetic analyses revealed that the remarkable burst of diversification in this family happened mostly synchronously with grassland expansion during the Miocene (Piacentini and Ramírez 2019). Lycosids are usually able to perform ballooning, and

thus are capable of transoceanic flights, turning them into formidable colonizers of remote islands. Consequently, lycosids can be found even in most islands of the world, including remote outposts such as Saint Helena (Tongiorgi 1977). Biogeographic patterns of the group, specially at species level, are frequently blurred by its high dispersal ability, which may help to maintain gene flow even among distantly located populations (Murphy et al. 2006, Piacentini and Ramírez 2019).

Lycosidae is a challenging group for taxonomists. Closely related species often have similar looking secondary genitalia, the main source of diagnostic characters for species identification among spiders. A possible explanation to the remarkable uniformity observed in genitalic characters is the presence in the group of complex mating rituals, probably associated to female sexual selection, which may replace the lock-and-key mechanisms as a prezygotic barrier to interspecific gene flow (Uetz and Roberts 2002, Stratton 2005, Vaccaro et al. 2010). The current taxonomic research on the group has also been hampered by former poor taxonomic revisions. Specifically, the publications of Roewer (Roewer 1960) created major problems, as a result of the erection and redefinition of genera based on invalid combinations of somatic characters (Langlands and Framenau 2010). Even with the use of molecular data, revising lycosid genera is a highly sensitive task, as species might be wrongly assigned, based on old descriptions.

Hogna is a genus of medium to large sized wolf spiders composed of 235 species distributed worldwide (World Spider Catalog 2021). As discussed above, the limits of the genus are elusive and some of its species may be wrongly placed. A recent molecular phylogenetic study by Piacentini & Ramírez (2019, 234: Fig. 4) revealed that *Hogna* is in fact paraphyletic, with several species well apart from the genus type species, *H. radiata* (Latreille, 1807).

Although continental species usually have wide distribution ranges, a number of *Hogna* lineages have diversified in small and remote islands, such as in the Galapagos archipelago (Baert et al. 2008). The evolutionary pathways of *Hogna* in Galapagos have been the object of recent studies. The seven endemic species seem to have diverged into coastal and montane habitats, with instances of introgression. Interspecific gene flow seems to have played a major role in driving parallel evolution in ecologically similar species (De Busschere et al. 2012, 2015).

Among the seven species of *Hogna* in Madeira archipelago, some have striking appearance, such as *H. ingens* (Blackwall, 1857), a giant species endemic to Deserta Grande. With a threatened status of Critically Endangered (Cardoso 2014), it is a case-study of conservation targeting invertebrate species (Crespo et al. 2014b). Unfortunately, poor descriptions, unavailability of type material and partial revisions have left a record of unsolved taxonomic problems in Madeiran *Hogna* (Wunderlich 1992, 1995), which has compromised advances in the understanding of the evolutionary history of this remarkable group.
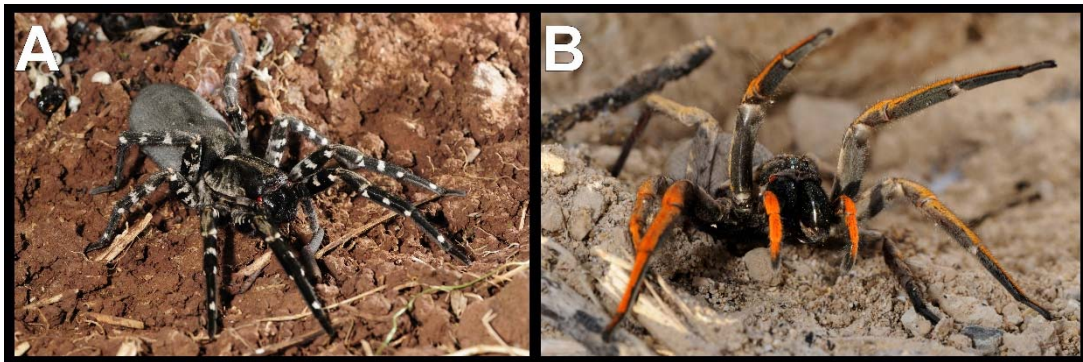
Figure 3. Two of the most striking species of Madeiran endemic *Hogna*. A: *H. ingens* (Blackwall, 1857). B: *H. maderiana* (Walckenaer, 1837). Photo credits: Pedro Cardoso.

Methodology fundamentals

- *An introduction to phylogenetic inference*

We can grossly say that phylogenetic inference is the attempt to reconstruct ancestry of a target set of biological taxa. This is usually based on the mapping of derived homologous characters, either morphological or molecular. Phylogenies allow us to understand the evolution of traits, their loss or gain, and identify instances of convergent or divergent evolution occurring across evolutionary time. Up until the 1970's, attempt to reconstruct ancestry of living organisms mostly a morphological endeavour (Telford and Budd 2003). These suffered from the questionable homology of traits across deeply divergent taxa and the limited availability of homologous characters for simple organisms, such as microorganisms (Delsuc et al. 2005). In the subsequent decades, the technological advances in molecular biology opened the door to the use of nucleotide and aminoacidic sequences as a source of massive number of homologous

characters. Target sequencing approaches (i.e. Sanger sequencing) revolutionized modern biological systematics and have been paramount to infer phylogenetic relationships among organisms and genes. Although second and third generation sequencing methods have somehow superseded target based approaches (Heather and Chain 2016), integrative taxonomy, including molecular identification techniques and single marker discovery methods such as DNA barcoding (Hebert et al. 2003), continue to strongly rely on Sanger sequencing. Molecular information has been fundamental to reveal overlooked species, provide quantitative phyletic surveys of environmental samples, or to inform conservation planning and forensic diagnostics, among other applications.

Molecular phylogenetic inference methods include both algorithm approaches based on genetic distances and those based on optimality criteria such as parsimony, maximum likelihood and Bayesian inference. In turn, one can distinguish between those inference methods based on explicit evolutionary models, from those that use an hypothetic-deductive approach based on character congruence (i.e. parsimony). Distance methods, such as neighbour-joining (Saitou and Nei 1987) or minimum evolution (Rzhetsky and Nei 1992), work on a distance matrix generated by explicit evolutionary models. Maximum Parsimony (MP) uses a different approach, in which it maps the history of mutations in a certain dataset and then generates a tree with the least required character changes to explain the dataset. A common program to run MP is TNT (Goloboff and Catalano 2016). This method has one disadvantage, which is the retrieval of solely one evolutionary pathway, which obscures the totality of available pathways, and the inability to account for convergent evolution in distantly related branches of the tree, the so-called "long-branch attraction", can cause distant branches to be closer under a parsimony framework (Holder and Lewis 2003). Maximum likelihood (ML) is a method able to correct for the presence of multiple mutational events at the same site. It generates the tree most likely to explain the observed data using an evolutionary model able to explain the probability of different mutations. Two widely used platforms to run ML analysis are RAxML (Stamatakis 2014) and IQTree (Minh et al. 2020). The downside of using ML is that the computational effort needed is much higher than any of the previous methods. Similar to ML, Bayesian inference (BI), uses an explicit evolutionary model. Unlike the former methods, BI relies on posterior distribution instead of single parameter estimates, searching for those trees and parameters that optimize the posterior probability given a set or informative and uninformative priors, using Markov Monte

Carlo chains. The posterior probability of a tree search is the result of the maximum likelihood multiplied by a prior probability. The major advantage of BI over ML is that it performs better when the number of parameters of the model is high and provides a measure of uncertainty around the parameter estimates. A common platform to run BI analyses is MrBayes (Ronquist et al. 2012).

One of the cases where additional parameters might contribute to evolutionary knowledge on a certain dataset is time estimation, which allow to contrast different biogeographic hypotheses. When molecular data was first available, the theory of the molecular clock emerged, which roughly dictated that the differences in homologous sequences is proportional to their time of divergence (Zuckerlandl and Pauling 1965). However, initial studies have resulted in extremely ancient divergence times for many lineages (Hedges et al. 1996, Wray et al. 1996, Heckman et al. 2001). This strict molecular clock contradicted paleontological evidences at first, but was the stepping stone for the development of better ways to estimate time, such as the lognormal relaxed clock (Donoghue and Yang 2016). In this case, particular branches of the tree must have an individual lognormal prior parameter, in the sense that the evolution rate changes independently across branch. We can also add calibration points to a certain node with either fossil or biogeographic information (taking care that the latter is not taken from the source data system). In the first case, the fossil provides a minimum date for the stem group, while in the second case the biogeographic events, such as emergence of islands or any other vicariant events, provide a basal threshold for the appearance of certain endemic lineages. This complex analysis can be implemented with the BEAST programme package (Bouckaert et al. 2019).

We are now standing in the age of phylogenomics, an area that surpasses the limitation of selecting target marker genes, by using a vast number of genes instead. The availability of multiple markers has also revealed the existence of frequent cases of incongruence among gene histories and between gene and species trees. This has in turn spurred the development of novel phylogenetic inference methods that explicitly incorporate the multiple coalescent and gene flow as additional sources of phylogenetic error, along with sampling and methodological ones. The computational infrastructures needed to operate these studies are, correspondingly, of a much greater magnitude, but it provides us with a powerful tool to advance in our goal of uncovering the Tree of Life and understanding its major drivers.

- *Methods of species delimitation*

Species are the fundamental units of evolution and the natural world. Much debate has occurred around the definition of the concept of species (Mayr 1982, de Queiroz 2005), due to the incompatible differences underlined by diverse group of biologists (Mayden 1997). In most cases, these differences are coupled to the definition of species boundaries, but all agree that a species is an independently evolving lineage delimited by specific barriers. The unified species concept includes the perception of a species as a metapopulational lineage, thus releasing the species concept free of requirements such as a morphological diagnostic, monophyly, reproductive isolation or ecological divergence (De Queiroz 2007), and uncoupling the definition of the concept from its empirical delimitation.

Several methods for species delimitation are available, some of them based on a single gene, which in the case of animals usually relies on the mitochondrial *cox1* barcode, while others are based on multilocus approaches. Model-based multilocus methods can explicitly account for gene tree versus species tree incongruences when estimating a tree, but the use of these methods in integrative taxonomic practise remains limited by the large amount of data required and the computational burden associated (Yang and Rannala 2010, Satler et al. 2013).

I mostly focused on single marker approaches to inform our taxonomic decisions. Some of the most widely used methods include the Automatic Barcode Gap Discovery (ABGD) (Puillandre et al. 2012), the Barcode Index Number (BIN) (Ratnasingham and Hebert 2013) the General Mixed Yule Coalescent model (GMYC) (Fujisawa and Barraclough 2013) and the multirate Poisson Tree Processes (mPTP) (Kapli et al. 2017) (see Chapters 1 and 3). The ABGD and BIN methods are distance-based methods that take pairwise differences and arrange those in a distribution dataset, pointing hypothetical species whenever a barcode gap is found between two distributions. The GMYC, is a method that tests if a particular branch in a tree either as inter- or intraspecific by maximizing the likelihood of a GMYC evolution model, thus testing for the onset of speciation versus coalescence. This method is one of the most popular, and was used in numerous works (Barraclough et al. 2009, Monaghan et al. 2009, Hamilton et al. 2011), with its robustness supported by several authors (Fujisawa and Barraclough 2013, Talavera et al. 2013, Tang et al. 2014). Finally, mPTP is the multiple rate version of the PTP model,

which seeks the transition in branch length between or within species (Zhang et al. 2013) given a Poisson distribution of branch lengths. This is done by either assuming one exponential distribution for speciation processes and another for coalescence, ignoring the stochastic variation among species and demographic histories (Blair and Bryson 2017), a problem overcome by the mPTP model (Kapli et al. 2017), which uses multiple independent distributions for each species to accommodate the aforementioned parameters. An advantage of mPTP is that unlike GMYC it does not require an ultrametric tree.

Objectives

The main goal of this work is to catalogue the species diversity of two highly diverse lineages in the Madeira archipelago, the spider genera *Dysdera* and *Hogna,* unravel their colonization pathways and evolutionary history and identify their main drivers of diversification. With that aim in mind, the following specific objectives are tackled:

1. To conduct an integrative taxonomic revision of the spider genera *Dysdera* and *Hogna* in the Madeira archipelago and the Azores;

2. To infer their phylogenetic relationships and internal structure using a multi-locus target gene approach;

3. To estimate a timeline for the diversification of the target genera to investigate their colonization history and evolutionary drivers;

4. To evaluate the species conservation status of the target groups.

Results

Chapter 1

Luís C. Crespo, Isamberto Silva, Alba Enguídanos, Pedro Cardoso and Miquel A. Arnedo (2021)

Integrative taxonomic revision of the woodlouse-hunter spider genus *Dysdera* (Araneae: Dysderidae) in the Madeira archipelago with notes on its conservation status

Integrative taxonomic revision of the woodlouse-hunter spider genus *Dysdera* (Araneae: Dysderidae) in the Madeira archipelago with notes on its conservation status

LUÍS C. CRESPO[1,3,*], ISAMBERTO SILVA[2], ALBA ENGUÍDANOS[1], PEDRO CARDOSO[3] and MIQUEL A. ARNEDO[1,©]

[1]*Department of Evolutionary Biology, Ecology and Environmental Sciences (Arthropods), Biodiversity Research Institute (IRBio), Universitat de Barcelona, Avenida Diagonal 645, 08028 Barcelona, Spain*
[2]*Instituto das Florestas e Conservação da Natureza IP-RAM, Jardim Botânico da Madeira, Caminho do Meio, Bom Sucesso, 9064–512, Funchal, Portugal*
[3]*Laboratory for Integrative Biodiversity Research (LIBRe), Finnish Museum of Natural History (LUOMUS), University of Helsinki, P.O. Box 17, 00014 Helsinki, Finland*

Dysdera is a highly speciose genus of mid-sized, nocturnal hunting spiders, mostly circumscribed to the Mediterranean. The genus managed to colonize all Macaronesian archipelagos, and underwent major diversification in the Canary Islands. Here, we report on an independent diversification event on the Madeira archipelago. Based on the integration of morphological and molecular evidence, we describe 8 new species to science, ***Dysdera dissimilis* sp. nov.**, ***Dysdera exigua* sp. nov.**, ***Dysdera isambertoi* sp. nov.**, ***Dysdera precaria* sp. nov.**, ***Dysdera recondita* sp. nov.**, ***Dysdera sandrae* sp. nov.**, ***Dysdera teixeirai* sp. nov.**, ***Dysdera titanica* sp. nov.** and redescribe *Dysdera coiffaiti*, *Dysdera diversa* and *Dysdera portisancti*. We synonymize *Dysdera longibulbis* and *Dysdera vandeli* under *D. coiffaiti* and *D. diversa*, respectively. Additionally, we use a multilocus target gene phylogeny to support a single colonization event of the archipelago followed by *in situ* diversification. We further discuss the discovered diversity patterns and their drivers. We conclude to that many of the species inhabit disturbed or fragile habitats and should be considered of high conservation concern.

ADDITIONAL KEYWORDS: Arachnida – biogeography – Desertas – island radiation – Macaronesia – phylogeny – Porto Santo – species delimitation – Synspermiata – Taxonomy.

INTRODUCTION

Oceanic islands have attracted the curiosity of naturalists and scholars for many centuries. As a newly emerged area surrounded by an inhospitable matrix, an oceanic island is subject to differential dynamic processes of immigration, extinction and speciation, and may additionally be impacted by volcanic activity and quiescence, i.e. island ontogeny (Whittaker *et al.*, 2017). The joint effect of biological, environmental and geological processes have, over evolutionary time, generated a large number of remarkable arthropod radiations in many archipelagos. Typical examples are the radiation of the long-jawed orb weaver spiders (*Tetragnatha* Latreille, 1804) in the Hawaiian Archipelago (Gillespie, 2004) or the net-winged beetles of the Indo-Pacific (Bocek & Bocak, 2019).

The genus *Dysdera* Latreille, 1804 provides one of the most remarkable examples of local diversification on oceanic islands within spiders. The genus is composed of 284 species of nocturnal ground-dwelling hunters distributed in the Western Palaearctic, mostly around the Mediterranean basin (World Spider Catalog, 2020).

*Corresponding author. E-mail: luiscarloscrespo@gmail.com

The westernmost limits of the genus are the Atlantic archipelagos of Madeira, the Selvagens, the Azores, the Canary Islands and Cabo Verde, collectively referred to as Macaronesia. When *Dysdera* colonized most of the Macaronesian archipelagos, it underwent an unparalleled diversification process on the Canary Islands, where 47 endemic *Dysdera* species are known (Wunderlich, 1987, 1992; Arnedo *et al.*, 1997, 2000, 2007; Arnedo & Ribera, 1997, 1999) and several more still await formal description (Arnedo, unpublished data). The remaining Macaronesian archipelagos harbour more modest numbers of endemic species. Cabo Verde and the Selvagens have one species each, *Dysdera vermicularis* Berland, 1936 and *Dysdera aneris* Macías-Hernández & Arnedo, 2010, respectively, and there is evidence in the Azores for an undescribed, possibly extinct species (Cardoso *et al.*, 2010).

Madeira is the only archipelago other than the Canary Islands to host several endemic *Dysdera* species. Prior to this study, five endemic species had been recorded. The first species of *Dysdera* described from Madeira was *Dysdera diversa* Blackwall, 1862, from a batch of spiders collected by Hamlet Clark. Almost a century passed before the next endemics were discovered. Jacques Denis, based on a study of material collected on an expedition to Madeira led by Albert Vandel in 1957, described *Dysdera vandeli* Denis, 1962, *Dysdera coiffaiti* Denis, 1962 and *Dysdera longibulbis* Denis, 1962. More recently, Jörg Wunderlich (1995) described a species from Porto Santo island, *Dysdera portisancti* Wunderlich, 1995, found among material collected by K. Groh in 1985.

The Madeira archipelago (Fig. 1) is situated in the Atlantic Ocean, 650 km south-west of the Iberian Peninsula and 450 km north of the Canary Islands. It is composed of Madeira island, Porto Santo island and adjacent islets and the Desertas islands. All islands originate from the same volcanic hotspot, with Porto Santo dating back to approximately 14 Mya, Madeira 7 Mya and the Desertas 5 Mya (Geldmacher & Hoernle, 2000; Schwarz *et al.*, 2005; Ramalho *et al.*, 2015). Several distinct habitats can be found in the archipelago, ranging from montane shrubland and laurel forest on Madeira island (Fig. 2A), secondary forests on Madeira and Porto Santo island and scrubland with sparse xerophytic plants in the coastal areas of eastern Madeira island, Porto Santo island and its neighbouring islets and the Desertas islands (Fig. 2B). This diversity of habitats, tied to a complex geomorphology and geologic history, allowed

Figure 1. Map of the Macaronesia and the Madeira archipelago [adapted from Borges *et al.* (2008) with author's permission].
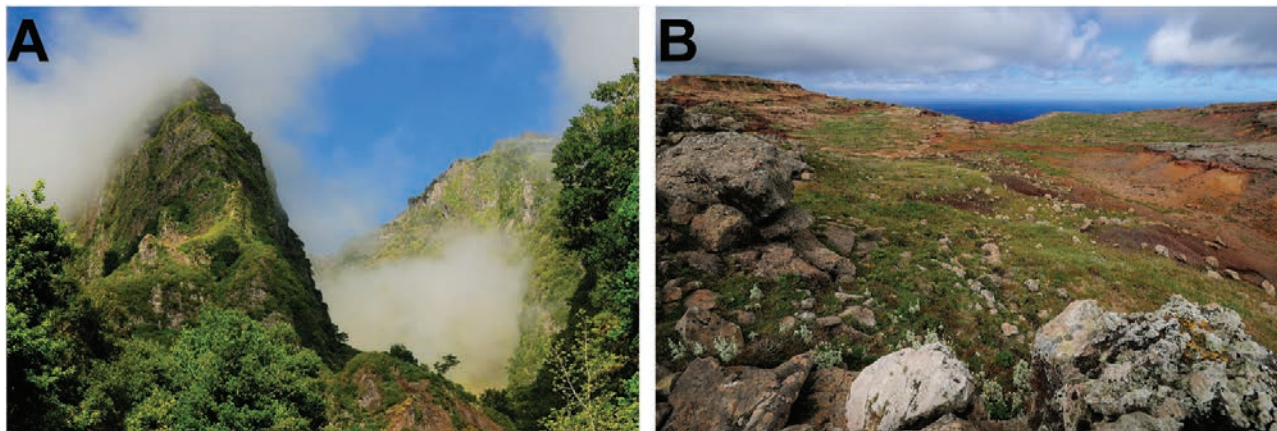
Figure 2. Landscapes. A, Fajã da Nogueira, Madeira island. B, Planalto Sul, Deserta Grande. Photo credits: Pedro Cardoso.

several taxa to diversify locally, such as the beetles *Laparocerus* Schönherr, 1834 and *Tarphius* Erichson, 1848 [see a regional checklist in Borges *et al.* (2008)]. In spiders, the most diverse taxa in the archipelago are the wolf spider genus *Hogna* Simon, 1885, with seven species, followed by the five aforementioned *Dysdera* species.

Over the course of the past years, the study of historical and newly collected material of *Dysdera* made available through general inventories and specific fieldwork campaigns led us to unravel a remarkable number of taxonomic novelties, including the discovery of new species and synonymies. Additionally, the inclusion of DNA barcoding information has offered us additional support for species delimitation and insights into phylogeographic patterns. The combined phylogenetic analyses of multiple loci from a sampling of island and continental species, confirmed that Madeiran species represent a diverse lineage that colonized the archipelago most likely only once and diversified *in situ*.

MATERIAL AND METHODS

FIELD WORK

The material studied here was made available through collections from general inventory projects, and from two expeditions specifically conducted to collect *Dysdera* specimens in Madeira archipelago in spring 2017 and 2018. Sampling was carried out in a wide variety of habitats, especially in areas where native vegetation, or its surrogates, could be found. This usually led us to the summits of the islands, because the low-elevation areas are either subject to a high levels of human disturbance, or are inaccessible (as is the case in the Desertas). The sampling localities and their coordinates are listed in Supporting Information

(Table S1). Sampling was done by manually lifting stones and removing tree bark (only in Madeira island) and retrieving *Dysdera* specimens manually or with the aid of an entomological aspirator. Each specimen was placed into a separate vial containing absolute ethanol.

MOLECULAR LABORATORY PROCEDURES

We used one leg III for DNA extractions, conducted with the Speedtools® Tissue DNA Extraction Kit (Biotools) or DNeasy® Blood & Tissue Kit (Qiagen) with the tissue protocol suggested by the respective manufacturer. Partial fragments of the mitochondrial cytochrome *c* oxidase subunit I (*COI*), i.e. the animal DNA barcode (Hebert *et al.*, 2003), 16S rRNA, tRNA Leu (*L1*), NADH dehydrogenase subunit 1 (*NAD1*), the nuclear large ribosomal subunit 28S rRNA (28S) and histone 3 (*H3*) were amplified. The primers used for amplification and sequencing, as well as the PCR conditions for the loci are listed in Supporting Information (Table S2). The final PCR product was sequenced by Macrogen Inc. (Seoul, South Korea). Sequences were edited and manipulated in Geneious v.8.1.9 (Kearse *et al.*, 2012).

MOLECULAR PHYLOGENETIC ANALYSIS

To test the monophyly and phylogenetic position of Madeiran endemics, we included the two specimens with the most divergent *COI* sequences of each Madeiran species and combined them with representatives of the spider family Dysderidae available in GenBank. The latter were automatically retrieved with the help of the R package *phylotaR* (Bennett *et al.*, 2018). In the final matrix we only included those Genbank species with three or more genes available and up to a maximum of two species per genus, except for *Dysdera,* where

all species available with the right number of genes were included. Ribosomal genes were aligned with the plugin available in Geneious of the automatic aligner MAFFT (Katoh, 2002; Katoh & Standley, 2013), using the L-INS-i option (conserved domain with long gaps). We treated gaps as missing data. Sequence edition, manipulation and concatenation were conducted in Geneious. We assessed sensitivity of the results to the use of alternative methods of phylogenetic inference by conducting analyses under three different approaches. We ran a uniformly weighted parsimony (MP) analysis as implemented in the computer program TNT v.1.5 (Goloboff *et al.*, 2008) constructing 1000 Wagner trees with random addition of taxa followed by Tree Bisection and Reconnection (TBR) branch swapping. Branches where minimum possible length in any most parsimonious reconstructions was zero were collapsed. Clade support was estimated by inferring the most parsimonious tree of 1000 jack-knife resampled matrices, with probability of character removal set to 0.33 (search strategy: mult 15 = TBR hold 20). Maximum likelihood (ML) inference was implemented with the program IQ-TREE v.1.6.12 (Nguyen *et al.*, 2015). We used IQ-TREE to first select the best-fit partitioning scheme and corresponding evolutionary models (Kalyaanamoorthy *et al.*, 2017), and then to infer the best tree and estimate clade support by means of 1000 replicates of ultrafast bootstrapping (Hoang *et al.*, 2018). Finally, we conducted a Bayesian inference (BI) analysis using the program MrBayes v.3.2.3 (Ronquist *et al.*, 2012). We first assessed the best partition scheme and corresponding evolutionary model with the help of the program PartitionFinder v.2.1.1 (Lanfear *et al.*, 2017). The best partition and models were defined in MrBayes and two Markov chain Monte Carlo (McMC) runs of eight chains and 0.05 temperature each were run for 10 million generations. We monitored the chain convergence (i.e. overlapping posterior distribution of key parameters), the chain mixing (ESS > 200) and the number of generations to discard as burn-in (25%) with Tracer v.1.7 (Rambaut *et al.*, 2018).

MOLECULAR SPECIES DELIMITATION

Morphology based delimitation was corroborated by conducting quantitative delimitation based on the DNA barcodes (*COI*) (676 bp) of a thorough sampling of specimens collected in all parts of the Madeiran archipelago (194 specimens, Supporting Information, Table S1). We implemented three different approaches: (1) based on distances [the Automatic Barcode Gap Discovery (ABGD) Puillandre *et al.* (2012)]; (2) based on the relative branch length estimated either from the best ML tree [the multirate Poisson Tree Processes (mPTP) Kapli *et al.* (2017)]; and (3) based on an ultrametric Bayesian tree

[the Generalized Mixed Yule-Coalescent (GMYC) Fujisawa & Barraclough (2013).

The ABGD method was conducted through the ABGD website (https://bioinfo.mnhn.fr/abi/public/abgd/abgdweb.html) using default options and uncorrected genetic distances. The mPTP method has been shown to outperform other delimitation methods by providing more stable outputs without requiring the ultrametric transformation of tree branches (Blair & Bryson, 2017). The mPTP model was implemented using a McMC approach, allowing estimates of support values on the delimitations, using the program available at https://github.com/Pas-Kapli/mptp.git. We ran five chains of 100 million generations each, removing the first 2 million as burn-in and discarding all branches with lengths smaller or equal to 0.0001. The mPTP analysis was conducted on the best ML tree obtained with IQ-TREE, using the same analyses settings specified above. To conduct the GMYC delimitation method, we first inferred an ultrametric tree using a Bayesian approach, as implemented in the program BEAST v.1.8.4 (Drummond *et al.*, 2012). We selected a coalescent tree prior (constant population size), which has been suggested to provide a more rigorous test of delimitation since the model assumes a single species as the null option (Monaghan *et al.*, 2009). We defined the best partition schemes and evolutionary models selected by PartitionFinder and assigned a single relaxed lognormal clock prior to the whole *COI* with the ucld.mean parameter arbitrarily set to 1 (relative branch lengths). Three chains of 10 million generations were run for each analysis. Correct mixing and burn-in was assessed with TRACER. The accompanying programs LOGCOMBINER and TREEANNOTATOR were used to remove the burn-in generations, to combine the results of three independent chains, and select the optimal distribution of posterior parameters and tree values. The GMYC cluster was identified with the help of the R package SPLITS (Ezard *et al.*, 2017).

We estimated inter- and intraspecific uncorrected genetic distances (p-distances, summarized in Table 1) with the program MEGA v.7.0.26 (Kumar *et al.*, 2016), using 500 iterations of bootstraps to estimate standard errors.

MORPHOLOGICAL STUDY

Morphological observations were carried out using a Leica MZ 16A stereomicroscope equipped with a Leica DFC450 digital camera. Individual raw photos were taken with the help of Leica Application Suite v.4.4 software and mounted with Helicon Focus software (Helicon Soft, Ltd.). Further editions were done with Paint Shop Pro v.21 (Corel Corporation). The vulva was removed from female specimens with the

Table 1. Genetic distance matrix (p-distance) based on the *COI* barcode of 194 samples, generated by MEGA. Average values in bold

	D. coiffaiti (Madeira)	D. coiffaiti (Desertas)	D. teixeirai	D. sandrae	D. exigua	D. diversa	D. recondita	D. precaria	D. isambertoi	D. dissimilis	D. portisancti
D. coiffaiti (Madeira)	**0.0322**										
D. coiffaiti (Desertas)	**0.0691** 0.0270–0.1081	**0.0224**									
D. teixeirai	**0.1305** 0.0811–0.2432	**0.1580** 0.1081–0.1892	**0.0314**								
D. sandrae	**0.1984** 0.1351–0.2432	**0.1616** 0.1351–0.1622	**0.2178** 0.1622–0.2432	**0.0068**							
D. exigua	**0.1489** 0.1081–0.1892	**0.0967** 0.0811–0.1351	**0.2138** 0.1892–0.2432	**0.0811** 0.0811–0.0811	**0.0000**						
D. diversa	**0.2141** 0.1351–0.2432	**0.2017** 0.1892–0.2432	**0.2813** 0.2432–0.3243	**0.1368** 0.1081–0.1622	**0.1486** 0.1351–0.1622	**0.0541**					
D. recondita	**0.1763** 0.1351–0.2162	**0.1507** 0.1351–0.1892	**0.2727** 0.2432–0.2973	**0.1892** 0.1892–0.1892	**0.1081** 0.1081–0.1081	**0.2162** 0.2162–0.2162	**0.0000**				
D. precaria	**0.2448** 0.1892–0.3243	**0.2254** 0.1622–0.2703	**0.2510** 0.1622–0.3243	**0.3064** 0.2703–0.3243	**0.2744** 0.2432–0.2973	**0.3358** 0.2973–0.3784	**0.2455** 0.2162–0.2703	**0.0735**			
D. isambertoi	**0.2338** 0.1892–0.3243	**0.2668** 0.2162–0.2703	**0.1919** 0.1622–0.2162	**0.3160** 0.2432–0.3243	**0.2899** 0.2162–0.2973	**0.3108** 0.2973–0.3243	**0.3096** 0.1622–0.3243	**0.2336** 0.1622–0.2703	**0.0270**		
D. dissimilis	**0.2561** 0.1892–0.3243	**0.2287** 0.2162–0.2973	**0.3008** 0.2703–0.3514	**0.1749** 0.1622–0.2432	**0.1445** 0.1351–0.1892	**0.2414** 0.1892–0.2973	**0.1351** 0.1081–0.1892	**0.1989** 0.1622–0.2432	**0.2636** 0.1351–0.2973	**0.0170**	
D. portisancti	**0.2810** 0.2162–0.2973	**0.2734** 0.2703–0.2973	**0.3759** 0.3514–0.4054	**0.1926** 0.1892–0.2162	**0.2162** 0.2162–0.2162	**0.1622** 0.1351–0.1892	**0.2162** 0.2162–0.2162	**0.3015** 0.2703–0.3243	**0.3468** 0.2973–0.3514	**0.1863** 0.1622–0.2162	**0.0000**

29

aid of hypodermic needles and forceps. To clear the membranous tissues surrounding the genitalic sclerites we manually removed muscular and membranous tissue with forceps and a needle, then immersed the structure in 30% KOH for 15 to 30 min, after which we cleaned the remaining patches of tissue. SEM images of the male copulatory bulb were obtained with a Q-200 (FEI Co.) scanning electron microscope (SEM). For the SEM images, each male palp was excised at the joint between the tarsus and the tibia. Samples were sonicated for roughly 30 s with a Nahita ZCC001 ultrasonic bath, dehydrated through immersion in increasing dilutions of ethanol, transferred to absolute ethanol, air dried and carbon or gold sputter-coated.

When available, we used five males and five females of each species to take somatic morphology measurements with an ocular micrometre in the stereoscope. Length of the cheliceral furrow was measured from the base of the distal condyle to the tip of the cheliceral basal lamina (Fig. 6C). All measurements are in millimetres (mm). Scoring of leg chaetotaxy followed Arnedo *et al.* (1996). The apical pair of ventral spines in the tibiae, which are always present, as well as spineless leg segments, are omitted from the spination description. Genital homologies and nomenclature followed Arnedo *et al.* (2000). Nevertheless, due to the complexity and taxonomic relevance of these structures, we hereby provide a general overview with a special focus on the species described in this study.

Male palp

The tegulum (T) is an orange cylindrical sclerite containing the coiled sperm duct, of which only the outermost sections are visible through transparency. The T bears at its distal retrolateral side, the posterior apophysis (P) (Fig. 3). Throughout the genus, this structure can have a wide array of shapes, some of which are a good indicator of the species-group to which a species belongs [see a compilation of male bulbs in Le Peru (2011)]. In most other *Dysdera* lineages, P is directed posteriorly. However, in the Madeiran lineage, it is shifted roughly 90 ° anteriorly, thus appearing directed retrolaterally. P is always short to moderately elongated, sclerotized, claw-shaped and well separated from other structures, with a sharp edge tilted dorsally (the case for most species) or posteriorly (see the new species *D. recondita*; Fig. 17A). The SEM photos show small ridges in the dorsal surface of the P for most of the species (Fig. 3B–D); however, these are difficult to discern under the stereomicroscope, and as such not included in the species diagnosis. The embolic or distal division (DD) includes a membranous distal hematodocha (DH) connected to internal and external sclerites (IS and ES, respectively). The relative length of the DD in relation to T varies across the genus; however,

in the Madeiran species the T is always clearly shorter than the DD. The IS are usually straight, serving as support for the DD, whereas the ES are variably curved, probably acting as conductors for the sperm duct. Each sclerite is differentially developed and can present different structures distally, which are of relevance for species diagnoses. In the Madeiran species, the tips of the IS often presents an arch-like ridge (AR), which is a membranous cavity opened to a variable extent [e.g. in *D. portisancti* it is open, spoon-shaped (Figs 15C, 32) whereas in *D. dissimilis* it is a fully encircled opening (Figs 10B, 28)]. However, in some species the AR is missing [e.g. *D. diversa*, *D. exigua* (Figs 12B, 13B, 29, 30) and *D. sandrae* (Figs 18A–B, 35)]. The crest (C) is a variably sclerotized prolateral process that usually forms the base of the AR. In some cases, the C ends in a membranous tip [e.g. *D. teixeirai* (Figs 19B, 36)], while in others it ends in a highly sclerotized process, hereafter referred to as internal sclerite distal apophysis [ISDA, e.g. *D. recondita* (Figs 17B, 34) and *D. sandrae* (Figs 18A–B, 35)]. Some species show an additional process or ridge at the distal, retrolateral margin of the IS: the lateral fold (LF). The opening of the embolus (EO) is usually difficult to discern under a normal stereomicroscope; however, observation of the contour of the sperm duct by transparency, couple to a detailed search of the opening on ventral view, allowed us to find the opening in most species, often being juxtaposed to the retrolateral margin of the tip of the IS. The tip of the ES is simpler, because it usually corresponds to the sclerotized edge of the medially membranous lateral sheet (L), hence we hereby treat it as an external side of the lateral sheet (eL). In the species concerned, the aspect of the eL ranges from small and thin [e.g. *D. precaria* (Figs 16A, 33D)] to massive and claw-shaped [e.g. *D. sandrae* (Figs 18A–B, 35)].

Female vulva

All copulatory structures of *Dysdera* females are internal. The epigastric opening leads to two pouches, the anterior diverticulum (AD) and the posterior diverticulum (PD), which are locked by the bursal valve (not illustrated), a thin sclerotized lamellar outgrowth of the transversal bar (TB), a massive semicircular sclerotized structure that constitutes the posterior margin of the AD and acts as a muscular attachment. All the PD of the species treated here are similar, oval or rounded, and are not illustrated. In *Dysdera*, the AD bears most of the diagnostic characters. This pouch is further subdivided in two compartments, namely the ventral arch (VA) and the dorsal arch (DA), which converge and fuse towards the frontal part, while tilting dorsally. The DA presents a small external fold, the dorsal fold (DF), which, in combination with the bursal valve, provides a lock
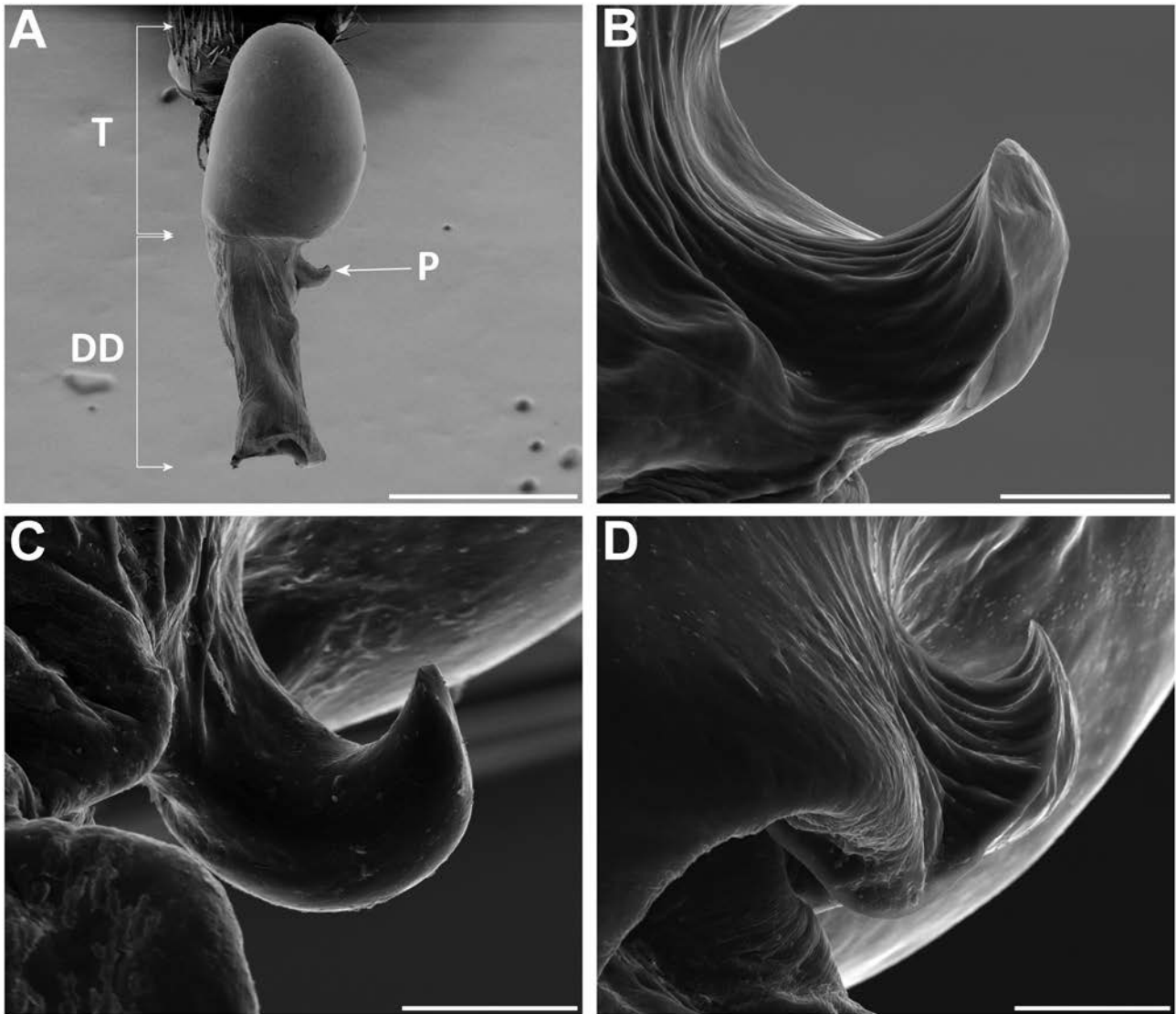
Figure 3. A, male palp of *D. diversa*, frontal. B, posterior apophysis of ***D. isambertoi* sp. nov.**, posterior. C, posterior apophysis of ***D. recondita* sp. nov.**, posterior. D, posterior apophysis of ***D. teixeirai***, posterior. Scale bars: A = 0.5 mm; B–D = 0.05 mm. Abbreviations: DD, distal division; P, posterior apophysis; T, tegulum.

system for the opening of the oviduct. The DA extends laterally in a variable manner, sometimes with sulci and folds visible in these extensions. The DA and VA are generally fused but can be distinguished by the presence of a lateral furrow separating both structures, the major fold (MF), usually recognised by the observation of lateral sclerotized lamellar outgrowths through transparency of the VA [e.g. *D. sandrae* (Fig. 18F)]. The DA and VA are readily apparent in some species, such as in the new species *D. precaria*, because of a distinct separation between the two structures (Fig. 16F), whereas in others, such as in *D. portisancti*, it is not clear where the border between the two structures lies (Fig. 15G). The ventral side of the VA presents different levels of

sclerotization across species and, sometimes, it presents additional folds, of which the degree of development may make apparent the shape of an additional ventral diverticulum (AVD). The membranous section of the VA usually shows, by transparency, the outline of the medial groove (MG), which is a membranous channel connecting the anterior spermatheca sclerite (S) to the VA. The S is usually a subtriangular sclerite, with more or less elongated lateral arms, and tips that are often tilted anteriorly or dorsally, and from which muscular tissues are attached. In some of the present species, a small dorsal diverticulum can be observed in the S [e.g. *D. coiffaiti* (Fig. 6E–F), *D. dissimilis* (Fig. 10E, G) or *D. teixeirai* (Fig. 19E–F, H–I)].

ABBREVIATIONS

Somatic characters: AME – anterior median eyes. B – basal tooth. CF – cheliceral furrow. D – distal tooth. fe – femur. M – median tooth. me – metatarsus. pa – patella. PLE – posterior lateral eyes. PME – posterior median eyes. ta – tarsus. ti – tibia.

Male genitalia: AR – arch-like ridge. DD – distal division. DH – distal hematodocha. eL – external margin of lateral sheet. EO – embolus opening. ES – external sclerite. IS – internal sclerite. ISDA – internal sclerite distal apophysis. L – lateral sheet. LF – lateral fold. P – posterior apophysis of tegulum. T – tegulum.

Female genitalia: AD – anterior diverticulum. AVD – additional ventral diverticulum. DA – dorsal arch. DF – dorsal fold. MG – medial groove. MF – major fold. PD – posterior diverticulum. S – spermathecae. SD – spermathecae diverticulum. TB – transversal bar. VA – ventral arch

Collections: CRBA – Centre de Recursos de Biodiversitat Animal, University of Barcelona, Barcelona, Spain. FMNH – Finnish Museum of Natural History, Helsinki, Finland. LCPC – Luís Crespo Personal Collection, Barcelona, Spain. MIZ – Museum and Institute of Zoology, Polish Academy of Sciences, Warsaw, Poland. MMF – Museu Municipal do Funchal, Funchal, Madeira, Portugal. MNHNP – Muséum National d'Histoire Naturelle, Paris, France. MZB – Museu de Ciències Naturals de Barcelona, Barcelona, Spain. OUMNH – Oxford University Museum of Natural History, Oxford, UK. SMF – Senckenberg Research Institute, Frankfurt am Main, Germany.

RESULTS

PHYLOGENY

PCR amplification was generally successful, except for samples of *D. diversa* collected in pitfall traps with liquids unsuitable for DNA conservation. We were unable to amplify large portions of the 28S gene (maximum of 159 bp obtained) or the *H3* gene of the last specimens. In addition, because of the old age (probably collected in the 19th century), we did not try to extract DNA from the single specimen of the new species *D. titanica*. All sequences newly obtained in this study are listed in Supporting Information (Table S1).

Results of phylogenetic analyses are summarized in Fig. 4. All analyses recover the monophyly of Madeiran species with high support – hereafter referred to as the Madeiran clade. Similarly, all analyses support the sister group relationship of the Madeiran clade

to a clade exclusively composed of species from the Iberian Peninsula and Morocco – hereafter referred as the Ibero-Moroccan clade. Support for both the Ibero-Moroccan clade and its internal structure is generally low. Interestingly, the Madeiran clade is not closely related to the endemic species of the Canary Islands, which are also retrieved as monophyletic, albeit with low support in the parsimony analysis, and a sister clade to the combined Madeiran and Ibero-Moroccan clades. The remaining *Dysdera* species, including mostly species from the eastern Mediterranean (except the Iberian *Dysdera scabricula* Simon, 1882) form a grade leading to the western Mediterranean lineages, within a well-supported monophyletic genus *Dysdera*.

Within the Madeiran clade, the four species of Porto Santo island form a well-supported clade in both model-based analyses, forming a sister clade to a well-supported clade that included the Madeira island and Desertas species. The parsimony analysis instead recovers the Porto Santo species as a grade, because *D. portisancti* is placed as a sister species to the remaining Madeiran clade. The internal structure of the Madeira-Desertas clade varied across analyses; however, *D. coiffaiti* and the new species *D. teixeirai* are always recovered as sister taxa with high support.

SPECIES DELIMITATION

Based on morphological traits traditionally used in spider taxonomy (i.e. genitalia, cheliceral teeth, leg spination) to delineate species, we distinguish ten putative morphospecies. In addition, the *D. coiffaiti* populations from Madeira island and Desertas present subtle differences in male genitalia and body size. The molecular species delimitation methods, on the other hand, retrieve a variable number of putative species, ranging from ten to 16 (Fig. 5). Of these, GMYC is the method that split the most, generating 16 clusters, followed by mPTP, which generate 13 clusters, while ABGD has ten groups, providing a perfect match with the morphological delimitation. In some cases, mPTP and GMYC identify clusters that correspond to geographical structure within morphologically diagnosable species, such as populations of *D. dissimilis* from different mountain ranges, or island populations from Madeira island and the Desertas of *D. coiffaiti* (GMYC only). However, in other cases GMYC and mPTP clusters did not reflect any obvious geographical or morphological features. We adopt a conservative approach and accept the species boundaries inferred with morphology and that are supported by the molecular ABGD approach. The additional clusters revealed by the GMYC and mPTP methods are interpreted as corresponding to intraspecific variability and population structuring. The inter- and intraspecific p-distances in *COI* are summarized in Table 1. Interspecific genetic distances
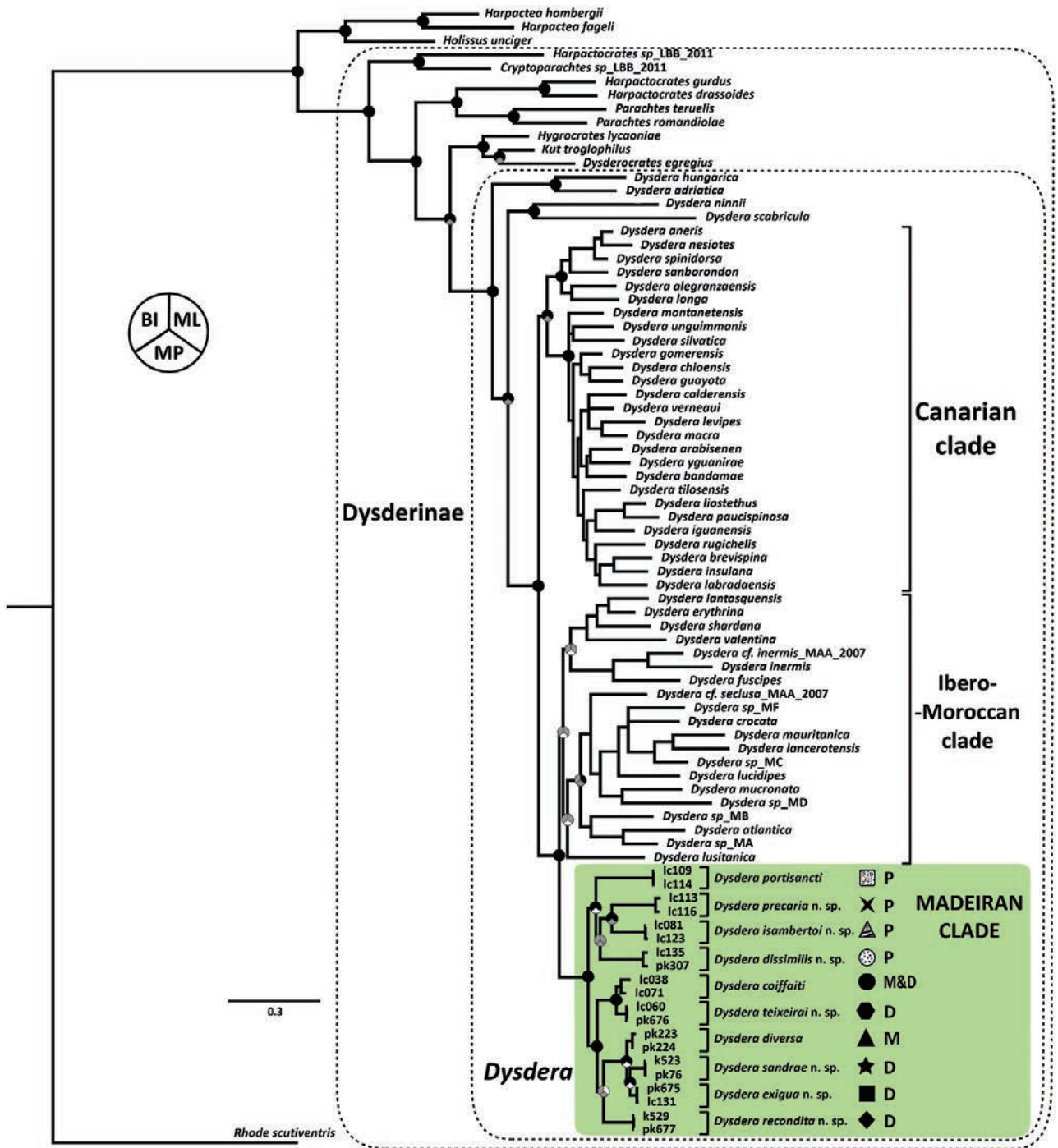
Figure 4. Bayesian majority rule consensus tree based on the multigene concatenate alignment. Nodes are split in three sections, respectively representing each method (see diagram on left): top left: BI; top right: ML; bottom: MP. Black indicates a supported node (Bayesian PP ≥ 0.95, ML Bootstrap ≥ 80% or MP Jackknife ≥ 70%), grey an unsupported node (Bayesian PP < 0.95, ML Bootstrap < 80% or MP Jackknife < 70%) and white an unrecovered node (only ML and MP). Terminal nodes in Madeiran clade are all supported. Terminal nodes in outgroup clades are not illustrated for simplification. Icons besides species names refer to the distribution maps (Figs 9, 10, 12). Letters refer to the island(s) of occurrence of each species, P: Porto Santo; M: Madeira; D: Desertas.

33
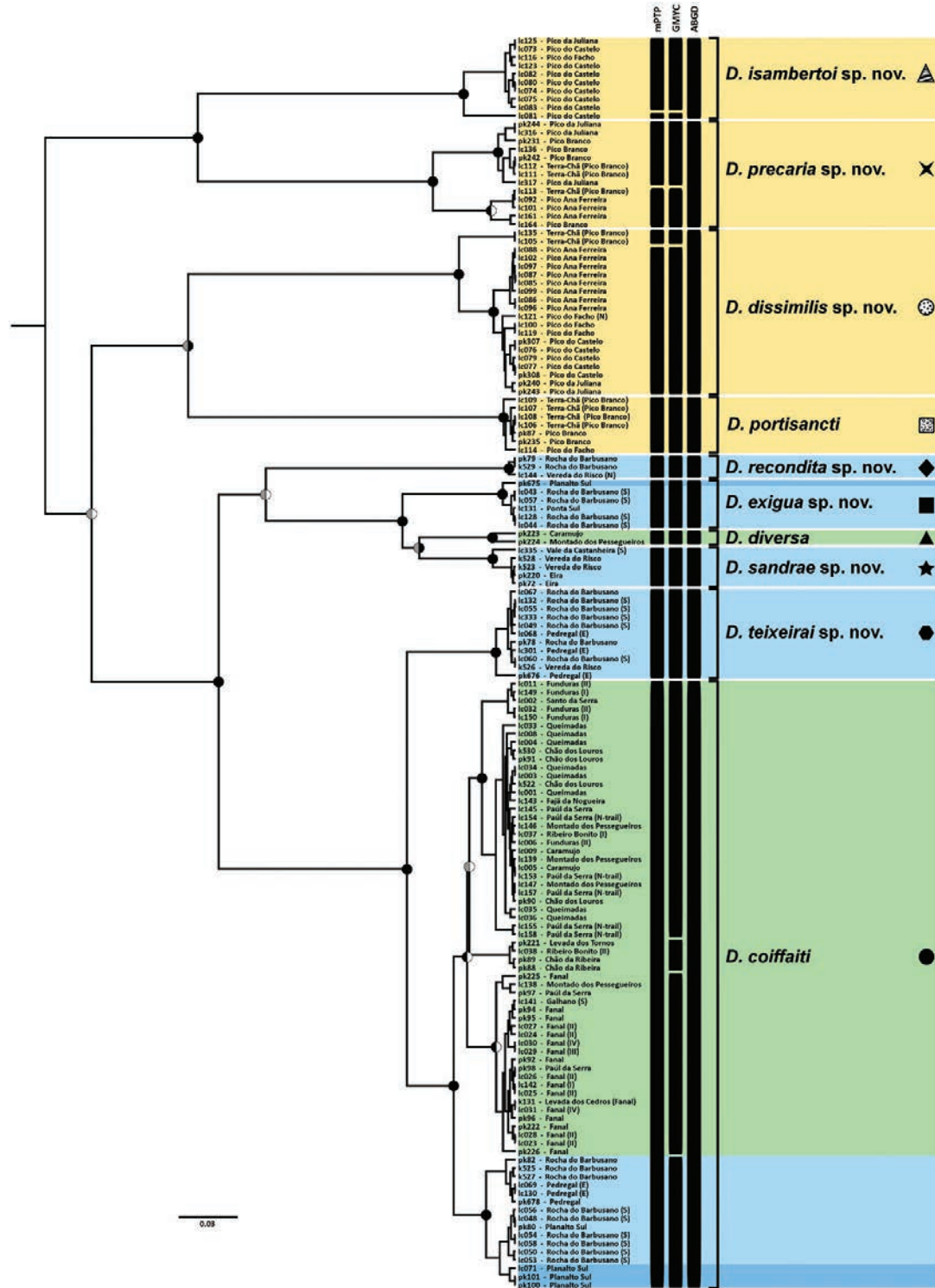
Figure 5. Bayesian majority rule consensus tree inferred from the mitochondrial cytochrome oxidase I locus (*COI*). Node circles are split to represent posterior probability (left) and bootstrap support level (right), in which black indicates a supported node (Bayesian PP ≥ 0.95 or Bootstrap ≥ 80%), grey an unsupported node (Bayesian PP < 0.95 or ML Bootstrap < 80%) and white an unrecovered node (only ML). Sampling sites are shown beside each sample code. Bars indicate groupings according to each method, namely GMYC, mPTP and ABGD. Icons besides species names refer to the distribution maps (Figs 8, 9, 11). Coloured boxes indicate the island of occurrence: yellow: Porto Santo; light blue: Deserta Grande; blue: Bugio; green: Madeira.

were always higher (> 8%) than any of the intraspecific values. Interestingly, the average p-distance (6.9%) between island populations (Madeira and Desertas) of *D. coiffaiti*, which display subtle morphological differences, was similar to the highest intraspecific values observed (e.g. *D. precaria* 7.4%), yet below the lowest interspecific p-distance recovered (e.g. *D. exigua* and *D. sandrae* 8%).

SYSTEMATICS

KEY TO THE *DYSDERA* SPECIES OF THE MADEIRA ARCHIPELAGO:

1	Males (male of *D. titanica* unknown).	2
	Females..	12
2	P separated from T, distally with bifid ridge and membranous base (Deeleman-Reinhold & Deeleman, 1988: p. 159, figs 23–24). ....*D. crocata*	
	P attached to T, distally with simple, sclerotized ridge (Figs 3, 6A–B, G–H, 10A–B, 12A–B, G–H, 13A–B, 14A–B, 15A–C, 16A–B, 17A–B, 18A–B, 19A–B)..	3
3	Species from Porto Santo.	4
	Species from Madeira or Desertas..	7
4	Prolateral bulge on well-developed base of IS (Figs 14B, 16B). Distal tooth in the distal half of cheliceral furrow (Figs 14C, 16C).	5
	Base of IS moderately or poorly developed (Figs 10B, 15B). Distal tooth at most in the midpoint of cheliceral furrow (Figs 10C, 15C).	6
5	DD roughly as long as T. eL stout (Fig. 14A–B). D robust, slightly larger than B (Fig. 14C). .... *D. isambertoi*	
	DD roughly twice as long as T. eL thin (Fig. 16A–B). D subequal or slightly smaller than B (Fig. 16C). ....*D. precaria*	
6	Tip of DD highly developed. eL massive and tilted dorsally (Fig. 10A–B). Cheliceral teeth poorly developed (Fig. 10C). Patella III with abundant small stout spines. ....*D. dissimilis*	
	Tip of DD poorly developed. eL moderate and rotated retrolaterally (Fig. 15A–C). Cheliceral teeth moderately developed (Fig. 15D). Patella III without spines...*D. portisancti*	
7	Tip of IS with an AR (Figs 6B, H, 19B).	8
	Tip of IS without an AR (Figs 12B, H, 13B, 17B, 18B).	9
8	DD roughly twice as long as T. C digitiform (Fig. 6B, H). Species from Madeira or Desertas. ....*D. coiffaiti*	
	DD roughly 1.5 times longer than T. C slender. A sclerotized sickle-shaped ridge between the AR and L (Fig. 19B). Species from Desertas. .... *D. teixeirai*	
9	IS with a massive ISDA. eL sclerotized, claw-shaped (Fig. 18A–B). D wide and blunt (Fig. 18C). Species from Desertas...*D. sandrae*	
	Tip of IS different, either with a pointed, thin ISDA (Fig. 17B) or a C. eL different (Figs 12A–B, G–H, 13A–B, 17A–B). D different (Figs 12C, I, 13C, 17C). Species from Desertas or Madeira.	10
10	IS with a pointed, thin ISDA. eL rod-shaped (Fig. 17A–B). Distal tooth trapezoidal (Fig. 17C). Species from Desertas. .... *D. recondita*	
	IS with a C and a LF. eL lanceolate (Figs 12A–B, G–H, 13A–B). Distal tooth triangular (Figs 12C, I, 13C). Species from Madeira or Desertas..	11
11	All teeth of similar size (Fig. 12C, I). Chelicerae without bulge (Fig. 22B, D). Species from Madeira. ....*D. diversa*	
	D smaller than B and M (Fig. 13C). Chelicerae with notorious bulge (Fig. 23B). Species from Desertas. ....*D. exigua*	
12	S with arms directed posteriorly (Deeleman-Reinhold & Deeleman, 1988: p. 159, Figs 25–27). ....*D. crocata*	
	S with arms directed anteriorly, laterally or dorsally (Figs 6D–F, 10D–G, 12D–F, 13D–F, 14D–F, 15E–G, 16D–F, 17D–F, 18D–F, 19D–I, 20A–C)..	13
13	Species from Porto Santo..	14
	Species from Madeira or Desertas..	17

14	S juxtaposed onto AVD (Figs 10D–G, 15E–G). D at most in the midpoint of cheliceral furrow (Figs 10C, 15D)... 15
	S inserted onto VA or AVD through a constricted sclerotized neck (Figs 14D–F, 16D–F). D in the distal half of cheliceral furrow (Figs 14C, 16C)... 16
15	S with bilobed SD dorsally. DA without wing-shaped lateral projections (Fig. 10D–G). Cheliceral teeth poorly developed (Fig. 10C). Patella III with abundant small stout spines..............*D. dissimilis*
	S without lobed SD. DA with wing-shaped projections (Fig. 15E–G). Cheliceral teeth moderately developed (Fig. 15D). Patella III without spines. ....*D. portisancti*
16	DA narrow. S compact, subtriangular, with tips projected dorsally (Fig. 14D–F). D robust, slightly larger than B (Fig. 14C)... *D. isambertoi*
	DA wide. S transverse, oval, with tips projected laterally (Fig. 16D–F). D subequal or slightly smaller than B (Fig. 16C). .... *D. precaria*
17	Prosoma length > 7 mm. D distinctly larger than M and B....................................*D. titanica*
	Prosoma length < 7 mm. D subequal or smaller than M and B. 18
18	AVD absent, or, at most, reduced to a small ventral triangular projection. S with a small slit-shaped or oval SD (Figs 6D–F, 19D–I).. 19
	AVD present. S without SD (Figs 12D–F, 13D–F, 17D–F, 18D–F).. 20
19	AVD absent. S with a slit-shaped SD dorsally (Fig. 6D–F)..*D. coiffaiti*
	AVD reduced to a small ventral sclerotization, which may be hard to discern. S with an oval SD dorsally (Fig. 19D–I). ....*D. teixeirai*
20	VA triangular in ventral view (Fig. 17D). D trapezoidal (Fig. 17C). *D. recondita*
	VA roughly quadrangular in ventral view (Fig. 12D, 13D, 18D). D triangular (Figs 12C, 13C) or wide, blunt (Fig. 18C).. 21
21	AVD clearly separated from VA (Fig. 18F). D wide, blunt (Fig. 18C). ....*D. sandrae*
	AVD juxtaposed to VA (Figs 12F, 13F). D triangular, small (Fig. 13C).. 22
22	Juxtaposition of DA and VA without constriction (Fig. 12E). All teeth of similar size (Fig. 12C, I). Chelicerae without bulge (Fig. 22B, D). Species from Madeira. ....*D. diversa*
	Juxtaposition of DA and VA with constriction (Fig. 13E). D smaller than B and M (Fig. 13C). Chelicerae with notorious bulge (Fig. 23B). Species from Desertas..*D. exigua*

DESCRIPTIONS

FAMILY DYSDERIDAE C.L. KOCH, 1837

GENUS *DYSDERA* LATREILLE, 1804

DYSDERA COIFFAITI DENIS, 1962

(FIGS 6, 21A–B, 27, 37A)

Dysdera longibulbis Denis, 1962: pp 24–25, figs 4–6. Holotype ♂ from Santo da Serra, Madeira; coll. 21.IV.1957, leg. Vandel *et al.*, stored at MNHNP, collection number AR5828. Examined (Fig. 6G–I). New synonym.

Holotype: 1 ♂ (left palp missing), 32.76642 °N 16.94775 °W, Caldeirão do Inferno (Denis refers to "Caldeira" do Inferno, while the vial label refers to "Caldeiro Juferno", respectively, therefore we find it necessary to present the correct locality name), Madeira, Portugal, coll. 25–30.IV.1957 (Denis refers to

the sampling period between 25th and 29th, we retain the largest period, cited on the vial label), leg. Vandel *et al.*, stored at MNHNP, collection number AR5855. Examined.

Paratypes: Madeira: São Vicente, 2 ♀♀ (MNHNP AR3459, one with extracted vulva, used for redescription), coll. 4.V.1957, (no collection method), leg. Vandel *et al*. Examined.

Additional material examined: Bugio: Planalto Sul, 2 ♀♀ (CRBA002500: pk100, CRBA002501: pk101), 28.VI.2012, hand collecting, leg. I. Silva, 1 juvenile (CRBALC0114: lc071), 13.IV.2017, hand collecting, leg. L. Crespo; Deserta Grande: Pedregal, 2 ♀♀ (CRBA002562: pk678, CRBA002563: pk679), 16.IV.2015, hand collecting, leg. I. Silva & D. Teixeira; Planalto Sul, 1 ♀ (CRBA002539: pk80), 18.IV.2011, hand collecting, leg. L. Crespo, I. Silva & P. Cardoso; Rocha do Barbusano, 2 ♀♀ (NMH001599: k525,
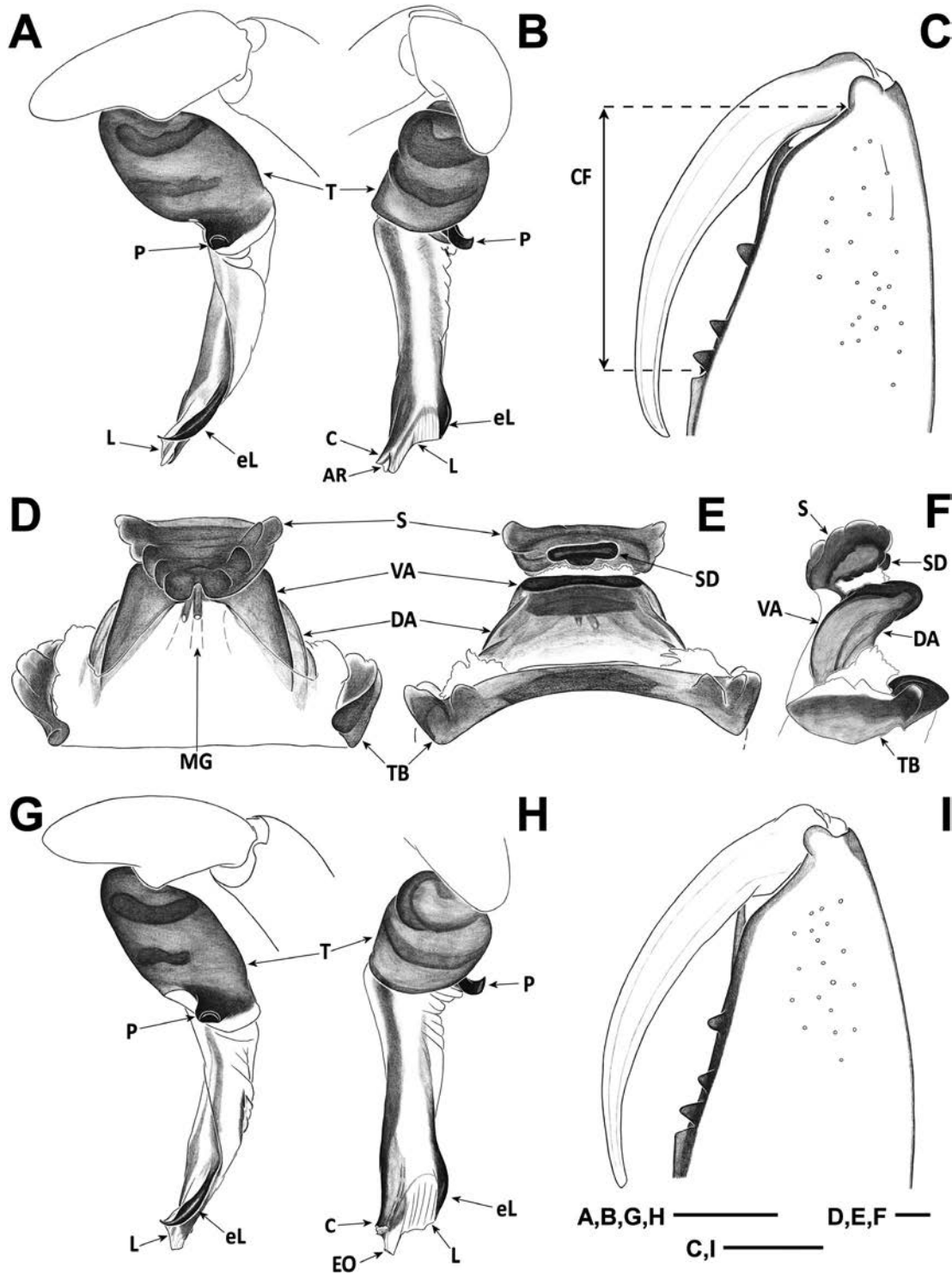
Figure 6. *D. coiffaiti*. A–C, holotype male: (A) mirrored image of right palp, retrolateral; (B) mirrored image of right palp, frontal; (C) mirrored image of right chelicera, ventral. D–F, female paratype (MNHNP AR3459); (D) vulva, ventral; (E) vulva, dorsal; (F) vulva, lateral. G–I, *D. longibulbis*: (G) mirrored image of right palp, retrolateral; (H) mirrored image of right palp, frontal; (I) mirrored image of right chelicera, ventral. Scale bars: A–C, G–I = 0.5 mm; D–F = 0.1 mm. Abbreviations, male palp: AR, arch-like ridge; C, crest; CF, cheliceral furrow; eL, external margin of lateral sheet; EO, embolus opening; L, lateral sheet; P, posterior apophysis; T, tegulum. Abbreviations, female vulva: DA, dorsal arch; MG, medial groove; S, spermatheca; SD, spermatheca diverticulum; TB, transversal bar; VA, ventral arch.

37

NMH001600: k527), 31.X.2009, leg. D. Hernández, 1 ♂ (CRBA002541: pk82), 1 ♀ (CRBA002540), 20.IV.2011, leg. L. Crespo, I. Silva & P. Cardoso, 1 ♂ (CRBALC0210: lc129), 8.IV.2017, hand collecting, leg. L. Crespo, 1 ♀ (CRBALC0211: lc130), 2 juveniles (CRBALC0112: lc069, CRBALC0113: lc070), 9.IV.2017, hand collecting, leg. L. Crespo; Vale da Castanheira (S), 1 ♀ (CRBALC0584), 25.III.2018, hand collecting, leg. L. Crespo; Rocha do Barbusano (S), 4 ♂♂ (CRBALC0076: lc048, CRBALC0106: lc063, CRBALC0107: lc064, CRBALC0108: lc065), 1 ♀ (CRBALC0109: lc066), 8 juveniles (CRBALC0078: lc050, CRBALC0081: lc053, CRBALC0082: lc054, CRBALC0084: lc056, CRBALC0101: lc058, CRBALC0102: lc059, CRBALC0104: lc061, CRBALC0105: lc062), 10.IV.2017, hand collecting, leg. L. Crespo & I. Silva; Madeira: near water deposit of Paúl da Serra, 1 ♀ (CRBALC0737), 21.VIII.2016, hand collecting, leg. I. Silva; Caramujo, 1 juvenile (CRBALC0009), 23.VIII.2016, hand collecting, leg. I. Silva, 1 ♀ (CRBALC0005: lc005), 27.VIII.2016, hand collecting, leg. L. Crespo & I. Silva, 1 ♂ (CRBALC0673), 1 ♀ (CRBALC0621), 06.IV.2018, hand collecting, leg. L. Crespo & A. Bellvert; Chão da Ribeira, 1 ♂ (MZB 2019-1961: pk88), 1 ♀ (CRBA002548: pk89), 1.V.2011, hand collecting, leg. L. Crespo, I. Silva & P. Cardoso; Chão dos Louros, 1 ♂ (MZB 2019-1960: k522), 1 ♀ (MZB 2019-1959: k530), 6.XI.2009, hand collecting, leg. D. Hernández, 2 ♂♂ (CRBA002549: pk90, LCPC: pk91), 12.II.2010, hand collecting, leg. I. Silva; Fajã da Nogueira, 1 ♀ (CRBALC0479: lc143), 5.IV.2017, hand collecting, leg. L. Crespo; Fanal, 1 ♀ (FMNH KN.17855: pk92), 11.XII.2011, hand collecting, leg. I. Silva, 3 ♂♂ (FMNH KN.17854: pk93, CRBA002553: pk94, MMF 47910: pk96), 1 ♀ (MZB 2019-1962: pk95), 1.V.2011, hand collecting, leg. L. Crespo, I. Silva & P. Cardoso; Fanal (I), 1 ♀ (CRBALC0478: lc142), 3.IV.2017, leg. P. Oromí; Fanal (II), 1 ♂ (CRBALC0023: lc023), 5 juveniles (CRBALC0024: lc024, CRBALC0025: lc025, CRBALC0026: lc026, CRBALC0027: lc027, CRBALC0028: lc028), 7–21.VIII.2016, pitfall trapping, leg. P. Borges *et al.*; Fanal (III), 1 juvenile (CRBALC0029: lc029), 7.VIII.2016, hand collecting, leg. J. Malumbres-Olarte; Fanal (IV), 1 ♂ (CRBALC0030: lc030), 1 juvenile (CRBALC0031: lc031), 8–22. VIII.2016, pitfall trapping, leg. P. Borges *et al.*; Fanal (V), 1 ♂ (CRBA002508: pk225) and 2 ♀♀ (CRBA002504: pk222, LCPC: pk226), 1.V.2012, hand collecting, leg. A. Serrano *et al.*; Funduras (I), 3 ♂♂ (CRBA3044: lc149, CRBA3048: lc152, CRBA3049: lc151), 1 ♀ (CRBA3046: lc150), 2.IV.2017, hand collecting, leg. M. Arnedo, L. Crespo & P. Oromí, 3 ♂♂ (CRBALC0611, CRBALC0612, CRBALC0675), 4 ♀♀ (CRBALC0624, CRBALC0638, CRBALC0674, CRBALC0676), 6.IV.2018, hand collecting, leg. L. Crespo & A. Bellvert;

Funduras (II), 1 ♀ (CRBALC0032: lc032), 5.VIII.2016, hand collecting, leg. L. Crespo, 1 ♂ (CRBALC0736), 2 ♀♀ (CRBALC0006: lc006, CRBALC0011: lc011), 19.VIII.2016, hand collecting, leg. L. Crespo & I. Silva; Galhano, 1 ♀ (CRBALC0477: lc141), 3.IV.2017, hand collecting, leg. P. Oromí; Ginjas, 1 juvenile (CRBALC0735), 23.VIII.2016, hand collecting, leg. L. Crespo; Levada dos Cedros (Fanal), 1 ♂ (ZMUC), 8.III1994, leg. Bjørn & Damgaard; Levada dos Tornos, 1 ♀ (MMF 47909: pk221), 2.V.2012, hand collecting, leg. A. Serrano *et al.*; Montado dos Pessegueiros, 3 ♀♀ (CRBALC0222: lc138, CRBALC0484: lc146, CRBALC0485: lc147), 28.III.2017, hand collecting, leg. L. Crespo & I. Silva, 1 ♀ (CRBA3061: lc156), 1 juvenile (CRBALC0457: lc139), 31.III.2017, hand collecting, leg. L. Crespo, M. Arnedo & P. Oromí, 1 ♀ (CRBALC0625), 4 juveniles (CRBALC0640, CRBALC0644, CRBALC0647, CRBALC0695), 4.IV.2018, hand collecting, leg. L. Crespo & A. Bellvert; Paúl da Serra, 2 ♀♀ (CRBA002556: pk97, CRBA002557: pk98), 26.II.2012. hand collecting, leg. I. Silva, 1 ♀ (CRBALC0482: lc145), 2 juveniles (CRBALC0475, CRBA3043: lc148), 28.III.2017, hand collecting, leg. L. Crespo & I. Silva; Queimadas, 1 ♂ (CRBALC0033: lc033), 3 ♀♀ (CRBALC0001: lc001, CRBALC0003: lc003, CRBALC0004: lc004), 4 juveniles (CRBALC0008: lc008, CRBALC0034: lc034, CRBALC0035: lc035, CRBALC0036: lc036), hand collecting, leg. L. Crespo; Ribeiro Bonito (I), 1 juvenile (CRBALC0037: lc037), 4.VIII.2016, hand collecting, leg. L. Crespo; Ribeiro Bonito (II), 1 juvenile (CRBALC0038: lc038), 4.VIII.2016, hand collecting, leg. F. Pereira; Ribeiro Bonito (III), 1 juvenile (CRBALC0039: lc039), 4–18. VIII.2016, pitfall trapping, leg. P. Borges *et al.*; Santo da Serra, 1 ♀ (CRBALC0002: lc002), 1 juvenile (CRBALC0738), 19.VIII.2016, hand collecting, leg. L. Crespo; trail from Paúl da Serra to Montado dos Pessegueiros, 3 ♂♂ (CRBA3058: lc153, CRBA3059: lc154, CRBA3060: lc155), 2 ♀♀ (CRBA3062: lc157, CRBA3063: lc158), 31.IV.2017, hand collecting, leg. L. Crespo, M. Arnedo & P. Oromí.

Diagnosis: D. coiffaiti males can be diagnosed from all other Madeiran *Dysdera* by: the C, digitiform, prolaterally projected (Figs 6B, 27A–C). Females are distinguished from other Madeiran *Dysdera*, except *D. precaria* and *D. teixeirai*, by: the AVD, absent (Fig. 6D, F); it can be differentiated from *D. precaria* and *D. teixeirai* by: the SD, small, slit-like (Fig. 6E).

Redescription – male holotype: (Figs 6A–C, 21A). Carapace length 4.75; maximum width 4.08; minimum width 3.13. Carapace reddish-brown, foveate at borders, anteriorly slightly rugose, posteriorly smoother. Frontal border roughly rounded, 3 wide;

anterior lateral borders parallel; lateral borders rounded; posterior margin straight, moderately wide. AME 0.28, oval; PLE 0.28, oval; PME 0.23, rounded; AME separated from anterior border by less than their diameter; AME separated from one another by less than their diameter; AME touching PLE; PME separated from PLE by roughly one-third of PME diameter; PME touching. Labium trapezoid, with base wider than distal part, as long as wide at base; distal part concave. Sternum reddish-brown, wrinkled, with scattered setae. Chelicerae (Fig. 6C) 2.72 long, about half of carapace length in dorsal view, straight, dorsolaterally and ventrally slightly wrinkled; dorsally and prolaterally with lightly sclerotized piliferous granulations; fang 2.35 long. Cheliceral furrow ~53% of length of basal segment, armed with three teeth and basal lamina, B = D > M; all teeth triangular, B close to lamina, M closer to B than D, D situated in the distal half of cheliceral furrow. Anterior legs and palp orange, posterior legs yellow. Lengths: fe1 4.08; pa1 2.58; ti1 3.6; me1 3.56; ta1 0.82; total 14.63; fe2 3.64; pa2 2.34; ti2 3.22; me2 3.3; ta2 0.82; total 13.32; fe3 2.94; pa3 1.72; ti3 1.9; me3 2.66; ta3 0.74; total 9.95; fe4 3.64; pa4 2.08; ti4 2.86; me4 3.4; ta4 0.82; total 12.79; relative length: 1 > 2 > 4 > 3; fe palp 2.46; pa palp 1.35; ti palp 1.04; ta palp 1.09; total 5.94. Spination: ti3d proximal 1.0.0, distal 1.0.0. Palpal coxae with lightly sclerotized piliferous granulations. Legs covered with setae, especially on tibiae, metatarsi and tarsi. Ventral setae of anterior metatarsi with sclerotized base. Metatarsi III and IV ventrally with dense tuft of setae in distal section. Claws with nine to ten teeth. Abdomen 6.22 long, cream-coloured, cylindrical; abdominal dorsal setae short, 0.02–0.03 long, thin, apically blunt, uniformly distributed. Male copulatory bulbus (Fig. 6A–B): T shorter than DD, external border sloped backwards. DD bent anteriorly in lateral view, more or less 30 °. IS longer and thicker than ES, uniformly sclerotized. ES more sclerotized distally. C present, digitiform, with tip projected prolaterally. AR present, small. L present, with eL sclerotized, lanceolate. P claw-shaped, fused to T through a wide sclerotized base, directed to retrolateral side, lateral length one-quarter of width of T in frontal view. Ridge present, not expanded, parallel to T. Remark: a small undetermined needle-shaped artifact is visible, emerging from DH below P.

Female paratype (MNHNP AR3459): (Fig. 6D–F). All characters as in male except: carapace length 5.19; maximum width 4.28; minimum width 3.09; AME separated from anterior border by half their diameter. Chelicerae 2.78 long; fang 2.56 long. Leg lengths: fe1 4.13; pa1 2.69; ti1 3.56; me1 3.44; ta1 0.86; total 14.67; fe2 3.64; pa2 2.4; ti2 3.13; me2 3.2; ta2 0.84; total 13.21; fe3 3.03; pa3 1.78; ti3 1.9; me3 2.64; ta3 0.78; total

10.13; fe4 3.84; pa4 2.21; ti4 2.86; me4 3.44; ta4 0.88; total 13.23; fe palp 2.48; pa palp 1.3; ti palp 0.95; ta palp 1.32; total 6.05. Abdomen 9 long. Vulva (Fig. 6D–F): PD oval. DA separated from VA. DA roughly twice as wide as long, anteriorly truncated. DF wide in dorsal view. MF moderately developed, visible only slightly ventrally or posteriorly. VA roughly as wide as long, membranous except in its anterior section, which is sclerotized and shaped as a quadrangle with rounded corners. AVD absent. Insertion of S projected onto VA through a short neck, S subtriangular in ventral view, with arms short and tips projected dorsally, with a slit-like diverticulum dorsally. Remark: two artefacts with an apparent duct aspect are seen attached to the insertion of the S.

Intraspecific variation: Male carapace varies from 4.1 to 5.63 in length and 3.06 to 4.48 in width, and female carapace from 4.6 to 5.38 in length and 3.58 to 4.33 in width. However, we observed that specimens found in Deserta Grande and Bugio are distinctly smaller than those found in Madeira (male and female prosoma length respectively range from 4.1 to 4.85 and 4.6 to 4.88 against 4.75 to 5.34 and 5 to 5.38 in the Madeira population), and that in addition male specimens from Deserta Grande present a proportionally longer DD in regard to the T. We substantiated our observations with additional measurements and a Mann-Whitney test for prosoma length (in a universe of 34 observations, 17 from each island, $U1 = 42.5 < U'^{(17,17)} = 87$, see also Fig. 7). Cheliceral length varies from 2.13 to 3.52 in males, and 2.05 to 3.24 in females. Teeth can vary slightly in size, so that all teeth are of equal size or B > M = D; after revising part of the abundant materials of *D. coiffaiti* available
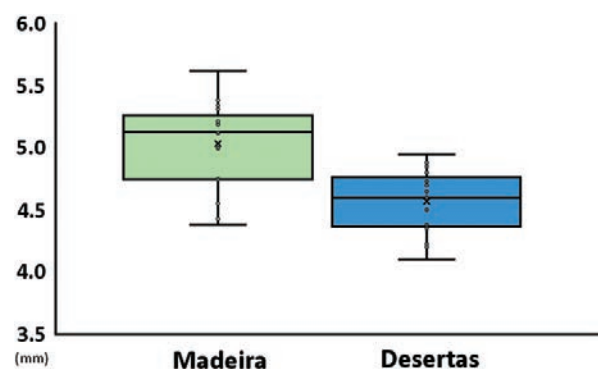

Figure 7. Box plot with the size distribution for the populations of *D. coiffaiti*. The *y* axis represents prosoma length measurements (*N* = 17, for both cases) and *x* separates the populations from Madeira island (left) and Desertas (right). Whiskers: minimum and maximum; boxes: limits of the first quartile, median and third quartile; crosses: mean markers.

for our study, we report that the left chelicera of the holotype male presents an abnormal conformation of teeth, with M juxtaposed to B. Spination variability: ti3d proximal 1.0.0, distal 1.0.0; ti4d proximal 0.0.0–1, distal 0–1.0.0–1; ti4v proximal 0–1.0.0, distal 0.0.0. We removed additional vulvas from our materials, and S can be found with more extended arms than those illustrated (Fig. 6D–F).

Distribution: This species is known from many locations in Madeira island, Deserta Grande and one location in Bugio, a smaller islet south of Deserta Grande (Figs 8–9).

Habitat: D. coiffaiti occurs in diverse habitats. In Madeira island, it can be found in the bark of tree trunks or under stones in habitats ranging from humid laurel forest, to *Erica* scrubland, to secondary forests. In Desertas, it can be found under stones or in sandstone crevices in dry, arid slopes or plateaus with few xerophytic herbs and shrubs.

Conservation: Given its observed range in Madeira island, coupled with the presence of native forest throughout the north coast of the island, we can assume that as long as efforts are made to maintain the patches of laurel forest, we will be able to find large populations of *D. coiffaiti* [see detailed conservation profile in Cardoso *et al.* (2017)]. The populations that live in Deserta Grande and Bugio inhabit a completely different habitat, devoid of any tree cover.

The presence of exotic species in Deserta Grande may have a two-fold effect. First, the introduction of the synanthropic species *Dysdera crocata* C.L. Koch, 1838 might contribute through competitive interactions to the ecological displacement of this endemic species (Crespo *et al.*, 2013), and second, vertebrate and plant species introduced by humans (e.g. goats, rabbits, *Nicotiana glauca* Graham, *Phalaris aquatica* L.) have severely altered the native communities of Deserta Grande and we can only speculate to which extent the endemic species can be resilient to habitat change and disturbance.

Remarks: D. coiffaiti and *D. longibulbis* were described as distinct species in the same publication (Denis, 1962), both using the left palps, which are now missing from the MNHNP vials. After comparing the types, it was readily apparent that both specimens belong to the same taxon. We here propose *D. longibulbis* as a junior synonym of *D. coiffaiti*. Although both species were described in the same publication, we selected *D. coiffaiti* as the name with priority, because the type locality of *D. coiffaiti*, Caldeirão do Inferno, is a site where native laurel forest can still be found and where it is currently relatively easy to find populations of this species. Conversely, no native forest is left at the type locality of *D. longibulbis*, Santo da Serra, and specimens of the latter population are not as easy to find. In addition, the only available male palp for *D. longibulbis* presents a broken tip of the IS (Fig. 6H), obscuring its interpretation.

Figure 8. Map of Madeira island, with the sampling localities. *D. coiffaiti* = circle; *D. diversa* = triangle. Dotted areas represent large sites from where several specimens were collected. Map provided by DROTA.

Figure 9. Map of the Desertas islands, with the sampling localities. *D. coiffaiti* = circle; ***D. exigua* sp. nov.** = square; ***D. recondita* sp. nov.** = rhombus; ***D. sandrae* sp. nov.** = pentagonal star; ***D. teixeirai* sp. nov.** = hexagon. Dotted areas represent large sites from where several specimens were collected. Map provided by DROTA.

DYSDERA DISSIMILIS CRESPO & ARNEDO, **SP. NOV.**

(Figs 10, 21C–D, 28, 37B)

urn:lsid:zoobank.org:act:176FB691-1D07-4A02-ABBC-3AAAA5B1BBBC

Holotype: 1 ♂, 33.08518 °N 16.32364 °W, Pico do Facho (N), Porto Santo, Portugal, coll. 22.IV.2017, hand collecting, leg. L. Crespo, stored at MZB, collection number 2019-1947, DNA code lc134.

Paratypes: Porto Santo: Pico Ana Ferreira, 1 ♂ (FMNH KN.17861: lc085), 2 ♀♀ (MZB 2019-1950: lc086, CRBALC0131: lc088), 20.IV.2017, hand collecting, leg. L. Crespo & I. Silva; Pico do Castelo, 1 ♂ (MZB 2019-1949: lc076) and 1 ♀ (MZB 2019-1948: lc077), 17.IV.2017, hand collecting, leg. L. Crespo & I. Silva; Pico do Facho, 1 ♂ (CRBALC0146: lc100), 22.IV.2017, hand collecting, leg. L. Crespo; Pico da Juliana, 1 ♂ (MMF 47916: pk243) and 1 ♀ (MMF 47917), 23.IV–7.V.2011, pitfall trapping, leg. A. Serrano *et al.*; Terra-Chã (Pico Branco), 1 ♀ (FMNH KN.17862: lc135), 21.IV.2017, hand collecting, leg. L. Crespo & I. Silva.

Additional material examined: Pico Ana Ferreira, 1 ♂ (LCPC: lc089) and 1 ♀ (CRBALC0130: lc087) and 7 juveniles (CRBALC0138: lc095, CRBALC0139: lc096, CRBALC0140: lc097, CRBALC0141: lc098, CRBALC0142: lc099, CRBALC0166: lc102, CRBALC0168: lc104), 20.IV.2017, hand collecting, leg. L. Crespo & I. Silva; Pico do Castelo, 2 ♀♀ (CRBA002529: pk307, LCPC: pk308), 1.VIII.2013, hand collecting, leg. I. Silva, 1 juvenile (CRBALC0122: lc079), 17.IV.2017, hand collecting, leg. L. Crespo & I. Silva, 1 juvenile (CRBALC0679), 8.IV.2018, hand collecting, leg. L. Crespo & A. Bellvert; Pico do Facho, 1 ♂ (CRBALC0145: lc165), 2 juveniles (CRBALC0184: lc119, CRBALC0185: lc120), 22.IV.2017, hand collecting, leg. L. Crespo, 1 juvenile (CRBALC0660), 9.IV.2018, hand collecting, leg. L. Crespo & A. Bellvert; Pico do Facho (N), 3 juveniles (CRBALC0186: lc121, CRBALC0187: lc122, CRBALC0189: lc124), 22.IV.2017, hand collecting, leg. L. Crespo; Pico da Juliana, 1 juvenile (CRBA002522: pk240), 23.IV–7.V.2011, pitfall trapping, leg. A. Serrano *et al.*, 1 juvenile (CRBALC0619), 10.IV.2018, hand collecting, leg. L. Crespo & A. Bellvert; Terra-Chã (Pico Branco), 1 ♂ (CRBALC0169: lc105), 21.IV.2017, hand collecting, leg. L. Crespo & I. Silva.

Etymology: The specific epithet, from the Latin adjective *dissimilis*, unlike, different, refers to a combination of traits, such as short and stout legs, densely spinate posterior legs and strongly reduced cheliceral teeth, that make this species different from all others in Madeira.
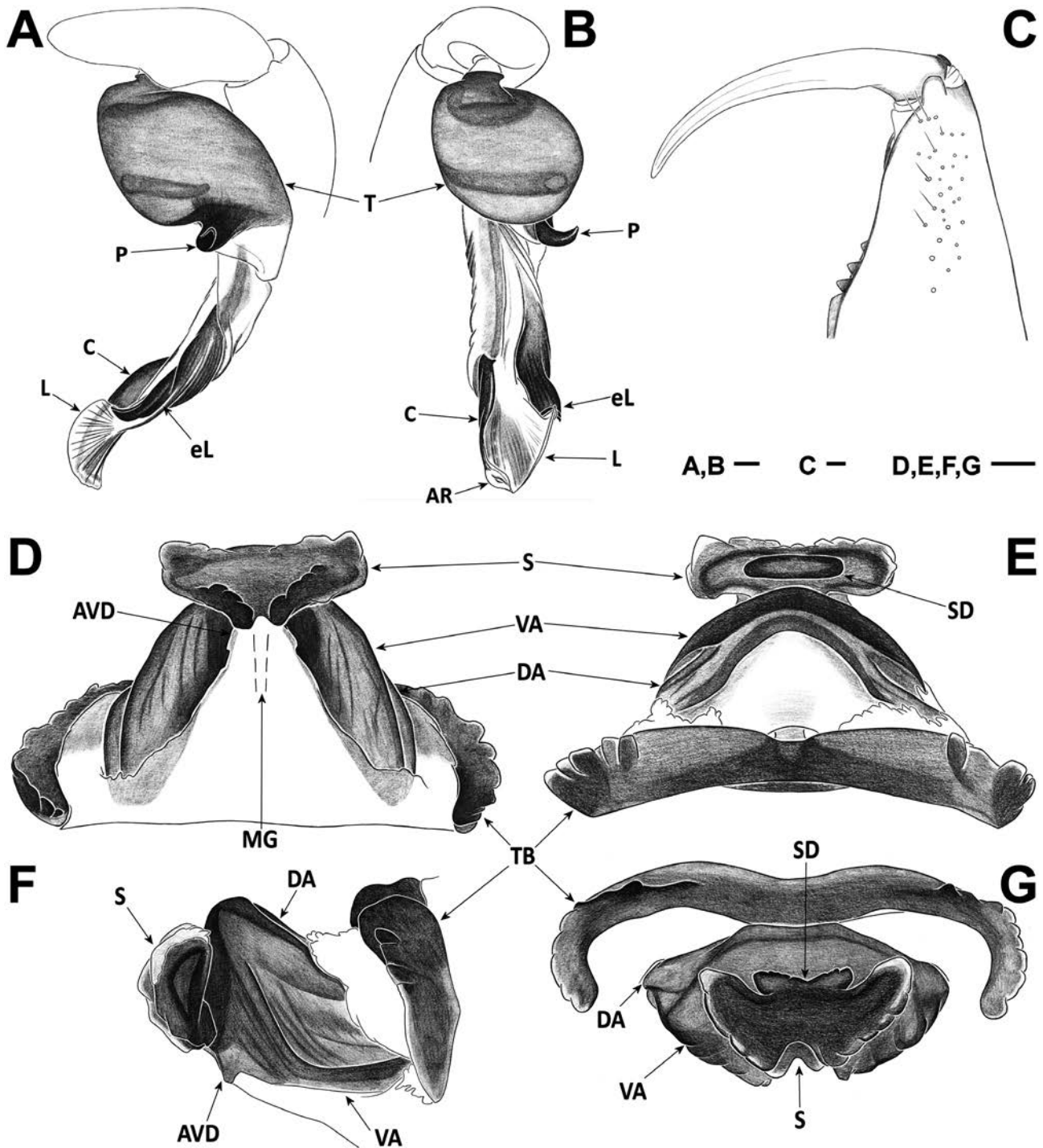
41

Figure 10. *D. dissimilis* **sp. nov.** A–C, holotype male: (A) left palp, retrolateral; (B) left palp, frontal; (C) left chelicera, ventral. D–G, female paratype (MZB 2019-1948): (D) vulva, ventral; (E) vulva, dorsal; (F) vulva, lateral; (G) vulva, anterior. Scale bars = 0.1 mm. Abbreviations, male palp: AR, arch-like ridge; C, crest; eL, external margin of lateral sheet; L, lateral sheet; P, posterior apophysis; T, tegulum. Abbreviations, female vulva: AVD, additional ventral diverticulum; DA, dorsal arch; MG, medial groove; S, spermatheca; SD, spermatheca diverticulum; TB, transversal bar; VA, ventral arch.

Diagnosis: D. dissimilis can be diagnosed from all other Madeiran species by the combination of the following somatic characters: reduced size of cheliceral teeth (Fig. 10C) and dense spination in posterior legs. Additionally, males by: the well developed, bent, striate eL and the C, bent (Fig. 10A–B); females by: the DA and VA, well developed and the presence of a bilobed SD (Fig. 10D–G).

Description – male holotype: (Figs 10A–C, 21C–D). Carapace length 4; maximum width 3.48; minimum width 2.38. Carapace blackish-brown, foveate at borders, smooth, with several small depressions radiating from the larger fovea. Frontal border roughly rounded, 2.15 wide; anterior lateral borders slightly divergent; lateral borders divergent, rounded around maximum width point to posterior margin; posterior margin straight, short. AME 0.18, rounded; PLE 0.2, oval; PME 0.16, oval; AME separated from anterior border by their diameter; AME separated from one another by their diameter; AME touching PLE; PME separated from PLE by roughly one-third of PME diameter; PME almost touching. Labium trapezoid, with base wider than distal part, longer than wide at base; distal part concave. Sternum brown, anteriorly darker, wrinkled, with setae. Chelicerae (Fig. 10C) 1.96 long, about two-fifths of carapace length in dorsal view, straight, smooth; fang 1.28 long. Cheliceral furrow ~51% of length of basal segment, armed with three teeth and basal lamina, B = M > D; all teeth triangular, B close to lamina, all teeth roughly equidistant. Except for coxae and femora I, brown, all legs greenish-brown. Lengths: fe1 2.88; pa1 1.97; ti1 2.03; me1 2.09; ta1 0.62; total 9.58; fe2 2.59; pa2 1.87; ti2 1.84; me2 2; ta2 0.59; total 8.89; fe3 2.35; pa3 1.36; ti3 1.28; me3 2.15; ta3 0.66; total 7.8; fe4 3; pa4 1.75; ti4 1.94; me4 2.88; ta4 0.72; total 10.29; relative length: 4 > 1 > 2 > 3; fe palp 2; pa palp 1.16; ti palp 0.9; ta palp 1.04; total 5.1. Spination: pa3d medial-proximal 1.0.0, medial-distal 1.0.0, distal 2.2.1; pa3v distal 1.0.0; ti3d proximal 2.2.1, medial-distal 1.2.0, distal 1.0.1; ti3v proximal 1.1.0, medial-proximal 0.1.0, distal 1.0.0; pa4d distal 1.0.1; ti4d proximal 1–2.2.1, medial-distal 0.2.0–1, distal 1.0.1; ti4v proximal 1.2–3.1, medial-distal 0.1–2.0, distal 0.0.1. Palpal coxae with moderately sclerotized piliferous granulations. Legs covered with setae, especially on tibiae, metatarsi and tarsi. All tibiae with dorsal dense patch of short, moderately thick, setae. All metatarsi with small dorsal distal patch of setae, III and IV ventrally also with dense tuft of setae in distal section. Claws with six to eight teeth. Abdomen 3.6 long, cream-coloured, cylindrical; abdominal dorsal setae short, 0.03–0.07 long, tapered, uniformly distributed. Male copulatory bulbus (Fig. 10A–B): T roughly half length of DD, external border sloped backwards. DD bent anteriorly

in lateral view, more or less 45 °. IS longer than ES, basally and medially moderately developed, well developed terminally. ES well developed only medially and terminally. C present, sclerotized, bent ventrally. LF absent. AR present, well developed. L present, with eL sclerotized, massive, striated and tilted dorsally at tip. P claw-shaped, fused to T, rotated to retrolateral side, lateral length one-third of width of T in frontal view. Ridge present, not expanded, parallel to T.

Female paratype (MZB 2019-1948): (Fig. 10D–G). All characters as in male except: carapace length 3.92; maximum width 3.26; minimum width 2.13; AME 0.17; PLE 0.16; PME 0.13; AME separated from anterior border by less than their diameter; AME almost touching PLE. Chelicerae 1.76 long; fang 1.56 long. All legs greenish-brown. Leg lengths: fe1 2.38; pa1 1.8; ti1 1.73; me1 1.82; ta1 0.54; total 8.27; fe2 2.25; pa2 1.72; ti2 1.58; me2 1.74; ta2 0.54; total 7.83; fe3 2.08; pa3 1.3; ti3 1.1; me3 1.9; ta3 0.6; total 6.98; fe4 2.75; pa4 1.6; ti4 1.82; me4 2.78; ta4 0.78; total 9.73; fe palp 1.52; pa palp 0.9; ti palp 0.64; ta palp 1.04; total 4.1. Spination: leg1, leg2 spineless; fe3 spineless, pa3d medial-proximal 1.0.0, medial-distal 1.0.1, distal 1.0.0; pa3v distal 1.0.0; ti3d proximal 3.2.1, medial-proximal 1.0.0, medial-distal 1.2.0, distal 1.0.1; ti3v proximal 1.2.0, distal 1.0.0; fe4d spineless; pa4d distal 1.0.1; ti4d proximal 1.2.2, medial-proximal 0.0–1.0, medial-distal 0–1.2.1, distal 1.0.1; ti4v proximal 1.2.1, medial-distal 0.1.0, distal 0–1.0.1. Claws with six to nine teeth. Abdomen 4.65 long; abdominal dorsal setae 0.07–1.2 long. Vulva (Fig. 10D–G): PD oval. DA separated from VA. DA roughly twice as wide as long, anteriorly domed and excavated, with striae laterally. DF wide in dorsal view. MF poorly developed, with no visible internal sclerotized plates ventrally. VA slightly wider than long, laterally well developed, projecting ventrally (see lateral view, Fig. 10F), with striae, and a well-defined membranous section leading to insertion of S. AVD present, reduced, shaped as a neck of a shirt, with triangular tips. Insertion of S projected onto AVD. S subtriangular in ventral view, with arms short, straight, tips projected dorsally, and a bilobed diverticulum posteriorly (see anterior view, Fig. 10G).

Intraspecific variation: Male carapace varies from 3.32 to 4 in length and 2.8 to 3.48 in width, female carapace from 3.76 to 4.55 in length and 2.91 to 3.72 in width. Cheliceral length from 1.5 to 1.96 in males, 1.63 to 2.3 in females. Spination variability: pa3d proximal 0.0.0, medial-proximal 1.0–1.0, medial-distal 1–2.0–1.0, distal 1–3.0–2.0–1; pa3v proximal 0.0.0, distal 1.0.0; ti3d proximal 1–3.0–3.0–1, medial-proximal 0–1.0–2.0–1, medial-distal 1.2.0–1, distal 1–2.0.0–1; ti3v proximal 0–1.1–2.0, medial-proximal 0–1.0–1.0–1,

distal 1.0.0; pa4d distal 1.0.1; ti4d proximal 1–2.1–2.1–2, medial-proximal 0.0–1.0, medial-distal 0–1.0–2.0–1, distal 1.0–2.0–1; ti4v proximal 1.2–3.1, medial-proximal 0.0–2.0–1, medial-distal 0.0–2.0, distal 1.0.0–1.

Distribution: This species is known from the summit of all the highest peaks of Porto Santo island: Pico do Facho (517 m), Pico Branco (450 m), Pico do Castelo (437 m), Pico da Juliana (447 m) and Pico Ana Ferreira (283 m) (Fig. 11).
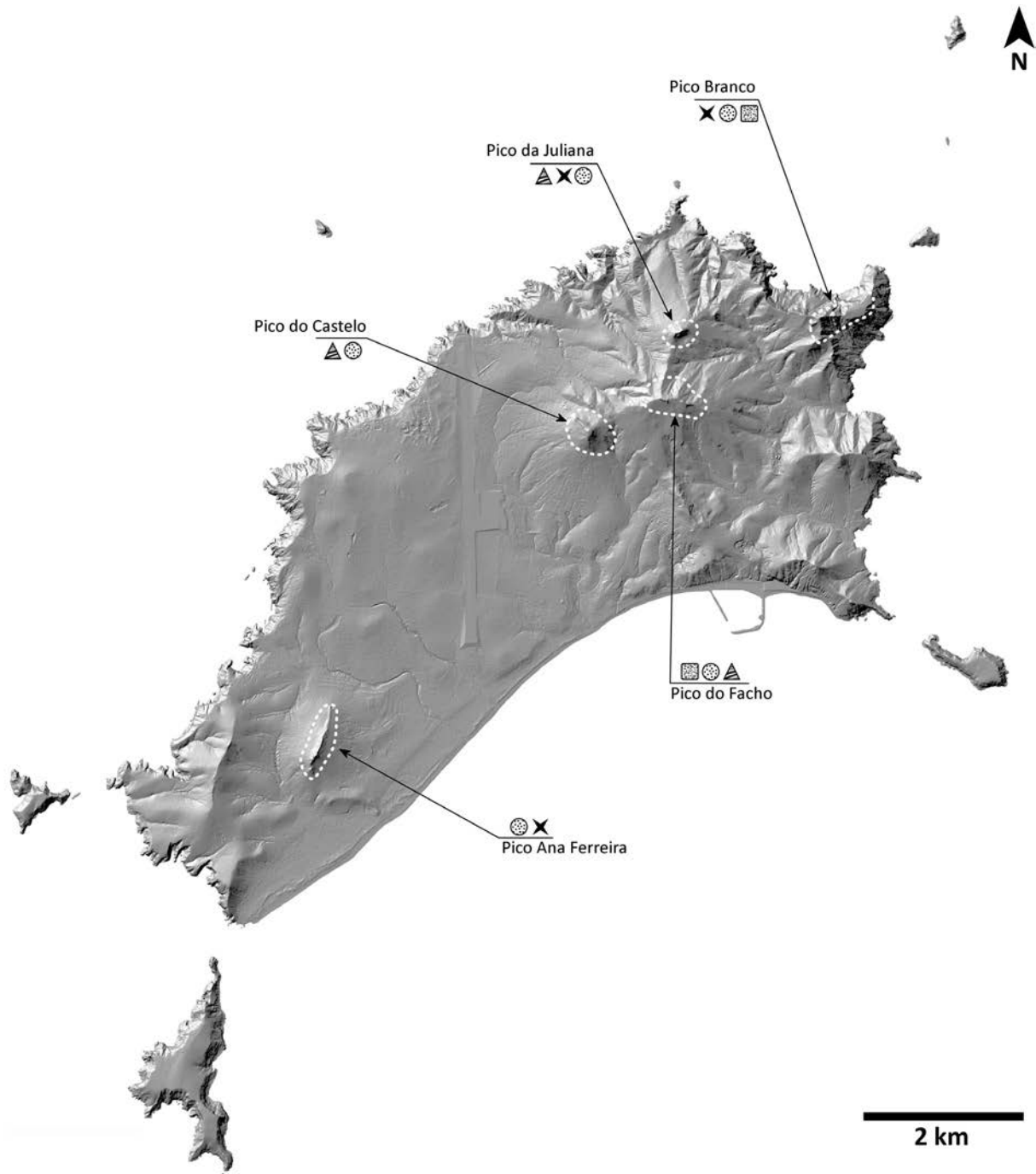

Figure 11. Map of Porto Santo and neighbouring islets, with the sampling localities. ***D. dissimilis* sp. nov.** = dotted circle; ***D. isambertoi* sp. nov.** = stripped triangle; ***D. precaria* sp. nov.** = four-pointed star; *D. portisancti* = patterned rounded square. Dotted areas represent large sites from where several specimens were collected. Map provided by DROTA.

Habitat: *D. dissimilis* occurs in the reduced areas of secondary forest in Porto Santo (43 km², maximum elevation of 517 m), composed mainly of *Cupressus macrocarpa* Hartw., *Juniperus turbinata* Guss., *Pinus* spp., occasionally with shrubland with dominant *Erica platycodon* (Webb & Berthel.) Rivas Mart. *et al.* There, it can be found under stones or in the bark of dead logs.

Conservation: Porto Santo has as an area of roughly 43 km², but if we sum the areas corresponding to the northern slopes of the mountains where *D. dissimilis* was found, we reach an extrapolated range of 0.52 km². This means that *D. dissimilis* and other endemics of Porto Santo are subsisting in a mosaic of islands within an island, threatened by both habitat loss and fragmentation.

DYSDERA DIVERSA BLACKWALL, 1862

(FIGS 12, 22, 29)

Dysdera vandeli Denis, 1962: pp 22–23, figs 1–3. Holotype ♂, 32.76642 °N 16.94775 ° W, Caldeirão do Inferno, Madeira (Denis refers to "Caldeira" do Inferno, while the vial label refers to "Caldeiro Juferno", respectively, therefore we find it necessary to present the correct locality name); coll. 25–29.IV.1957, leg. A. Vandel *et al.*, stored at MNHNP, collection number AR5843. Examined (Figs 12G–I, 22C–D). New synonym.

Holotype: 1 ♂ (no location), Madeira, Portugal, (no collection date), (no collection method), leg. H. Clark, stored at OUMNH (no collection number). Examined.

Additional material examined: Madeira: Caramujo, 1 ♀ (MMF 47902: pk223), 25.V–8.VI.2012, pitfall trapping, leg. A. Serrano *et al.*; Montado dos Pessegueiros, 1 ♂ (MMF 47903: pk224), 2–19.VI.2012, pitfall trapping, leg. A. Serrano *et al.*

Diagnosis: *D. diversa* differs from all other Madeiran *Dysdera*, except *D. exigua*, in males by: LF, short (Fig. 12B). *D. diversa* can be diagnosed from *D. exigua* by: chelicera more gracile, with more widely separated, equal teeth (Fig. 12C), in males, by: C, longer, LF, shorter (Figs 12A–B, 29A–C), in females by: the AVD, less developed (Fig. 12F).

Redescription – male holotype: (Figs 12A–C, 22A–B). Carapace length 3.46; maximum width 2.77; minimum width 1.8. Carapace dark brown, foveate at borders, anteriorly slightly rugose, posteriorly smooth. Frontal border roughly rounded, 1.74 wide; anterior lateral borders slightly convergent; lateral border rounded;

posterior margin straight, short. AME 0.15, rounded; PLE 0.17, oval; PME 0.15, rounded; AME separated from anterior border by less than their diameter; AME separated from one another by more than their diameter; AME touching PLE; PME almost touching PLE; PME almost touching. Labium trapezoid, with base wider than distal part, longer than wide at base; distal part concave. Sternum brown, wrinkled, without setae. Chelicerae (Fig. 12C) 1.46 long, about one-third of carapace length in dorsal view, slightly concave dorsally, dorsally and prolaterally with sparse sclerotized piliferous granulations; fang 1.16 long. Cheliceral furrow ~48% of the length of basal segment, armed with three teeth and basal lamina, B > M = D; all teeth triangular, B close to lamina, M closer to B than D, D situated in distal half of cheliceral furrow. Anterior legs and palp orange, posterior legs yellow. Lengths: fe1 2.44; pa1 1.62; ti1 2; me1 1.8; ta1 0.56; total 8.42; fe2 2.2; pa2 1.51; ti2 1.79; me2 1.76; ta2 0.54; total 7.8; fe3 1.8; pa3 1.1; ti3 1.12; me3 1.52; ta3 0.48; total 6.02; fe4 2.31; pa4 1.32; ti4 1.66; me4 2.06; ta4 0.56; total 7.92; relative length: 1 > 4 > 2 > 3; fe palp 1.61; pa palp 0.91; ti palp 0.82; ta palp 0.77; total 4.11. Spination: ti3d proximal 1.1.1, distal 1.0.1; ti3v proximal 1.1.0, distal 1.0.0; fe4d 2–3 spines, 1–3 rows; ti4d proximal 1.0–1.1–2, medial-proximal 0.0–1.0, medial-distal 0.0–1.0, distal 1.0–1.1; ti4v proximal 1.1–2.1, medial-distal 0.0.0–1, distal 1.0.0–1. Palpal coxae with moderately sclerotized piliferous granulations. Legs covered with setae, especially tibiae, metatarsi and tarsi. All metatarsi distally with small dorsal patch of setae, III and IV also with dense tuft of setae in distal ventral section. Claws with nine to ten teeth. Abdomen 3.98 long, cream-coloured, cylindrical; abdominal dorsal setae short, 0.01–0.02 long, thick, apically blunt, uniformly distributed. Male copulatory bulbus (Fig. 12A–B): T shorter than DD, external border sloped backwards. DD bent anteriorly in lateral view, more or less 45 °. IS roughly as long as ES, uniformly sclerotized, with a small medial retrolateral extension. ES more uniformly sclerotized. C present, its tip projected frontally. LF present, moderately developed, projected dorsally with a lightly sclerotized border. AR absent. L present, with eL sclerotized, lanceolate. P claw-shaped, fused to T, rotated to retrolateral side, lateral length one-quarter of width of T in frontal view. Ridge present, not expanded, parallel to T.

Female (MMF 47902): (Fig. 12D–F). All characters as in male except: carapace length 3.64; maximum width 2.89; minimum width 2.84; AME 0.18, oval; PLE 0.2; AME separated from anterior border by more than their diameter; PME separated from PLE by roughly one-third the diameter of the former. Chelicerae 1.69 long; fang 1.24 long; sclerotized piliferous granulations almost
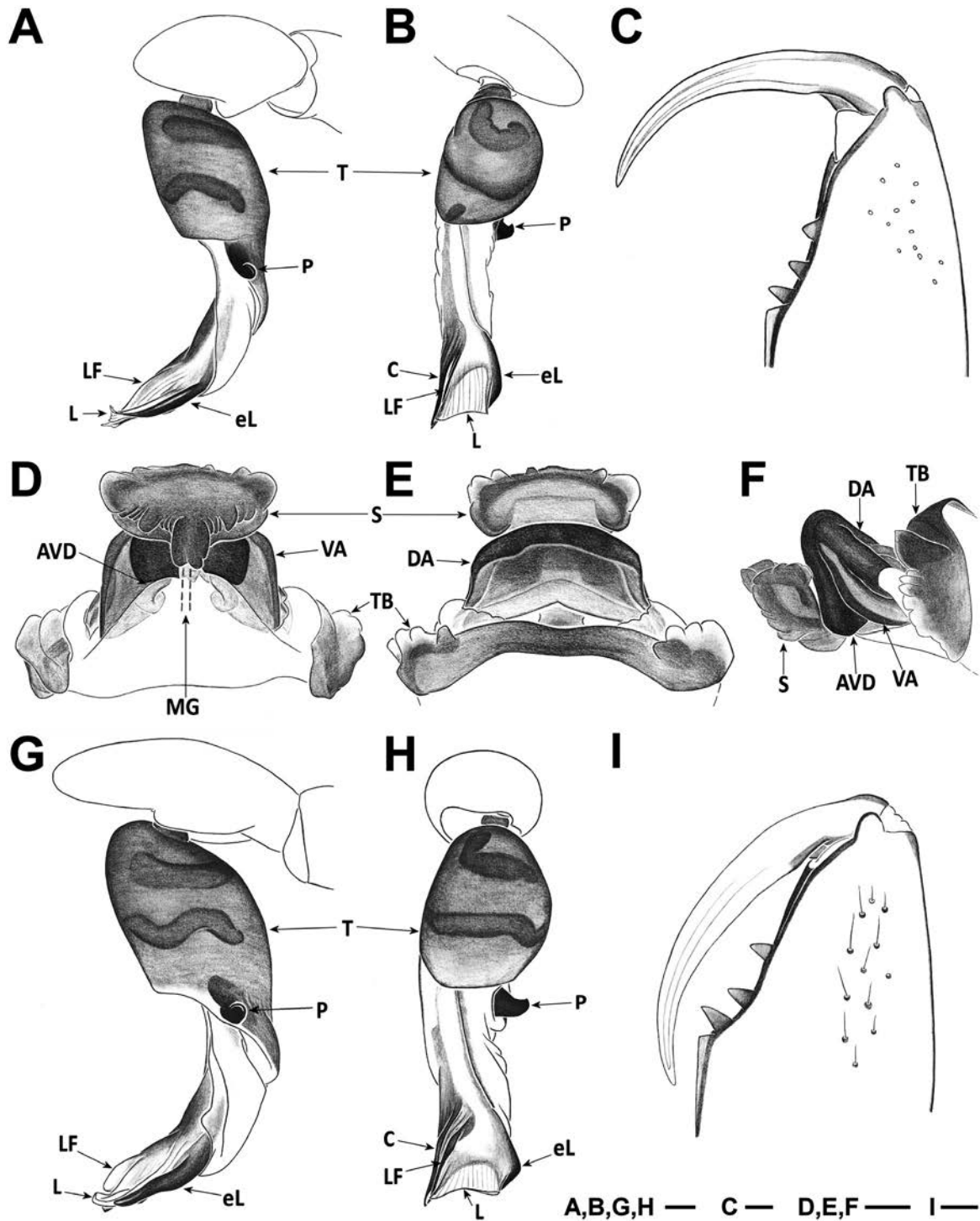
Figure 12. *D. diversa*. A–C, holotype male: (A) left palp, retrolateral; (B) left palp, frontal; (C) left chelicera, ventral. D–F, female (MMF 47902): (D) vulva, ventral; (E) vulva, dorsal; (F) vulva, lateral. G–I, *D. vandeli*: (G) left palp, retrolateral; (H) left palp, frontal; (I) left chelicera, ventral. Scale bars = 0.1 mm. Abbreviations, male palp: C, crest; eL, external margin of lateral sheet; L, lateral sheet; LF, lateral fold; P, posterior apophysis; T, tegulum. Abbreviations, female vulva: AVD, additional ventral diverticulum; DA, dorsal arch; MG, medial groove; S, spermatheca; TB, transversal bar; VA, ventral arch.

absent. Teeth conformation as in male, but shape of teeth trapezoid. Legs orange, anterior pair and palp darker than posterior pair. Leg lengths: fe1 2.38; pa1 1.62; ti1 1.8; me1 1.68; ta1 0.55; total 8.03; fe2 2.16; pa2 1.51; ti2 1.63; me2 1.57; ta2 0.56; total 7.43; fe3 1.73; pa3 1.1; ti3 1.03; me3 1.38; ta3 0.52; total 5.76; fe4 2.25; pa4 1.35; ti4 1.58; me4 1.97; ta4 0.59; total 7.74; fe palp 1.47; pa palp 0.82; ti palp 0.63; ta palp 0.72; total 3.64. Spination: ti3d proximal 1.2.1, distal 1.0.1; ti3v proximal 1.1.0, distal 1.0.0.0; fe4d 2 spines, 2 rows; ti4d proximal 1.0–1.1–2, medio-proximal 0.0–1.0, medio-distal 0.0–1.0, distal 1.0–1.1; ti4v proximal 1.2.1, medio-proximal 0.0.0–1, medio-distal 0.0.0–1, distal 0–1.0.1. Abdomen 3.88 long; abdominal dorsal setae long, 0.05–0.1 long, unmodified, with tapered tip. Vulva (Fig. 12D–F): PD oval. DA separated from VA. DA roughly twice as wide as long, anteriorly domed. DF wide in dorsal view. MF moderately developed, visible only slightly ventrally or posteriorly. VA roughly as wide as long, membranous except in its anterior section, which is sclerotized and shaped as a quadrangle with rounded corners. AVD present, as wide neck reaching base of S, with folds visible by transparency in ventral view. Insertion of S projected onto AVD through sclerotized protuberant neck, S subtriangular in ventral view, with arms short and tips blunt.

Intraspecific variation: Male carapace varies from 3.46 to 3.6 in length and from 2.66 to 2.77 in width. AME vary from 0.15 to 0.2; PLE from 0.17 to 0.2; AME separated from one another by more or less than their diameter; PME almost touching PLE or separated by roughly one-third the diameter of the former; PME almost touching or touching. Cheliceral length from 1.3 to 1.62 in males. The trapezoid shape of the teeth of the single available female present a remarkable discrepancy from the males, which generally have triangular teeth (but not exclusively, i.e. the D of the right chelicera in the holotype male is, likewise, trapezoid), but we attribute this variation to individual life history of each specimen. Spination variability: ti3d proximal 1.0–2.1, distal 1.0.1; ti3v proximal 1.1.0, distal 1.0.0.0; fe4d 1–3 spines, 1–3 rows; ti4d proximal 1.0–1.1–2, medial-proximal 0.0–1.0, medial-distal 0.0–1.0, distal 1.0–1.1; ti4v proximal 1.1–2.1–2, medial-proximal 0–1.0.0–1, medial-distal 0.0.0–1, distal 0–1.0.0–1.

Distribution: This species is known from three locations in Madeira island, spanning a maximum length of 14.7 km (Fig. 8) and an elevational range from 1000 m (Montado dos Pessegueiros and Caldeirão do Inferno) to 1270 m (Caramujo).

Habitat: The known distribution of this species corresponds to locations within laurel forest patches on the northern and central mountainous areas of Madeira island.

Conservation: The last two specimens collected, dating from 2012, were collected by pitfall traps, which suggests a secluded lifestyle, compared with its ubiquitous sympatric congener, *D. coiffaiti*. The data is too sparse to provide accurate insights on the actual range of the species; however, we can assume that as long as efforts to maintain the patches of laurel forest are made, we will be able to find specimens of *D. diversa*. See detailed conservation profile in Cardoso *et al.* (2017).

Remarks: The holotype specimen of *D. diversa* and that of its new junior synonym *D. vandeli* show some differences, both in the male genitalia, such as the slightly more dorsally pronounced LF in *D. vandeli* (Fig. 12G) and the more aculeate eL in *D. diversa* (Fig. 12A), and also somatically, such as a more granulated carapace and chelicerae in *D. vandeli* (Fig. 22C–D). At the same time, both are similar in size, leg spination and teeth arrangement. Denis described *D. vandeli* after revising Blackwall's holotype of *D. diversa* (Denis, 1962), but provided no reliable characters to diagnose one from the other, except for a small inference on leg spination of a female cited by Kulczynski (1899), which he believed to be *D. vandeli*. Leg spination can be of use to diagnose certain species with a peculiar spine conformation, but it is not of any use if the spine conformation is overall similar between the species for which a diagnosis is needed. This is especially so when, in addition, the available specimens are few, such as the case with the specimens cited as *D. diversa* or *D. vandeli*. We required a loan to the MIZ, in order to revise the females cited as *D. diversa* by Kulczynski (1899: pp 340 "Madera; feminae adultae duae") and were astonished to find a surprisingly strange large specimen instead of the expected *D. diversa* (see below *D. titanica*), which is even stranger due to the fact that Kulczynski reported prosoma length of 3.5 mm and prosoma width of 2.9 mm (Kulczynski, 1899: pp 341), which is consistent with all *D. diversa* specimens we found.

The only specimens of *D. diversa* found in the last decades in Madeira island were a male and a female collected by pitfall trapping in two locations separated by approximately 4 km. The male palp is similar to either *D. diversa* or *D. vandeli*, as well as size, leg spination or teeth arrangement, therefore we propose the synonymization of these two species, and provide the first illustrated description of the female.

DYSDERA EXIGUA CRESPO & CARDOSO, **SP. NOV.**

(Figs 13, 23A–B, 30, 37C)

urn:lsid:zoobank.org:act:D5D3CFA3-8564-4C0B-AAE5-BFD3719557D9

Holotype: 1 ♂, 32.53168 °N 16.51471 °W, Rocha do Barbusano (S), Deserta Grande, Portugal, coll. 27.III.2018, hand collecting, leg. L. Crespo, stored at MZB, collection number 2019-1936.

Paratypes: Bugio: Planalto Sul, 1 ♂ (MZB 2019-1939: pk675), 4.XI.2014, hand collecting, leg. I. Silva. Deserta Grande: Rocha do Barbusano, 1 ♂ (CRBA002542), 20.IV.2011, hand collecting, leg. L. Crespo, I. Silva & P. Cardoso; Rocha do Barbusano (S), 2 ♂♂ (FMNH KN.17856: lc045, MMF 47914), 4 ♀♀ (MZB 2019-1937: lc043, MZB 2019-1938: lc044, FMNH KN.17857: lc046, MMF 47915), 10.IV.2017, hand collecting, leg. L. Crespo & I. Silva; Ponta Sul, 1 ♀ (CRBALC0212: lc131), 11.IV.2017, hand collecting, L. Crespo & I. Silva col.

Additional material examined: Deserta Grande: Rocha do Barbusano (S), 4 ♂♂ (CRBALC0072 – dried prosoma only, CRBALC0196, CRBALC0213, LCPC: lc047), 1 ♀ (LCPC) and 5 juveniles (CRBALC0079: lc051, CRBALC0080: lc052, CRBALC0085: lc057, CRBALC0202, CRBALC0205: lc128), 10.IV.2017, hand collecting, leg. L. Crespo & I. Silva, 1 ♂ (CRBALC0582), 1 ♀ (CRBALC0589), 1 juvenile (CRBALC0580), 27.III.2018, hand collecting, leg. L. Crespo; Ponta Sul, 1 juvenile (CRBALC0203: lc162), 11.IV.2017, hand collecting, leg. L. Crespo & I. Silva.

Etymology: The specific epithet, from the Latin adjective *exiguus*, small, short or meager, refers to its small size.

Diagnosis: It is the smallest *Dysdera* in the Madeira archipelago. It differs from all other Madeiran *Dysdera*, except *D. diversa,* by male C combined with LF, short. *D. exigua* can be diagnosed from *D. diversa* by bulgier chelicera; teeth clumped together, D smallest; in males by C, shorter; LF, longer; in females by well-developed AVD (Fig. 13F).

Description – male holotype (MZB 2019-1936): (Figs 13A–C, 23A–B). Carapace length 2.94; maximum width 2.22; minimum width 1.58. Carapace blackish, foveate at borders, anteriorly slightly rugose while posteriorly smooth, with two small circular depressions, one behind cephalic region, other near posterior margin. Frontal border roughly rounded, 1.4 wide; anterior lateral borders parallel; lateral borders divergent, rounded around maximum width point, after converging to posterior margin; posterior margin straight, short. AME 0.15, oval; PLE 0.12, oval; PME 0.12, oval; AME separated from anterior border by less than their diameter; AME separated from one another by their diameter; AME touching PLE; PME separated from PLE by roughly less than half PME diameter; PME almost touching. Labium trapezoid, with base wider than distal part, longer than wide at base; distal part slightly concave, with some setae. Sternum brown, darkened anteriorly, wrinkled, with scattered setae. Chelicerae (Fig. 13C) 1.2 long, about one-third of carapace length in dorsal view, slightly concave dorsally, dorsally and ventrally with abundant sclerotized piliferous granulations; fang 0.92 long. Cheliceral furrow ~38% of the length of basal segment, armed with three teeth and basal lamina, B > M > D; all teeth triangular, B close to lamina, M closer to B than D, D situated roughly at groove midpoint. Legs orange, coxae and femora of anterior pairs slightly darker. Lengths: fe1 1.94; pa1 1.29; ti1 1.59; me1 1.54; ta1 0.48; total 6.84; fe2 1.76; pa2 1.2; ti2 1.45; me2 1.43; ta2 0.46; total 6.3; fe3 1.4; pa3 0.87; ti3 0.87; me3 1.23; ta3 0.4; total 4.77; fe4 1.76; pa4 1.04; ti4 1.31; me4 1.62; ta4 0.47; total 6.2; relative length: 1 > 2 > 4 > 3; fe palp 1.3; pa palp 0.72; ti palp 0.64; ta palp 0.67; total 3.33. Spination: ti3d proximal 1.0.1, distal 1.0.0; ti3v proximal 1.1.0, distal 0.0.0; ti4d proximal 1.0.1, distal 1.0.1; ti4v proximal 1.1.0, distal 0.0.0. Palpal coxae with slightly sclerotized piliferous granulations. Legs covered with setae, especially on tibiae, metatarsi and tarsi. Anterior metatarsi ventrally with sclerotized piliferous granulations. Metatarsi III and IV with dense tuft of setae in distal ventral section. Claws with seven to eight teeth. Abdomen 2.92 long, salmon-coloured, cylindrical; abdominal dorsal setae short, 0.04–0.07 long, simple, uniformly distributed. Male copulatory bulbus (Fig. 13A–B): T shorter than DD, external border sloped backwards. DD bent anteriorly in lateral view, more or less 30 °. IS roughly as long as ES, differentially sclerotized, poorly so at base, with medial sclerotized section extending retrolaterally, ES more uniformly sclerotized. C present, tip membranous and projected prolaterally. LF present, moderately developed, with sclerotized border. AR absent. L present, with eL sclerotized, lanceolate. P claw-shaped, fused to T, rotated to retrolateral side, lateral length one-third of width of T in frontal view. Ridge present, not expanded, parallel to T.

Female paratype (MZB 2019-1937): (Fig. 13D–F). All characters as in male except: carapace length 3; maximum width 2.35; minimum width 1.7; AME 0.16; PME 0.14; AME separated from one another by more than their diameter. Chelicerae 1.3; fang 1.08. Leg lengths: fe1 2.1; pa1 1.4; ti1 1.67; me1 1.57; ta1 0.43; total 7.17; fe2 1.9; pa2 1.31; ti2 1.53; me2 1.48; ta2 0.42; total 6.64; fe3 1.55; pa3 0.96; ti3 0.97; me3 1.34; ta3 0.4; total 5.22; fe4 2; pa4 1.16; ti4 1.48; me4 1.8; ta4 0.46; total 6.9; fe palp 1.28; pa palp 0.68; ti palp 0.52; ta palp 0.67; total 3.15. Spination: ti3v proximal 1.0.0, distal 0.0.0; fe4d
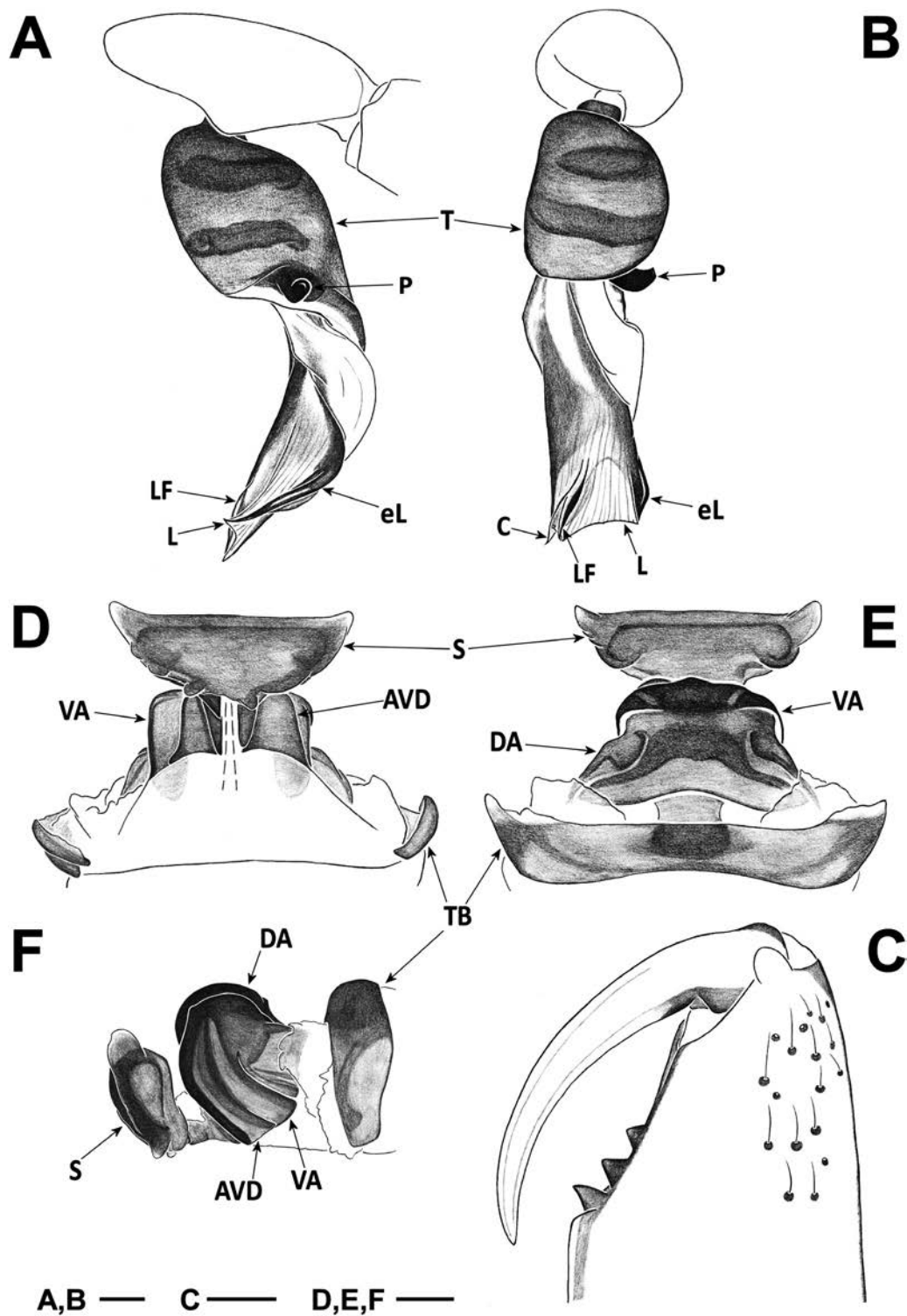
Figure 13. ***D. exigua* sp. nov.** A–C, holotype male: (A) left palp, retrolateral; (B) left palp, frontal; (C) left chelicera, ventral. D–F, female paratype (MZB 2019-1937): (D) vulva, ventral; (E) vulva, dorsal; (F) vulva, lateral. Scale bars = 0.1 mm. Abbreviations, male palp: C, crest; eL, external margin of lateral sheet; L, lateral sheet; LF, lateral fold; P, posterior apophysis; T, tegulum. Abbreviations, female vulva: AVD, additional ventral diverticulum; DA, dorsal arch; MG, medial groove; S, spermatheca; TB, transversal bar; VA, ventral arch.

spineless; ti4d proximal 0.0.1, distal 0.0.1; ti4v proximal 0.1.0, distal 0.0.0. Abdomen 3.68 long; abdominal dorsal setae long, 0.05–0.1. Vulva (Fig. 13D–F): PD oval. DA separated from VA. DA roughly twice as wide as long, anteriorly truncated, with central small elevation. DF wide in dorsal view. MF moderately developed, visible in ventral and lateral views. VA roughly as wide as long, membranous except in anterior sclerotized section. AVD present, well developed. Insertion of S as sclerotized neck projected onto AVD, S subtriangular in ventral view, with arms moderately elongated and tips slightly extended dorsally.

Intraspecific variation: Male carapace varies from 2.81 to 2.95 in length and 2.22 to 2.31 in width, female carapace from 2.72 to 3.24 in length and 2.08 to 2.5 in width. Cheliceral length from 1.2 to 1.29 in males, 1.2 to 1.3 in females. The position of D in the cheliceral furrow is slightly variable, most often being separated from M by its width at base, more rarely closer to M. The female vulva varies in shape, namely in the shape of the DA (from anteriorly truncated to triangular, in dorsal view) and the development of the AVD. Spination variability: ti3d proximal 1.0.1, distal 1.0.0; ti3v proximal 0–1.0–1.0, distal 0.0.0; ti4d proximal 0–1.0.1–2, distal 0–1.0.1; ti4v proximal 0–1.0–2.0, medial-proximal 0.0–1.0, distal 0.0.0.

Distribution: This species is known from several localities along the entire length of Deserta Grande and from one locality in Bugio (Fig. 9), spanning an elevational range of roughly 300 m to 450 m.

Habitat: On both islands the habitats are similar, mainly composed of rocky scarps practically devoid of vegetation, except for a few xerophytic herbs and shrubs. There, *D. exigua* can be found under stones or in sandstone crevices.

Conservation: The extrapolated range of the species is 11 km², with a maximum elevation in Deserta Grande of 479 m and of 388 m in Bugio. The conservation concerns are similar to those reported for the population of *D. coiffaiti* present in Deserta Grande and Bugio.

DYSDERA ISAMBERTOI CRESPO & CARDOSO, **SP. NOV.**

(Figs 14, 23C–D, 31)

urn:lsid:zoobank.org:act:B786FE57-BFC1-47B5-B90E-C9F54EFF4028

Holotype: 1 ♂, 33.09270 °N 16.32186 °W, Pico da Juliana, Porto Santo, Portugal, coll. 24.IV.2017, hand collecting, leg. L. Crespo, stored at MZB, collection number 2019-1951.

Paratypes: Porto Santo: Pico do Castelo, 2 ♂♂ (MZB 2019-1953: lc073, FMNH KN.17863: lc075) and 2 ♀♀ (FMNH KN.17864, MZB 2019-1954: lc074), 17.IV.2017, hand collecting, leg. L. Crespo & I. Silva, 1 ♂♂ (CRBALC0614) and 1 ♀ (CRBALC0636), 8.IV.2018, hand collecting, leg. L. Crespo & A. Bellvert; Pico da Juliana, 1 ♀ (MZB 2019-1952: lc126), 24.IV.2017, hand collecting, leg. L. Crespo, 1 ♂ (MMF 47920), 23.IV–7.V.2011, pitfall trapping, A. Serrano *et al.* col.; Pico do Facho, 1 ♂ (CRBALC0683) and 1 ♀ (MMF 47921), IV.2018, hand collecting, leg. I. Silva.

Additional material examined: Porto Santo: Pico do Castelo, 2 ♂♂ (CRBALC0143, CRBALC0163) and 5 juveniles (CRBALC0121, CRBALC0123: lc080, CRBALC0124: lc081, CRBALC0125: lc082, CRBALC0126: lc083), 17.IV.2017, hand collecting, leg. L. Crespo & I. Silva, 2 ♂♂ (CRBALC0693, LCPC), 8.IV.2018, hand collecting, leg. L. Crespo & A. Bellvert; Pico da Juliana, 1 juvenile (CRBALC0190: lc125), 24.IV.2017, hand collecting, leg. L. Crespo; Pico do Facho, 1 ♀ (LCPC: lc116) and 1 juvenile (CRBALC0183: lc118), 22.IV.2017, hand collecting, leg. L. Crespo; Pico do Facho (N), 1 juvenile (CRBALC0188: lc123), 22.IV.2017, hand collecting, L. Crespo col.

Etymology: The specific epithet is a patronym in honour of Isamberto Silva, who for the past decades has provided researchers with biological material and information concerning the endemic biota of the Madeira archipelago. His support in the field was pivotal for the discovery of the hidden diversity of *Dysdera* in the Desertas.

Diagnosis: *D. isambertoi* can be diagnosed from all other Madeiran *Dysdera* by D, larger, distal (Fig. 14C); males by eL, stout, conical (Fig. 14A–B); females by VA with radial spine-like sclerotizations (Fig. 14D).

Description – male holotype: (Figs 14A–C, 23C). Carapace length 5.16; maximum width 4.1; minimum width 2.88. Carapace blackish-brown, foveate at borders, smooth, with several small depressions at the margin of the cephalic area, larger depression at fovea center and just anteriorly of the posterior margin. Frontal border roughly rounded, 2.66 wide; anterior lateral borders parallel; lateral borders divergent, rounded around maximum width point to posterior margin; posterior margin straight, wide. AME 0.26, rounded; PLE 0.23, oval; PME 0.23, oval; AME separated from anterior border by less than their diameter; AME separated from one another by roughly half their diameter; AME touching PLE; PME separated from PLE by roughly one-third PME diameter; PME touching. Labium trapezoid, with base wider than distal part, longer than wide at
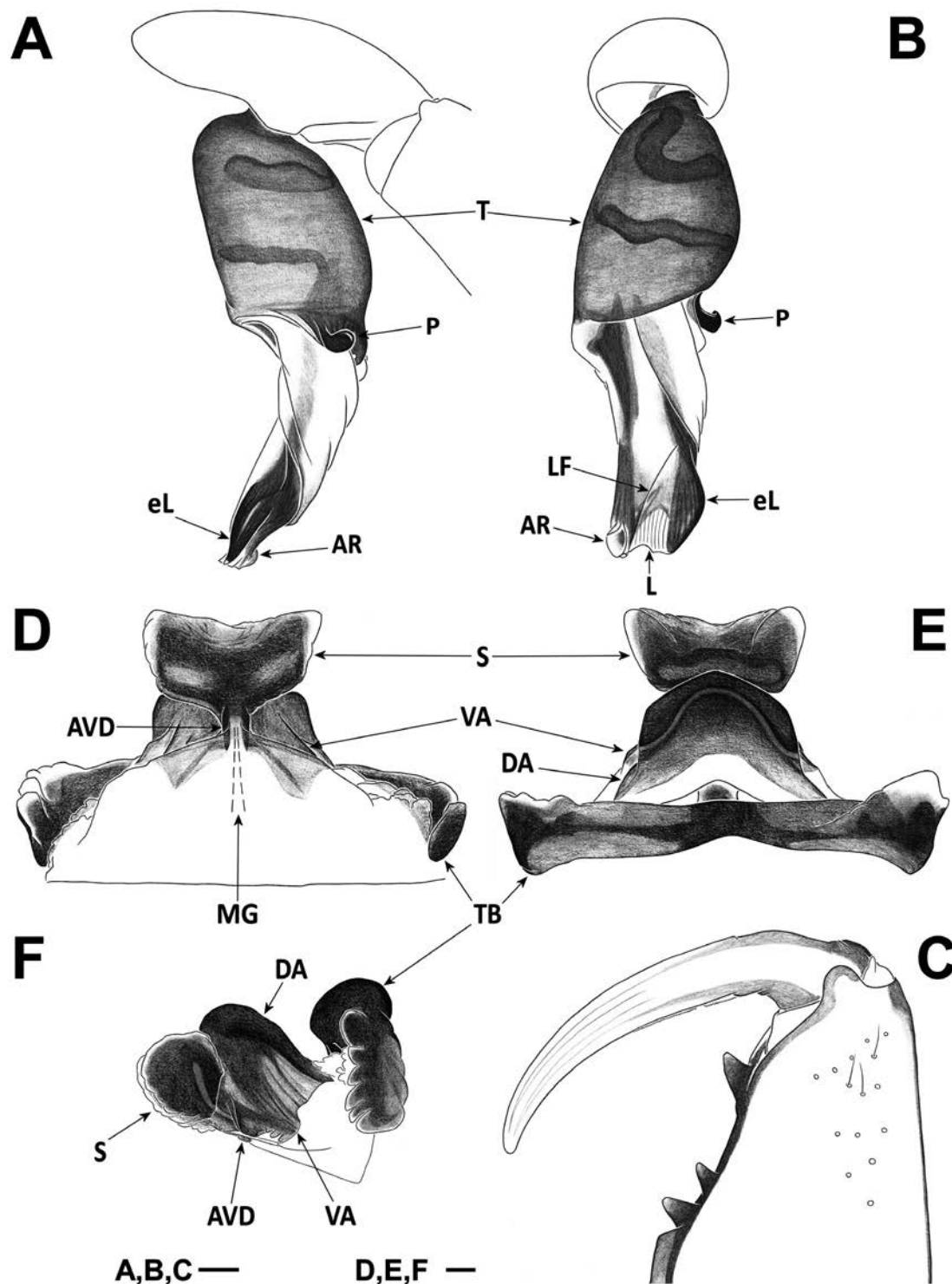
Figure 14. *D. isambertoi* **sp. nov.** A–C, holotype male: (A) left palp, retrolateral; (B) left palp, frontal; (C) mirrored image of right chelicera, ventral. D–F, female paratype (MZB 2019-1952): D, vulva, ventral; E, vulva, dorsal; F, vulva, lateral. Scale bars = 0.1 mm. Abbreviations, male palp: AR, arch-like ridge; eL, external margin of lateral sheet; L, lateral sheet; LF, lateral fold; P, posterior apophysis; T, tegulum. Abbreviations, female vulva: AVD, additional ventral diverticulum; DA, dorsal arch; MG, medial groove; S, spermatheca; SD, spermatheca diverticulum; TB, transversal bar; VA, ventral arch.

base; distal part concave. Sternum brown, anteriorly darker, wrinkled, without setae. Chelicerae (Fig. 14C) 2.2 long, about one-quarter of carapace length in dorsal view, slightly concave, dorsally and prolaterally with sclerotized piliferous granulations; fang 1.68 long. Cheliceral furrow ~44% of length of basal segment, armed with three teeth and basal lamina, D > B > M; all teeth triangular, B close to lamina, M closer to B than D, D massive, situated in distal half of cheliceral furrow. All legs and palp orange, anterior pairs and palp darker than posterior pairs. Lengths: fe1 4.05; pa1 2.53; ti1 3.18; me1 3.24; ta1 0.78; total 13.78; fe2 3.72; pa2 2.38; ti2 2.98; me2 3.03; ta2 0.78; total 12.89; fe3 2.97; pa3 1.71; ti3 1.8; me3 2.66; ta3 0.71; total 9.85; fe4 3.84; pa4 2.18; ti4 2.75; me4 3.52; ta4 0.82; total 13.11; relative length: 1 > 4 > 2 > 3; fe palp 2.29; pa palp 1.31; ti palp 1.18; ta palp 1.08; total 5.86. Spination: leg1, leg2 spineless; fe3, pa3 spineless; ti3d proximal 1.0.1, distal 1.0.1; ti3v proximal 1.1.0, distal 1.0.0; fe4d 2 spines, 1–2 rows; ti4d proximal 1.0.1, distal 1.0.1; ti4v proximal 1.1.1, distal 1.0.1. Palpal coxae with moderately sclerotized piliferous granulations. Legs covered with setae, especially on tibiae, metatarsi and tarsi. Anterior tibiae distally with a dorsal dense patch of short setae. Ventral setae of anterior tibiae and metatarsi with sclerotized base. All metatarsi with a small dorsal distal patch of setae, III and IV ventrally also with dense tuft of setae in distal section. Claws with eight to nine teeth. Abdomen 5.53 long, cream-coloured, cylindrical; abdominal dorsal setae short, 0.01–0.02, thick, apically blunt, uniformly distributed. Male copulatory bulbus (Fig. 14A–B): T roughly as long as DD, external border slightly sloped backwards. DD bent anteriorly in lateral view, more or less 30 °. IS roughly as long as ES, but thicker, especially basally, with a prolateral sclerotized outgrowth. ES more uniformly sclerotized. C absent. LF present, small. AR present, well developed. L present, with eL sclerotized, stout, conical. P claw-shaped, fused to T, rotated to retrolateral side, lateral length one-quarter of the width of T in frontal view. Ridge present, not expanded, parallel to T.

Female paratype (MZB 2019-1952): (Fig. 14D–F). All characters as in male except: carapace length 5.25; maximum width 3.88; minimum width 2.63; AME 0.24, oval; PLE 0.24; PME 0.2, rounded; AME separated from anterior border by roughly half their diameter; AME separated from one another by less than their diameter; PME almost touching. Chelicerae 2 long; fang 1.58 long. Legs greenish-orange, anterior pairs and palp darker than posterior pairs. Leg lengths: fe1 3.78; pa1 2.48; ti1 3.02; me1 3.05; ta1 0.82; total 13.14; fe2 3.42; pa2 2.31; ti2 2.78; me2 2.92; ta2 0.78; total 12.22; fe3 2.91; pa3 1.73; ti3 1.8; me3 2.66; ta3 0.78; total 9.87; fe4 3.84; pa4 2.2; ti4 2.91; me4 3.56; ta4 0.92; total 13.43; fe palp 2.09; pa palp 1.16; ti palp 0.97; ta palp 1.36; total 5.58. Spination: leg1, leg2 spineless; fe3, pa3 spineless;

ti3d proximal 1.0.1, distal 1.0.1; ti3v proximal 1.1.0, distal 1.0.0; fe4d 2–3 spines, 2 rows; ti4d proximal 1.0.1, distal 1.0.1; ti4v proximal 1.1.1, medio-distal 1.0.0–1, distal 0.0.0–1. Abdomen 5.88 long; abdominal dorsal setae short, 0.03–0.07 long. Vulva (Fig. 14D–F): PD oval. DA well separated from VA. DA roughly twice as wide as long, anteriorly domed. DF wide in dorsal view. MF poorly developed, indistinct. VA roughly as wide as long, poorly developed, membranous except in its anterolateral section, which is sclerotized and striate. AVD present, rebordered anteriorly by two sclerotized lanceolate projections. S projected onto AVD through a wrinkled sclerotized neck, S triangular in ventral view, with arms short and tips extended dorsally.

Intraspecific variation: Male carapace varies from 4.55 to 5.16 in length and 3.58 to 4.1 in width, female carapace from 4.65 to 5.31 in length and 3.86 to 4.3 in width. Cheliceral length from 1.84 to 2.2 in males, 1.87 to 2.15 in females. Spination variability: fe3d 0–1 spine, 0–1 rows; ti3d proximal 1.0.1, distal 1.0.1; ti3v proximal 1.1.0–1, distal 1.0.0; fe4d 0–3 spines, 0–2 rows; ti4d proximal 0–1.0.1, medial-proximal 0–1.0.0, distal 1.0.1; ti4v proximal 1–2.1–2.1–2, medial-proximal 0.0–1.0, medial-distal 0–1.0.0–1, distal 0–1.0.0–1.

Distribution: This species is known from the summits of the central peaks of Porto Santo island: Pico do Castelo (437 m), Pico do Facho (517 m) and Pico da Juliana (447 m) (Fig. 11).

Habitat: The same as that of *D. dissimilis* (see above). Likewise, *D. isambertoi* can be found under stones or in the bark of dead logs.

Conservation: The extrapolated range is of 0.38 km². The conservation concerns are the same as those reported for *D. dissimilis* (e.g. habitat loss, fragmentation).

Dysdera portisancti Wunderlich, 1995
(Figs 15, 24A–B, 32, 37D)

Holotype: 1 ♂, 33.09428 °N 16.30137 °W, Pico Branco, Porto Santo, Portugal, coll. 14.VIII.1985, (no collection method), leg. K. Groh, stored at SMF, collection number 37633. Examined.

Additional material examined: Porto Santo: Pico Branco, 1 ♀ (CRBA002546: pk87), 6.IV.2011, hand collecting, leg. I. Silva, 4 ♂♂ (MMF 47906: pk228, LCPC: pk233, MMF 47904: pk235, FMNH KN.17865: pk238) and 4 ♀♀ (MMF 47907, LCPC: pk233, MMF 47908: pk239, MMF 47905: pk241), 23.IV–7.V.2011, pitfall

trapping, leg. A. Serrano *et al.*, 2 ♀♀ (CRBALC0204, CRBALC0215), 21.IV.2017, hand collecting, leg. L. Crespo & I. Silva; Terra-Chã (Pico Branco), 4 ♂♂ (MZB 2019-1955: lc109, MZB 2019-1957: lc110, CRBALC0175, CRBALC0214) and 3 ♀♀ (FMNH KN.17866: lc106, MZB 2019-1958: lc107, MZB 2019-1956: lc108), 21.IV.2017, hand collecting, leg. L. Crespo & I. Silva, 4 ♂♂ (CRBALC0641, CRBALC0646, CRBALC0649, CRBALC0650), 4 ♀♀ (CRBALC0626, CRBALC0643, CRBALC0669, CRBALC0672) and 4 juveniles (CRBALC0652, CRBALC0655, CRBALC0656, CRBALC0686), 10.IV.2018, hand collecting, leg. L. Crespo & A. Bellvert; Pico do Facho, 1 juvenile (CRBALC0179: lc114), 22.IV.2017, hand collecting, leg. L. Crespo, 3 ♂♂ (CRBALC0613, CRBALC0617, CRBALC0677), 7 ♀♀ (CRBALC0620, CRBALC0623, CRBALC0634, CRBALC0635, CRBALC0639, CRBALC0668, CRBALC0671), 9.IV.2018, hand collecting, leg. L. Crespo & A. Bellvert.

Diagnosis: D. portisancti can be diagnosed from all other Madeiran *Dysdera* in males by: the distally narrow DD, with a spoon-shaped AR (Figs 15A–C, 32), and in females by: the AVD, the DA, with lateral wing-shaped projections (Fig. 15E–G).

Redescription – male holotype: (Figs 15A–D, 24A). Carapace length 3.6; maximum width 2.89; minimum width 2.05. Carapace brown, foveate at borders, anteriorly slightly rugose, posteriorly smooth. Frontal border roughly rounded, 2.03 wide; anterior lateral borders slightly convergent; lateral borders rounded; posterior margin straight, wide. AME 0.22, oval; PLE 0.17, oval; PME 0.16, rounded; AME separated from anterior border by less than their diameter; AME separated from one another by more than their diameter; AME touching PLE; PME separated from PLE by roughly one-third of PME diameter; PME touching. Labium trapezoid, with base wider than distal part, longer than wide at base; distal part concave. Sternum orange, wrinkled, with abundant setae. Chelicerae (Fig. 15D) 1.72 long, about two-fifths of carapace length in dorsal view, slightly concave especially ventrally, smooth, without sclerotized piliferous granulations; fang 1.28 long. Cheliceral furrow ~44% of length of basal segment, armed with three teeth and basal lamina (remark: left chelicera presents an abnormal teeth conformation with two distal teeth instead of one, visible on Fig. 24A), B = D > M; all teeth triangular, B close to lamina, M closer to B than D, D situated at midpoint of cheliceral furrow. First pair of legs orange, second pair light orange, posterior pairs yellow. Lengths: fe1 2.63; pa1 1.62; ti1 1.8; me1 1.5; ta1 0.44; total 7.99; fe2 2.33; pa2 1.47; ti2 1.69; me2 1.48; ta2 0.48; total 7.45; fe3 1.9; pa3 1.11; ti3 1.21; me3 1.47; ta3 0.42; total

6.11; fe4 2.38; pa4 1.34; ti4 1.72; me4 1.92; ta4 0.5; total 7.86; relative length: 1 > 4 > 2 > 3; fe palp 1.57; pa palp 0.74; ti palp 0.64; ta palp 0.68; total 3.63. Spination: ti3d proximal 0.0.0, distal 1.0.0; ti3v proximal 0.1.0, distal 0.0.0; ti4v proximal 0.1.0, distal 0.0.0. Palpal coxae with non-sclerotized piliferous granulations. Legs covered with setae, especially on tibiae, metatarsi and tarsi. All metatarsi with a small dorsal distal patch of setae (setae lost in first pair of legs), in addition to the dense tuft of setae in distal ventral section. Six to seven teeth in each claw. Abdomen 4.08 long, cream-coloured, cylindrical; abdominal dorsal setae short, 0.03–0.07, slender, apically blunt, uniformly distributed. Male copulatory bulbus (Fig. 15A–C): T shorter than DD, external border sloped backwards. DD narrowing apically, bent anteriorly in lateral view, more or less 30 °, and rotated retrolaterally. IS roughly as long as ES, although much less developed, thin and lightly sclerotized. Both sclerites descending through DD juxtaposed to each other. ES thicker, uniformly sclerotized. C absent. LF absent. AR present, spoon-shaped. L present, with eL sclerotized, lanceolate. P claw-shaped, fused to T, rotated to retrolateral side, lateral length one-third of the width of T in frontal view. Ridge present, not expanded, parallel to T.

Female (MZB 2019-1956): (Fig. 15E–G). All characters as in male except: carapace length 3.28; maximum width 2.75; minimum width 1.82. Frontal border 1.78. AME 0.15, oval; PLE 0.14, oval; PME 0.14, rounded; PME separated from PLE by almost half the diameter of the former. Chelicerae 1.4; fang 1.25. Cheliceral furrow ~52% of the length of basal segment. Legs greenish-orange, anterior pair darker than others. Leg lengths: fe1 2.25; pa1 1.42; ti1 1.43; me1 1.26; ta1 0.43; total 6.79; fe2 2.08; pa2 1.32; ti2 1.43; me2 1.22; ta2 0.41; total 6.46; fe3 1.74; pa3 1.05; ti3 1.06; me3 1.28; ta3 0.4; total 5.53; fe4 2.16; pa4 1.24; ti4 1.53; me4 1.74; ta4 0.44; total 7.11; relative length: 4 > 1 > 2 > 3; fe palp 1.38; pa palp 0.62; ti palp 0.48; ta palp 0.7; total 3.18. Spination: leg1, leg2 spineless; fe3, pa3 spineless; ti3d proximal 1.0.0, distal 1.0.0; ti3v proximal 1.0.0, distal 0.0.0; fe4d spineless; ti4d proximal 0.0.1, distal 0.0.0; ti4v proximal 0.1.0, distal 0.0.0. Abdomen 3.6 long; abdominal dorsal setae 0.04–0.08. Vulva (Fig. 15E–G): PD oval. DA separated from VA. DA more than twice as wide as long, anteriorly domed, in ventral view with lateral wing-shaped outgrowths. DF wide in dorsal view. MF poorly developed, indistinct in ventral view. VA wider than long, membranous except in anterior, sclerotized section, quadrangle shaped with rounded corners. AVD present, strongly reduced, with triangular tips surrounding insertion of S (in ventral view). S subtriangular in ventral view, with arms moderately elongated and tips extended laterally.
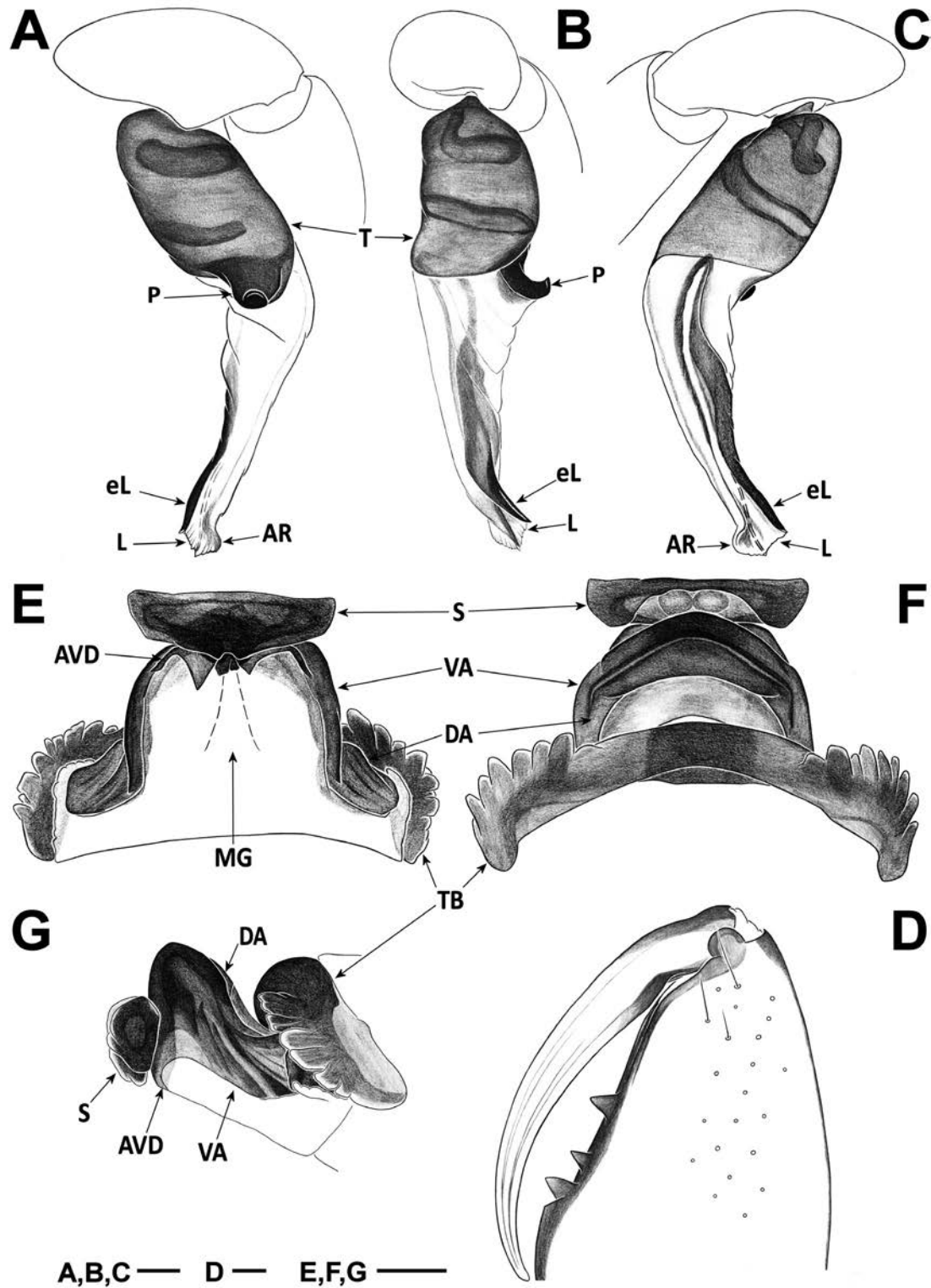
Figure 15. *D. portisancti*. A–D, holotype male: (A) left palp, retrolateral; (B) left palp, frontal; (C) left palp, prolateral; (D) mirrored image of right chelicera, ventral. E–G, female (MZB 2019-1956): (E) vulva, ventral; (F) vulva, dorsal; (G) vulva, lateral. Scale bars = 0.1 mm. Abbreviations, male palp: AR, arch-like ridge; eL, external margin of lateral sheet; L, lateral sheet; P, posterior apophysis; T, tegulum. Abbreviations, female vulva: AVD, additional ventral diverticulum; DA, dorsal arch; MG, medial groove; S, spermatheca; TB, transversal bar; VA, ventral arch.

Intraspecific variation: Male carapace varies from 2.88 to 3.6 in length and 2.34 to 2.89 in width, female carapace from 3.06 to 3.4 in length and 2.56 to 2.88 in width. Cheliceral length from 1.24 to 1.72 in males, 1.24 to 1.55 in females. Cheliceral basal tooth can vary slightly in relative size, so that in addition to the holotype teeth conformation we can have D > M = B. Spination variability: ti3d proximal 0–1.0.0, medial-proximal 0–1.0.0, medial-distal 0–1.0.0, distal 1.0.0; ti3v proximal 0–1.0–1.0, distal 0.0.0; ti4d proximal 0.0.0–1, distal 0.0.0–1; ti4v proximal 0–1.1–3.0, medial-proximal 0.0–1.0, distal 0–1.0.0.

Distribution: This species is known from the summit of the two highest peaks of Porto Santo island, Pico do Facho (517 m) and Pico Branco (450 m) ([Fig. 11](#)).

Habitat: The same as that of *D. dissimilis* (see above). *D. portisancti* can be found under stones, pine needles or under the bark of dead logs.

Conservation: The conservation concerns are the same as those reported for *D. dissimilis*. (see above) with the increased risk factor of an even smaller known distribution, because *D. portisancti* is only known from two mountains, the range not surpassing 0.30 km². See detailed conservation profile in [Cardoso *et al.* (2017)](#).

DYSDERA PRECARIA CRESPO, SP. NOV.

([Figs 16](#), [24C–D](#), [33](#), [37E](#))
urn:lsid:zoobank.org:act:92ADD5AA-52E9-49D4-B5B6-92DA3E97BB31

Holotype: 1 ♂, 33.09447 °N 16.29839 °W, Terra-Chã (Pico Branco), Porto Santo, Portugal, coll. 21.IV.2017, hand collecting, leg. L. Crespo & I. Silva, stored at MZB, collection number 2019-1940, DNA code lc111.

Paratypes: Porto Santo: Pico Ana Ferreira, 3 ♂♂ (MZB 2019-1942, FMNH KN.17858: lc092, MMF 47918), 1 ♀ (MZB 2019-1943), 20.IV.2017, hand collecting, leg. L. Crespo & I. Silva, 1 ♂ (CRBALC0632), 1 ♀ (CRBALC0633), 9.IV.2018, hand collecting, leg. L. Crespo & A. Bellvert; Pico Branco, 1 ♀ (FMNH KN.17859: lc136), 21.IV.2017, hand collecting, leg. L. Crespo & I. Silva; Pico da Juliana, 1 ♀ (MMF 47919: pk244), 23.IV–7.V.2011, pitfall trapping, leg. A. Serrano *et al.*; Terra-Chã (Pico Branco), 1 ♀ (MZB 2019-1941: lc112), 21.IV.2017, hand collecting, leg. L. Crespo & I. Silva.

Additional material examined: Porto Santo: Pico Ana Ferreira, 2 ♂♂ (CRBALC0137, CRBALC0164), 1 ♀ (CRBALC0165) and 2 juveniles (CRBALC0162: lc101, CRBALC0167: lc103), 20.IV.2017, hand collecting,

leg. L. Crespo & I. Silva, 4 ♂♂ (CRBALC0616, CRBALC0637, CRBALC0645, LCPC) and 2 juveniles (CRBALC0658, CRBALC0681), 9.IV.2018, hand collecting, leg. L. Crespo & A. Bellvert; Pico Branco, 1 ♀ (LCPC: pk242) and 1 juvenile (CRBA002513: pk231), 23.IV–7.V.2011, pitfall trapping, A. Serrano *et al.* col., 1 ♂ (CRBALC0144), 21.IV.2017, hand collecting, leg. L. Crespo & I. Silva; Pico da Juliana, 2 juveniles (CRBALC0195: lc316, CRBALC0199: lc317), 24.IV.2017, hand collecting, leg. L. Crespo, 1 juvenile (CRBALC0648), 10.IV.2018, hand collecting, leg. L. Crespo & A. Bellvert; Terra-Chã (Pico Branco), 1 ♂ (CRBALC0221) and 1 juvenile (CRBALC0178: lc113), 21.IV.2017, hand collecting, leg. L. Crespo & I. Silva, 2 ♂♂ (CRBALC0615, CRBALC0642) and 5 juveniles (CRBALC0657, CRBALC0663, CRBALC0667, CRBALC0682, CRBALC0687), 10.IV.2018, hand collecting, leg. L. Crespo & A. Bellvert.

Etymology: The specific epithet, from the Latin adjective *precarius*, obtained from entreaty, referring to the precarious state of the habitat of this species. It is also a hint to call attention to the current employment situation of many taxonomists.

Diagnosis: *D. precaria* can be diagnosed from all other Madeiran *Dysdera* in males by: the well-developed, membranous LF and the thin, poorly developed eL ([Fig. 16A–B](#)); females by: the wide and short VA ([Fig. 16D–F](#)).

Description – male holotype: ([Figs 16A–C](#), [24C](#)). Carapace length 4.88; maximum width 3.84; minimum width 2.39. Carapace blackish-brown, foveate at borders, smooth, in lateral view flattened. Frontal border roughly rounded, 2.38 wide; anterior lateral borders parallel; lateral borders divergent, rounded around maximum width point, after converging to posterior margin; posterior margin straight, wide. AME 0.25, oval; PLE 0.23, oval; PME 0.19, rounded; AME separated from anterior border by roughly half their diameter; AME separated from one another by roughly half their diameter; AME touching PLE; PME separated from PLE by roughly one-third of PME; PME touching. Labium trapezoid, with base wider than distal part, longer than wide at base; distal part concave. Sternum brown, anteriorly darker, wrinkled, with setae. Chelicerae ([Fig. 16C](#)) 1.9 long, about one-quarter of carapace length in dorsal view, straight, dorsally and prolaterally with sclerotized piliferous granulations; fang 1.56 long. Cheliceral furrow ~46% of length of basal segment, armed with three teeth and basal lamina, B = D > M; all teeth triangular, B close to lamina, M closer to B than D, D situated in the distal half of cheliceral furrow. First pair of legs and
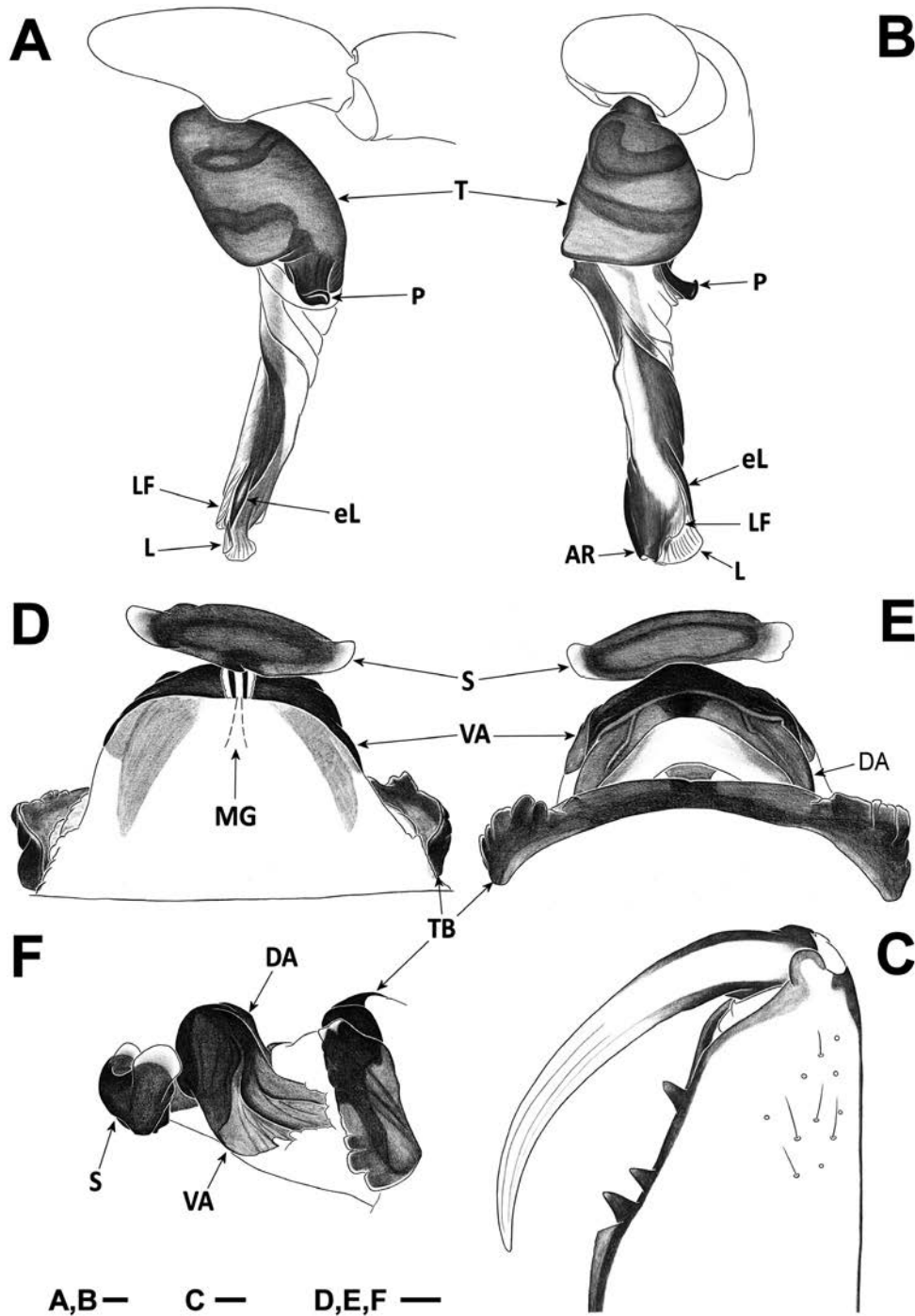
Figure 16. *D. precaria* **sp. nov.** A–C, holotype male: (A) left palp, retrolateral; (B) left palp, frontal; (C) mirrored image of right chelicera, ventral. D–F, female paratype (MZB 2019-1941): (D) vulva, ventral; (E) vulva, dorsal; (F) vulva, lateral. Scale bars = 0.1 mm. Abbreviations, male palp: AR, arch-like ridge; eL, external margin of lateral sheet; L, lateral sheet; LF, lateral fold; P, posterior apophysis; T, tegulum. Abbreviations, female vulva: DA, dorsal arch; MG, medial groove; S, spermatheca; SD, spermatheca diverticulum; TB, transversal bar; VA, ventral arch.

palp orange, other legs yellow. Lengths: fe1 3.98; pa1 2.56; ti1 3.44; me1 3.28; ta1 0.78; total 14.04; fe2 3.52; pa2 2.31; ti2 3; me2 2.97; ta2 0.74; total 12.54; fe3 2.78; pa3 1.66; ti3 1.76; me3 2.39; ta3 0.58; total 9.17; fe4 3.66; pa4 1.69; ti4 2.84; me4 3.24; ta4 0.76; total 12.19; relative length: 1 > 2 > 4 > 3; fe palp 1.57; pa palp

0.74; ti palp 0.64; ta palp 0.68; total 3.63. Spination: ti3d proximal 1.1.1, distal 1.0.1; ti3v proximal 1.1.1, distal 1.0.0; fe4d 3 spines, 2–3 rows; ti4d proximal 1.0.1–2, distal 1.0.1; ti4v proximal 1–2.1–2.1, medial-proximal 0.1.0, medial-distal 1.0.0, distal 1.0.1. Palpal coxae with moderately sclerotized piliferous granulations. Legs covered with setae, especially on tibiae, metatarsi and tarsi. Ventral setae of anterior metatarsi with sclerotized base. All metatarsi with small dorsal distal patch of setae, III and IV also with dense tuft of setae in distal ventral section. Claws with six to eight teeth. Abdomen 5.53 long, cream-coloured, cylindrical; abdominal dorsal setae short, 0.02–0.05, thick, apically blunt, uniformly distributed. Male copulatory bulbus (Fig. 16A–B): T shorter than DD, external border sloped backwards. DD bent anteriorly in lateral view, more or less 30 °. IS roughly as long as ES, but differentially developed, more so basally, showing a prolateral sclerotized outgrowth. ES more developed medially. C absent. LF present, emerging from prolateral margin of AR, leading to base of eL. AR present, well developed. L present, with eL thin, sclerotized, lanceolate. P claw-shaped, fused to T, rotated to retrolateral side, lateral length one-quarter of width of T in frontal view. Ridge present, not expanded, parallel to T.

Female paratype (MZB 2019-1941): (Fig. 16D–F). All characters as in male except: carapace length 5.13; maximum width 3.96; minimum width 2.66; AME 0.23; PLE 0.21; PME 0.18; AME separated from one another by roughly their diameter; PME separated from PLE by roughly half PME diameter. Chelicerae 2 long; piliferous granulations only prolaterally; fang 1.63 long. Legs orange, anterior pairs and palp darker than posterior pairs. Leg lengths: fe1 3.8; pa1 2.52; ti1 3.16; me1 3.05; ta1 0.77; total 13.29; fe2 3.48; pa2 2.35; ti2 2.84; me2 2.91; ta2 0.76; total 12.34; fe3 2.86; pa3 1.74; ti3 1.84; me3 2.45; ta3 0.64; total 9.53; fe4 3.84; pa4 2.28; ti4 3.03; me4 3.4; ta4 0.88; total 13.43; fe palp 1.96; pa palp 1.15; ti palp 0.96; ta palp 1.3; total 5.37. Spination: ti3d proximal 1.0.1, distal 1.0.1; ti3v proximal 1.1.0, distal 0.0.0; fe4d 2 spines, 1–2 rows; ti4d proximal 1.0.1, distal 1.0.1; ti4v proximal 1.1.1, distal 1.0.1. Abdomen 6.6 long; abdominal dorsal setae 0.03–0.06. Vulva (Fig. 16D–F): PD oval. DA separated from VA. DA roughly twice as wide as long, anteriorly domed. DF wide in dorsal view. MF poorly developed, visible only ventrally and posteriorly. VA roughly twice as wide as long, membranous except in anterolateral section, sclerotized and domed. AVD absent. Insertion of S projected onto VA through sclerotized neck, S oval in ventral view, with arms of moderate length and tips extended dorsolaterally.

Intraspecific variation: Male carapace varies from 4.15 to 4.97 in length and 3.2 to 3.84 in width, female carapace from 4.3 to 5.13 in length and 3.34 to 3.96 in width. Cheliceral length from 1.65 to 1.9 in males, 1.57 to 2.05 in females. Spination variability: ti3d proximal 1.0–1.1, distal 1.0.0–1; ti3v proximal 1.1.0–1, distal 0–1.0.0; fe4d 2–3 spines, 1–3 rows; ti4d proximal 1.0.1–2, distal 1.0.1; ti4v proximal 1–2.1–2.1, medial-proximal 0.0–1.0, medial-distal 0–1.0.0, distal 0–1.0–1.1.

Distribution: This species is known from the summit of the following peaks of Porto Santo island: Pico Branco (450 m), Pico da Juliana (447 m) and Pico Ana Ferreira (283 m) (Fig. 11).

Habitat: The same as that of *D. dissimilis*. *D. precaria* can be found under stones or beneath the bark of dead logs.

Conservation: The predicted geographical range of this species is 0.15 km². The conservation concerns are the same as those reported for *D. dissimilis* (e.g. habitat loss, fragmentation).

DYSDERA RECONDITA CRESPO & ARNEDO, **SP. NOV.**
(Figs 17, 25A–B, 34)
urn:lsid:zoobank.org:act:0533F035-A285-416E-8B0E-4F5CF5CBD822

Holotype: 1 ♂, 32.52571 °N 16.51131 °W, Vereda do Risco (N), Deserta Grande, Portugal, coll. 21.X.2016, hand collecting, leg. I. Silva, stored at MZB, collection number 2019-1944, DNA code lc144.

Paratypes: Deserta Grande: Rocha do Barbusano, 1 ♂ (MZB 2019-1946: k529), 31.X.2009, hand collecting, leg. P. Oromí & I. Silva; Vereda do Risco (N), 1 ♂ (FMNH KN.17860: pk677), 16.IV.2015, hand collecting, leg. I. Silva & D. Teixeira, 1 ♀, (MZB 2019-1945: lc334), 27.III.2018, hand collecting, leg. L. Crespo.

Additional material examined: Deserta Grande: Rocha do Barbusano, one juvenile (CRBA002538: pk79), 20.IV.2011, hand collecting, leg. L. Crespo, I. Silva & P. Cardoso.

Etymology: The specific epithet, from the Latin adjective *reconditus*, hidden, abstruse or secluded, refers to the restricted distribution of this species.

Diagnosis: *D. recondita* can be diagnosed from all other Madeiran *Dysdera* by: the D, trapezoidal, in both sexes (Fig. 17C). Males are further recognized
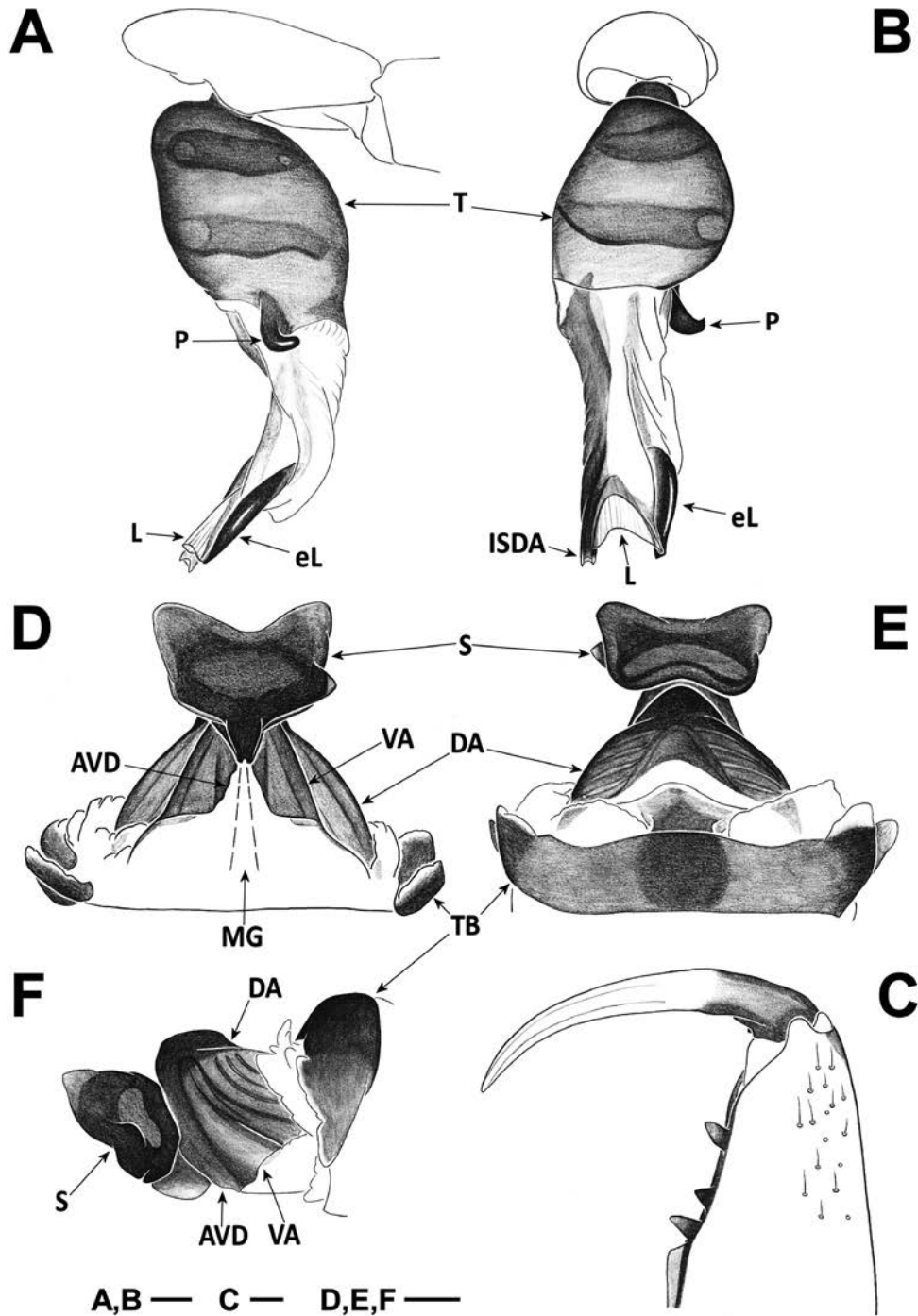
Figure 17. *D. recondita* **sp. nov.** A–C, holotype male: (A) left palp, retrolateral; (B) left palp, frontal; (C) left chelicera, ventral. D–F, female paratype (MZB 2019-1945): (D) vulva, ventral; (E) vulva, dorsal; (F) vulva, lateral. Scale bars = 0.1 mm. Abbreviations, male palp: eL, external margin of lateral sheet; ISDA, internal sclerite distal apophysis; L, lateral sheet; P, posterior apophysis; T, tegulum. Abbreviations, female vulva: AVD, additional ventral diverticulum; DA, dorsal arch; MG, medial groove; S, spermatheca; TB, transversal bar; VA, ventral arch.

by: the eL, rod-shaped (Fig. 17A–B) and females by: the VA, constricted, triangular and the AVD markedly constricted (Fig. 17D–F).

Description – male holotype (MZB 2019-1944): (Fig. 17A–C). Carapace length 3; maximum width 2.4; minimum width 1.6. Carapace brown, foveate at borders, with scanty dark grains scattered through its otherwise smooth surface. Frontal border roughly rounded, 1.46 wide; anterior lateral borders parallel; lateral borders divergent, rounded around maximum width point, after converging to posterior margin; posterior margin straight, wide. AME 0.15, oval; PLE 0.15, oval; PME 0.13, oval; AME separated from anterior border by less than their diameter; AME separated from one another by less than their diameter; AME touching PLE; PME separated from PLE by roughly one-third of PME diameter; PME touching. Labium trapezoid, with base wider than distal part, longer than wide at base; distal part concave. Sternum brown, wrinkled, with scattered setae. Chelicerae (Fig. 17C) 1.35 long, about one-third of carapace length in dorsal view, straight, dorsally and prolaterally with sclerotized piliferous granulations, their degree of sclerotization increasing towards prolateral side; fang 1.07 long. Cheliceral furrow ~44% of length of basal segment, armed with three teeth and basal lamina, D > B > M; B close to lamina, triangular, M closer to B than D, triangular, D situated in the distal half of cheliceral furrow, trapezoid. Legs greenish-yellow, coxae I slightly darker. Lengths: fe1 2.25; pa1 1.44; ti1 1.66; me1 1.63; ta1 0.5; total 7.48; fe2 2.09; pa2 1.46; ti2 1.64; me2 1.65; ta2 0.49; total 7.33; fe3 1.76; pa3 1.01; ti3 1; me3 1.46; ta3 0.46; total 5.69; fe4 1.89; pa4 1.3; ti4 1.7; me4 2.21; ta4 0.54; total 7.64; relative length: 4 > 1 > 2 > 3; fe palp 1.4; pa palp 0.8; ti palp 0.7; ta palp 0.62; total 3.52. Spination: ti3d proximal 1.1.1, distal 1.0.1; ti3v proximal 1.1.0, medial-distal 1.0.0, distal 0.0.0; fe4d 0–1 spine; ti4d proximal 1.1.1, distal 1.0–1.1; ti4v proximal 1.1.1, distal 1.0.1. Palpal coxae with moderately sclerotized piliferous granulations. Legs covered with setae, especially on tibiae, metatarsi and tarsi. Metatarsi III and IV with dense tuft of setae in distal ventral section. Claws with nine teeth. Abdomen 3.26 long, cream-coloured with dark irregular spots, cylindrical; abdominal dorsal setae short, 0.02–0.04, thick, apically blunt, uniformly distributed. Male copulatory bulbus (Fig. 17A–B): T slightly shorter than DD, external border sloped backwards. DD bent anteriorly in lateral view, more or less 30 °. IS longer and wider than ES, uniformly sclerotized, ES slightly sclerotized. ISDA present, as sclerotized pointed ridge supporting small opening at level of EO. AR hardly recognizable. L present, with eL sclerotized, rod-shaped. P claw-shaped, fused to T,

rotated retrolaterally and posteriorly, lateral length one-quarter of width of T in frontal view. Ridge present, small, perpendicular to T.

Female paratype (MZB 2019-1945): (Fig. 17D–F). All characters as in male except: carapace length 3.44; maximum width 2.78; minimum width 2.66; carapace dark brown. AME 0.18; PLE 0.15; PME 0.14. Chelicerae 1.5 long; fang 1.25 long; sclerotized piliferous granulations almost absent. Legs greenish-orange. Leg lengths: fe1 2.33; pa1 1.6; ti1 1.74; me1 1.74; ta1 0.52; total 7.93; fe2 2.23; pa2 1.52; ti2 1.64; me2 1.68; ta2 0.52; total 7.59; fe3 1.92; pa3 1.14; ti3 1.1; me3 1.65; ta3 0.5; total 6.31; fe4 2.63; pa4 1.5; ti4 1.92; me4 2.44; ta4 0.6; total 9.08; fe palp 1.36; pa palp 0.76; ti palp 0.58; ta palp 0.9; total 3.6. Spination: ti3d proximal 1.1.1, distal 1.0.1; ti3v proximal 1.1.1, distal 1.0.0; fe4d 0–1 spine; ti4d proximal 1.1.1, medio-proximal 0.0–1.1, distal 1.1.1; ti4v proximal 1.2.1, distal 1.0.1. Abdomen 3.74 long; abdominal dorsal setae long, 0.08–0.14, unmodified, with tapered tip. Vulva (Fig. 17D–F): PD oval. DA separated from VA. DA roughly twice as wide as long, anteriorly domed, dorsolaterally with 4 to 5 small inner ridges visible by transparency. DF wide in dorsal view. MF moderately developed, visible only slightly ventrally or posteriorly. VA roughly as wide as long, membranous except in its anterior section, which is sclerotized and domed. AVD present, a tubular neck reaching base of S, with poorly developed folds. Insertion of S projected onto AVD through sclerotized neck, S triangular in ventral view, with arms short and tips extended anteriorly.

Intraspecific variation: Male carapace varies from 3.0 to 3.4 in length and from 2.4 to 2.78 in width. Cheliceral length from 1.32 to 1.48 in males. Colour of carapace can vary from brown to blackish-purple. Colour of legs can vary from dark orange to pale brown. Spination variability: ti3d proximal 1.1–2.1, distal 1.0.1; ti3v 1.1–2.0–1, medial-distal 0–1.0.0, distal 0–1.0.0; fe4d 0–1 spines, 0–1 rows; t4d proximal 1.1.1, medial-proximal 0.0–1.0–1, distal 1.0–1.1; ti4v proximal 1.1–2.1, medial-proximal 0.0.0–1, distal 1.0.1.

Distribution: This species is known from the central region of Deserta Grande (Fig. 9).

Habitat: The same as that of *D. exigua*, but restricted to the island of Deserta Grande. There, it can be found under stones or in sandstone crevices.

Conservation: The conservation concerns are the same as those reported for *D. exigua* (invasive species, habitat loss, fragmentation) with the increased risk factor of an even smaller known distribution. So far

only five specimens have been found in an area of no more than 3 km².

DYSDERA SANDRAE CRESPO, **SP. NOV.**

(FIGS 18, 25C–D, 35, 37F)

urn:lsid:zoobank.org:act:CCAA1A02-5EF7-4B3A-9828-B838CD90BD69

Holotype: 1 ♂, 32.50596 °N 16.49986 °W, Planalto Sul, Deserta Grande, Portugal, coll. 18.IV.2012, hand collecting, leg. L. Crespo, I. Silva & P. Cardoso, stored at MZB, collection number 2019-1929.

Paratypes: Deserta Grande: Eira, 1 ♂ (MZB 2019-1930: pk72), 17.IV.2011, hand collecting, leg. L. Crespo, I. Silva & P. Cardoso, 1 ♂ (MMF 47911: pk220), 9–23.V.2012, hand collecting, leg. A. Serrano *et al.*; Planalto Sul, 1 ♀ (MZB 2019-1931), 18.IV.2012, hand collecting, leg. L. Crespo, I. Silva & P. Cardoso; Vale da Castanheira (S), 1 ♀ (FMNH KN.17851: lc335), 25.III.2018, hand collecting, leg. L. Crespo; Vereda do Risco, 1 ♂ (NMH001593: k523), 1 ♀ (MZB 2019-1932: k528), 31.X.2009, hand collecting, leg. I. Silva & P. Oromí, 1 ♀ (MMF 47912: pk72), 19.IV.2011, hand collecting, leg. L. Crespo, I. Silva & P. Cardoso, 1 ♂ (FMNH KN.17850: pk77), 11.IV.2012, hand collecting, leg. L. Crespo, I. Silva & P. Cardoso.

Additional material examined: Deserta Grande: Poço da Fajã Grande, 1 ♂ (LCPC: pk75), 10.IV.2012, hand collecting, leg. L. Crespo, I. Silva & P. Cardoso.

Etymology: The specific epithet is a patronym in honour of Sandra Videira, partner of the first author, for the unconditional help, support and kindness given throughout the years.

Diagnosis: D. sandrae can be diagnosed from all other Madeiran *Dysdera* by: the D, short, blunt, in both sexes (Fig. 18C). Males are further recognized by: eL, claw-shaped, ISDA, massive (Fig. 18A–B) and females by: the AD, highly constricted and AVD, well developed (Fig. 18D–F).

Description – male holotype (MZB 2019-1930): (Figs 18A–C, 25C–D). Carapace length 3.36; maximum width 2.56; minimum width 1.74. Reddish-brown; foveate at borders, with scanty dark grains scattered through its otherwise smooth surface. Frontal border roughly rounded, 1.6 wide; anterior lateral borders slightly divergent; lateral borders rounded; posterior margin straight, short. AME 0.16, nearly rounded; PLE 0.15, oval; PME 0.13, rounded; AME separated from anterior border by slightly less

than their diameter; AME separated from one another by less than their diameter; AME touching PLE; PME separated from PLE by roughly one-third of PME diameter; PME almost touching. Labium trapezoid, with base wider than distal part, longer than wide at base; distal part slightly concave, with some setae. Sternum dark orange, darkened on lateral borders, wrinkled, with scattered straight setae. Chelicerae (Fig. 18C) 1.24 long, about one fifth of carapace length in dorsal view; fang 0.9 long; basal segment basally protuberant, straight, dorsally and ventrally with abundant sclerotized piliferous granulations. Cheliceral furrow ~35% of length of basal segment, armed with three teeth and basal lamina, B > M > D; B close to lamina, triangular, M close to B, triangular, D situated at groove midpoint, wide and short. Legs orange, anterior pairs slightly darker than posterior pairs. Lengths: fe1 2.66; pa1 1.62; ti1 2.15; me1 2.20; ta1 0.52; total 9.15; fe2 2.43; pa2 1.56; ti2 1.97; me2 2.13; ta2 0.5; total 8.58; fe3 2; pa3 1.14; ti3 1.28; me3 1.86; ta3 0.48; total 6.76; fe4 2.63; pa4 1.48; ti4 2.08; me4 2.66; ta4 0.58; total 9.42; relative length: 4 > 1 > 2 > 3; fe palp 1.59; pa palp 0.9; ti palp 0.74; ta palp 0.85; total 4.08. Spination: ti3d proximal 1.0.1, distal 1.0.1; ti3v proximal 1.1.0, distal 0.0.0; fe4d 1–2 spines, 1 row; ti4d proximal 1.0.1, distal 1.0.1; ti4v proximal 1.1.1, distal 1.0.1. Palpal coxae with lightly sclerotized piliferous granulations. Legs covered with setae, especially on tibiae, metatarsi and tarsi. Metatarsi III and IV with dense tuft of setae in distal ventral section. Claws with eight to nine teeth. Abdomen 3.88 long, greyish yellow, cylindrical; abdominal dorsal setae short, 0.01–0.02, thick, apically blunt, uniformly distributed. Male copulatory bulbus (Fig. 18A–B): T shorter than DD, external border sloped backwards. DD bent anteriorly in lateral view, more or less 30 °. IS as long as ES, both sclerites distally more sclerotized than basally. ISDA present, as massive laminar outgrowth. AR absent. L present, with external margin heavily sclerotized, claw-shaped. P claw-shaped, fused to T, directed to retrolateral side, lateral length one-quarter of width of T in frontal view. Ridge present, not expanded, parallel to T.

Female paratype (MZB 2019-1931): (Fig. 18D–F). All characters as in male except: carapace length 4.2; maximum width 3.22; minimum width 2.13; AME 0.2, PME and PLE 0.1; AME separated from one another by more than their diameter. Chelicerae 1.5 long; fang 1.1 long. Leg lengths: fe1 2.75; pa1 1.8; ti1 2.25; me1 2.24; ta1 0.62; total 9.66; fe2 2.63; pa2 1.68; ti2 2.1; me2 2.1; ta2 0.62; total 9.13; fe3 2.19; pa3 1.28; ti3 1.4; me3 1.96; ta3 0.52; total 7.35; fe4 3; pa4 1.68; ti4 2.35; me4 2.75; ta4 0.68; total 10.46; fe palp 1.46; pa palp 0.84; ti palp 0.66; ta palp 0.96; total 3.92. Spination:
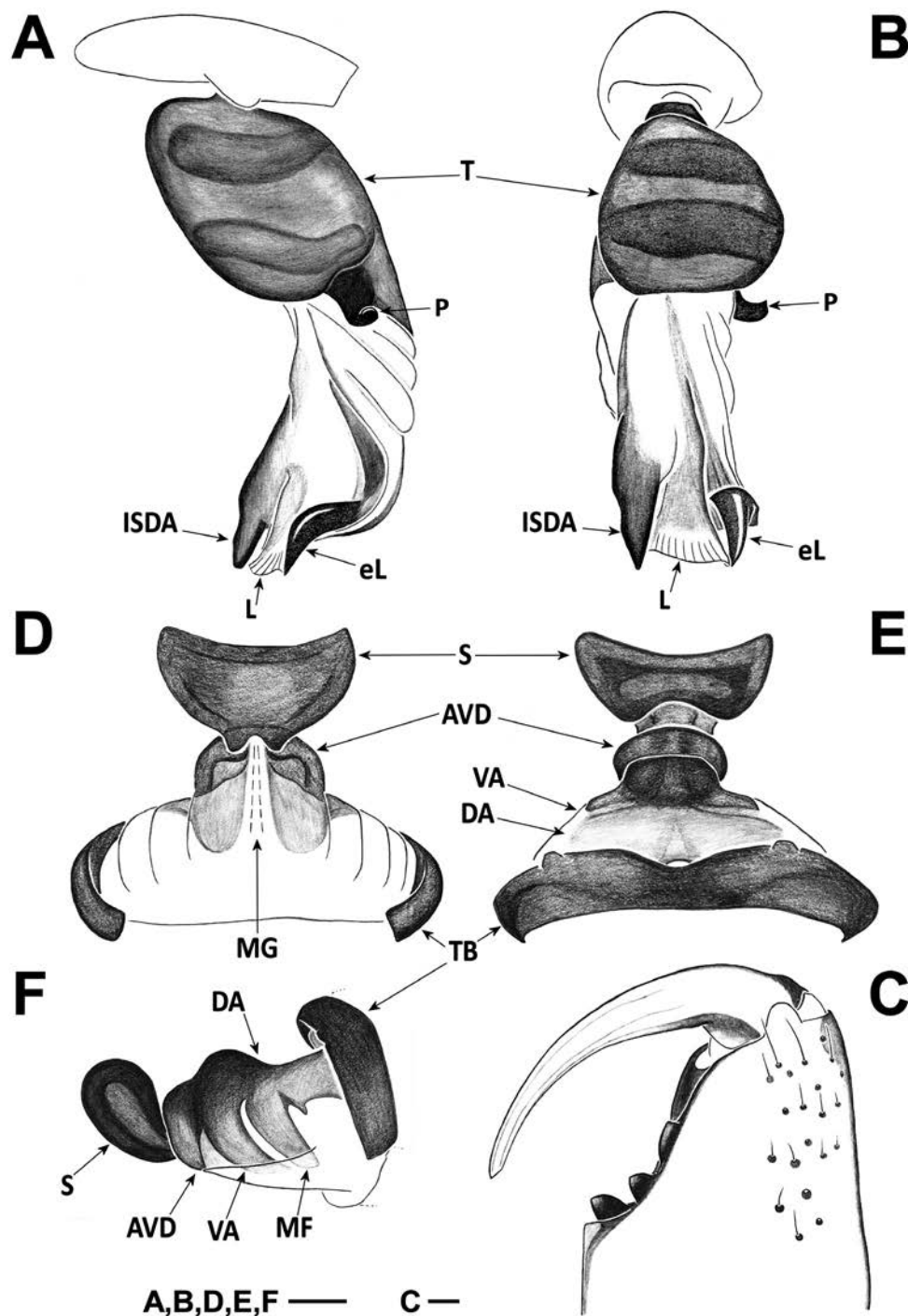
Figure 18. *D. sandrae* **sp. nov.** A–C, holotype male: (A) left palp, retrolateral; (B) left palp, frontal; (C) left chelicera, ventral. D–F, female paratype (MZB 2019-1931): (D) vulva, ventral; (E) vulva, dorsal; (F) vulva, lateral. Scale bars = 0.1 mm. Abbreviations, male palp: eL, external margin of lateral sheet; ISDA, internal sclerite distal apophysis; L, lateral sheet; P, posterior apophysis; T, tegulum. Abbreviations, female vulva: AVD, additional ventral diverticulum; DA, dorsal arch; MG, medial groove; S, spermatheca; TB, transversal bar; VA, ventral arch.

ti3v proximal 1.1.0, distal 1.0.0; fe4d 3 spines, 2 rows; ti4d proximal 1.1.1, distal 1.0.1; ti4v proximal 1.1.1–2, medial-proximal 0.0.1, distal 1.0.1. Abdomen 4.45 long; abdominal dorsal setae short, 0.03–0.07. Vulva (Fig. 18D–F): PD oval. DA separated from VA. DA roughly twice as wide as long. DF wide in dorsal

view. MF well developed, sclerotized, well visible in ventral and lateral views. VA roughly as wide as long, membranous except in its anterior section, sclerotized. AVD present, sclerotized. Insertion of S projected onto AVD, S ventrally subtriangular, dorsally concave both anteriorly and posteriorly, with arms short and tips slightly curved anteriorly.

Intraspecific variation: Male carapace varies from 3.2 to 3.8 in length and 2.47 to 2.97 in width, female carapace from 3.48 to 4.2 in length and 2.72 to 3.22 in width. Cheliceral length from 1.18 to 1.44 in males, and 1.2 to 1.5 in females. Carapace coloration ranges from reddish-brown to dark-brown. Female vulva from specimen FMNH KN.17851 (the single specimen collected from the northern half of Deserta Grande island) presents an AVD slightly more extended ventrally than the illustrated specimen. Spination variability: ti3d proximal 1.0–1.1, medial-proximal 0.0–1.0–1, distal 1.0.1; ti3v proximal 1.1.0, distal 0–1.0.0; fe4d 1–4 spines, 1–3 rows; ti4d proximal 1.0–2.1–2, medial-proximal 0.0–1.0, distal 0–1.0–1.0–1; ti4v proximal 1.1–3.0–2, medial-proximal 0.0–1.0–1, medial-distal 0–1.0.0, distal 0–1.0.0–1.

Distribution: This species is known from several locations along the entire length of the island of Deserta Grande.

Habitat: The same as that of *D. exigua* (see above), but restricted to the island of Deserta Grande. There, it can be found under stones or in sandstone crevices.

Conservation: The predicted geographical range of the species is 8 km². The conservation concerns are the same as those reported for *D. coiffaiti* (invasive species, habitat loss, fragmentation), but the species is restricted to the island of Deserta Grande.

DYSDERA TEIXEIRAI Crespo & Cardoso, **SP. NOV**.

(Figs 19, 26A–B, 36)

urn:lsid:zoobank.org:act:6CB21C01-112F-4815-BD06-F597EC8BD11B

Holotype: 1 ♂, 32.53168 °N 16.51471 °W, Rocha do Barbusano (S), Deserta Grande, Portugal, coll. 10.IV.2017, hand collecting, leg. L. Crespo & I. Silva, stored at MZB, collection number 2019-1933, DNA code lc049.

Paratypes: Deserta Grande: Vereda do Risco, 1 ♂ (NMH001596: k526), 31.X.2009, hand collecting, leg. I. Silva & P. Oromí; Rocha do Barbusano, 1 ♂ (MMF 47913: pk78), 20.IV.2011, hand collecting, leg.

L. Crespo, I. Silva & P. Cardoso; Rocha do Barbusano (S), 1 ♀ (MZB 2019-1934), 27.III.2018, hand collecting, leg. L. Crespo; Pedregal (E), 1 ♂ (MZB 2019-1935: pk676), 16.IV.2015, hand collecting, leg. I. Silva & D. Teixeira, 1 ♂ (FMNH KN.17852: lc068), 8.IV.2017, hand collecting, leg. I. Silva, 1 ♀ (FMNH KN.17853: lc301), 9.IV.2017 (reared in captivity, found adult, dried, on 14.VIII.2017), hand collecting, leg. L. Crespo.

Additional material examined: Deserta Grande: Rocha do Barbusano, 1 juvenile (CRBALC0110: lc067), 8.IV.2017, hand collecting, leg. L. Crespo; Rocha do Barbusano (S), 3 juveniles (CRBALC0083: lc055, CRBALC0103: lc060, CRBALC0198: lc132), 10.IV.2017, hand collecting, leg. L. Crespo & I. Silva, 1 ♂ (LCPC) and 3 juveniles (CRBALC0583, CRBALC0588: lc333, CRBALC0685), 27.III.2018, hand collecting, leg. L. Crespo.

Etymology: The specific epithet is a patronym in honour of Dinarte Teixeira, malacologist at Madeira's Instituto das Florestas e Conservação da Natureza (IFCN), who called our attention to the existence of a great number of new species of *Dysdera* in the Madeira archipelago.

Diagnosis: *D. teixeirai* can be diagnosed from all other Madeiran *Dysdera* in males by: eL, sickle-shaped, C, membranous, thin (Fig. 19A–B), in females by: AVD, reduced, SD, oval (Fig. 19D–I).

Description – male holotype (MZB 2019-1933): (Figs 19A–C, 26A–B). Carapace length 3.76; maximum width 3.06; minimum width 2.15. Carapace blackish, foveate at borders, with scanty dark grains scattered through its otherwise smooth surface, with two small circular depressions, one behind cephalic region, the other near the posterior margin. Frontal border roughly rounded, 2.1 wide; anterior lateral borders parallel; lateral borders divergent, rounded around maximum width point, after converging to posterior margin; posterior margin straight, wide. AME 0.21, oval; PLE 0.19, oval; PME 0.16, rounded; AME separated from anterior border by less than their diameter; AME separated from one another by less than their diameter; AME touching PLE; PME separated from PLE by roughly one-third of PME diameter; PME almost touching. Labium trapezoid, with base wider than distal part, longer than wide at base; distal part slightly concave, with some setae. Sternum brown, darkened on lateral borders, wrinkled, with scattered straight setae. Chelicerae (Fig. 19C) 1.76 long, about one-third of carapace length in dorsal view, straight, dorsally with sclerotized piliferous granulations and abundantly wrinkled; fang 1.5 long. Cheliceral furrow ~51% of length of basal segment,
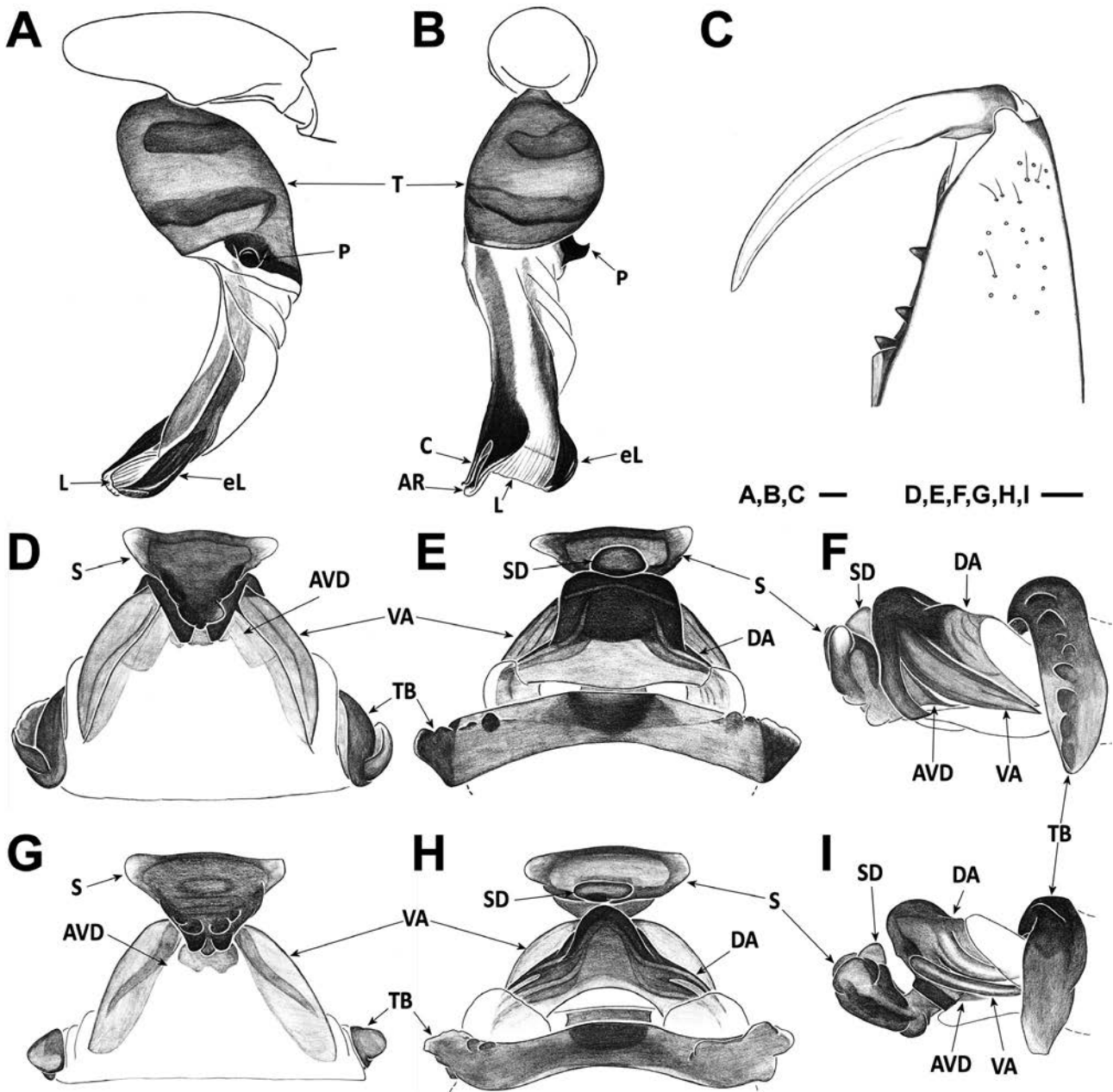
Figure 19. *D. teixeirai* **sp. nov.** A–C, holotype male: (A) left palp, retrolateral; (B) left palp, frontal; (C) left chelicera, ventral. D–F, female paratype (MZB 2019-1934): (D) vulva, ventral; (E) vulva, dorsal; (F) vulva, lateral. G–I, female paratype (FMNH KN.17853): (G) vulva, ventral; (H) vulva, dorsal; (I) vulva, lateral. Scale bars = 0.1 mm. Abbreviations, male palp: AR, arch-like ridge; C, crest; eL, external margin of lateral sheet; L, lateral sheet; P, posterior apophysis; T, tegulum. Abbreviations, female vulva: AVD, additional ventral diverticulum; DA, dorsal arch; MG, medial groove; S, spermatheca; SD, spermatheca diverticulum; TB, transversal bar; VA, ventral arch.

armed with three teeth and basal lamina, B = M = D; all teeth triangular, B close to lamina, M closer to B than D, D situated in distal half of cheliceral furrow. Legs greenish-yellow, coxae and femora of anterior pairs slightly darker. Lengths: fe1 2.75; pa1 1.8; ti1 2.2; me1 2.23; ta1 0.57; total 9.55; fe2 2.48; pa2 1.66; ti2 1.96; me2 2.08; ta2 0.56; total 8.73; fe3 2.13; pa3 1.24; ti3 1.24; me3 1.76; ta3 0.51; total 6.88; fe4 2.66; pa4 1.58; ti4 1.94; me4 2.45; ta4 0.59; total 9.22; relative length: 1 > 4 > 2 > 3; fe palp 1.74; pa palp 1; ti palp 0.88;

ta palp 0.86; total 4.48. Spination: ti3d proximal 1.1.1, distal 1.0.1; ti3v proximal 1.1.0, distal 1.0.0; fe4d 1–3 spines, 1–2 rows; ti4d proximal 1.0.1, distal 1.0.1; ti4v proximal 1.1.1, medial-distal 1.0.0, distal 0.0.0. Palpal coxae with sclerotized piliferous granulations. Legs covered with setae, especially on tibiae, metatarsi and tarsi; anterior metatarsi with sclerotized piliferous granulations ventrally. Metatarsi III and IV with dense tuft of setae in distal ventral section. Claws with seven to eight teeth. Abdomen 4.25 long, greyish, cylindrical; abdominal dorsal setae short, 0.01–0.03, thick, apically blunt, uniformly distributed. Male copulatory bulbus (Fig. 19A–B): T shorter than DD, external border sloped backwards. DD bent anteriorly in lateral view, more or less 45 °. IS as long as ES, wider, more sclerotized than ES. C present, thin. AR present, small. Sickle-shaped ridge present roughly medially. L present, with eL sclerotized, sickle-shaped. P claw-shaped, fused to T, rotated to retrolateral side,

lateral length one fifth of width of T in frontal view. Ridge present, not expanded, parallel to T.

Female paratype (MZB 2019-1934): (Fig. 19D–F). All characters as in male except: carapace length 3.36; maximum width 2.69; minimum width 1.84; AME 0.19. Chelicerae 1.65; fang 1.39. Leg lengths: fe1 2.38; pa1 1.6; ti1 1.88; me1 1.9; ta1 0.52; total 8.28; fe2 2.2; pa2 1.46; ti2 1.7; me2 1.78; ta2 0.54; total 7.68; fe3 1.86; pa3 1.1; ti3 1.08; me3 1.56; ta3 0.5; total 6.1; fe4 2.52; pa4 1.45; ti4 1.85; me4 2.29; ta4 0.56; total 8.66; fe palp 1.37; pa palp 0.77; ti palp 0.61; ta palp 0.9; total 3.65. Spination: fe3 1 spine; ti3d proximal 1.0.1, distal 1.0.1; ti3v proximal 1.1.0, distal 0–1.0.0; fe4d 3–4 spines, 1–3 rows; ti4v proximal 1.1.1, medial-proximal 0.0–1.0, distal 1.0.0. Abdomen 4.58 long; abdominal dorsal setae variable, 0.04–0.15. Vulva (Fig. 19D–F): PD rounded. DA separated from VA. DA roughly twice as wide as long, anteriorly truncated. DF
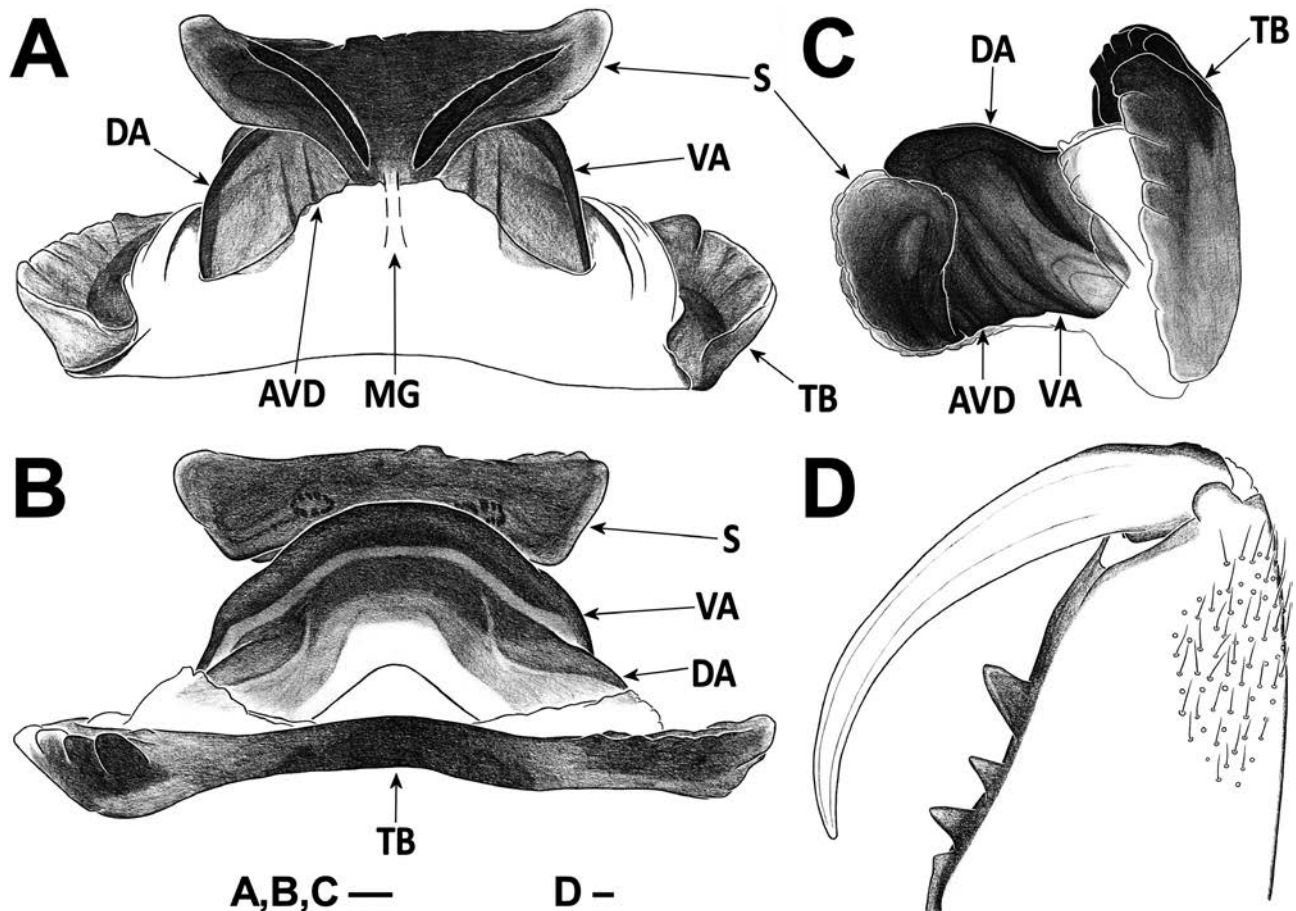

Figure 20. *D. titanica* **sp. nov.** A–D, holotype female: (A) vulva, ventral; (B) vulva, dorsal; (C) vulva, lateral; (D) mirrored image of right chelicera, ventral. Scale bars = 0.1 mm. Abbreviations: AVD, additional ventral diverticulum; DA, dorsal arch; MG, medial groove; S, spermatheca; SD, spermatheca diverticulum; TB, transversal bar; VA, ventral arch.
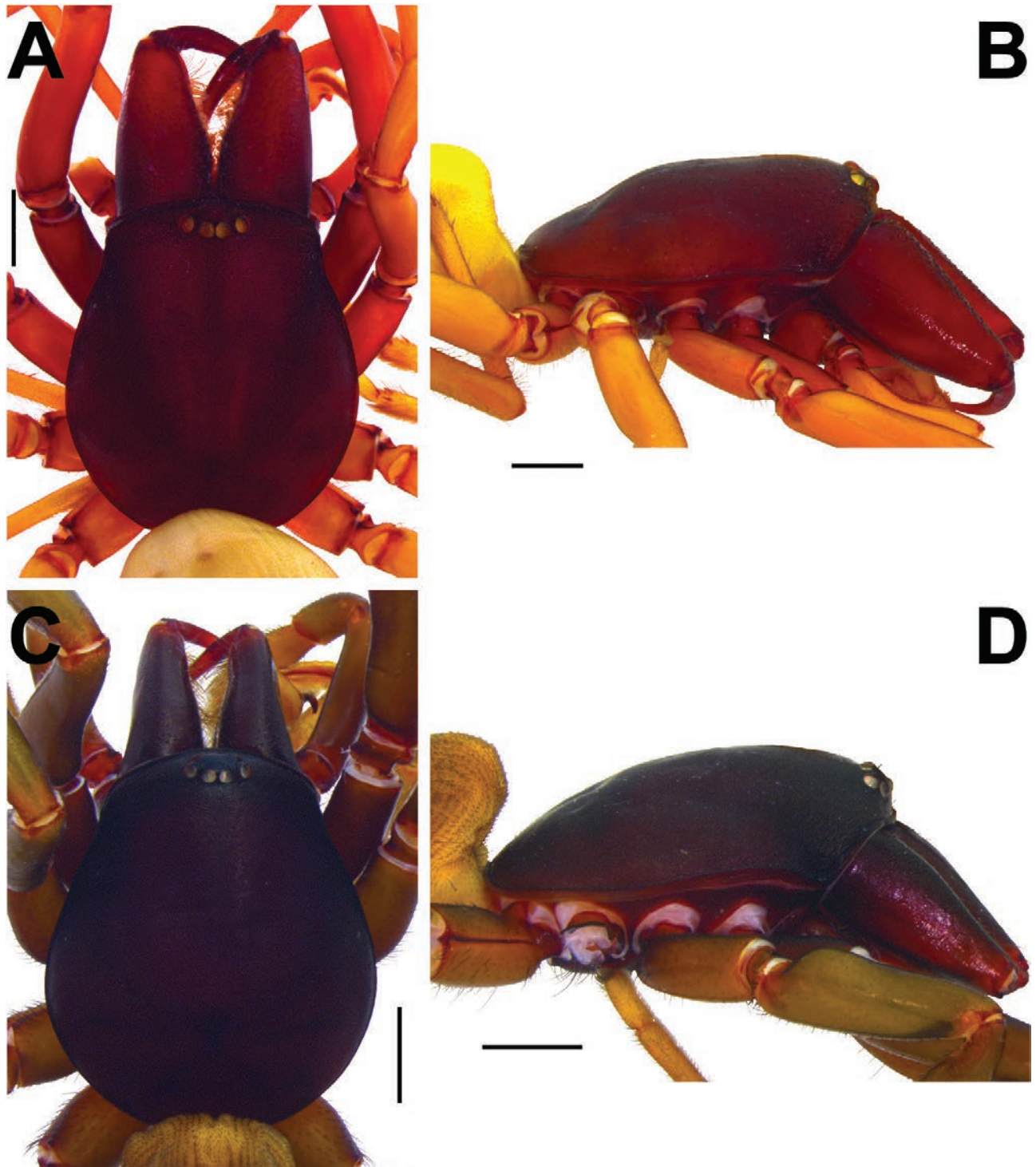
Figure 21. A–B, *D. coiffaiti*: (A) holotype male (MNHNP AR5855), prosoma, dorsal; (B) male (MZB 2019-1959), prosoma, lateral; C–D, ***D. dissimilis* sp. nov.**, holotype male (MZB 2019-1947): (C) prosoma, dorsal; (D) prosoma, lateral. Scale bars = 1 mm.
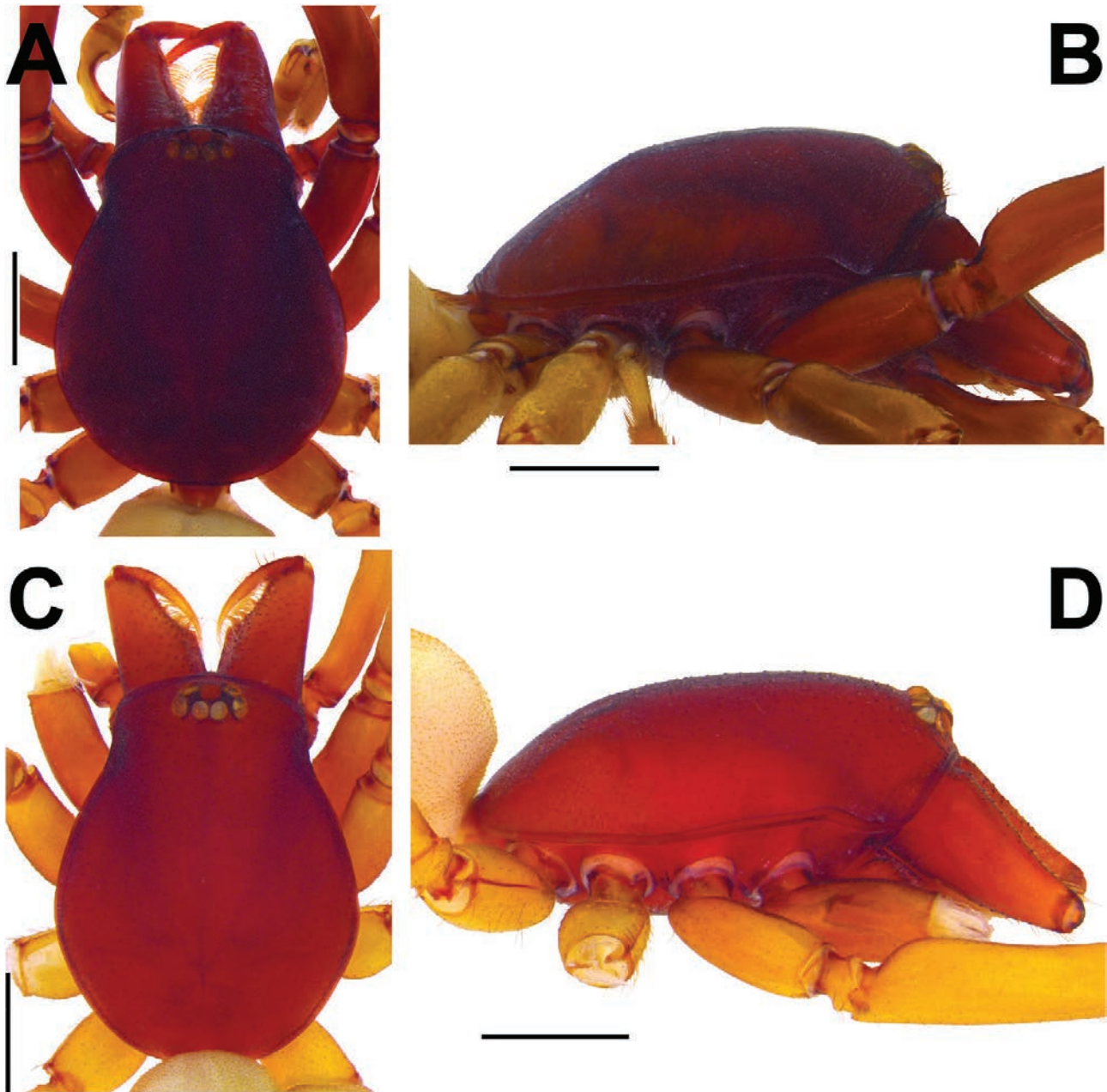
Figure 22. A–D, *D. diversa*. A–B, holotype male (OUMNH): (A) prosoma, dorsal; (B) prosoma, lateral; C–D, *D. vandeli*, male (MNHNP AR5843): (C) prosoma, dorsal; (D) prosoma, lateral. Scale bars = 1 mm.

wide in dorsal view. MF moderately developed, lightly sclerotized. VA slightly wider than long, membranous except in its anterior section, which is sclerotized. AVD present, small. Insertion of S projected onto AVD through sclerotized neck, S triangular in ventral view, with arms short and tips slightly extended laterally, with small ovoid diverticulum dorsally.

Intraspecific variation: Male carapace varies from 3.48 to 3.76 in length, from 2.72 to 3.06 in width,

female from 3.36 to 3.4 in length and 2.66 to 2.69 in width. Cheliceral length from 1.6 to 1.76 in males, and 1.52 to 1.65 in females. The vulva of the only two females available varies considerably in sclerotization and shape, namely in the shape of the DA, which can be anteriorly truncated to triangular (in dorsal view) and can have variable differentiation of lateral sulci (in lateral and anterior view, the latter not illustrated) and the small diverticulum present in the S, which can be ovoid to slit-shaped (see vulva of paratype FMNH
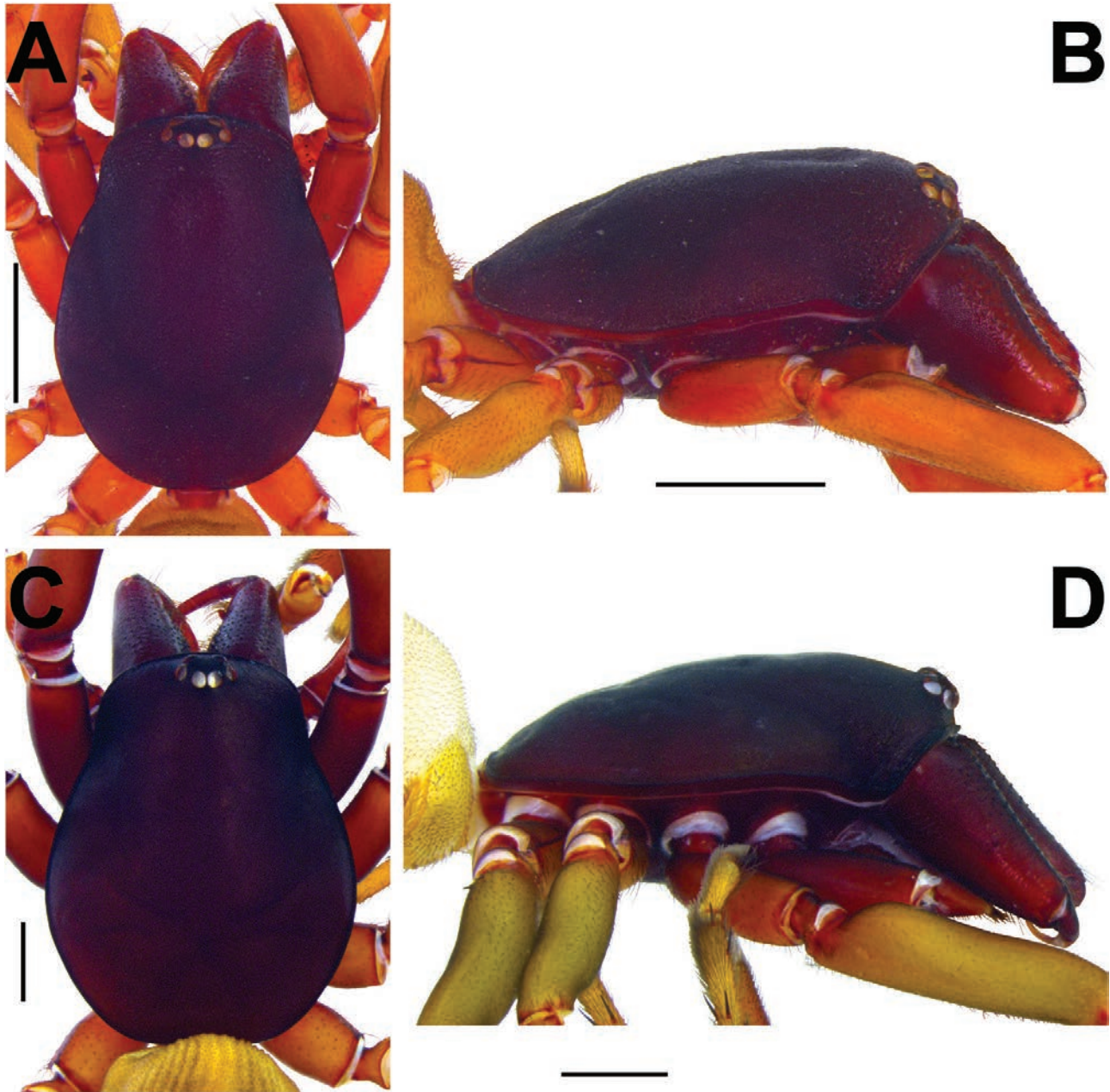
Figure 23. A–B, ***D. exigua* sp. nov.**, holotype male (MZB 2019-1936): (A) prosoma, dorsal; B, prosoma, lateral. C–D, ***D. isambertoi* sp. nov.**: (C) holotype male (MZB 2019-1951), prosoma, dorsal; (D) male (CRBALC0693), prosoma, lateral. Scale bars = 1 mm.

KN.17853, Fig. 19G–I). Spination variability: fe3d 0–1 spines, 1 row; ti3d proximal 1.0–1.1–2, distal 1.0.1; ti3v proximal 0–1.0–1.0–1, medial-distal 0–1.0.0, distal 0–1.0–1.0; fe4d 1–4 spines, 1–3 rows; ti4d proximal 1.0.1–2, distal 1.0.1; ti4v proximal 1.1–2.1, medial-proximal 0.0–1.0, medial-distal 0–1.0.0, distal 0–1.0.0–1.

Distribution: This species is known from several locations across the entire length of the island of Deserta Grande (Fig. 9).

Habitat: The same as that of *D. exigua* (see above), but restricted to the island of Deserta Grande. There, it can be found under stones or in sandstone crevices.
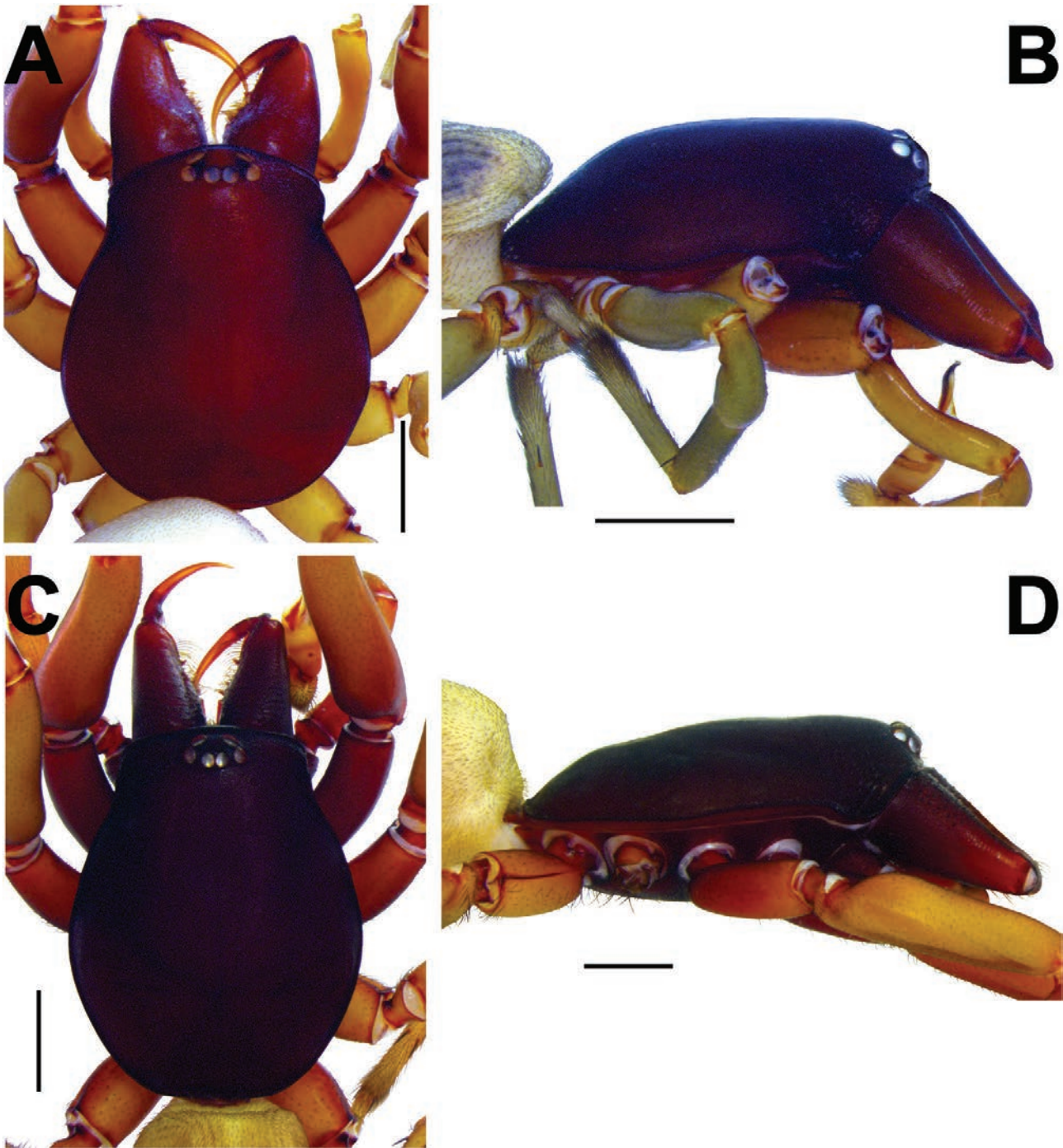
Figure 24. A–B, *D. portisancti*: (A) holotype male (SMF 37633), prosoma, dorsal; (B) male (MZB 2019-1957), prosoma, lateral. C–D, ***D. precaria* sp. nov.**: (C) holotype male (MZB 2019-1940), prosoma, dorsal; (D) paratype male (MMF 47918), prosoma, lateral. Scale bars = 1 mm.

Conservation: The predicted geographical range of the species is 5 km². The conservation concerns are the same as those reported for *D. coiffaiti* (invasive species, habitat loss, fragmentation), but the species is restricted to the island of Deserta Grande.
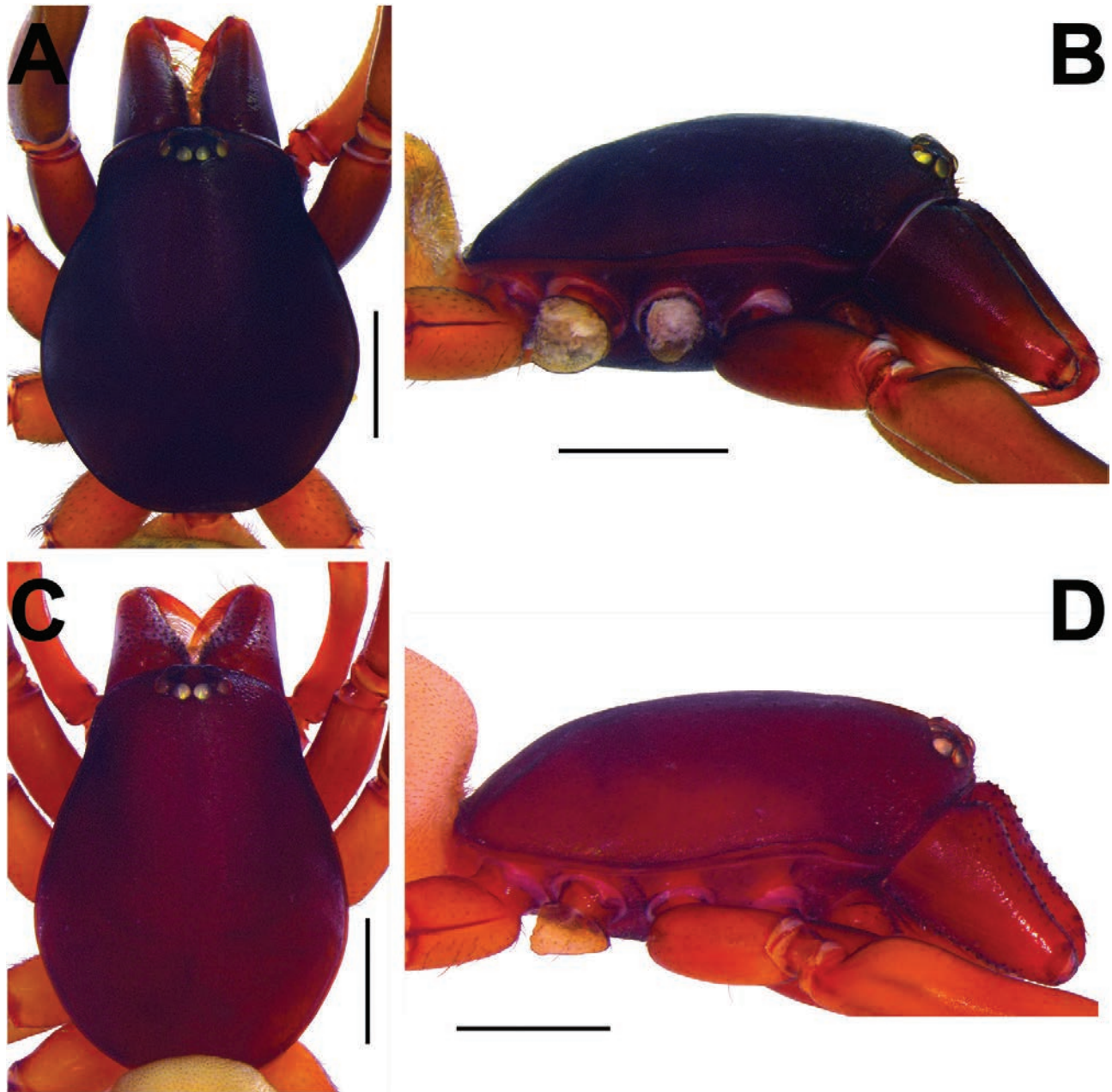
Figure 25. A–B, *D. recondita* **sp. nov.**, paratype male (FMNH KN.17860): (A) prosoma, dorsal; (B) prosoma, lateral. C–D, *D. sandrae* **sp. nov.**, holotype male (MZB 2019-1929): (C) prosoma, dorsal; (D) prosoma, lateral. Scale bars = 1 mm.

DYSDERA TITANICA CRESPO & ARNEDO, **SP. NOV.**

(Figs 20, 26C–D)

urn:lsid:zoobank.org:act:F588C592-F367-4159-9EB3-ED66AAEDE2A9

Holotype: 1 ♀ (with detached vulva), (no location), Madeira (the vial label refers to "Madera"), Portugal, (no collection information), stored at MIZ, collection number 144509, determined by W. Kulczynski.

Etymology: The specific epithet is derived from Ancient Greek Τιτάν, a race of giant sun gods, and the Greek suffix, -ικός, pertaining to. Combined, this forms the adjective titanic, which in English usually refers to something large, in this case the large size of the species.

Diagnosis: This species can be differentiated from all other Madeiran *Dysdera* by its large body size and the D, clearly larger than B and M (Fig. 20D).
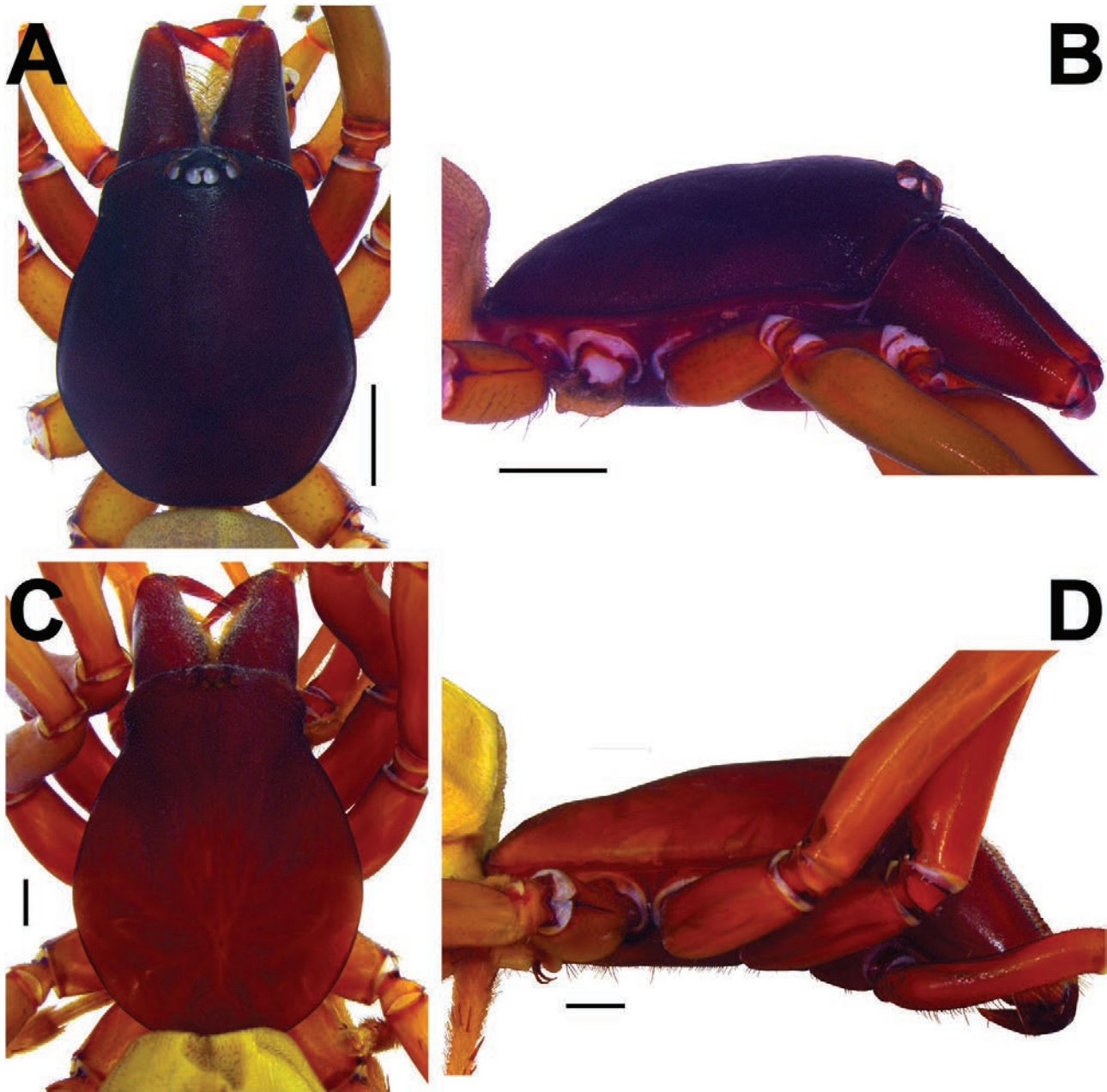
Figure 26. A–B, ***D. teixeirai* sp. nov.**, holotype male (MZB 2019-1933): (A) prosoma, dorsal; (B) prosoma, lateral. C–D, ***D. titanica* sp. nov.**, holotype female (MIZ 144509): (C) prosoma, dorsal; (D) prosoma, lateral. Scale bars = 1 mm.

Description – female holotype (MIZ 144509): ([Figs 20](#), [26C–D](#)). Carapace length 8.3; maximum width 6.56; minimum width 4. Carapace brown, foveate at borders, smooth. Frontal border roughly rounded, 4 wide; anterior lateral borders slightly convergent; lateral borders divergent until maximum width point, then converging to posterior margin, around maximum width point carapace surpasses lateral fovea (best seen in dorsal view); posterior margin straight, wide. AME 0.31, oval; PLE 0.29, oval; PME 0.26, rounded;

AME separated from anterior border by more than their diameter; AME separated from one another by more than their diameter; AME touching PLE; PME separated from PLE by roughly one-third of PME diameter; PME touching. Labium trapezoid, with base wider than distal part, longer than wide at base; distal part concave. Sternum brown, wrinkled, with setae. Chelicerae ([Fig. 20D](#)) 3.68 long, about one-third of carapace length in dorsal view, straight, dorsally and ventrally with abundant sclerotized piliferous

Figure 27. A–D, SEM mirrored images of distal left palp of *D. coiffaiti*, male: (A) ventral detail, 800×; (B) apical, 200×; (C) fr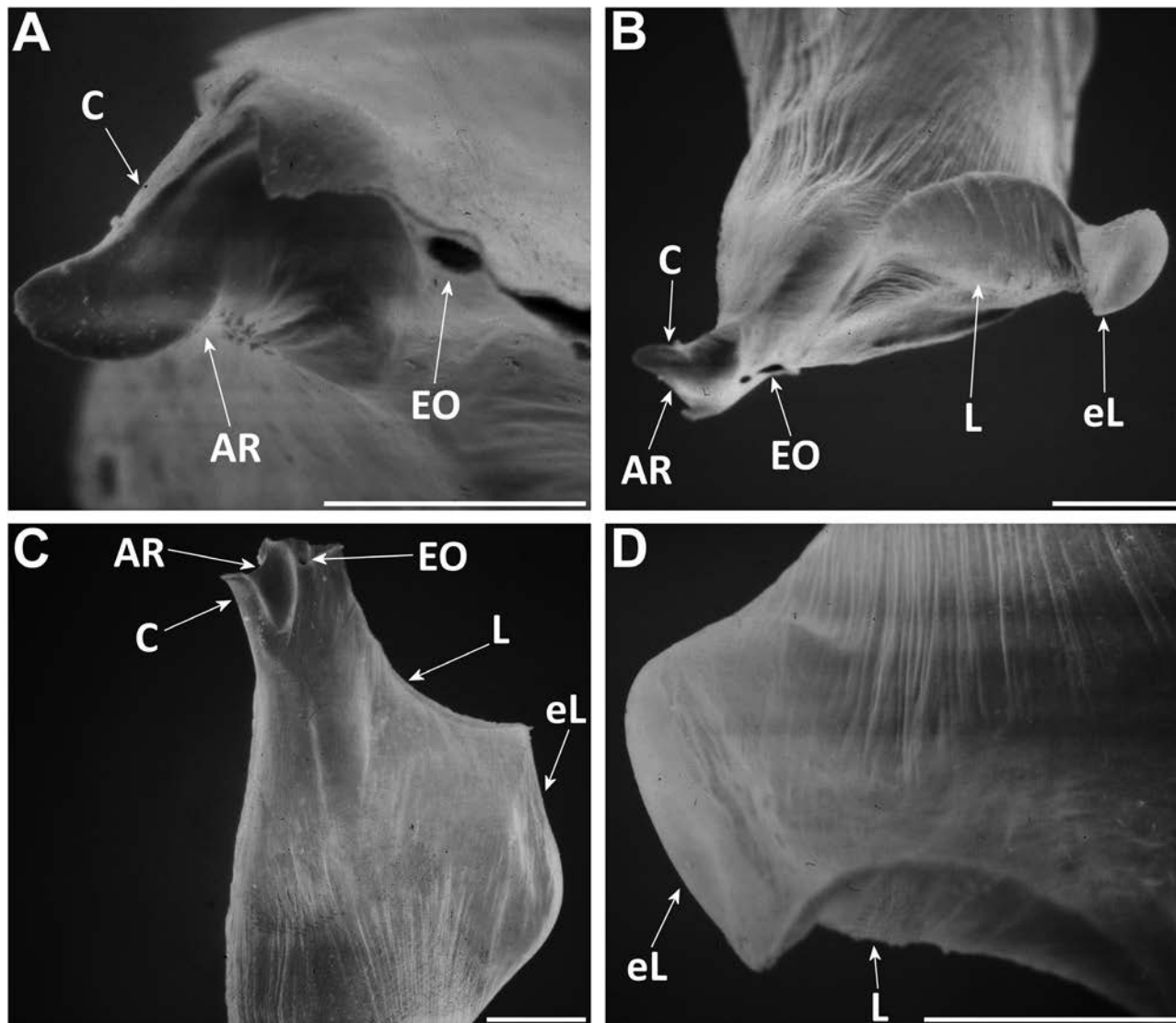ontal, 150×; (D) anterior retrolateral detail, 400×. Scale bars: A = 0.05 mm; B, C, D = 0.1 mm. Abbreviations: AR, arch-like ridge; C, crest; eL, external margin of lateral sheet; EO, embolus opening; L, lateral sheet.

granulations; fang 3.05 long. Cheliceral furrow ~46% of length of basal segment, armed with three teeth and basal lamina, D > B > M; all teeth triangular, B close to lamina, M slightly closer to B than D, D situated at groove midpoint. Anterior legs and palp orange, posterior legs light orange. Lengths: fe1 7.52; pa1 5.25; ti1 6.88; me1 6.64; ta1 1.22; total 27.51; fe2 6.92; pa2 4.55; ti2 6.13; me2 6.13; ta2 1.2; total 24.92; fe3 5.63; pa3 3.32; ti3 4.1; me3 5.38; ta3 1.24; total 19.66; fe4 7.28; pa4 3.96; ti4 5.69; me4 7.2; ta4 1.34; total 25.47; relative length: 1 > 4 > 2 > 3; fe palp 4.7; pa palp 2.38; ti palp 2.28; ta palp 2.43; total 11.78. Spination: fe3 1–2 spines, 1–2 rows; ti3d proximal 1.0.1–2, medial-proximal 1.0.1, medial-distal 0–1.0.0, distal 1.0.1; ti3v proximal 0–1.1.0, medial-proximal 1–2.1.1,

medial-distal 0–1.1–2.0, distal 0–1.0.1; fe4d 7–8 spines, 6–7 rows; ti4d proximal 1.0.2, medial-proximal 1.0.1, medial-distal 0.0.0, distal 1.0.1; ti4v proximal 1–2.1–3.1, medial-proximal 1.1–3.1–2, medial-distal 2.2–3.1–2, distal 2–3.0–1.0–1. Palpal coxae with few moderately sclerotized piliferous granulations. Legs covered with setae, especially on tibiae, metatarsi and tarsi. All tibiae with dorsal dense patch of short, moderately thick, setae. All metatarsi with small dorsal distal patch of setae, III and IV also with dense tuft of setae in distal ventral section. Claws with seven to nine teeth. Abdomen 10.88 long, yellow, cylindrical; abdominal dorsal setae (most are torn off, only a small patch is present), 0.1–0.15, of intermediate thickness, tapered, uniformly distributed. Vulva (Fig. 20A–C): PD
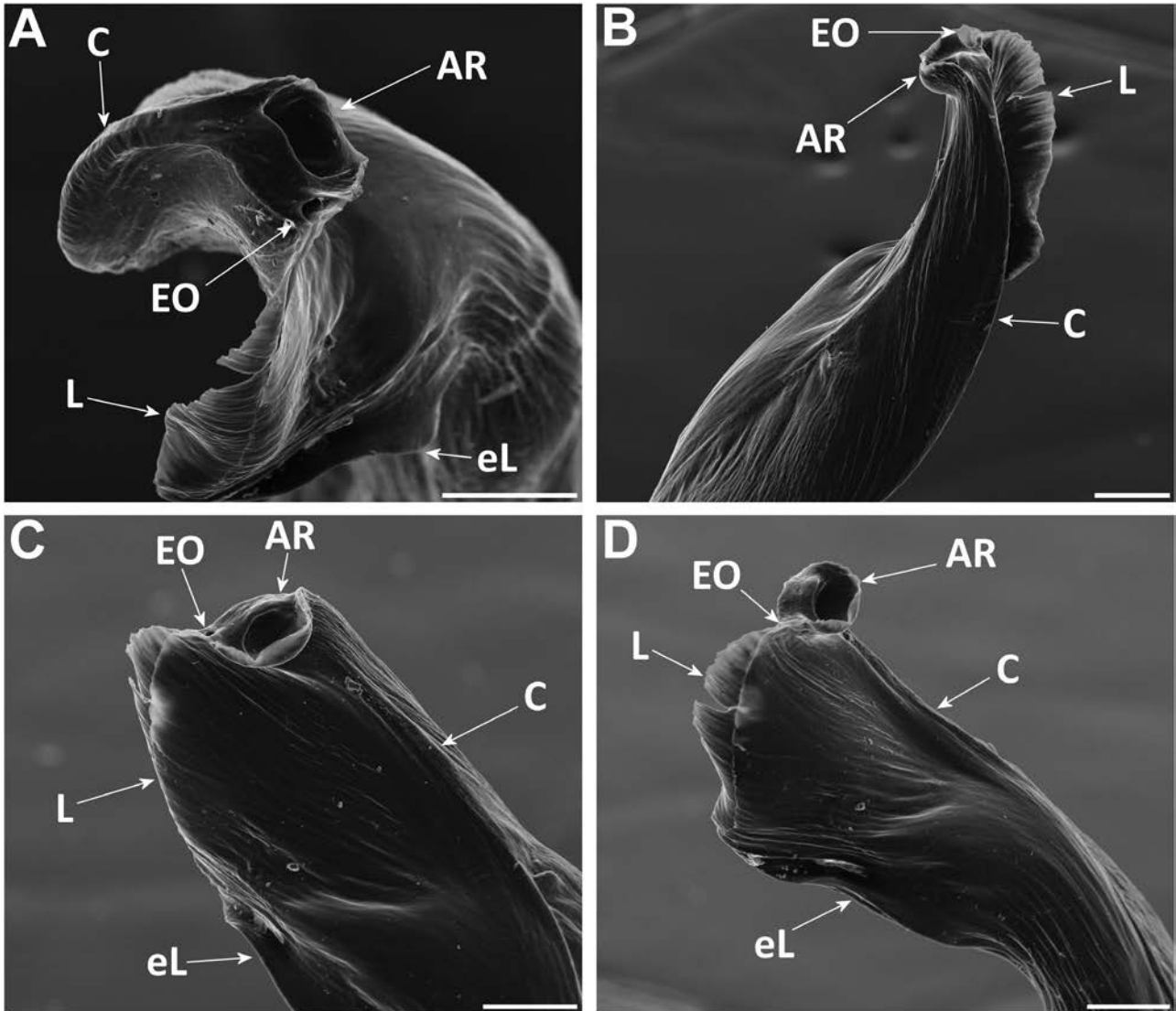
Figure 28. A–D, SEM images of distal right palp of **D. dissimilis sp. nov.**, paratype male (MZB 2019-1949): (A) ventral detail, 696×; (B) prolateral, 388×; (C) frontal, 486×; (D) retrolateral, 428×. Scale bars = 0.1 mm. Abbreviations: AR, arch-like ridge; C, crest; eL, external margin of lateral sheet; EO, embolus opening; L, lateral sheet.

oval. DA separated from VA. DA more than twice as wide as long, anteriorly domed. DF narrow in dorsal view. MF well developed, with sclerotized ventral outgrowth visible by transparency surpassing the edge of VA. VA wider than long, membranous except its anterior section, sclerotized and quadrangle shaped with rounded corners. AVD present, as tubular compartment with unapparent folds, visible by transparency in ventral and lateral view. Insertion of S projected directly onto AVD, S as rod-shaped transverse bar in ventral view, with arms as long as DA and tips projected anteriorly.

Distribution: This species is reported from Madeira island, but without any information on its exact locality.

Habitat: Unknown, none provided together with the single known specimen.

Remarks: The single specimen of *D. titanica* was discovered through a loan to the MIZ, requesting all specimens of the genus present in the Kulczynski collection, especially because two females of *D. diversa* were cited by Kulczynski (1899: pp 340). Although the cited females were not accounted for, we were surprised
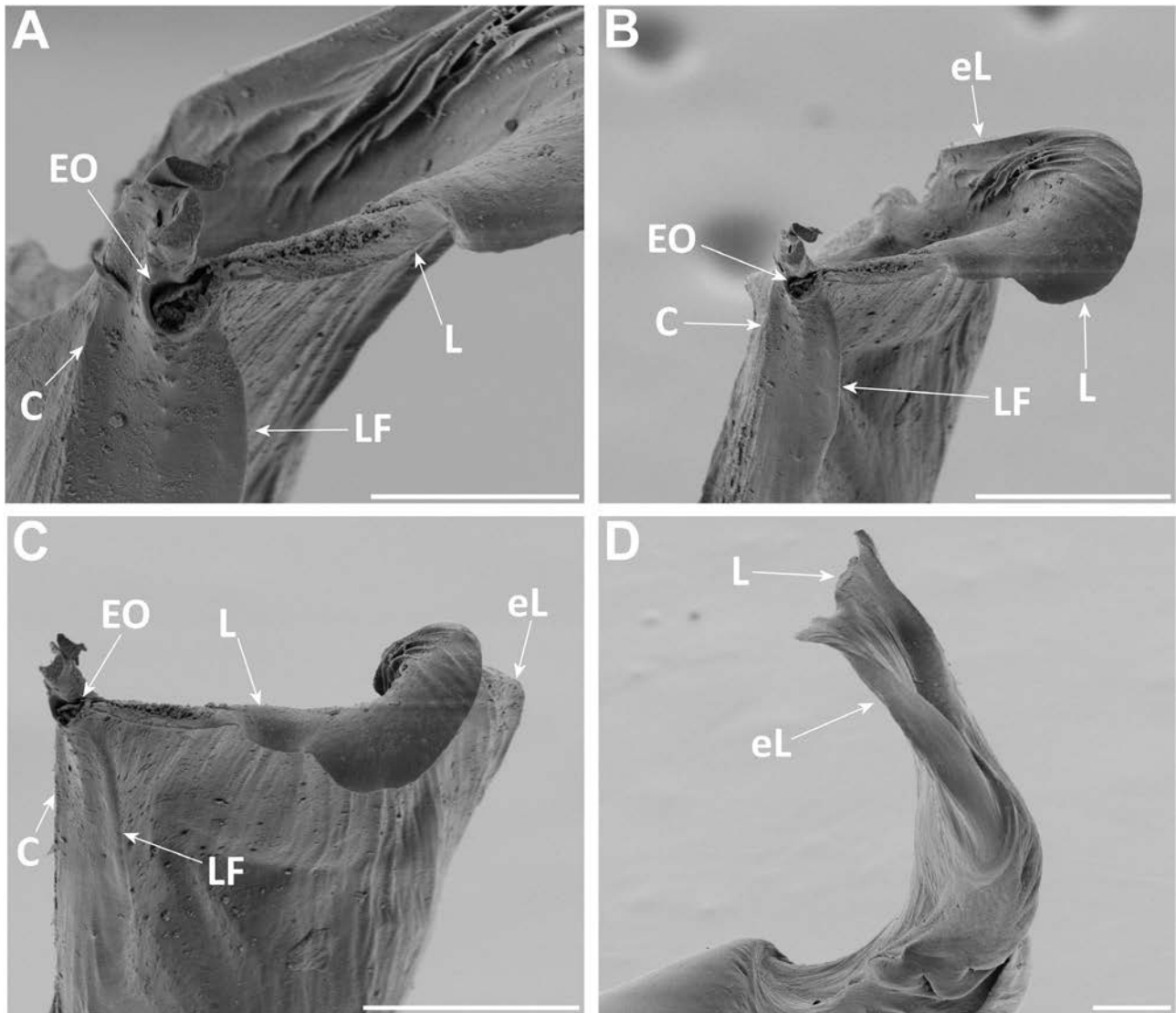
Figure 29. A–D, SEM images of distal right palp of *D. diversa*, male (MMF 47903): (A) prolateral detail, 1074×; (B) prolateral, 500×; (C) frontal, 557×; (D) retrolateral, 200×. Scale bar: A = 0.05 mm; B, C, D = 0.1 mm. Abbreviations: C, crest; eL, external margin of lateral sheet; EO, embolus opening; L, lateral sheet; LF, lateral fold.

to see this large single specimen of *D. titanica*. This discovery is remarkable, because the new species more closely resembles similarly large species from the Canary Islands (e.g. *Dysdera ambulotenta* Ribera, Ferrández & Blasco, 1985, *Dysdera gibbifera* Wunderlich, 1991 or *Dysdera labradaensis* Wunderlich, 1992) than any of the remaining Madeiran species. No precise locality is given in the vial label other than "Madera".

DISCUSSION

ORIGINS OF THE MADEIRAN CLADE

Our phylogenetic analyses suggest that the Madeira archipelago was colonized once, most likely from the mainland. We can only speculate about the actual colonization pathway, but it is worth mentioning that present day seamounts of Ormonde, Ampère, Coral Patch and Seine were once emerged islands (Geldmacher & Hoernle, 2000), which could have provided a stepping stone pathway facilitating colonization of, at least, Porto Santo, from the Iberian Peninsula. The use of rafting and floating islands, on the other hand, has been put forward to explain the colonization of the Canary Islands, which are much closer to the continent, and could have also facilitated arrival from the continent to Madeira archipelago (Arnedo *et al.*, 2001). The closer relationships of the species of Madeira island and Desertas can be easily explained by their geographic
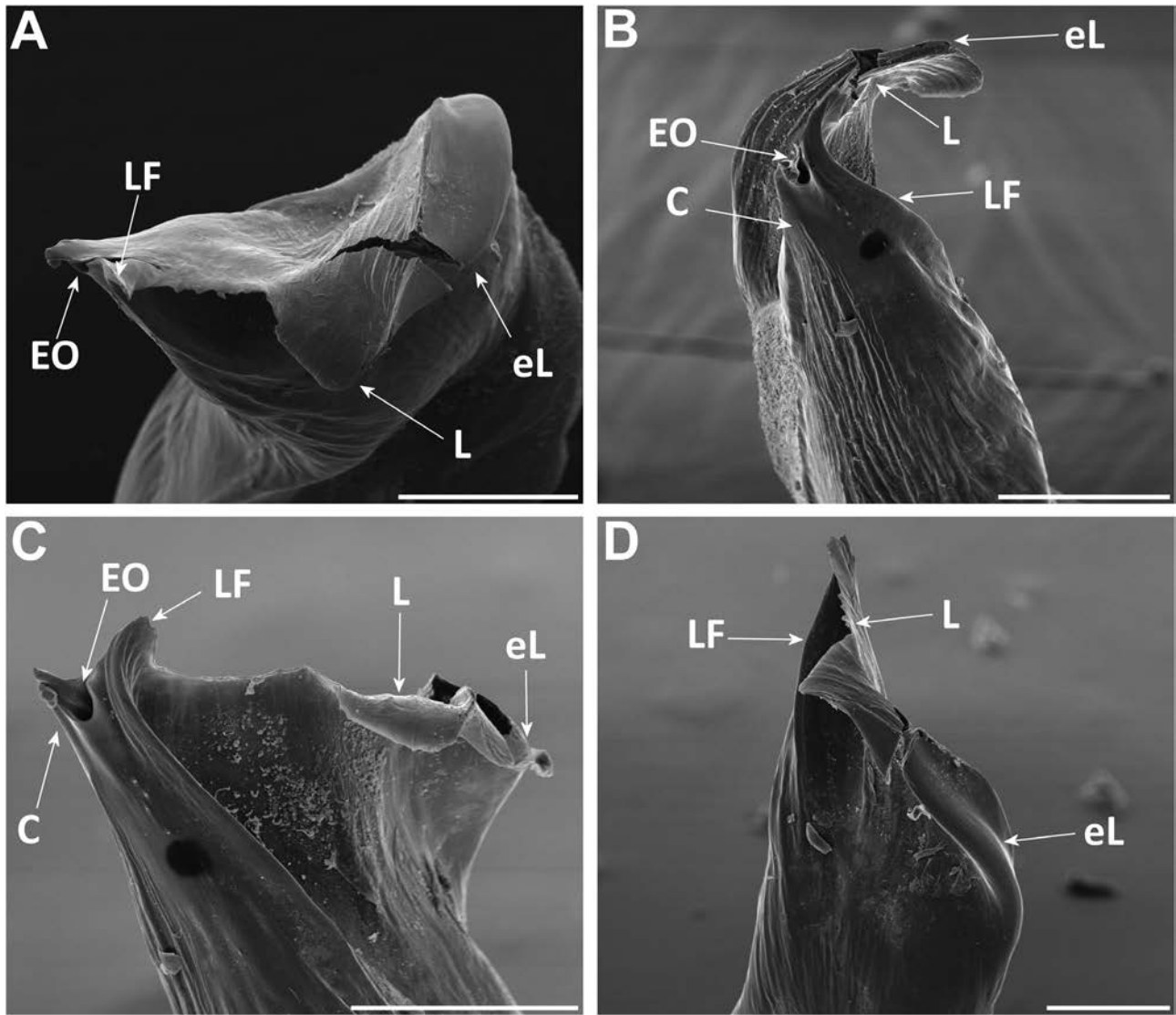
Figure 30. A–D, SEM images of distal right palp of ***D. exigua* sp. nov.**, paratype male (CRBA002542): (A) ventral detail, 929×; (B) prolateral, 887×; (C) frontal, 1173×; (D) retrolateral, 636×. Scale bars = 0.1 mm. Abbreviations: C, crest; eL, external margin of lateral sheet; EO, embolus opening; L, lateral sheet; LF, lateral fold.

proximity. Although the Desertas ridge represents a discrete volcanic system (Schwarz *et al.*, 2005), it is likely that the submarine ridge connecting the eastern side of Madeira island to Ilhéu Chão was exposed during Pleistocene eustatic sea level changes or that a more substantial connection was broken by landslide erosion (Cameron & Cook, 1999).

Regarding the actual source of colonization, the sparse sampling of continental species and the low support recovered for some of the deeper relationships preclude identification of the actual mainland sister group of the Madeiran lineage. Interestingly, the parsimony analyses pinpointed the Portuguese species *Dysdera lusitanica* (Kulczynski, 1915) as the closest

relative of the Madeiran clade albeit with low support and not recovered in the model-based analyses. We revised the descriptions of Iberian and Moroccan *Dysdera* species scouting for morphological affinities to the Madeiran clade. The main morphological synapomorphies of the Madeiran clade appear to be the retrolaterally oriented, claw-shaped P, and the well separated sclerites of the DD (ES and IS, respectively). We identified several Iberian species that share the short, well sclerotized, retrolaterally oriented, claw-shaped P, including *Dysdera alentejana* Ferrández, 1996 or *Dysdera bicornis* Fage, 1931. However, unlike the Madeiran clade, the Iberian species present palpal sclerites with fused bases. Future phylogenetic

Figure 31. A–D, SEM images of distal right palp of *D. isambertoi* **sp. nov.**, paratype male (MZB 2019-1953): (A) ventral detail, 1463×; (B) prolateral, 605×; (C) frontal, 933×; (D) retrolateral, 757×. Scale bars = 0.1 mm. Abbreviations: AR, arch-like ridge; eL, external margin of lateral sheet; EO, embolus opening; L, lateral sheet; LF, lateral fold.

analyses will have to include Iberian species with male bulb similarities to the Madeiran clade to confirm their putative shared ancestry.

One additional loose end remains in our hypothesis of the colonization of Madeira archipelago by *Dysdera*. The enigmatic species *D. titanica* found in the Kulczynski collection, is more similar in appearance to some of the larger species found in the Canary Islands. If this overall similarity reflected phylogenetic relatedness, it could be indicative of an independent colonization event, most likely from the Canary Islands to Madeira, as the former are richer in species, geologically older and closer to the continent (Fernández-Palacios *et al.*, 2011). Unfortunately, we

lack any information about this specimen other than collected in "Madera" and its old age (over a century) precludes molecular analyses using Sanger sequencing techniques. The implementation of high throughput sequencing approach to the Madeiran species may allow in the future to include Kulczynski's specimen and resolve this conundrum.

A CASE OF ADAPTIVE RADIATION?

Adaptive radiation is usually defined as the rapid proliferation of species involving ecophenotypic change in sibling species (Soulebeau *et al.*, 2015), commonly referred as ecomorphs (Gillespie, 2004). Oceanic
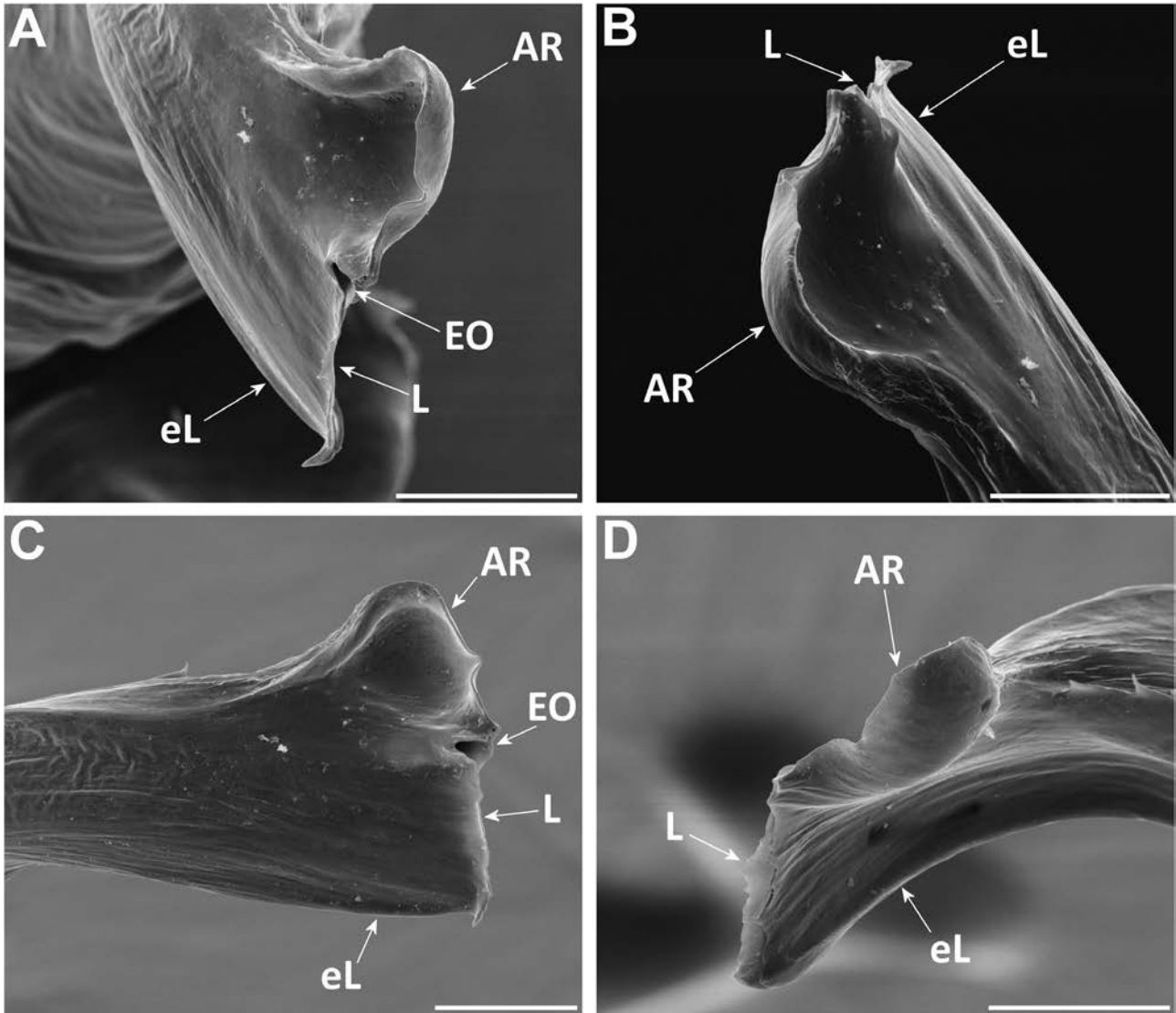
Figure 32. A–D, SEM images of distal right palp of *D. portisancti*, male (MZB 2019-1955): (A) ventral detail, 1870×; (B) prolateral, 2302×; (C) frontal, 1467×; (D) posterior, 1873×. Scale bars = 0.05 mm. Abbreviations: AR, arch-like ridge; eL, external margin of lateral sheet; EO, embolus opening; L, lateral sheet.

archipelagos provide some of the most renowned examples of adaptive radiations (Grant, 1998). Several lines of evidence suggest that the Madeiran clade may constitute a case of adaptive radiation. At least nine of the endemic species of Madeiran *Dysdera* share a common ancestor and are the result of local diversification. Although the emergence date of the oldest island (Porto Santo, 14 Mya), could limit the time window for the diversification of the lineage, the existence nearby of much older once emerged submarine volcanoes prevents ruling out a much older age for the diversification of Madeiran *Dysdera*. Within each island, almost all species show overlapping distributions, which may hint to a differentiation in the ecological niche among species. This pattern is

most remarkable in Deserta Grande, an elongate outcrop of 11 km² that harbours five *Dysdera* species. Some phenotypic differences are evident among co-occurring species. In spiders, like other generalist hunters, predator size limits the size range of potential prey (Nentwig & Wissel, 1986) and hence differences in predator size may ultimately reflect dietary differences (Nyffeler, 1999). Additionally, it has been shown that the size and morphology of the chelicera in *Dysdera* is related to both the level of trophic specialization, namely generalist vs. oniscophagous species, and the prey capture strategy used to subdue prey (Rezac *et al.*, 2008). In Porto Santo, for instance, where four species co-occur in the remaining summits of the island, *D. portisancti* is clearly smaller, whereas *D. isambertoi*
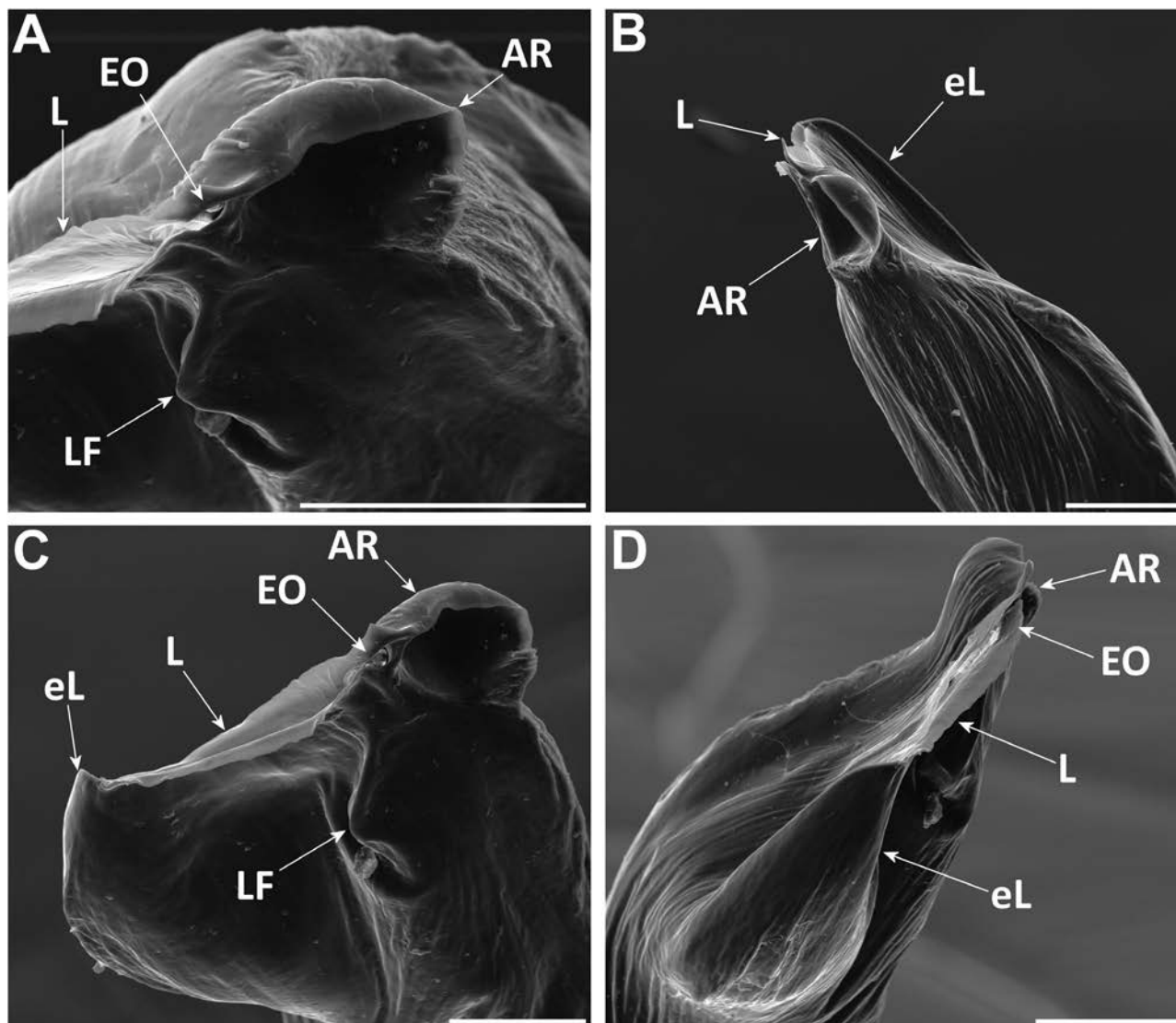
Figure 33. A–D, SEM images of distal right palp of **D. precaria sp. nov.**, paratype male (MZB 2019-1942): (A) ventral detail, 1034×; (B) prolateral, 878×; (C) frontal, 559×; (D) retrolateral, 756×. Scale bars = 0.1 mm. Abbreviations: AR, arch-like ridge; eL, external margin of lateral sheet; EO, embolus opening; L, lateral sheet; LF, lateral fold.

and *D. precaria* are large species. Interestingly, the mid-sized *D. dissimilis* bears long chelicerae, which presumably indicates a trophic specialization to prey on woodlice. Although these former evidences hint at the involvement of competition in the diversification of Madeiran *Dysdera*, quantitative measurement of the phenotypic differences and a comparative analysis of those differences in a phylogenetic framework will be required to properly assess the adaptive nature of the diversification processes undergone by *Dysdera* in Madeira archipelago.

HABITAT LOSS AND THREATS TO BIODIVERSITY

Each community of *Dysdera* species in the Madeira archipelago is subject to different pressures, depending on its range and preferred habitat. Porto Santo, the older island, is under an advanced stage of its geological ontogeny, with small hills surrounded by an unhospitable (for *Dysdera*) matrix of dry habitats. Human colonization caused massive deforestation throughout the entire island, degrading native habitats to a point where later attempts to reforest the mountains could only be done with surrogate tree species. The remarkably small ranges of the four species found in Porto Santo suggest that local

Figure 34. A–D, SEM images of distal right palp of **D. recondita sp. nov.**, paratype male (MZB 2019-1946): (A) ventral detail, 1234×; (B) prolateral, 851×; (C) frontal, 1012×; (D) retrolateral, 777×. Scale bar: A = 0.05 mm; B, C, D = 0.1 mm. Abbreviations: eL, external margin of lateral sheet; EO, embolus opening; ISDA, internal sclerite distal apophysis; L, lateral sheet.

extinctions, driven by dwindling suitable habitats, have already occurred and are likely to continue.

Similarly, the five species from the Desertas show small ranges, and are only found at the top of the islands, where the high aridity is buffered by regular fog and where only few herbs and xerophytic shrubs can be found. According to malacological fossil fauna surveys (Cameron & Cook, 1999), it is suggested that, in the past, the vegetation was probably taller and microclimates were wetter. Given the small size and steep topography of the Desertas, we believe that the greatest threats to these species are the introduction of exotic species (goats, rabbits, rodents, exotic plants), coupled with habitat loss by erosion and landslides,

which probably contribute to the increasing aridity of the Desertas. In the particular case of Bugio, the ecological restoration efforts due to the conservation of the Desertas petrel, *Pterodroma deserta* Mathews, 1934, led to the successful eradication of goats, rabbits and rodents, by which ecological restoration processes might take place at a quicker pace than on its neighbouring islands. However, it is also possible that, as in Deserta Grande, the impacts of the introduction of exotic species during attempts of colonization by humans have caused irreversible changes in the native communities of Bugio.

Surprisingly, only two species occur in Madeira island, a much larger and forested island. Although

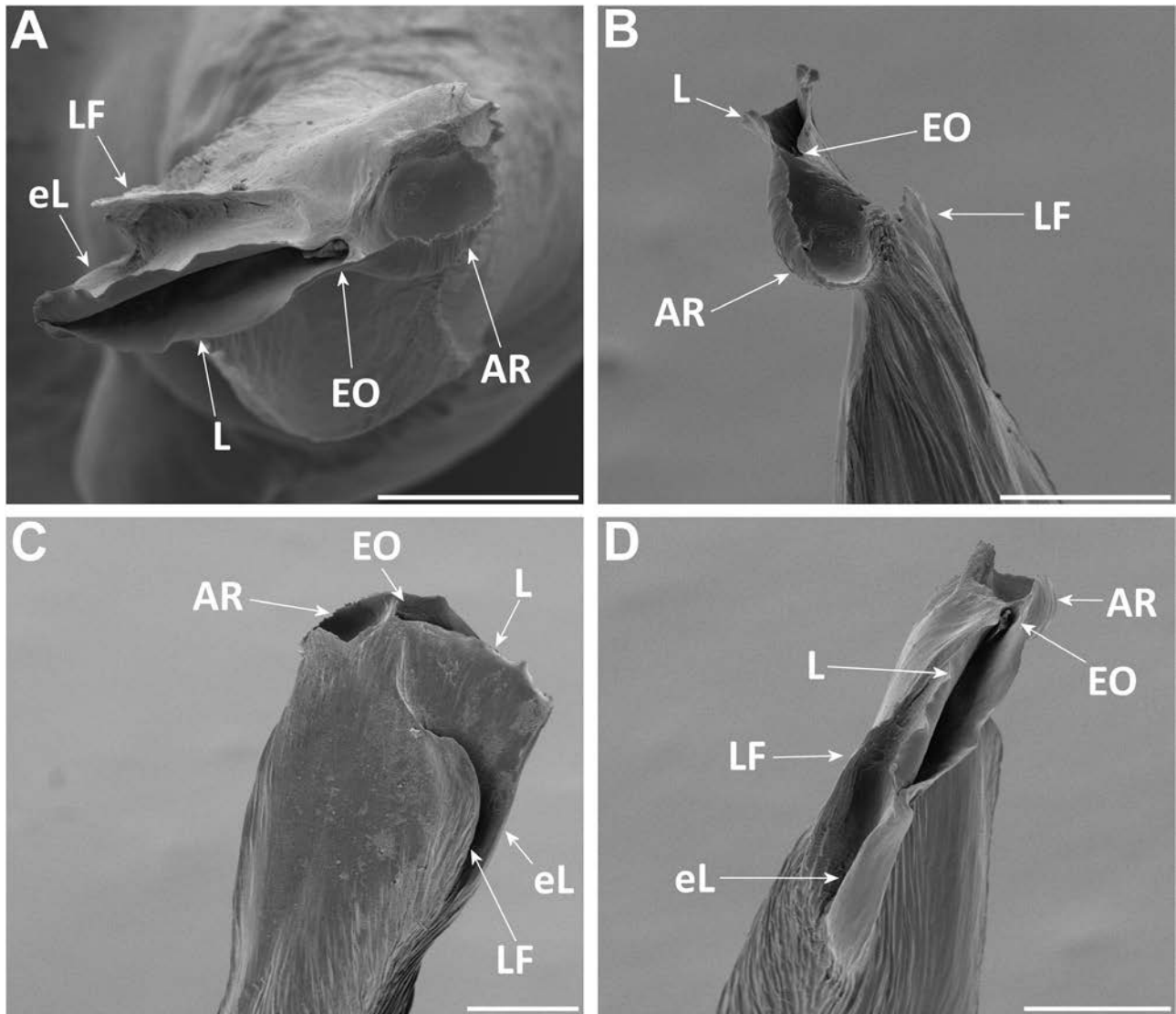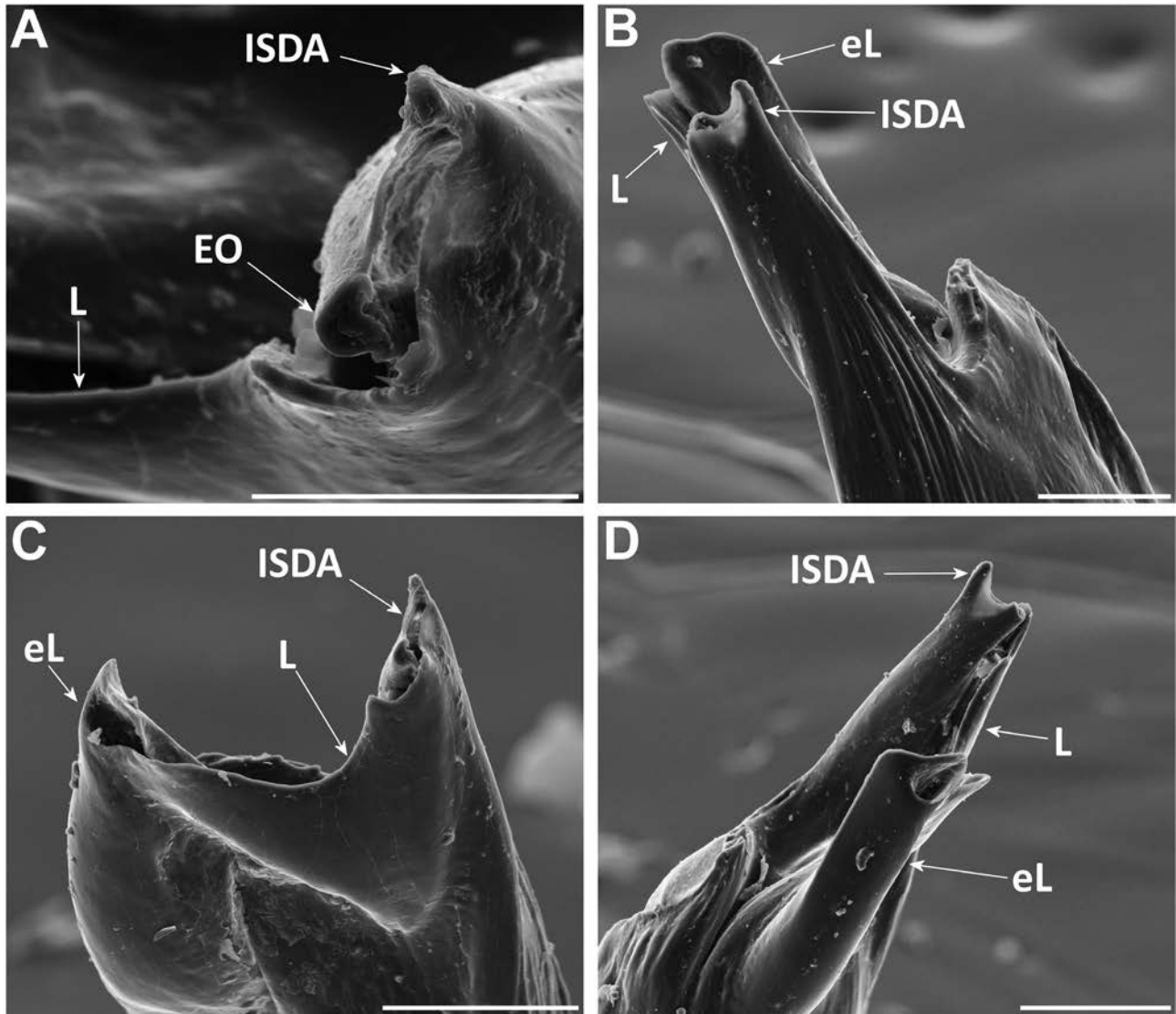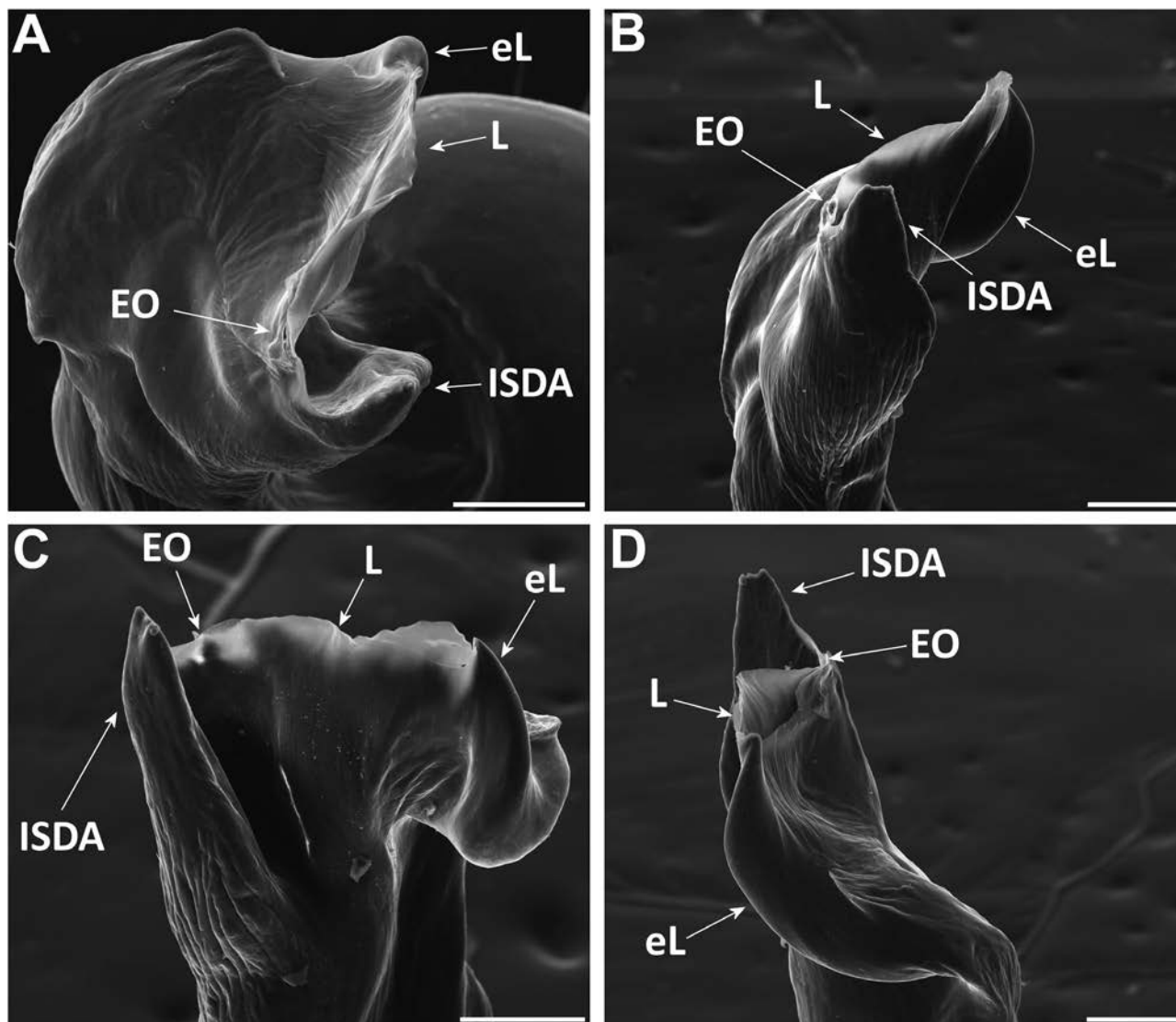**Figure 35.** A–D, SEM images of distal right palp of **D. sandrae sp. nov.**, paratype male (MZB 2019-1930): (A) ventral detail, 675×; (B) prolateral, 473×; (C) frontal, 640×; (D) retrolateral, 488×. Scale bars = 0.1 mm. Abbreviations: eL, external margin of lateral sheet; EO, embolus opening; ISDA, internal sclerite distal apophysis; L, lateral sheet.

D. coiffaiti is found ubiquitously across Madeiran forest patches, the other species is difficult to find. In fact, we have made thorough efforts (twice) to find specimens of *D. diversa* at both localities where each of the two known specimens were found in pitfall traps in 2012 and did not find any *Dysdera* apart from *D. coiffaiti*. The rugged and steep geomorphology also creates a physical impediment for a good inventory of Madeira island, with many inaccessible slopes and secluded valleys left to sample. Both species mainly occur in the area inside the Madeira laurel forest Unesco World Heritage Site (Unesco World Heritage Committee, 1999), a conservation rank which should safe keep the native habitats where both species are found (Cardoso *et al.*, 2017).

For those species facing major threats (i.e. showing smaller ranges, inhabiting highly perturbated habitats), a recovery programme of native vegetation combined with *ex situ* conservation attempts could be implemented to guarantee their future survival. Joint *in situ* and *ex situ* conservation efforts were already successful for the survival of the Desertas wolf spider (*Hogna ingens* Blackwall, 1857; Crespo *et al.*, 2014), and a similar approach could be tested for the *Dysdera* from Porto Santo and Desertas.

79
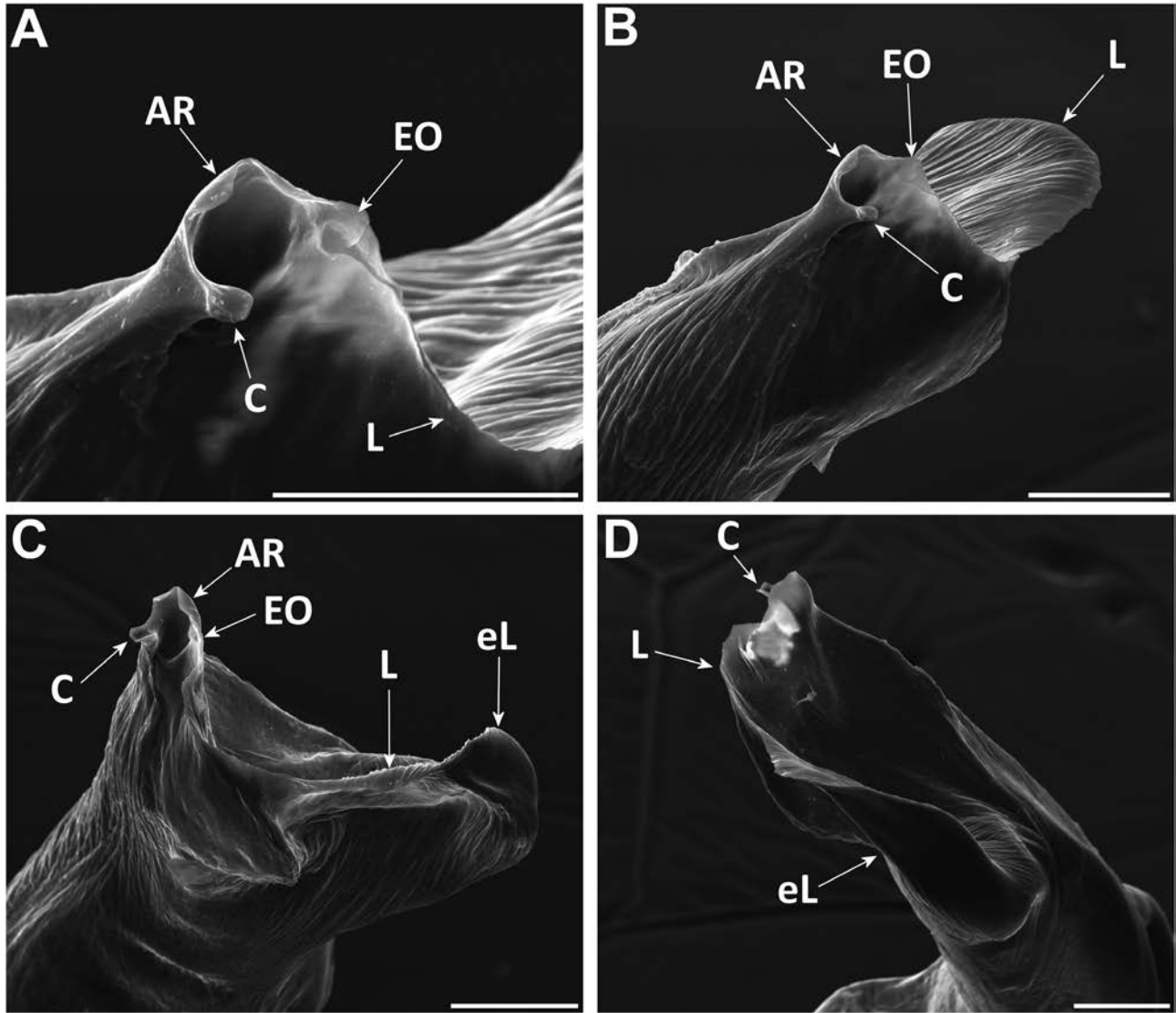
Figure 36. A–D, SEM images of distal right palp of **D. teixeirai sp. nov.**, paratype male (NMH001596): (A) prolateral detail, 1579×; (B) prolateral, 732×; (C) frontal, 565×; (D) retrolateral, 497×. Scale bars = 0.1 mm. Abbreviations: AR, arch-like ridge; C, crest; eL, external margin of lateral sheet; EO, embolus opening; L, lateral sheet.

CONCLUSION

Dysdera is now the most species-rich spider genus in the Madeira archipelago. A successful lineage, composed mostly of species new to science, colonized the archipelago from the mainland. Although basal resolution of the Madeiran clade is equivocal, because of its older age it is possible that an ancestral colonizer arrived first to Porto Santo. Subsequently, *Dysdera* would have hopped to and diversified on the remaining islands, according through some lines of evidence undergoing an adaptive radiation process. An enigmatic specimen discovered in the Kulczynski collection might represent an independent colonization event from a distinct source, the Canary Islands. Species-richness patterns in Madeiran *Dysdera* are exceptional in the fact the largest and second oldest island harbours the lowest number of species. Conversely, in the small, steep and highly eroded Desertas, five species occur sympatrically. Finally, the species from Porto Santo and Desertas represent cases worthy of attention for conservation biologists and competent authorities, since they are either found in small, surrogate woodlands, or in steep, narrow islands that lost native vegetation and are subject to high

Figure 37. A, *Dysdera coiffaiti,* female (CRBA002548). B, **D. dissimilis sp. nov.**, holotype male (MZB 2019-1947). C, **D. exigua sp. nov.**, paratype female (CRBALC0212). D, *D. portisancti*, female (CRBALC0215). E, **D. precaria sp. nov.**, male (CRBALC0221). F, **D. sandrae sp. nov.**, undetermined male specimen. Photo credits: A and F, by Pedro Cardoso. B, C, D and E, by courtesy of Emídio Machado.

erosion. The discovery of hidden diversity in highly perturbed habitats should serve to put more efforts and funding into the management and conservation of the remaining wild habitats of the Madeira archipelago. A consequent effort should also be made to list most species of Madeiran *Dysdera* in regional protected species legislation and international agreements such as the European Habitats Directive.

loaned materials and those who facilitated storage of the type series of the new species are hereby acknowledged: B. Caballero, Y. Gonçalves, J.E. Hogan, P. Jaeger, C. Rollard and W. Wawer. Thanks are also due to the IFCN of the Madeira Regional Secretariat of Environment, Natural Resources and Climate Change for coordinating the logistical arrangements, and for providing collection and transport permits, namely to C. Santos and D. Menezes, and for field work support to the entire team of rangers, especially during the stays of the first author at the Desertas. The Portuguese Navy is acknowledged for allowing transportation to the Desertas in the 2017 expedition. We thank P. Mazzuca who extracted and amplified the first sequences coming from Madeira archipelago. Original distribution maps were provided, under copyright agreement, by DROTA. Live photos of some of the species treated here were provided by courtesy of E. Machado. Finally, we acknowledge A. Henrard, I. Agnarsson and two anonymous reviewers for their comments and suggestions on an early version of the manuscript, which helped us to improve the quality of the article.

REFERENCES

Arnedo M, **Oromí P**, **Múrria C**, **Macías-Hernández N**, **Ribera C. 2007.** The dark side of an island radiation: systematics and evolution of troglobitic spiders of the genus *Dysdera* Latreille (Araneae: Dysderidae) in the Canary Islands. *Invertebrate Systematics* **21:** 623–660.

Arnedo M, **Oromí P**, **Ribera C. 1996.** Radiation in the genus *Dysdera* (Araneae, Dysderidae) in the Canary Islands: the western islands. *Zoologica Scripta* **27:** 604–662.

Arnedo M, **Oromí P**, **Ribera C. 2000.** Systematics of the genus *Dysdera* (Araneae, Dysderidae) in the eastern Canary Islands. *Journal of Arachnology* **28:** 261–292.

Arnedo M, **Oromí P**, **Ribera C. 2001.** Radiation of the spider genus *Dysdera* (Araneae, Dysderidae) in the Canary Islands: cladistic assessment based on multiple data sets. *Cladistics* **17:** 313–353.

Arnedo M, **Ribera C. 1997.** Radiation of the genus *Dysdera* (Araneae, Haplogynae, Dysderidae) in the Canary Islands: the island of Gran Canaria. *Zoologica Scripta* **26:** 205–243.

Arnedo M, **Ribera C. 1999.** Radiation of the spider genus *Dysdera* (Araneae, Dysderidae) in the Canary Islands: the island of Tenerife. *Journal of Arachnology* **27:** 604–662.

Bennett DJ, **Hettling H**, **Silvestro D**, **Zizka A**, **Bacon CD**, **Faurby S**, **Vos RA**, **Antonelli A. 2018.** PhylotaR: an automated pipeline for retrieving orthologous DNA sequences from GenBank in R. *Life* **8:** 1–11.

Blair C, **Bryson RW. 2017.** Cryptic diversity and discordance in single-locus species delimitation methods within horned lizards (Phrynosomatidae: *Phrynosoma*). *Molecular Ecology Resources* **17:** 1168–1182.

Bocek M, **Bocak L. 2019.** The origins and dispersal history of the trichaline net-winged beetles in Southeast Asia, Wallacea, New Guinea and Australia. *Zoological Journal of the Linnean Society* **185:** 1079–1094.

Borges PA, **Abreu C**, **Aguiar AF**, **Carvalho P**, **Jardim R**, **Melo I**, **Oliveira P**, **Sérgio C**, **Serrano AR**, **Vieira P. 2008.** *A list of the terrestrial fungi, flora and fauna of Madeira and Selvagens archipelagos.* Funchal and Angra do Heroísmo: Direcção Regional do Ambiente da Madeira and Universidade dos Açores.

Cameron RAD, **Cook LM. 1999.** Land snail faunas of the Deserta Islands, Madeiran archipelago, past and present. *Journal of Conchology* **36:** 1–12.

Cardoso P, **Arnedo M**, **Triantis K**, **Borges P. 2010.** Drivers of diversity in Macaronesian spiders and the role of species extinctions. *Journal of Biogeography* **37:** 1034–1046.

Cardoso P, **Crespo L**, **Silva I**, **Borges P**, **Boieiro M. 2017.** Species conservation profiles of endemic spiders (Araneae) from Madeira and Selvagens archipelagos, Portugal. *Biodiversity Data Journal* **5:** e20810.

Crespo L, **Silva I**, **Borges P**, **Cardoso P. 2013.** Rapid biodiversity assessment, faunistics and description of a new spider species (Araneae) from Desertas Islands and Madeira (Portugal). *Revista Iberica de Aracnología* **23:** 11–23.

Crespo L, **Silva I**, **Borges P**, **Cardoso P. 2014.** Assessing the conservation status of the strict endemic Desertas wolf spider, *Hogna ingens* (Araneae, Lycosidae). *Journal for Nature Conservation* **22:** 516–524.

Deeleman-Reinhold C, **Deeleman P. 1988.** Revision des Dysderinae (Araneae, Dysderidae), les espèces Mediterranéennes occidentales exceptées. *Tijdschrift voor Entomologie* **131:** 141–269. Available at: https://www.biodiversitylibrary.org/part/66464

Denis J. 1962. Les araignées de l'Archipel de Madère (Mission du Professeur Vandel). *Publicações do Instituto Zoologia Doutor Augusto Nobre* **79:** 1–118.

Drummond AJ, **Suchard MA**, **Xie D**, **Rambaut A. 2012.** Bayesian phylogenetics with BEAUti and the BEAST 1.7. *Molecular Biology and Evolution* **29:** 1969–1973.

Ezard T, **Fujisawa T**, **Barraclough T. 2017.** *SPLITS: SPecies' LImits by Threshold Statistics.* Available at: https://r-forge.r-project.org/projects/splits/

Fernández-Palacios JM, **de Nascimento L**, **Otto R**, **Delgado JD**, **García-del-Rey E**, **Arévalo JR**, **Whittaker RJ. 2011.** A reconstruction of palaeo-Macaronesia, with particular reference to the long-term biogeography of the Atlantic island laurel forests. *Journal of Biogeography* **38:** 226–246.

Fujisawa T, **Barraclough TG. 2013.** Delimiting species using single-locus data and the generalized mixed yule coalescent approach: a revised method and evaluation on simulated data sets. *Systematic Biology* **62:** 707–724.

Geldmacher J, **Hoernle K. 2000.** The 72 Ma geochemical evolution of the Madeira hotspot (eastern North Atlantic): recycling of Paleozoic (≤500 Ma) oceanic lithosphere. *Earth and Planetary Science Letters* **183:** 73–92.

Gillespie R. 2004. Community assembly through adaptive radiation in Hawaiian spiders. *Science* **303:** 356–359.

Goloboff P, **Farris J**, **Nixon K. 2008.** TNT, a free program for phylogenetic analysis. *Cladistics* **24:** 774–786.

Grant PR. 1998. *Evolution on islands.* Oxford: Oxford University Press.

Hebert PDN, **Cywinska A**, **Ball SL**, **DeWaard JR. 2003.** Biological identifications through DNA barcodes. *Proceedings of the Royal Society B: Biological Sciences* **270:** 313–321.

Hoang DT, **Chernomor O**, **von Haeseler A**, **Minh BQ**, **Vinh LS. 2018.** UFBoot2: improving the ultrafast bootstrap approximation. *Molecular Biology and Evolution* **35:** 518–522.

Kalyaanamoorthy S, **Minh BQ**, **Wong, TKF**, **von Haeseler A**, **Jermiin LS. 2017.** ModelFinder: fast model selection for accurate phylogenetic estimates. *Nature Methods* **14:** 587–589.

Kapli P, **Lutteropp S**, **Zhang J**, **Kobert K**, **Pavlidis P**, **Stamatakis A**, **Flouri T. 2017.** Multi-rate Poisson tree processes for single-locus species delimitation under maximum likelihood and Markov chain Monte Carlo. *Bioinformatics* **33:** 1630–1638.

Katoh K. 2002. MAFFT: a novel method for rapid multiple sequence alignment based on fast Fourier transform. *Nucleic Acids Research* **30:** 3059–3066.

Katoh K, **Standley DM. 2013.** MAFFT multiple sequence alignment software version 7: improvements in performance and usability. *Molecular Biology and Evolution* **30:** 772–780.

Kearse M, **Moir R**, **Wilson A**, **Stones-Havas S**, **Cheung M**, **Sturrock S**, **Buxton S**, **Cooper A**, **Markowitz S**, **Duran C**, **Thierer T. 2012.** Geneious basic: an integrated and extendable desktop software platform for the organization and analysis of sequence data. *Bioinformatics* **28:** 1647–1649.

Kulczynski, W. 1899. Arachnoidea opera Rev. E. Schmitz collecta in insulis Maderianis et in insulis Selvages dictis. *Rozprawy i Sprawozdania z Posiedzen Wydzialu Matematyczno Przyrodniczego Akademji Umiejetnosci, Krakow* **36:** 319–461.

Kumar S, **Stecher G**, **Tamura K. 2016.** MEGA7: molecular evolutionary genetics analysis version 7.0 for bigger datasets. *Molecular Biology and Evolution* **33:** 1870–1874.

Lanfear R, **Frandsen PB**, **Wright AM**, **Senfeld T**, **Calcott B. 2017.** Partitionfinder 2: new methods for selecting partitioned models of evolution for molecular and morphological phylogenetic analyses. *Molecular Biology and Evolution* **34:** 772–773.

Le Peru B. 2011. The spiders of Europe, a synthesis of data: volume 1 Atypidae to Theridiidae. *Mémoires de La Société Linnéenne de Lyon* **2:** 1–522.

Monaghan MT, **Wild R**, **Elliot M**, **Fujisawa T**, **Balke M**, **Inward DJ**, **Lees DC**, **Ranaivosolo R**, **Eggleton P**, **Barraclough TG**, **Vogler AP. 2009.** Accelerated species inventory on Madagascar using coalescent-based models of species delineation. *Systematic Biology* **58:** 298–311.

Nentwig W, **Wissel C. 1986.** A comparison of prey lengths among spiders. *Oecologia* **68:** 595–600.

Nguyen LT, **Schmidt HA**, **von Haeseler A**, **Minh BQ. 2015.** IQ-TREE: a fast and effective stochastic algorithm for estimating maximum-likelihood phylogenies. *Molecular Biology and Evolution* **32:** 268–274.

Nyffeler M. 1999. Prey selection of spiders in the field. *Journal of Arachnology* **27:** 317–324.

Puillandre N, **Lambert A**, **Brouillet S**, **Achaz G. 2012.** ABGD, automatic barcode gap discovery for primary species delimitation. *Molecular Ecology* **21:** 1864–1877.

Ramalho RS, **Brum da Silveira A**, **Fonseca PE**, **Madeira J**, **Cosca M**, **Cachão M**, **Fonseca MM**, **Prada SN. 2015.** The emergence of volcanic oceanic islands on a slow-moving plate: the example of Madeira Island, NE Atlantic. *Geochemistry, Geophysics, Geosystems* **16:** 522–537.

Rambaut A, **Drummond AJ**, **Xie D**, **Baele G**, **Suchard MA. 2018.** Posterior summarization in Bayesian phylogenetics using Tracer 1.7. *Systematic Biology* **67:** 901–904.

Rezac M, **Pekàr S**, **Lubin Y. 2008.** How oniscophagous spiders overcome woodlouse armour. *Journal of Zoology* **275:** 64–71.

Ronquist F, **Teslenko M**, **Van der Mark P**, **Ayres DL**, **Darling A**, **Höhna S**, **Larget B**, **Liu L**, **Suchard MA**, **Huelsenbeck JP. 2012.** MrBayes 3.2: efficient Bayesian phylogenetic inference and model choice across a large model space. *Systematic Biology* **61:** 539–542.

Schwarz S, **Klügel A**, **Van den Bogaard P**, **Geldmacher J. 2005.** Internal structure and evolution of a volcanic rift system in the eastern North Atlantic: the Desertas rift zone, Madeira archipelago. *Journal of Volcanology and Geothermal Research* **141:** 123–155.

Soulebeau A, **Aubriot X**, **Gaudeul M**, **Rouhan G**, **Hennequin S**, **Haevermans T**, **Dubuisson JY**, **Jabbour F. 2015.** The hypothesis of adaptive radiation in evolutionary biology: hard facts about a hazy concept. *Organisms Diversity and Evolution* **15:** 747–761.

Unesco World Heritage Committee. **1999.** *Twenty-third session: convention concerning the protection of the cultural and natural heritage.* Marrakesh: World Heritage Committee. Available at: http://whc.unesco.org/archive/1999/whc-99-conf209-22e.pdf

Whittaker RJ, **Fernández-Palacios JM**, **Matthews TJ**, **Borregaard MK**, **Triantis KA. 2017.** Island biogeography: taking the long view of nature's laboratories. *Science* **357:** eaam8326.

World Spider Catalog. **2020.** *World spider catalog. Version 21.0.* Bern: Natural History Museum. Available at: https://doi.org/10.24436/2

Wunderlich J. 1987. *Die Spinnen der Kanarischen Inseln und Madeiras: adaptive Radiation, Biogeographie, Revisionen und Neubeschreibungen.* Langen: Triops Verlag.

Wunderlich J. 1992. Die Spinnen-Fauna der Makaronesischen Inseln: taxonomie, Ökologie, biogeographie und evolution. *Beiträge zur Araneologie* **1:** 1–619.

Wunderlich J. 1995. Zu Ökologie, Biogeographie, Evolution und Taxonomie einiger Spinnen der Makaronesischen Inseln (Arachnida: Araneae). *Beiträge zur Araneologie* **4:** 385–439.

SUPPORTING INFORMATION

Additional Supporting Information may be found in the online version of this article at the publisher's web-site:

Table S1. List of specimens used in the molecular analysis with voucher specifications, GenBank accession numbers and collecting data. Sequences with DNA codes were newly generated in the present study. Superscript letters in *COI* indicate shared haplotypes. Subfamily, genus, species: taxonomic category; sex: life cycle stage; type: type material status of the specimen; collection code: collection number of the specimen; DNA code: DNA extraction code; *COI*, 16S, *NAD1*, 28S, *H3*: accession numbers for the corresponding genes; country, island, locality: locality information; additional site information: habitat characteristics; coordinates: decimal latitude and longitude; elevation: in metres as inferred from the GPS coordinates with https://www.freemaptools.com/elevation-finder.htm
Table S2. Primers and amplification conditions used in the present study

Chapter 2

Luís C. Crespo, Isamberto Silva, Alba Enguídanos, Pedro Cardoso and Miquel A. Arnedo (in press)

The Atlantic connection: Coastal habitat favoured long distance dispersal and colonization of Azores and Madeira by *Dysdera* spiders (Araneae: Dysderidae)

(text presented as in the accepted manuscript)

Abstract

The woodlouse hunter *Dysdera* spiders have colonized all Macaronesian archipelagos. We report here for the first time an evolutionary connection between the Iberian Peninsula, Madeira, and the remote archipelago of Azores. Based on museum specimens from the 1950's, we describe the first endemic *Dysdera* species from the Azores. Additionally, we report the recent collection of immature individuals related yet probably not conspecific to the new species, rejecting previous suggestions that the endemic lineage had gone extinct. A multi-locus target phylogeny revealed that an undescribed species from Madeira was the closest relative to the Azores lineage, and that both island taxa were in turn sister to an Iberian endemic species, within a mostly Iberian clade. Interestingly, the Madeiran relative was not closely related to the remaining endemic species reported in the archipelago, suggesting an independent colonization. A divergence time estimation analyses unravelled that *Dysdera* colonised both archipelagos early after their emergence. The colonisation pathway remains ambiguous, but the Iberian Peninsula acted as the ultimate source of the ancestral colonisers. Finally, we describe the new species *Dysdera cetophonorum* Crespo & Arnedo sp. nov. from Pico and *Dysdera citauca* Crespo & Arnedo, sp. nov. from Ilhéu de Cima (Porto Santo) and redescribe and illustrate the female genitalia for the first time of their poorly known closest relative, *Dysdera flavitarsis* Simon, 1882 from north-western Iberian Peninsula.

Keywords

ZooBank LSID

Introduction

Community assembly in oceanic islands is largely dependent on the interplay between colonisation and extinction processes (MacArthur & Wilson, 1967). The relative contribution

of both factors may vary along geologic and evolutionary time (Whittaker, Fernández-Palacios, Matthews, Borregaard, & Triantis, 2017; Whittaker, Triantis, & Ladle, 2008) and are, in turn, intrinsically linked to the differential dispersal ability of species (Carvalho & Cardoso, 2014). Species with greater dispersal ability are expected to colonize islands more frequently, but the continuation of gene flow with the mainland source will hamper differentiation of the island populations. Conversely, species with poor dispersal abilities will have slim chances of reaching an island. Both empirical and theoretical studies (Agnarsson, Cheng, & Kuntner, 2014; Ashby, Shaw, & Kokko, 2020; Claramunt, Derryberry, Remsen, & Brumfield, 2012) have confirmed that high levels of endemism in insular systems are often associated with organisms showing intermediate dispersal ability. In this case, colonization events are rare enough to prevent high levels of gene flow with the source populations yet allow, from time to time, long distance dispersal events that grant access to the exploitation of new resources, driving to local speciation and diversification processes.

Active airborne transport is the most obvious mechanism for long distance dispersal across marine barriers for terrestrial organisms. Alternatively, organisms may reach oceanic islands passively, transported by ocean drift, on the wind, or by transport on or in a flying animal. In spite of the accidental nature of passive dispersal, it has been suggested that biogeographic patterns and evolutionary outcomes following colonisation events can be predicted from the knowledge on the dispersal vector, their geographical and biological drivers, and the ability of the organisms to use them (Gillespie *et al.*, 2012).

Macaronesia comprises several archipelagos of volcanic origin, located in the north-eastern Atlantic Ocean, spanning approximately 3,000 km (Fig. 1A). The wide latitudinal range covered (14.8° N to 39.7° N) reflects in a strong climatic gradient, ranging from temperate to warm arid climates (Fernández-Palacios *et al.*, 2011), which partly explains its high species richness and levels of endemism. The validity of the region as a biogeographic unit has been repeatedly questioned. Plants and several arthropod groups from the Cape Verde islands suggest stronger affinities of this archipelago with sub-Saharan Africa, while marine organisms further support the separation of the Azores from the remaining archipelagos, namely the Canary Islands, Madeira and the Selvagens (Freitas *et al.*, 2019).
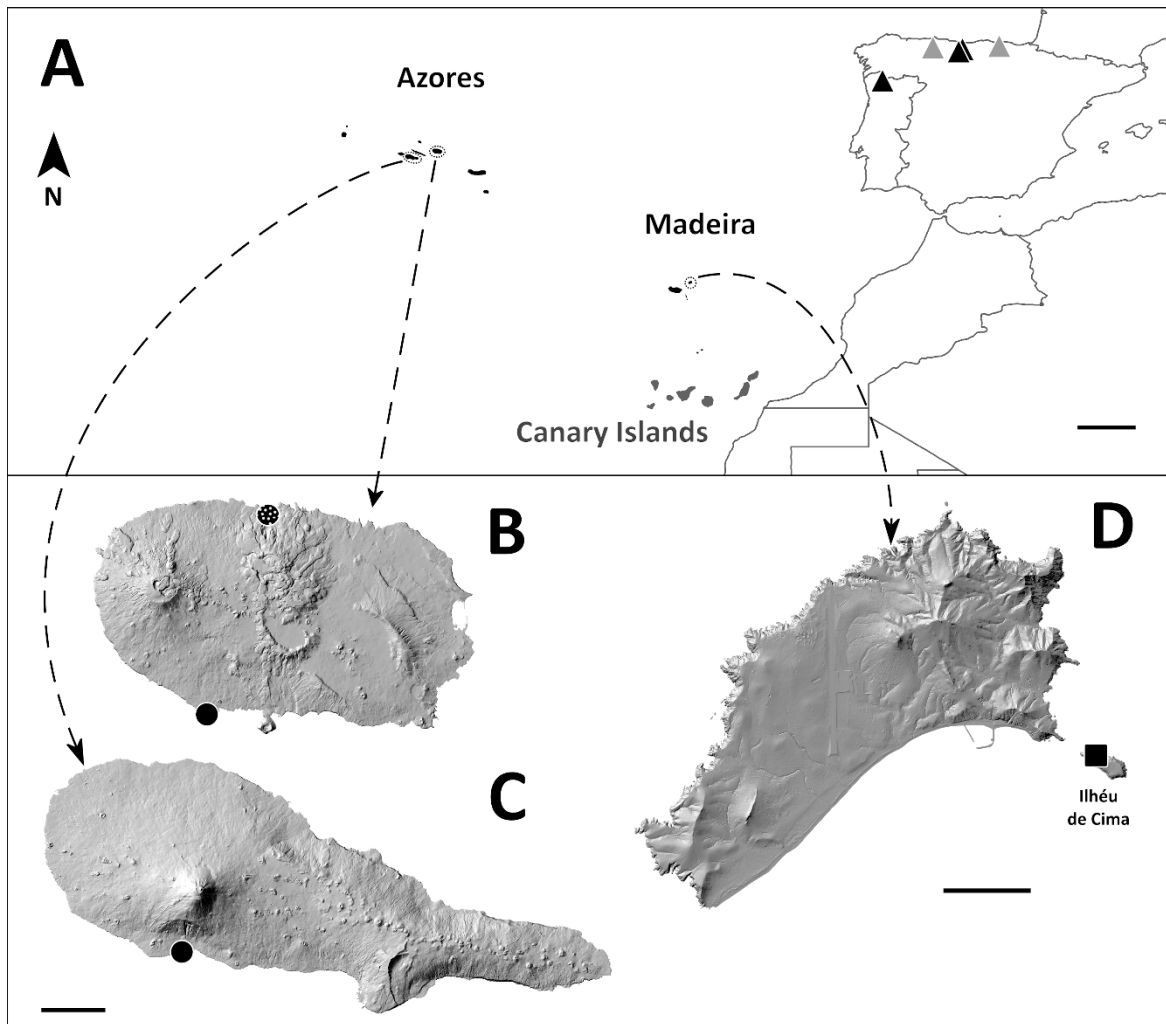
Figure 1. A, map of the Macaronesia (adapted from Borges *et al.*, 2008, with author's permission, Cape Verde omitted). B, map of Terceira. C, map of Pico. D, map of Porto Santo. Scale bars: A = 200 km; B, C = 5 km; D = 2 km. Shapes: Full circles, locations where specimens of "SPJ" were found; dotted circle, location where a moult attributed to the former species was found; square, location where *D. citauca* sp. nov. was found; black triangles, locations where *D. flavitarsis* was found; grey triangles, previous citations of *D. flavitarsis*, taken from literature.

The Madeira archipelago is situated roughly 500 km North from the Canary Islands, 600 km West from Africa and 1000 km from the Iberian Peninsula. It is composed by Porto Santo island (and neighbouring islets), Madeira and Desertas. The Madeira archipelago is currently in an intermediate stage of island ontogeny, with subaerial geologic ages spanning from 14 to 11 million years (my) of Porto Santo to 5 to 7 my of Desertas and Madeira, respectively (Geldmacher & Hoernle, 2000; Ramalho *et al.*, 2015; Schwarz, Klügel, van den

Bogaard, & Geldmacher, 2005). The Azores is the most isolated archipelago of the Macaronesia. It lays roughly 1,600 km west from Europe and 1,000 km from Madeira. Its westernmost island, Flores, is roughly located at the midpoint between Europe and the Americas (Newfoundland). The Azores is also the youngest Macaronesian archipelago. Santa Maria, the oldest island, has been dated approximately at 6 Mya (Ramalho *et al.*, 2017). The islands have been extensively depauperated of their native forests since humans settled in the 15th century. The laurel forest that once covered almost all islands and where most endemic species are concentrated, currently only represents 3% of the total area of the archipelago (Gaspar, Gaston, Borges, & Cardoso, 2011).

Dysdera Latreille, 1804 is a genus of nocturnal, ground-dwelling wandering hunter spiders, which occurs throughout the Mediterranean region. It successfully colonized the Macaronesian archipelagos and underwent remarkable local diversification in the Canary Islands and Madeira. To date, 47 and 11 endemic species have been documented in the Canary Islands and Madeira, respectively (Arnedo, Oromí, Múrria, Macías-Hernández, & Ribera, 2007; Arnedo, Oromí, & Ribera, 2001; Bidegaray-Batista, Macías-Hernández, Oromí, & Arnedo, 2007; Crespo, Silva, Enguídanos, Cardoso, & Arnedo, 2020; Macías-Hernández, Bidegaray-Batista, Emerson, Oromí, & Arnedo, 2013; Macías-Hernández, Bidegaray-Batista, Oromí, & Arnedo, 2013; Macías-Hernández, Oromí, & Arnedo, 2008, 2010). Single endemic species have been reported in Cabo Verde, *D. vermicularis* Berland, 1936, and in the Selvagens, *D. aneris* Macías-Hernández & Arnedo, 2010.

Despite extensive sampling efforts, the only species of *Dysdera* known from the Azorean forests is the synanthropic and most likely introduced *D. crocata* C. L. Koch, 1838. Interestingly, the presence of an undescribed, endemic *Dysdera* species presumably extinct was reported by Cardoso et al (Cardoso, Arnedo, Triantis, & Borges, 2010), based on a series of 2 male and 1 female specimens from the island of Pico collected in the 1950's, stored at the Natural History Museum in London (NHMUK).

In recent collecting campaigns conducted in the context of a taxonomic revision of *Dysdera* in the Madeira archipelago (Crespo *et al.*, 2021), we found a new species in the spray zone of coastal areas on Ilhéu de Cima (an islet of Porto Santo), with clear morphological affinities to the Azorean specimens stored at BMNH. A new collection trip to the Azores specifically aimed at search for the supposedly endemic species in similar habitats to those

reported in Madeira, yielded some juvenile specimens in the Islands of Terceira and Pico, with clear morphological similarities to both former species.

In the present study we use a multilocus target gene approach to confirm that the littoral Azorean and Madeiran specimens are each other's closest relatives. Additionally, we formally describe the two new endemic species from Azores and Madeira, respectively, and redescribe the Iberian species *D. flavitarsis* Simon, 1882, which is supported in our analyses as their sister species. We further discuss the colonization pathways and evolutionary history of this newly discovered Atlantic faunal connection under the light of a divergence time estimation analysis.

Materials and methods

Field work

We collected Madeiran specimens in Ilhéu de Cima, a small islet (30 Ha, 120m high) 400 meters off the east coast of Porto Santo Island in 2017, by manually lifting stones and retrieving specimens manually or with the aid of an entomological aspirator. We conducted an expedition to Terceira and Pico islands, in the Azores archipelago, in 2018, where *Dysdera* specimens were collected following the same protocol as mentioned above. Each specimen was placed into a separate vial. We obtained specimens of *D. flavitarsis* from a former study (Carvalho *et al.*, 2020; Crespo *et al.*, 2018; Domènech, Crespo, Enguídanos, & Arnedo, 2020; Malumbres-Olarte *et al.*, 2020).

Molecular lab procedures

We generated sequences of partial fragments of the mitochondrial cytochrome *c* oxidase subunit I (*COI*), i.e. the animal DNA barcode (Hebert, Cywinska, Ball, & DeWaard, 2003), 16S rRNA, tRNA Leu (*L1*), NADH dehydrogenase subunit 1 (*NAD1*), the nuclear large ribosomal subunit 28S rRNA (*28S*) and histone 3 (*H3*) for *D. citauca* sp. nov., *D. flavitarsis* and *D.* sp. 'SPJ' (listed in Supplementary Materials A), and added these to the Dysderidae samples published by Crespo *et al.* (C. *et al.*, 2021). Outgroup taxa were grabbed from the Spider Tree

of Life project (Wheeler et al., 2017). Methods for extraction, DNA amplification, sequencing and sequence edition followed Crespo *et al* (C. *et al.*, 2021).

Phylogenetic analyses

We combined the DNA sequences newly generated in the present study with the data matrix available for Madeiran *Dysdera* in Crespo *et al* (C. *et al.*, 2021). Additional outgroup species within the superfamily Dysderoidea available in Genbank from former studies were also included to provide fossil calibration points for divergence time estimation analysis (see Supplementary Materials A).

The ribosomal genes were automatically aligned using the Geneious Prime® 2021.0.3 (https://www.geneious.com) plugin of the alignment program MAFFT v. 1.4.0 (Katoh, Misawa, Kuma, & Miyata, 2002), using the G-INS-i algorithm with default options. Protein coding genes were aligned using the Translation Align option in Geneious also with the MAFFT alignment program and the G-INS-i algorithm, using the BLOSUM62 scoring matrix. All genes were concatenated in a super matrix for subsequent phylogenetic analyses with the help of the program Sequence Matrix (Vaidya, Lohman, & Meier, 2011).

Parsimony analysis of the concatenated matrix was conducted with the program TNT v1.5 (Goloboff & Catalano, 2016). For parsimony analyses gaps were recoded as absence/presence characters using the simple coding method proposed by Simmons & Ocheterena (Simmons & Ochoterena, 2000) implemented in the computer program SeqState (Müller, 2005). Following Soto *et al.* (S. *et al.*, 2017), we use a combination of the 'New Technologies' search strategies in TNT, namely sectorial searches, tree fusing, drift and ratchet. Tree searches were driven to hit independently 10 times the optimal scoring, followed by TBR branch swapping. Support values were estimated by jackknifing frequencies derived from 1000 resampled matrices using 15 random addition sequences, retaining 20 trees per replication, followed by TBR, and TBR collapsing to calculate the consensus. The best maximum likelihood tree was inferred with IQ-TREE v. 2.1.2 (Minh *et al.*, 2020). We used ModelFinder to first select the best-fit partitioning scheme and corresponding evolutionary models (Kalyaanamoorthy, Minh, Wong, Von Haeseler, & Jermiin, 2017), and then to infer the best tree and estimate clade support by means of 1000 replicates of standard non-parametric

bootstrapping. For Bayesian analyses, the best partition scheme and evolutionary model was first selected with help of the computer program Partition Finder v2.1.1 (Lanfear, Frandsen, Wright, Senfeld, & Calcott, 2017). Bayesian inference was implemented with MrBayes v3.2.6 (Ronquist *et al.*, 2012). The analysis was run for 10 million generations, sampling every 1000, with eight simultaneous Markov Chain Monte Carlo (MCMC) chains, 'heating temperature' of 0.15, and a relative initial burn-in of 25%. Support values were calculated as posterior probabilities. Convergence of the chains, correct mixing and the number of burn in generations were monitored with Tracer v. 1.7 (Rambaut, Drummond, Xie, Baele, & Suchard, 2018). Model based analyses were run remotely at the CIPRES Science Gateway (Miller, Pfeiffer, & Schwartz, 2010). The phylogenetic tree was edited using FIGTREE (http://tree.bio.ed.ac.uk/software/figtree/).

Divergence time estimation

A timeframe for the diversification of focal taxa was inferred in a Bayesian framework using non-correlated relaxed clocks as implemented in Beast 2.6.3 (Bouckaert *et al.*, 2019). We use a scheme partition by gene to reduce the parameter space, with the corresponding unlinked evolutionary models as selected by PartitionFinder 2. We assigned the Birth-Death model as tree prior and defined individual relaxed lognormal clocks for each gene partition. We selected uniform distributions with a (0.0001 to 1.0) as prior for the ucld.mean parameters. A monophyly constraint for relationships within Dysderoidea were defined following results of a recent transcriptomic analysis of spiders (Kallal *et al.*, 2020), such as Segestriidae, Oonopidae, Orsolobiidae and Dysderidae form a clade, and Segestriidae was sister to all other families. Absolute divergence time were inferred based on fossil calibration points. We followed the interpretation of relevant fossil taxa provided by Magalhaes et al (Magalhaes, Azevedo, Michalik, & Ramírez, 2020). The fossil *Dasumiana emicans* Wunderlich, 2004 from Baltic Amber, age estimated at a minimum of 43 my old was considered a crown Harpacteinae, and thus provided a minimum age of 43 my to the crown group. Similarly, *Ariadna parva* Wunderlich, 2008 and *Vetsegestria quinquespinosa* Wunderlich, 2004, also from Baltic Amber, considered stem species of the two main subfamilies within Segestriidae, provided a minimum age of 43 my to the crown age of the family. Several fossil species from

Mesozoic amber inclusions have been assigned to the oonopid subfamily Orchestininae (see Dunlop, JA, Penney, D & Jekel, 2018), suggesting that the family had already diversified by the Cretaceous (minimum age of 98.17 my). Since Orchestininae is presumably the sister lineage to the remaining Oonopidae, but was not included in the present study, we played safe and assigned these fossils to the stem Oonopidae. We incorporated fossil calibration information as lognormal distributed priors on specific target nodes. Values for Harpacteinae and Segestriidae crowns were as follows: mean in real space=15, standard deviation=0.75, offset=43.0 (Median 54.3, 97.5% HPD=45.6-92.2), and for Oonopidae stem: mean in real space=15, standard deviation=0.75, offset=98.17 (Median 109, 97.5% HPD=101-147). We included three additional biogeographic calibration points. The divergence time between the two *Parachtes* Alicata, 1964 has been shown to correspond to a vicariant event as a result of the Hercynian belt opening, which has been dated at 33–25 Myr (Bidegaray-Batista & Arnedo, 2011). Consequently, we constrained a normal prior distribution on the corresponding node with mean 29 Myr and standard deviation 2.5 (Median 29, 97.5% HPD=24.1-33.9). The oldest age of the Western Canary Island and the Eastern Canary Islands, respectively, provided maximum ages for the diversification of the endemic species on each island group as they were found to form well supported exclusive clades (see results). Therefore, we defined a uniformly distributed prior to the crown of the Western Canary Islands and the Eastern Canary Island clades, ranging from 1 my to 15 or 22 my, based on the oldest evidence for emerged land in the Western and Eastern island groups, respectively (Fernández-Palacios *et al.*, 2011). Finally, we constrained the root of the complete tree by assigning a uniform prior ranging from 125 to 270 my, based on recent estimates of the timeline of spider evolution (Kallal *et al.*, 2020; Magalhaes *et al.*, 2020). We ran three independent runs of 100,000,000 generations each, saving parameters and trees every 10,000 generations, remotely on CIPRES Science Gateway. Convergence and correct mixing were assessed with Tracer, results for each chain combined after burn in of 10% of the generations with LogCombiner and the maximum clade credibility tree estimated with TreeAnnotator using median heights for the nodes.

Morphological study

We carried morphological observations through a stereomicroscope Leica MZ 16A equipped with a digital camera Leica DFC450. We took individual raw photos with the help

of the software Leica Application Suite v4.4 and mounted with the software Helicon Focus (Helicon Soft, Ltd.). Further editions were done with Paint Shop Pro v21 (Corel Corporation). We removed Female vulva from specimens with the aid of hypodermic needles and forceps. To clear the membranous tissues surrounding the sclerites of genitalia, we manually removed muscular and membranous tissue with forceps and a needle, then also immersed the structure in KOH 30% for 15 to 30 minutes, after which we cleaned the remaining patches of tissue. SEM images of the male copulatory bulb were obtained with a Q-200 (FEI Co.) scanning electron microscope (SEM). For the SEM images, each male palp was excised at the joint between tarsus and tibia. Samples were sonicated for roughly 30 seconds with ultrasonic bath Nahita ZCC001, dehydrated through immersion in increasing dilutions of ethanol, transferred to absolute ethanol and carbon or gold sputter coated.

We took measurements using an ocular micrometre in the stereoscope. We measured length of the cheliceral furrow from the base of the distal condyle to the tip of cheliceral basal lamina. All measurements are in millimetres (mm). We followed Arnedo, Oromí, & Ribera, 1996 for scoring leg chaetotaxy, and Arnedo, Oromí, & Ribera, 2000 for establishing genital homologies and nomenclature. We added an additional character, the prolateral lateral sheet (pL), a membranous fin-like outgrowth, bordering the tip of the IS (Fig. 9C).

Abbreviations

AME - anterior median eyes

PLE - posterior lateral eyes

PME - posterior median eyes

B - basal tooth

M - median tooth

D - distal tooth

T - tegulum

ES - external sclerite

IS - internal sclerite

pL - prolateral lateral sheet

eL - external margin of lateral sheet

L - lateral sheet

P - posterior apophysis of tegulum

AD - anterior diverticle

PD - posterior diverticle

DA - dorsal anterior diverticle

VA - ventral anterior diverticle

S - spermathecae

TB - transversal bar

Collections

NHMUK - British Museum of Natural History, London, UK

CRBA - Centre de Recursos de Biodiversitat Animal, University of Barcelona, Barcelona

FMNH - Finnish Museum of Natural History, Helsinki

MZB - Museu de Ciències Naturals de Barcelona, Barcelona

MMF - Museu Municipal do Funchal, Funchal

RESULTS

Phylogenetic analyses

The concatenated matrix included 107 terminals and 2,913 characters corresponding to 676 bp of the COI, 414 bp of the *nad1*, 658 aligned positions of the 16S+L1, 328 bp of the H3, 837

bp of the 28S. Parsimony analyses of the concatenated matrix with gaps coded and absence/presence characters yielded 8 trees of 15,105 steps. Results of the parsimony and model-based analyses are summarized in Fig. 2. The Iberian *Dysdera flavitarsis*, the Azorean *Dysdera sp.* 'SPJ' and the Madeiran *D. citauca* sp. nov. formed a well-supported clade and the island species were supported as sister taxa. The species *D. citauca* sp. nov. was never inferred as closely related to the remaining Madeiran endemics, which form a well-supported clade.
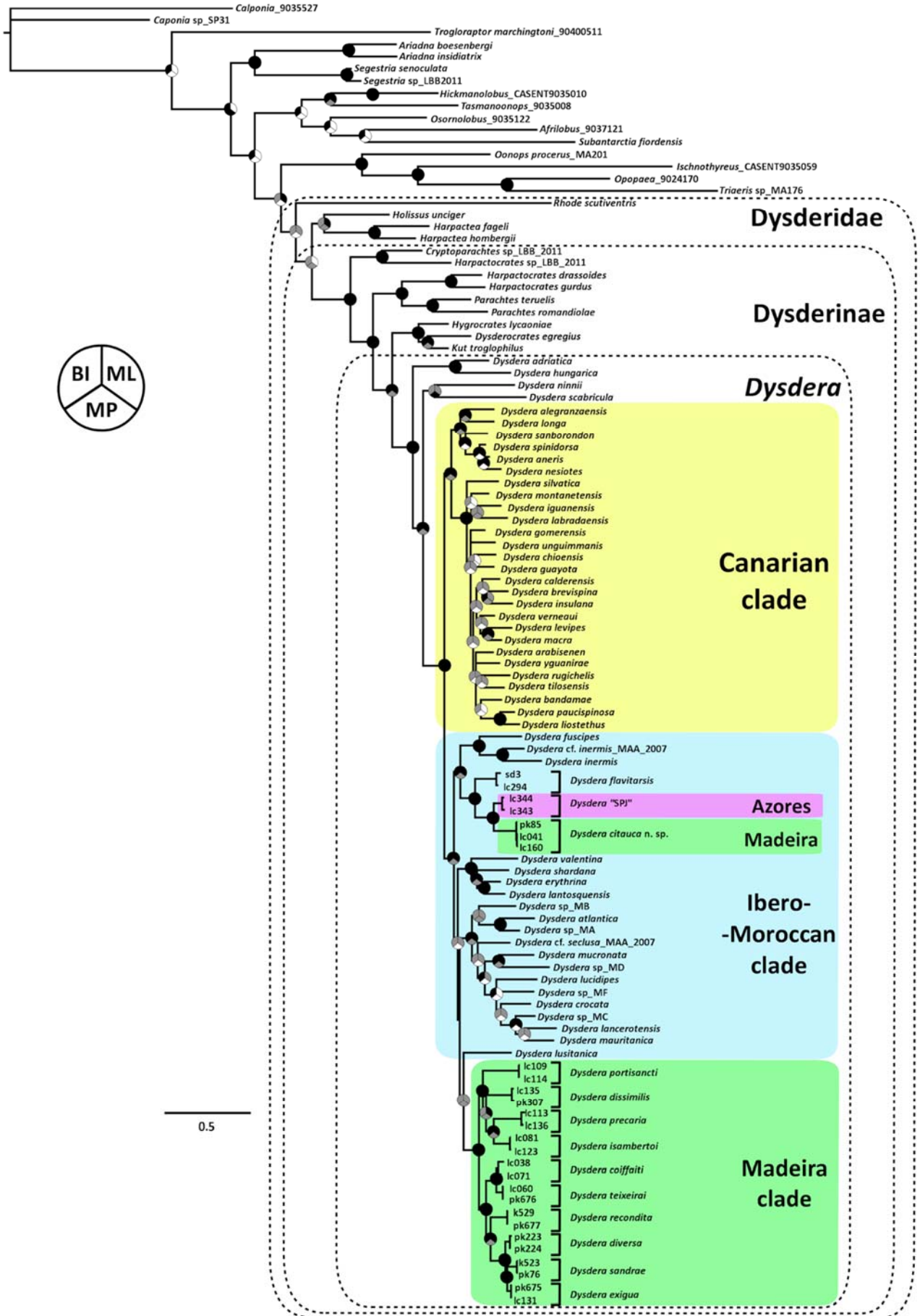
Figure 2. Bayesian majority rule consensus tree based on the multigene concatenate alignment. Nodes are split in three sections, respectively representing each method (see diagram on left): top left: BI; top right: ML; bottom: MP. Black indicates a supported node (Bayesian PP ≥ 0.95, ML ultrafast Bootstrap ≥ 95% or MP Jackknife ≥ 75%), grey an unsupported node (Bayesian PP < 0.95, ML ultrafast Bootstrap < 95% or MP Jackknife < 75%) and white an unrecovered node (only ML and MP). Coloured boxes signal the main groups of treated species in the genus *Dysdera*. Dashed boxes indicate major taxonomic divisions within Dysderidae.

Results of the time estimation analyses are illustrated in Fig. 3 (non *Dysdera* outgroups were removed, full tree available in Supplementary Materials B). The Azores and Madeira sister species split form their Iberian closest relative, *D. flavitarsis*, in the early to middle Miocene (18.5 my, 95% HPD 13.9-23.3), and the insular species diverged from one another during in the late Miocene (8.1 my, 4.9-12). Our analysis also provided the first time estimates for the origin and diversification of the Madeiran-clade (Crespo *et al.* 2021), which diverged from its mainland relatives during the Oligocene (31.2 my, 28.4-36.2) and extant species started diversifying in the early Miocene (18.7 my, 15.5-22.2). In this clade, endemic species from Porto Santo (*D. dissimilis* Crespo & Arnedo, 2021, *D. isambertoi* Crespo & Cardoso, 2021, *D. portisancti* Wunderlich, 1995 and *D. precaria* Crespo, 2021) are among the earliest to have diverged from their most recent common ancestor up to the mid-Miocene. From here on, the remaining diversification events occurred in species from Madeira and Desertas, with most species diverging in the Pliocene. Overall, for the Madeiran clade divergence time estimated slightly predated the age of the subaerial stages of the islands reported in the literature.
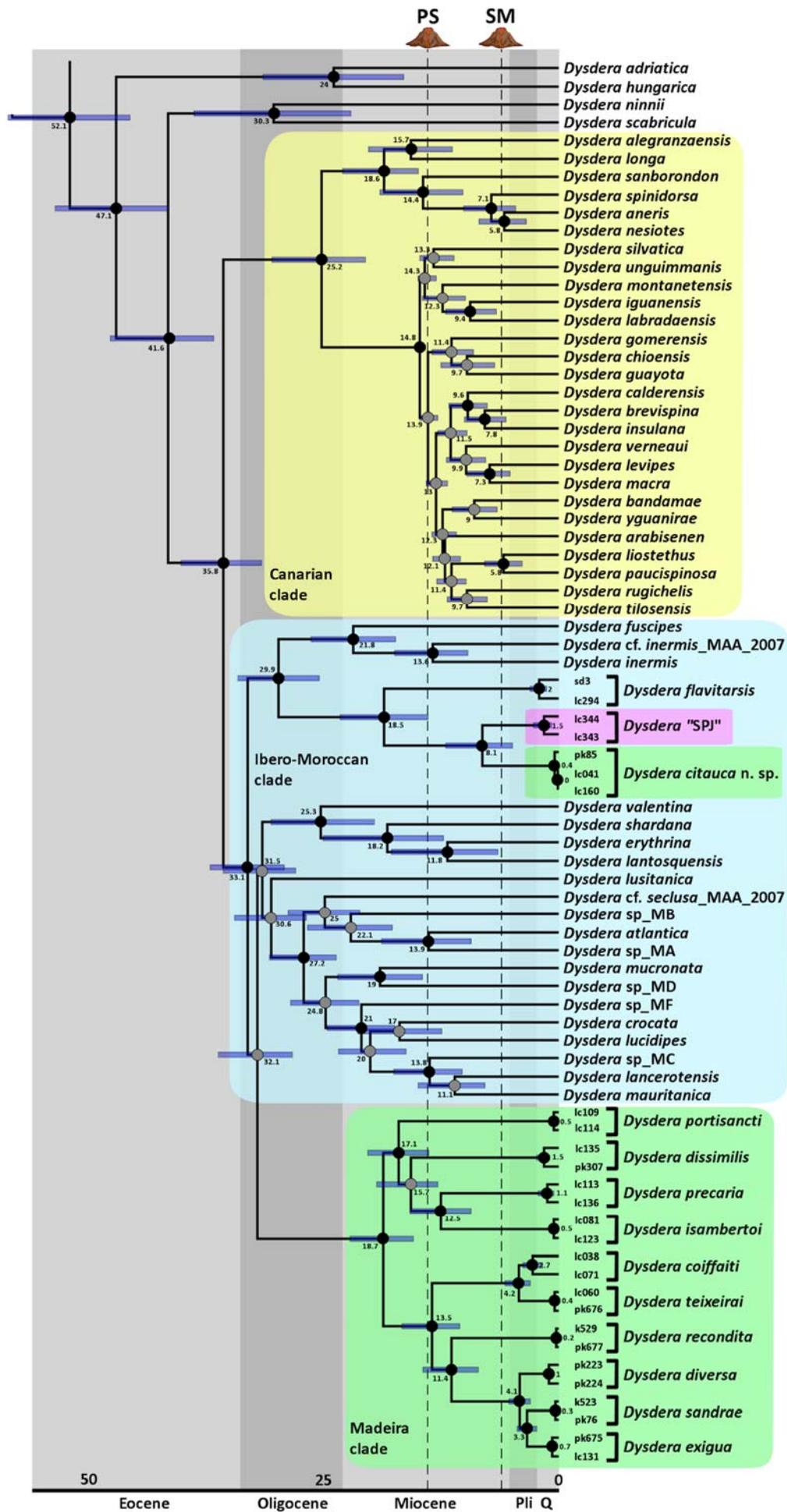
Figure 3. Maximum clade credibility tree retrieved with time estimation analysis in a Bayesian framework using BEAST. Black indicates a supported node (Bayesian PP ≥ 0.95), grey an unsupported node (Bayesian PP < 0.95). Colored boxes signal the main groups of treated species in the genus *Dysdera*. Dashed lines indicate the emergence of Porto Santo (PS) and Santa Maria (SM) islands. Geological eras are shown below (abbreviations: Pli – Pliocene, Q – Quaternary).

Taxonomy

FAMILY DYSDERIDAE C.L. KOCH, 1837

GENUS *DYSDERA* LATREILLE, 1804

Dysdera cetophonorum Crespo & Arnedo, **sp. nov.**

urn:lsid:zoobank.org:act:C67C9924-F941-4BE0-A1A7-117CEE79FFF8

(Figs 4–6)

HOLOTYPE: 1 ♂, stored at NHMUK, collection number 010305619.

PARATYPES: **Pico:** 1 ♂ and 1 ♀ (collection number the same as holotype, female with extracted vulva).

TYPE LOCALITY: (undetermined location), Pico, 300-1000 m, Azores Archipelago, Portugal.

ETYMOLOGY: The specific epithet, is a latinized genitive plural from the Greek 'keto-phonos', which means 'killing sea monsters', refers to the historical relevance of whaling for both the cultural identity and the economy of the Azores, which lasted until 1987. Today the islands are renowned as world-class spot for whale watching.

DIAGNOSIS: *D. cetophonorum* sp. nov. can be diagnosed from both its closely related species, *D. citauca* sp. nov. and *D. flavitarsis*, and the sympatric *D. crocata* by presence of a well projected P with a dorsal toothed ridge in the male palp (Figs 4A, 6A), the more developed anteroventral sclerotization of the female vulva VA (Fig. 4D), and its cheliceral dentition, presenting 4 teeth instead of 2 or 3 in the other species (Fig. 4C).

DESCRIPTION:

MALE HOLOTYPE (Figs 4A–C, 5–6):

CARAPACE: length 4.35; maximum width 3.56; minimum width 2.48. Brownish orange, foveate at borders, smooth, inclined (Fig. 5). Frontal border roughly rounded, 4.95 wide; anterior lateral borders slightly convergent; lateral borders divergent, rounded after maximum width point while converging to back margin; back margin bilobed, wide.

EYES: AME 0.24, oval; PLE 0.24, oval; PME 0.22, oval; AME separated from anterior border by less than their diameter; AME separated by one another by roughly their diameter; AME touching PLE; PME separated by PLE by roughly a third of PME diameter; PME touching.

LABIUM: trapezoid, with base wider than distal part, longer than wide at base; distal part concave.

STERNUM: orange, smooth, with setae.

CHELICERAE (Fig. 4C): 2.35 long, about one third of carapace length in dorsal view, dorsally and prolaterally with sparse sclerotized piliferous granulations; fang 1.9. Cheliceral furrow approximately 45% of the length of basal segment, armed with 4 teeth and basal lamina, D > B = M1 = M2; all teeth triangular, B close to lamina, M1 closer to B than M2, M2 situated roughly in the midpoint of D situated in the distal half of cheliceral furrow.

LEGS: orange, the first pair darker. Lengths: Leg I: 12.24 (3.64, 2.19, 2.88, 2.81, 0.72); Leg II: 11.54 (3.34, 2.09, 2.69, 2.69, 0.74); Leg III 9.09 (2.73, 1.55, 1.72, 2.35, 0.74); Leg IV 11.81 (3.48, 1.92, 2.52, 3.11, 0.78); relative length: 1 > 4 > 2 > 3; palp 5.35 (2.13, 1.16, 1, 1.06, 5.35). Legs covered with hairs, especially so in tibiae, metatarsi and tarsi. Metatarsi III and IV with dense tuft of hairs in distal ventral section. Eight to nine teeth in each claw.

SPINATION: ti3d proximal 1.0.0.

ABDOMEN: 6 long, cream colored, cylindrical; abdominal dorsal hairs very short, 0.01, apically blunt.

MALE GENITALIA (Figs 4A–B, 6): T shorter than DD, external border sloped backwards. DD bent anteriorly in lateral view, more or less 30°. IS shorter and thicker than ES. ES poorly developed. C present, short. pL present. LF absent. AR absent. L present, without sclerotized external margin. LA absent. F absent. AL absent. P unfused to T, rotated posteriorly, lateral

length roughly half of the width of T in retrolateral view. Ridge present, perpendicular to T, showing 4 teeth, not projected.

FEMALE PARATYPE (CRBALC0045) (Figs 4D–F):

All characters as in male except:

CARAPACE: length 5; maximum width 4.08; minimum width 2.65.

EYES: AME 0.27; PLE, 0.25; PME, 0.24.

CHELICERAE: 2.72; fang 2.04.

LEGS: Leg I: 13.45 (4, 2.44, 3.24, 3.03, 0.74); Leg II: 12.67 (3.72, 2.25, 2.97, 2.97, 0.76); Leg III: 10.17 (2.91, 1.74, 2, 2.72, 0.8); Leg IV: 13.59 (3.88, 2.19, 3, 3.6, 0.92); ; relative length: 4 > 1 > 2 > 3; palp 5.73 (2.24, 1.19, 0.98, 1.32).

SPINATION: leg1, leg 2 spineless; fe3, pa3 spineless; ti3d proximal 1.0.0, distal 1.0.0; ti3v spineless; leg4 spineless.

ABDOMEN: 8.1 long; abdominal dorsal hairs short, 0.03–0.06 in length, slender, uniformly distributed.

FEMALE GENITALIA (Figs 4D–F): PD oval. DA in close contact to VA. DA more than twice as wide as long, anteriorly with a small hump. DF wide in dorsal view. MF hard to discern, apparently small. VA roughly twice as wide as long, membranous except in its sclerotized anterolateral section, shaped as a quadrangle with rounded corners. Insertion of S projected onto VA through a sclerotized neck, S roughly oval in ventral view, with arms of moderate length and tips short, dorsally with irregularly shaped tubercles.

INTRASPECIFIC VARIATION: Male carapace varies from 4.35 to 5.72 in length, from 3.56 to 4.25 in width. Cheliceral length from 2.43 to 2.81 in males.

DISTRIBUTION AND ECOLOGY: This species is known from an undetermined locality comprised between 300 and 900 m of elevation, in the island of Pico, in the Azores (Fig. 1C).

CONSERVATION: The species was mentioned as presumably extinct in Cardoso *et al.* (Cardoso *et al.*, 2010). In spite of intense biological surveys conducted in the Azorean forests in the last

70 years, following the collection of the specimens here described, no more specimens were found.
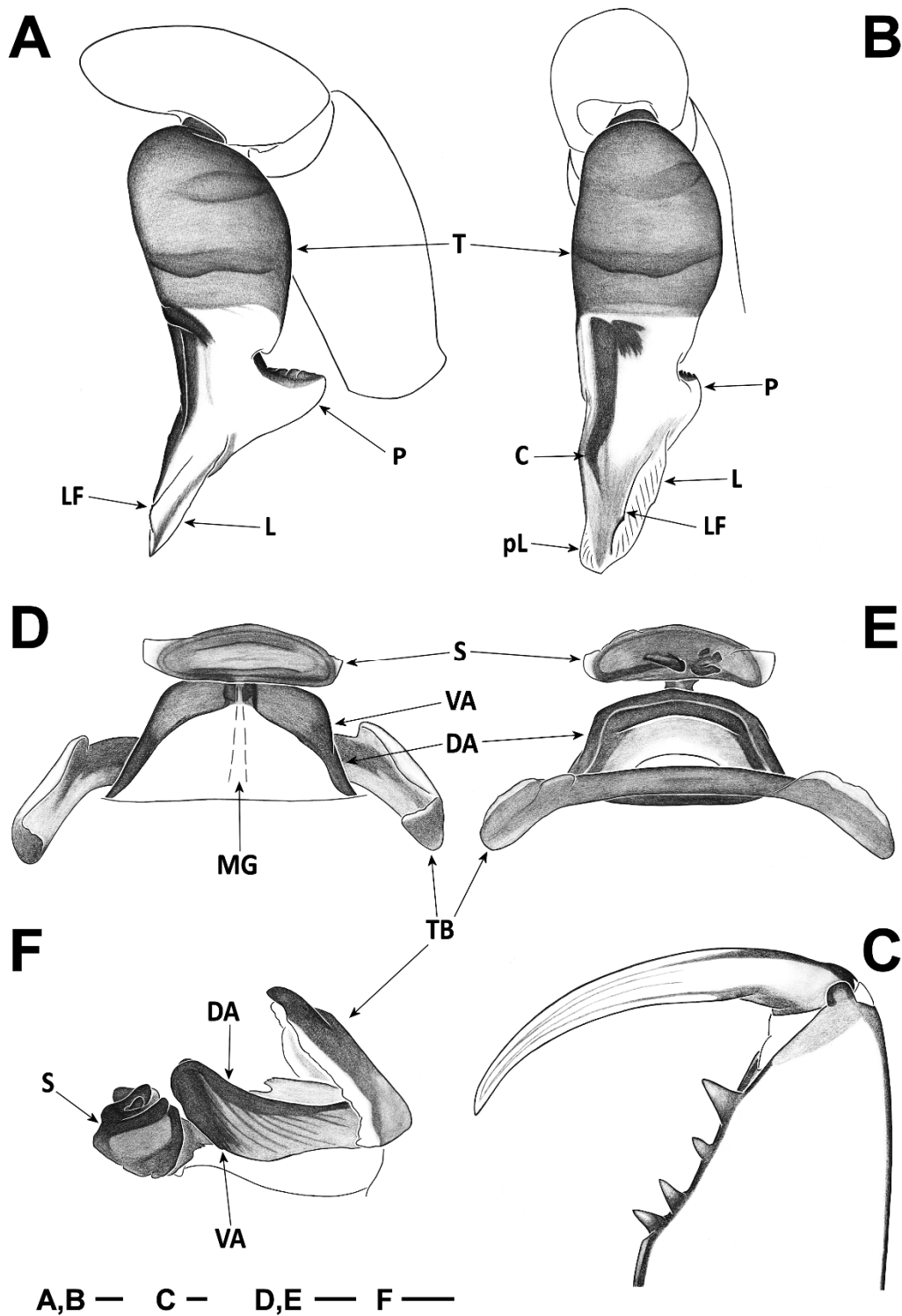
Figure 4. *D. cetophonorum* Crespo & Arnedo, sp. nov. A – C, holotype male; A, left palp, retrolateral; B, left palp, anterior; C, left chelicera, ventral; D – F, female paratype

(NHMUK 010305619); D, vulva, ventral; E, vulva, dorsal; F, vulva, lateral. Scale bars = 0.1 mm.

Figure 5. A – B, *D. cetophonorum* Crespo & Arnedo, sp. nov., holotype male (NHMUK 010305619): A, prosoma, dorsal; B, prosoma, lateral. Scale bars = 1 mm.
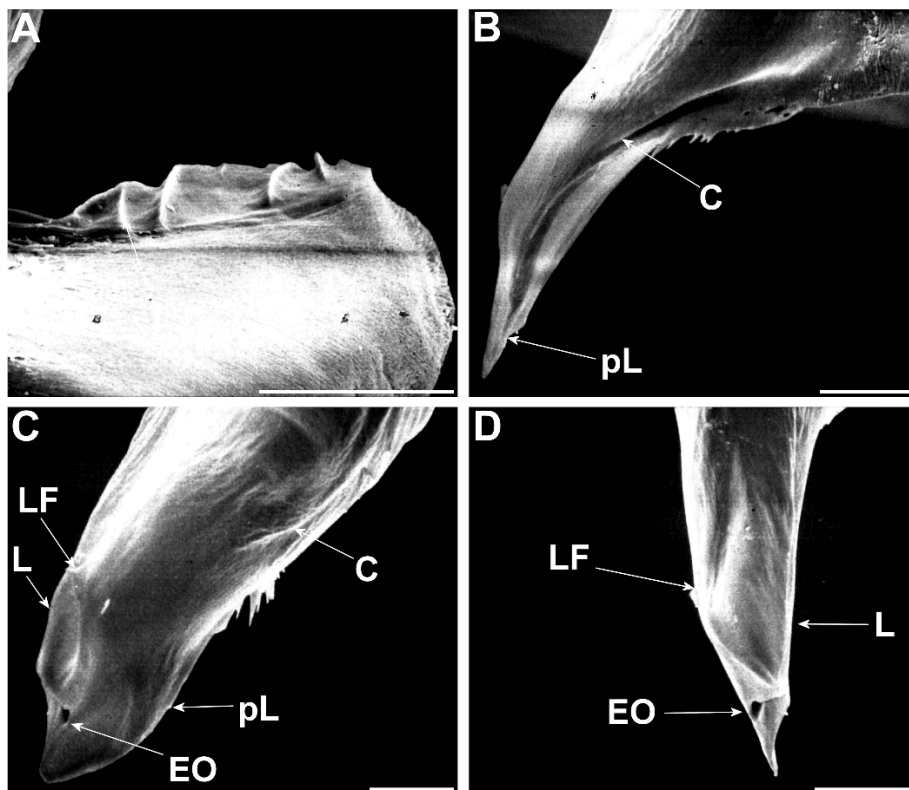
Figure 6. A – D, SEM mirrored images of distal left palp of *D. cetophonorum* Crespo & Arnedo, sp. nov., paratype male (NHMUK 010305619): A, retrolateral detail of the P, showing the toothed ridge; B, prolateral; C, anterior; D, retrolateral. Scale bars = 0.1 mm.

Dysdera citauca Crespo & Arnedo, **sp. nov.**

urn:lsid:zoobank.org:act:2CC697A6-F09D-49AD-8BCE-A5D5CA128264

(Figs 7–10)

HOLOTYPE: 1 ♂, MZB, collection number 2020-0755.

PARATYPES: Ilhéu de Cima (Porto Santo): erosion cave at NE side of islet, 1 ♂ (MMF 48021) and 3 ♀♀ (CRBALC0053, MZB 2020-0757, CRBALC0056), 19.IV.2017, direct hand sampling, leg. L. Crespo & I. Silva, 2 ♀♀ (CRBA002543, MMF 48022), 17.X.2011, direct hand sampling, leg. I. Silva; pebble beach at NE side of islet, 1 ♂ (FMNH KN.20930), 2 ♀♀ (MZB 2020-0756, FMNH KN.20931), 19.IV.2017, direct hand sampling, leg. L. Crespo & I. Silva.

ADDITIONAL MATERIAL*:* Ilhéu de Cima (Porto Santo): erosion cave at NE side of islet, 1 juvenile (CRBALC0054), 19.IV.2017, direct hand sampling, leg. L. Crespo & I. Silva, 1 ♀ (CRBA002545), 17.X.2011, direct hand sampling, leg. I. Silva; pebble beach at NE side of islet, 1 juvenile (CRBALC0052), 19.IV.2017, direct hand sampling, leg. L. Crespo & I. Silva.

TYPE LOCALITY: N33.05698° W16.2865°, erosion cave at NE side of islet, Ilhéu de Cima (Porto Santo), Madeira Archipelago, Portugal, coll. 19.IV.2017, direct hand sampling, leg. L. Crespo & I. Silva,

ETYMOLOGY: The species name in apposition refers to the fictional sea creature race that marauded at night the shores of a forsaken rocky island, portrayed in the novel Cold Skin by Catalan writer Albert Sanchez Piñol.

DIAGNOSIS*: D. citauca* sp. nov. can be diagnosed from its closely related species, *D. cetophonorum* sp. nov. and *D. flavitarsis*, by the presence of a P in close apposition to the base of the T (Fig. 7A) in the male palp, the combination of a reduced anteroventral sclerotization and a large length of the female vulva VA (Fig. 7D), and from *D. cetophonorum*

sp. nov. by its cheliceral dentition, presenting 3 teeth instead of 4 (Fig. 7C). Additionally, it can be diagnosed from other Madeira archipelago congeners by its flattened carapace and robust chelicerae (Fig. 8).

DESCRIPTION:

MALE HOLOTYPE (Figs 7A–C, 8–9):

CARAPACE: length 4.3; maximum width 3.38; minimum width 2.3. Brown, foveate at borders, smooth, with a posterior central depression, in lateral view flattened (Fig. 8). Frontal border roughly rounded, 2.4 wide; anterior lateral borders convergent; lateral borders divergent, rounded after maximum width point while converging to back margin; back margin slightly raised, wide.

EYES: AME 0.24, oval; PLE 0.2, oval; PME 0.18, oval; AME separated from anterior border by less than half their diameter; AME separated by one another by roughly their diameter; AME touching PLE; PME separated by PLE by roughly a third of PME diameter; PME touching.

LABIUM: trapezoid, with base wider than distal part, longer than wide at base; distal part concave.

STERNUM: orange, wrinkled.

CHELICERAE (Fig. 7C): 2.35 long, about two fifths of carapace length in dorsal view, robust (see lateral view), dorsally and prolaterally with sclerotized piliferous granulations; fang 1.77. Cheliceral furrow approx. 45% of the length of basal segment, armed with 3 teeth and basal lamina, D > B = M; all teeth triangular, B close to lamina, M closer to B than D, D situated in the distal half of cheliceral furrow.

LEGS: Posterior legs yellow, anterior legs orange, the first pair darker. Lengths: Leg I: 14.16 (3.88, 2.38, 3.6, 3.46, 0.84); Leg II: 13.1 (3.56, 2.24, 3.24, 3.24, 0.82); Leg III: 9.94 (2.81, 1.68, 2.04, 2.59, 0.82); Leg IV: 12.98 (3.64, 2.06, 3, 3.3, 0.98, 12.98); relative length: 1 > 2 > 4 > 3; palp 5.38 (2.18, 1.16, 1, 1.04). Legs covered with hairs, especially so in tibiae, metatarsi and tarsi. Metatarsi III and IV with dense tuft of hairs in distal ventral section. Six to seven teeth in each claw.

SPINATION: all legs spineless.

ABDOMEN: 5.19 long, cream coloured, cylindrical; abdominal dorsal hairs very short, 0.01–0.03, apically blunt, smaller hairs concentrated above cardiac region. MALE GENITALIA (Figs 7A–B, 9): T shorter than DD, external border sloped backwards. DD bent anteriorly in lateral view, more or less 30°. IS shorter and thicker than ES. ES basally poorly developed, apically well developed. C present, short. pL present. LF present. AR absent. L present, without sclerotized external margin. LA absent. F absent. AL absent. P unfused to T, rotated posteriorly, lateral length roughly half of the width of T in retrolateral view. Ridge present, perpendicular to T, showing 4 to 5 teeth, not projected.

FEMALE PARATYPE (MZB 2020-0756) (Figs 7D–F):

All characters as in male except:

CARAPACE: length 4.25; maximum width 3.52; minimum width 2.4.

EYES: AME 0.22.

CHELICERAE: 2.35; fang 1.73.

LEGS: Leg I: 14.48 (3.96, 2.5, 3.64, 3.54, 0.84); Leg II: 13.18 (3.68, 2.3, 3.2, 3.24, 0.76); Leg III: 10.53 (3.03, 1.8, 2.13, 2.73, 0.84); Leg IV: 13.89 (3.84, 2.19, 3.4, 3.5, 0.96); relative length: 1 > 4 > 2 > 3; palp: 5.7 (2.21, 1.17, 1.02, 1.3).

SPINATION: all legs spineless.

ABDOMEN: 7.72 long; a small patch of longer abdominal dorsal hairs with tapered tips can be found anterodorsally, 0.08–0.18 in length.

FEMALE GENITALIA (Figs 7D–F): PD oval. DA clearly separated from VA. DA roughly twice as wide as long, anteriorly with a small hump. DF wide in dorsal view. MF elongated posteriorly. VA roughly twice as wide as long, membranous except in its sclerotized anterolateral section, shaped as a quadrangle with rounded corners. Insertion of S projected onto VA through a membranous neck, with several sclerotized interior plaques, S trapezoidal in ventral view, with arms of moderate length and tips extended dorsolaterally.

INTRASPECIFIC VARIATION: Male carapace varies from 4.25 to 4.75 in length, from 3.34 to 3.64 in width, female from 3.8 to 4.65 in length and 2.89 to 3.64 in width. Cheliceral length from 2.35 to 2.72 in males, 1.86 to 2.48 in females.

DISTRIBUTION AND ECOLOGY: This species is known solely from the NE rocky shore of Ilhéu de Cima, an islet of Porto Santo (Fig. 1D). Interestingly, the species was collected in the spray zone. This is an infrequent habitat for *Dysdera*, but the presence in the intertidal and spray zone has also been reported in the Canarian endemics *D. curvisetae* Wunderlich, 1987 and *D. mahan* Macías-Hernández & Arnedo, 2010 (Macías-Hernández *et al.* 2016).

CONSERVATION: Extremely limited distribution probably diminishing due to the invasive *D. crocata* that occupies most of the island.
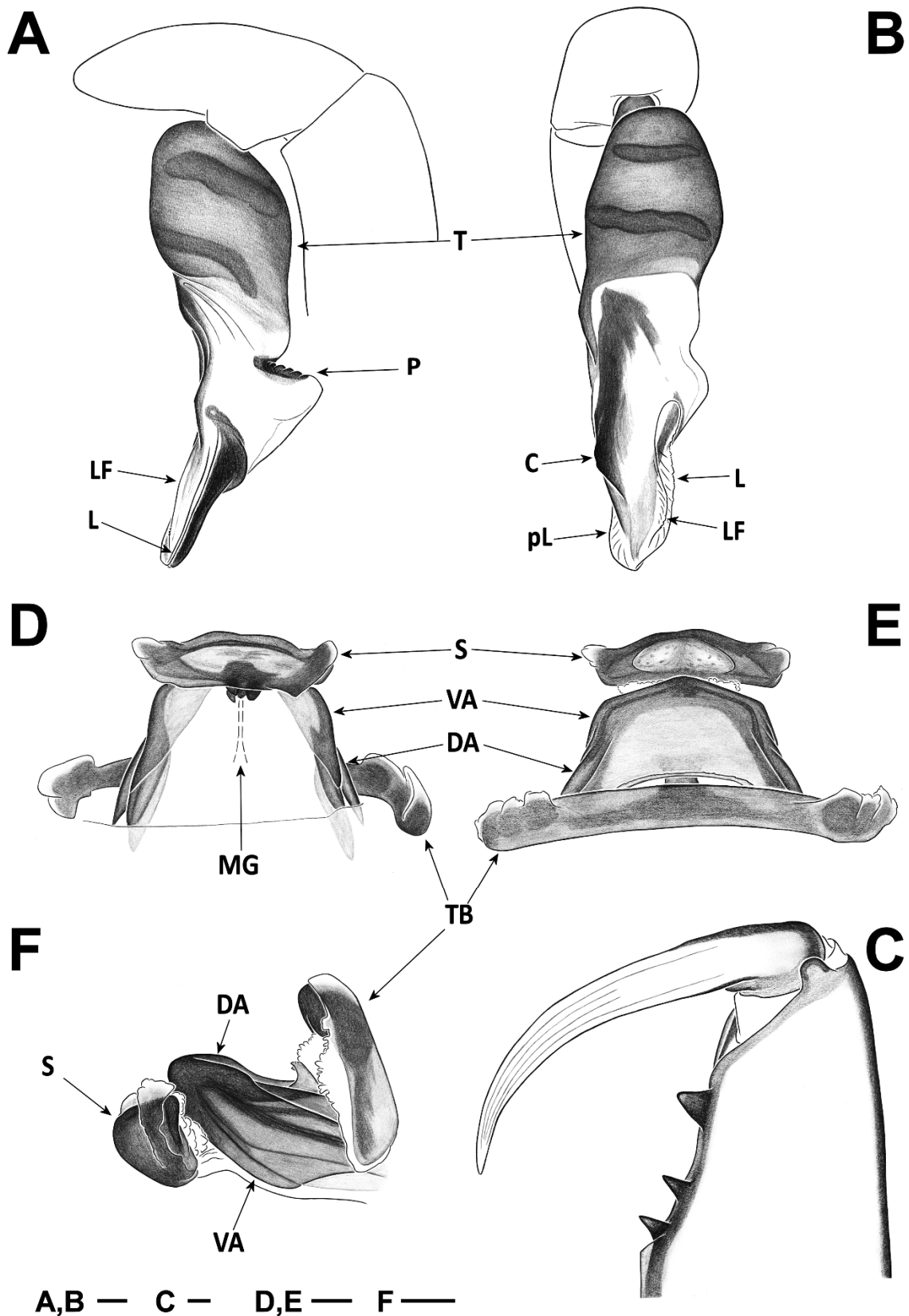
Figure 7. *D. citauca* Crespo & Arnedo, sp. nov. A – C, holotype male; A, left palp, retrolateral; B, left palp, anterior; C, left chelicera, ventral; D – F, female paratype (MZB 2020-0756); D, vulva, ventral; E, vulva, dorsal; F, vulva, lateral. Scale bars = 0.1 mm.

Figure 8. A – B, D. citauca Crespo & Arnedo, sp. nov., holotype male: A, prosoma, dorsal; B, prosoma, lateral. Scale bars = 1 mm.
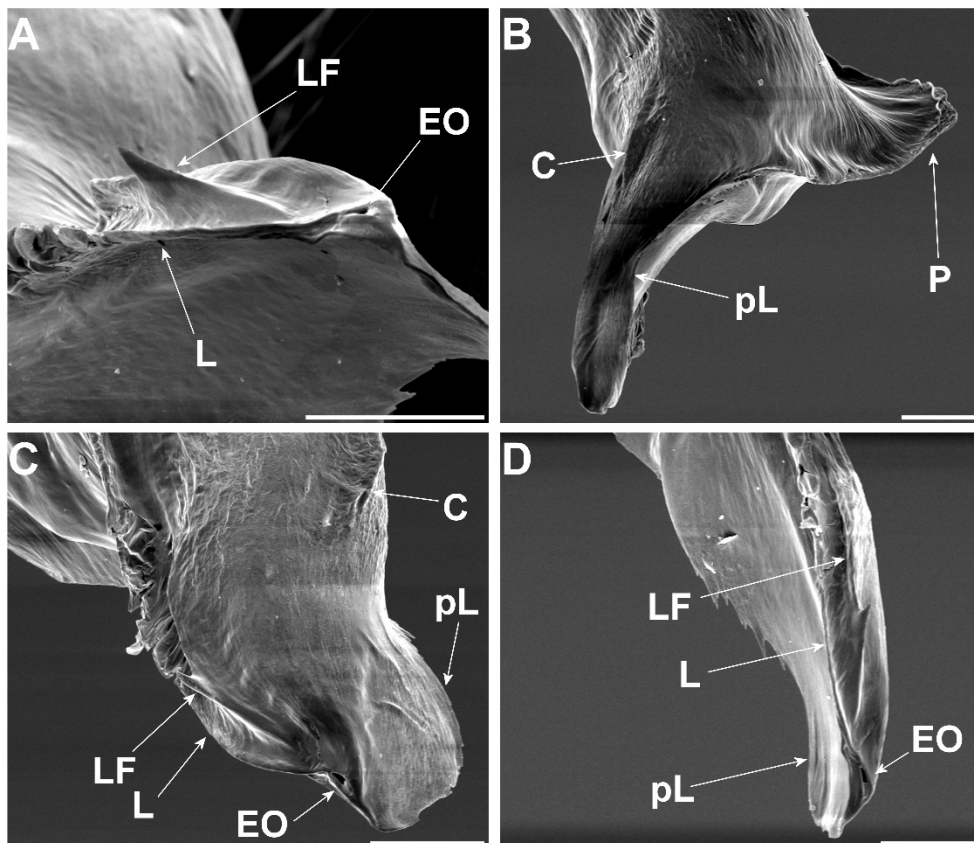
Figure 9. A – D, SEM images of distal right palp of *D. citauca* Crespo & Arnedo, sp. nov., paratype male (FMNH KN.20930): A, apical detail; B, prolateral; C, anterior; D, retrolateral. Scale bars = 0.1 mm.

Figure 10. A, *D. citauca* Crespo & Arnedo, sp. nov., paratype female (FMNH KN.20931). Photo credits: by courtesy of Emídio Machado.

Dysdera flavitarsis Simon, 1882

(Figs 11–13)

HOLOTYPE: 1 ♂, stored at MNHNP, collection number, 1167 jar 542 (according to Ferrández, unpublished information). Not examined.

ADDITIONAL MATERIAL: Portugal: Mata de Albergaria, Terras de Bouro, 1 ♂, 4–11.VI.2005, pitfall trapping, 1 ♂ and 2 ♀♀ (ZMUC), 15.VI.2005, direct hand sampling, leg. P. Cardoso *et al.*; Ponte de São Miguel, Terras de Bouro, 1 ♂ (CRBA), 7.V.2008, direct hand sampling, leg. G. Giribet; Spain: Joyoguelas, Leon, 8 ♂♂ and 2 ♀♀ (CRBA), 7–22.VI.2013, pitfall trapping, leg. M. Arnedo *et al.*; Las Arroyas, Leon, 2 ♂♂ and 3 ♀♀ (CRBA), 8–23.VI.2013, pitfall trapping, leg. M. Arnedo *et al.*

TYPE LOCALITY: Pajares, Oviedo, Asturias, Spain, (no collection date).

DIAGNOSIS: *D. flavitarsis* can be diagnosed from its closely related species *D. cetophonorum* sp. nov. and *D. citauca* sp. nov., as well as its sympatric Iberian congeners by presenting a P with large blades in the male palp (Fig. 11A), the combination of a reduced anteroventral

sclerotization and a reduced length of the VA in the female vulva (Fig. 11D), and its cheliceral dentition, presenting 2 teeth instead of 3 or 4 in the other species (Fig. 11C).

REDESCRIPTION:

MALE (CRBA2131) (Figs 11A–B, 12–13):

CARAPACE: length 2.63; maximum width 2.14; minimum width 1.36. Brown, foveate at borders, rugose, inclined (Fig. 12). Frontal border roughly rounded, 1.38 wide; anterior lateral borders slightly convergent; lateral borders divergent, rounded after maximum width point while converging to back margin; back margin slightly raised, narrow.

EYES: AME 0.16, oval; PLE 0.15, oval; PME 0.13, rounded; AME separated from anterior border by less than their diameter; AME separated by one another by less than their diameter; AME touching PLE; PME almost touching PLE; PME touching.

LABIUM: trapezoid, with base wider than distal part, longer than wide at base; distal part concave.

STERNUM: orange, smooth.

CHELICERAE (Fig. 11C): 1.3 long, about one third of carapace length in dorsal view, concave-shaped in lateral view, without sclerotized piliferous granulations; fang 1.09 long. Cheliceral furrow approx. 48% of the length of basal segment, armed with 2 teeth and basal lamina, B = M; all teeth triangular, B close to lamina, M close to B.

LEGS: yellow, except anterior femora and ti1, orange. Lengths: Leg I: 7.3 (2.13, 1.3, 1.67, 1.62, 0.58); Leg II: 6.86 (2.13, 1.3, 1.67, 1.62, 0.58); Leg III: 5.18 (1.6, 0.9, 0.96, 1.26, 0.46); Leg IV: 7.07 (2.08, 1.1, 1.5, 1.86, 0.53); relative length: 1 > 4 > 2 > 3; palp 3.44 (1.3, 0.72, 0.68, 0.74). Legs covered with hairs, especially so in tibiae, metatarsi and tarsi. All metatarsi with tuft of hairs in distal ventral section, posterior tufts dense. Five to eleven teeth in each claw.

SPINATION: ti3d proximal 1.0.0, distal 1.0.0; ti4d proximal 1.0.0.

ABDOMEN: 3.08 long, cream colored with gray spots, cylindrical; abdominal dorsal hairs short, 0.04–0.06, tapered, uniformly distributed.

MALE GENITALIA (Figs 11A–B, 13): T shorter than DD, external border sloped backwards. DD bent anteriorly in lateral view, more or less 30°. IS longer and thicker than ES. ES basally not

sclerotized. C present, its base separated from medial part of IS by a small fissure. LF present, with tip ending in small apophysis. AR absent. L present, with sclerotized eL. P unfused to T, rotated posteriorly, lateral length roughly half of the width of T in retrolateral view. Ridge present, perpendicular to T, showing 3 juxtaposed sclerotized sulci, projected dorsally.

FEMALE (CRBALC0045) (Figs 11D–F):

All characters as in male except:

CARAPACE: length 3.28; maximum width 2.66; minimum width 1.69. Dark brown.

EYES: AME 0.22.

CHELICERAE: 1.52; fang 1.36.

LEGS: Leg I: 7.94 (2.34, 1.48, 1.78, 1.74, 0.6); Leg II: 7.44 (2.34, 1.48, 1.78, 1.74, 0.6); Leg III: 5.85 (1.76, 1.02, 1.08, 1.48, 0.51); Leg IV: 7.98 (2.33, 1.3, 1.68, 2.05, 0.62); relative length: 4 > 1 > 2 > 3; palp 3.55 (1.37, 0.7, 0.62, 0.86, 3.55).

ABDOMEN: 4.13 long.

FEMALE GENITALIA (Figs 13D–F): PD oval. DA clearly separated from VA. DA three times as wide as long, anteriorly domed. DF wide in dorsal view. MF short. VA roughly twice as wide as long, membranous except in its sclerotized anterolateral section, wide, rounded. Insertion of S projected onto VA through a short, lightly sclerotized neck, S trapezoidal in ventral view, with arms of moderate length and tips extended laterally, dorsal SD present, bilobed.

INTRASPECIFIC VARIATION: Male carapace varies from 2.63 to 3.02 in length, from 2.14 to 2.49 in width, female from 2.97 to 3.52 in length and 2.4 to 2.97 in width. Cheliceral length from 1.2 to 1.38 in males, 1.32 to 1.7 in females. Spination variability: ti3d proximal 1.0.0, medial-proximal 0–1.0.0, distal 1.0.0; ti4d proximal 0–2.0–1.0, distal 0–1.0.0; ti4v proximal 0.0–1.0.

REMARKS: Part of the additional materials collected in Spain cited above correspond to those of an unidentified *Dysdera* cited as '*Dysdera* sp08' in Crespo *et al.*, 2018 (C. *et al.*, 2018). Although we did not see Simon's holotype, we identified our materials based on the unpublished redescription of Ferrández, who had seen the holotype.

DISTRIBUTION AND ECOLOGY: This species is known from the NW of the Iberian Peninsula (Fig. 1A). Recent projects have found it in oak woodlands (*Quercus* spp.) (Cardoso *et al.*, 2008; Crespo *et al.*, 2018).
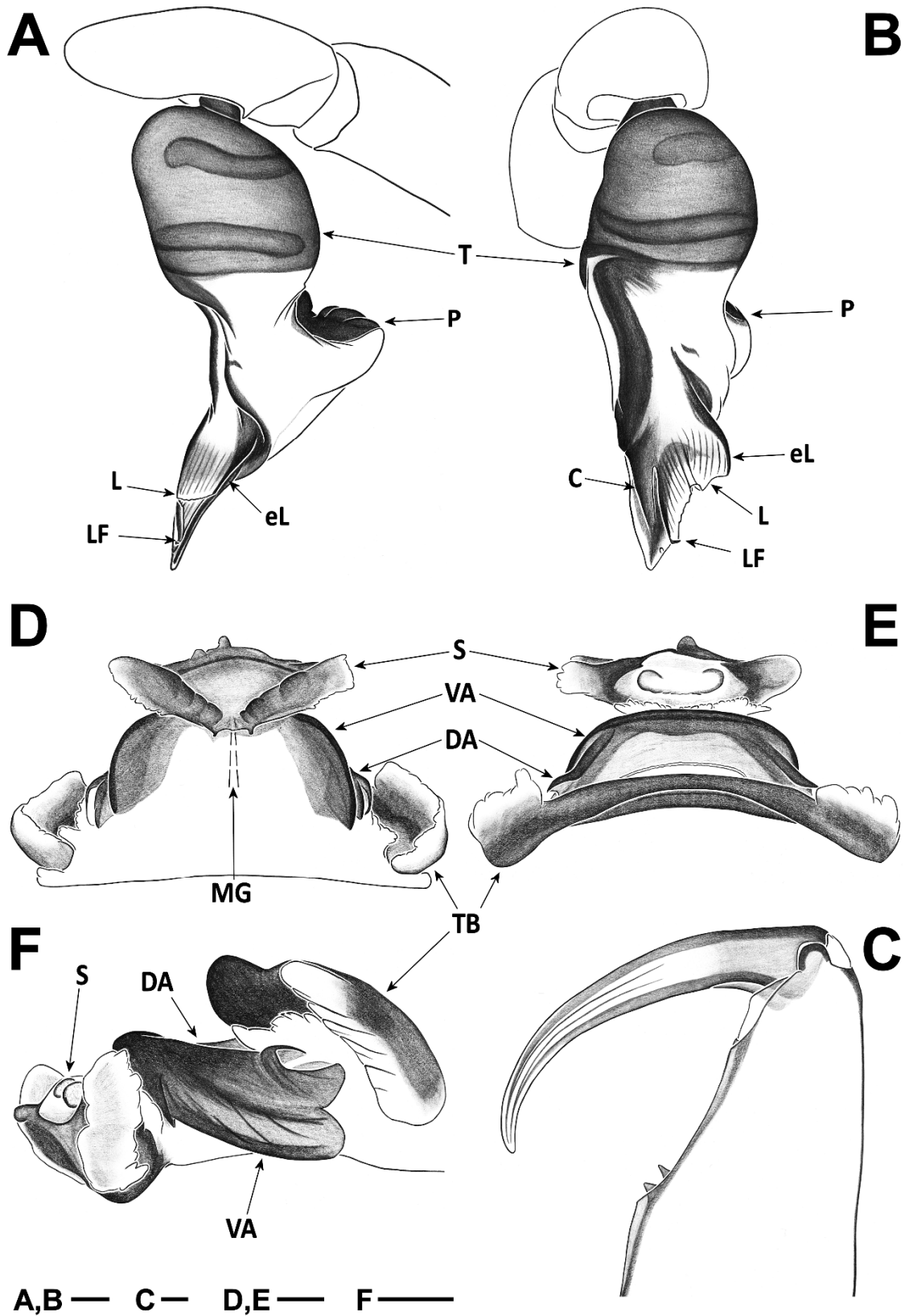
(previous page) Figure 11. *D. flavitarsis* Simon, 1882. A – C, male (CRBA2131); A, left palp, retrolateral; B, left palp, anterior; C, left chelicera, ventral; D – F, female (CRBALC0045); D, vulva, ventral; E, vulva, dorsal; F, vulva, lateral. Scale bars = 0.1 mm.

Figure 12. A – B, *D. flavitarsis* Simon, 1882, male (CRBA2131): A, prosoma, dorsal; B, prosoma, lateral. Scale bars = 1 mm.
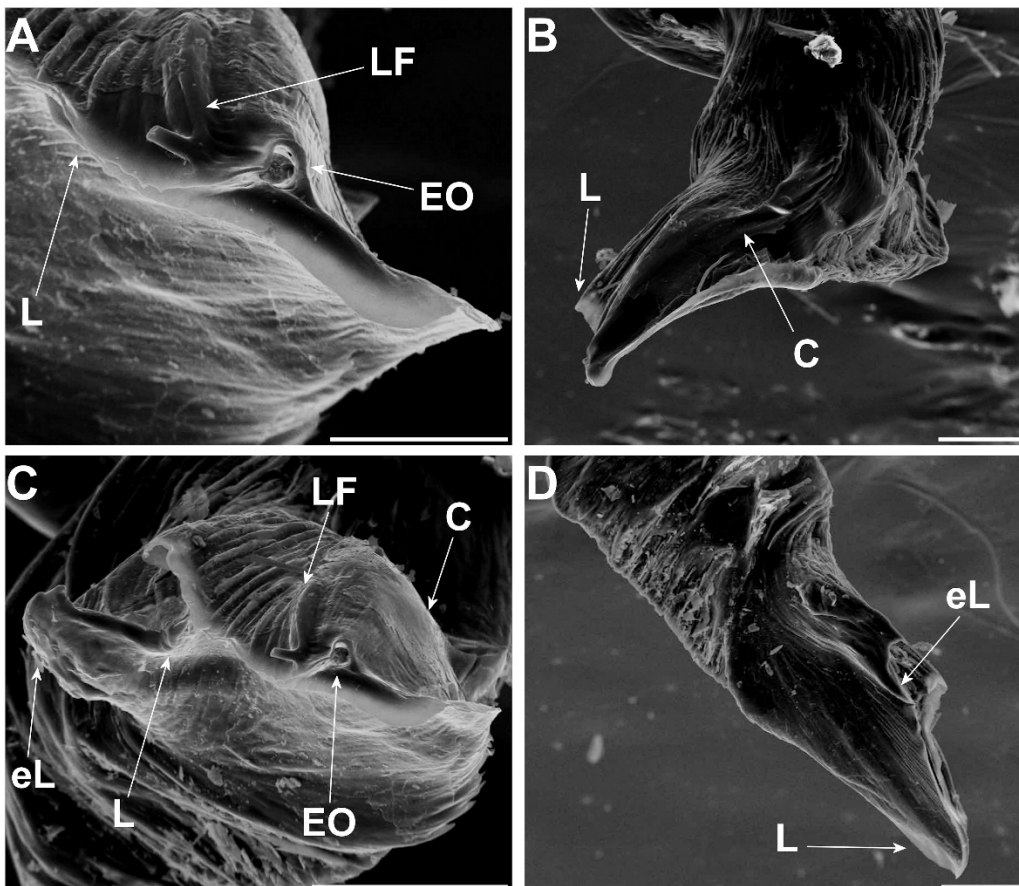
(previous page) Figure 13. A – D, SEM images of distal right palp of *D. flavitarsis* Simon, 1882, male (CRBA2131): A, apical detail; B, prolateral; C, anteroventral; D, retrolateral. Scale bars = 0.1 mm.

Dysdera sp. 'SPJ'

(Fig 14)

MATERIAL EXAMINED: Portugal: Azores archipelago: Pico Island: Praia do Caminho de Cima, Madalena do Pico, 7 juveniles (CRBALC0721, CRBALC0722, CRBALC0723, CRBALC0724, CRBALC0725, CRBALC0728, CRBALC0729), 30.VII.2018, 2 juveniles (CRBALC0726, CRBALC0727), direct hand sampling, leg. L. Crespo & S. Videira; Terceira Island: São Mateus da Calheta, Angra do Heroísmo, 1 juvenile (CRBALC0598), 26.VII.2018, 1 juvenile (CRBALC0720), direct hand sampling, leg. L. Crespo.

REMARKS: These specimens closely resemble *D. cetophonorum* sp. nov. by their overall appearance, the unique presence of four cheliceral teeth (instead of the canonical three teeth in *Dysdera*) and the extremely reduced leg chaetotaxy (only 1 small tibial spine present in leg III). However, the prosoma of *D.* sp. 'SPJ' is seemingly longer and more flattened than that of *D. cetophonorum* sp. nov., and the chelicerae of the latter species are more robust and projected than that of the former (Figs. 5, 14). Despite these differences, the lack of adult material prevented us from describing the littoral specimens as a new species. Future surveys in this underexplored habitat in the Azores will provide information the necessary information on the genital traits to determine if the littoral specimens belong to a different species.

DISTRIBUTION AND ECOLOGY: Like Madeiran *D. citauca* sp. nov., specimens tentatively referred as *Dysdera* sp. 'SPJ' were found on the spray zones of rocky beaches in both Pico and Terceira Islands. After removing the initial layer of rocks exposed to the sun, we found the typical silken cocoons of *Dysdera* attached to fragments of dried algae near the humid ground. One subadult male specimen was found in a much more densely woven cocoon.

CONSERVATION: Extremely limited distribution probably diminishing due to the invasive *D. crocata* that occupies most of both islands, which was found by the authors in the same areas where *Dysdera sp.* 'SPJ' was collected.

Figure 14. A – B, *D.* sp. 'SPJ' (CRBALC0720): A, prosoma, dorsal; B, prosoma, lateral. Scale bars = 1 mm.

Discussion

Here we report for the first time a direct evolutionary connection between the spider fauna of the Azores and Madeira and confirm the presence of endemic species of *Dysdera* in the former archipelago.

Long distance dispersal

The presence of native *Dysdera* species in the Azores further corroborate the ability of the genus to disperse by way of a sea crossing, already evident by the presence of endemic species in all the remaining Macaronesian archipelagos, as well as in all the main Mediterranean islands. Unlike many other spiders, *Dysdera* has rarely been observed to conduct ballooning, a form or airborne dispersal using silk. For example, Blandenier (Blandenier, 2009) reported 1 immature specimen of Dysderidae among 15,000 spiders collect in 10-year survey of ballooning spiders in Switzerland. Alternatively, island colonization by *Dysdera* has been suggested to be most likely mediated by rafting on plant and soil debris

(Arnedo *et al.*, 2001). Similarly, oceanic drifting was invoked to explain the Gondwanan distribution of *Amaurobioides* (Anyphaenidae) ghost spiders, which would have been favoured by the coastal habitat and the ability for immersion of these spiders, and the presence of the Antarctic Circumpolar Current and the West Wind Drift (Ceccarelli *et al.*, 2016). Interestingly, the new species here described inhabit the spray zone of their respective islands. Moreover, experimental evidence suggest that *Dysdera* species can remain active after 10 days if submerged while in their silk nests, which act as a physical gill and most likely represent an adaptation to regular flooding of their soil habitats (Rovner, 1986). The prevailing currents in the Azorean islands flow eastward and south-eastward, with little changes through the year or even during glacial maxima (Freitas *et al.*, 2019). While the main North Atlantic circulation system further aided by the north-eastern trade winds most likely facilitated the colonisation of Madeira from the continent, or even the Azores, they may have represented an impediment for reaching the Azores. It has been estimated that at the current velocity and direction of the slow and generally southward-flowing Portugal Current, the main oceanic drift system between continental Portugal and the Azores, oceanic drift between Europe and the archipelago would require at least 18 months, with little variation during past glacial cycles (Esteves *et al.*, 2015). Dispersal by birds, as suggested for fleshy fruited plants (Esteves *et al.*, 2015), could provide an alternative. Tenebrionid beetles, for example, have been shown to endure consumption and regurgitation by sea gulls, and population genetic analyses suggest that may have used this vector to disperse between islands (Nogales, López, & Emerson, 2019). However, this possibility seems highly improbable in the case of *Dysdera*. Although spiders are an important component of bird's diet, the main target groups include web building and diurnal wandering spiders (Gunnarsson, 2007). In addition, spiders are less protected than beetles to survive digestive enzymes. On the other hand, molecular studies have revealed the possibility for recurrent counter current migration (Foighil *et al.*, 2001). Recent studies conducted in the Canaries, have also revealed the important role of massive landslides in driving between island colonization (García-Olivares *et al.*, 2017), although dispersal events were mostly limited to nearby islands.

Colonization pathways

Our best supported trees are compatible with both the independent colonisation of Azores and Madeira from the mainland, or with a steppingstone model, with either Azores or Madeira acting as a source for the next archipelago. The divergence time estimates do not offer any additional insight since they were mostly compatible with the time of emergence of the islands.

The island species closely resemble each other both in morphology and habitat. Unlike the concave chelicera observed in their continental relative, *D. flavitarsis*, which has been suggested being related with dietary specialisation to feed on woodlouse, the island taxa bore unmodified chelicera, which suggest a generalised diet. The sister clade to *D. flavitarsis* and the island taxa, which includes *D. inermis* and *D. fuscipes*, also shows cheliceral modifications for catching woodlice, but instead of concave, the chelicera are short, and stout and the fang is flat and wide. These observations may hint at a derived state of the presumed generalist diet of the island taxa, which, along with its preference for coastal habitats, instead of the forest and woodlands preferred by their mainland relatives, would have facilitated overseas dispersal. In this regard, it is interesting to note that *Dysdera lata* Reuss, 1834, and other members of the *lata* group (Deeleman-Reinhold & Deeleman, 1988), which includes species typically inhabiting littoral and low land habitats, show wide distribution ranges throughout the Mediterranean coastal areas and islands, suggesting that this type of habitat would facilitate dispersal.

Diversification patterns

Surprisingly, *D. citauca* sp. nov., found in a single secluded location, the splash zone of an erosion cave in an islet 400 m off the east coast of Porto Santo, was not related to the eleven endemic *Dysdera* species that inhabit higher elevations across the rest of the archipelago (Crespo *et al.*, 2021). Our time estimates suggest that the arrival of the ancestor of *D. citauca* sp. nov. to Madeira post-dated the colonization of the highly diversified clade. Consequently, the presence of congeneric endemics occupying the inland habitats may have prevented the subsequent diversification of the littoral lineage. The situation is different for the Azorean *Dysdera* endemics. The specimens inhabiting the spray zone were collected in two different islands, eastern Pico and southern Terceira, about 230 km apart, while the new

species here described was collected more than 70 years ago in an undetermined location above 300m in Pico. Although we have tentatively rendered the coastal and forest specimens as non-conspecific, they all clearly belong to the same evolutionary lineage. The only other *Dysdera* species present in the archipelago is the synanthropic *D. crocata*, which has been introduced all over the world by man from its native range in the western Mediterranean, and probably reached the Azores not earlier that the first settlers in the 15th century.

The spider fauna of the Azores is highly depauperated, even compared with other Macaronesian archipelagos, and many species are introduced. Approximately 132 spider species have been reported in the Azores, only 30% of which are native and 19% endemic, compared with 218 species, 71% native and 27% endemic, from the much smaller Madeira (800 square km vs. 2,350 square km) (Borges & Cardoso, pers. comm.,) or the 526 from the Canary Islands (7,490 square km), 62% of which are endemic (http//:www.biodiversidadcanarias.es\biota, visited on March 2nd, 2021). Several hypotheses have been put forward to explain the low terrestrial species richness and level of endemism of the Azores, namely their remoteness, relatively young age, or the prevalence of recent unrecorded extinctions (both because of higher rate of natural disappearance and human driven) (Cardoso *et al.*, 2010). Additionally, comparative analyses in plants have revealed that the stable climatic conditions in the Azores further reduced the opportunities for diversification (Carine & Schaefer, 2010). However, molecular studies on *Tarphius* beetles (Amorim *et al.*, 2012) and *Pseudoniphargus* subterranean amphipods (Stokkan *et al.*, 2018) have uncovered the occurrence of incipient allopatric speciation mostly associated to inter-island colonization events in absence of clear morphological divergences. The uncorrected genetic distances in COI between the coastal populations of the *D. sp.* 'SPJ' (3%) fell within the average intraspecific divergence reported in Madeiran endemics (Crespo *et al.*, 2021), which in combination with the absence of clear morphological differences, although no adult specimens were available for comparison, would suggest they are conspecific. However, the estimated divergence between the Terceira and Pico populations (~1.5 my) is in the range reported for different species of *Tarphius* bettles in the same islands. Unfortunately, no fresh material for molecular analyses was available for *D. cetophonorum* sp. nov., which shows differences both in habitat (mid to high elevation) and in morphology (see diagnosis). If *D. cetophonorum* sp. nov. is confirmed extinct (Cardoso *et al.*, 2010), the only chances to retrieve

molecular information will be the use of high-throughput sequencing approaches effectively streamlined for their use in ethanol preserved museum material (Derkarabetian, Benavides, & Giribet, 2019). New collections in the largely unexplored coastal habitat in the Azores may also uncover additional population of endemic *Dysdera* in other islands and locations and provide adult material from additional morphological discrimination.

Conservation status

All the insular species here described seem to be both extremely restricted in range, probably extinct in the case of *D. cetophonorum* sp. nov., and may be threatened by the introduction on all islands of the currently widespread mainland species *D. crocata*. Being asynanthropic species which has been introduced worldwide, *D. crocata* most probably is outcompeting the endemic species from their native range, both in coastal areas of Ilhéu de Cima, Terceira and Pico and the middle to high elevation forests of Pico. Given that the invasive species is spread across each island we estimate one location *sensu* the International Union for the Conservation of Nature (IUCN) for *D. citauca*, two for *D.* sp. 'SPJ' and none for *D. cetophonorum.* This would result in IUCN assessments of Extinct for the later, Critically Endangered for *D. citauca* sp. nov. and Endangered for *D.* sp. 'SPJ'.

Conclusions

We add an important piece to complete the evolutionary jigsaw posed by the colonization and diversification of *Dysdera* species in the Macaronesia. We confirm the presence of endemic species in the Azores and report their presence in at least two islands, Terceira and Pico. In addition, we discovered and describe a new endemic species in Madeira, not related to the highly diversified lineage already documented in this archipelago. The new species described are each other closest relatives, and we were able to trace their origins back to the Iberian Peninsula, where their closest relatives currently dwell. The colonization pathways remain inconclusive, but the uncommon spray zone habitat of the species probably favoured their overseas dispersal, in some cases against prevailing wind and marine currents. Unfortunately, their highly localized distribution and the ecological pressure exerted by

introduced synanthropic species may have already brought the new species to the verge of extinction.

Acknowledgements

References

Agnarsson, I., Cheng, R. C., & Kuntner, M. (2014). A multi-clade test supports the intermediate dispersal model of biogeography. *PLoS ONE*, *9*(1). https://doi.org/10.1371/journal.pone.0086780

Amorim, I. R., Emerson, B. C., Borges, P. A. V, & Wayne, R. K. (2012). Phylogeography and molecular phylogeny of Macaronesian island Tarphius (Coleoptera: Zopheridae): Why

are there so few species in the Azores? *Journal of Biogeography*, *39*(9), 1583–1595. https://doi.org/10.1111/j.1365-2699.2012.02721.x

Arnedo, M., Oromí, P., Múrria, C., Macías-Hernández, N., & Ribera, C. (2007). The dark side of an island radiation: Systematics and evolution of troglobitic spiders of the genus Dysdera Latreille (Araneae:Dysderidae) in the Canary Islands. *Invertebrate Systematics*, *21*(6), 623–660. https://doi.org/10.1071/IS07015

Arnedo, M., Oromí, P., & Ribera, C. (1996). Radiation in the genus Dysdera (Araneae, Dysderidae) in the Canary Islands: The western islands. *Zoologica Scripta*, *27*(3), 604–662. Retrieved from http://www.jstor.org/stable/3706342%5Cnhttp://www.americanarachnology.org/JoA_free/JoA_v27_n3/arac_27_03_0604.pdf

Arnedo, M., Oromí, P., & Ribera, C. (2000). Systematics of the Genus Dysdera (Araneae, Dysderidae) in the Eastern Canary Islands. *Journal of Arachnology*, *28*(3), 261–292. https://doi.org/10.1636/0161-8202(2000)028[0261:SOTGDA]2.0.CO;2

Arnedo, M., Oromí, P., & Ribera, C. (2001). Radiation of the spider genus Dysdera (Araneae, Dysderidae) in the Canary Islands: Cladistic assessment based on multiple data sets. *Cladistics*, *17*(4), 313–353. https://doi.org/10.1006/clad.2001.0168

Ashby, B., Shaw, A. K., & Kokko, H. (2020). An inordinate fondness for species with intermediate dispersal abilities. *Oikos*, *129*(3), 311–319. https://doi.org/10.1111/oik.06704

Bidegaray-Batista, L., & Arnedo, M. (2011). Gone with the plate: The opening of the Western Mediterranean basin drove the diversification of ground-dweller spiders. *BMC Evolutionary Biology*, *11*(1). https://doi.org/10.1186/1471-2148-11-317

Bidegaray-Batista, L., Macías-Hernández, N., Oromí, P., & Arnedo, M. (2007). Living on the edge: Demographic and phylogeographical patterns in the woodlouse-hunter spider Dysdera lancerotensis Simon, 1907 on the eastern volcanic ridge of the Canary Islands. *Molecular Ecology*, *16*(15), 3198–3214. https://doi.org/10.1111/j.1365-294X.2007.03351.x

Blandenier, G. (2009). Ballooning of spiders (Araneae) in Switzerland: General Results from

an Eleven-Year Survey. *Arachnology*, *14*(7), 308–316.
https://doi.org/10.13156/arac.2009.14.7.308

Bouckaert, R., Vaughan, T. G., Barido-Sottani, J., Duchêne, S., Fourment, M., Gavryushkina, A., … Drummond, A. J. (2019). BEAST 2.5: An advanced software platform for Bayesian evolutionary analysis. *PLoS Computational Biology*, *15*(4), e1006650. https://doi.org/10.1371/journal.pcbi.1006650

Cardoso, P. (2008). Rapid biodiversity assessment of spiders (Araneae) using semi-quantitative sampling: a case study in a Mediterranean forest. *Insect Conservation and Diversity*, *1*(1), 71–84. https://doi.org/10.1111/j.1752-4598.2007.00008.x

Cardoso, P., Arnedo, M., Triantis, K., & Borges, P. (2010). Drivers of diversity in Macaronesian spiders and the role of species extinctions. *Journal of Biogeography*, *37*(6), 1034–1046. https://doi.org/10.1111/j.1365-2699.2009.02264.x

Carine, M. A., & Schaefer, H. (2010). The Azores diversity enigma: why are there so few Azorean endemic flowering plants and why are they so widespread? *Journal of Biogeography*, *37*(1), 77–89. https://doi.org/https://doi.org/10.1111/j.1365-2699.2009.02181.x

Carvalho, José C., Malumbres-Olarte, J., Arnedo, M. A., Crespo, L. C., Domenech, M., & Cardoso, P. (2020). Taxonomic divergence and functional convergence in Iberian spider forest communities: Insights from beta diversity partitioning. *Journal of Biogeography*, *47*(1), 288–300. https://doi.org/10.1111/jbi.13722

Carvalho, José Carlos, & Cardoso, P. (2014). Drivers of beta diversity in Macaronesian spiders in relation to dispersal ability. *Journal of Biogeography*, *41*(10), 1859–1870. https://doi.org/10.1111/jbi.12348

Ceccarelli, F., Opell, B., Haddad, C., Raven, R., Soto, E., & Ramírez, M. (2016). Around the world in eight million years: Historical biogeography and evolution of the spray zone spider Amaurobioides (Araneae: Anyphaenidae). *PLoS ONE*, *11*(10), 1–20. https://doi.org/10.1371/journal.pone.0163740

Claramunt, S., Derryberry, E. P., Remsen, J. V., & Brumfield, R. T. (2012). High dispersal ability inhibits speciation in a continental radiation of passerine birds. *Proceedings of*

the Royal Society B: Biological Sciences, *279*(1733), 1567–1574.
https://doi.org/10.1098/rspb.2011.1922

Crespo, L., Domènech, M., Enguídanos, A., Malumbres-Olarte, J., Cardoso, P., Moya-Laraño,
J., … Arnedo, M. (2018). A DNA barcode-assisted annotated checklist of the spider
(Arachnida, Araneae) communities associated to white oak woodlands in Spanish
National Parks. *Biodiversity Data Journal*, *6*. https://doi.org/10.3897/bdj.6.e29443

Crespo, L., Silva, I., Enguídanos, A., Cardoso, P., & Arnedo, M. (2021). Integrative taxonomic
revision of the woodlouse-hunter spider genus Dysdera (Araneae: Dysderidae) in the
Madeira archipelago with notes on its conservation status. *Zoological Journal of the
Linnean Society*, *192*(2), 356–415. https://doi.org/10.1093/zoolinnean/zlaa089

Deeleman-Reinhold, C., & Deeleman, P. (1988). Revision des Dysderinae (Araneae,
Dysderidae), les especes mediterraneennes occidentales exceptees. *Tijdschrift Voor
Entomologie*, *131*(2), 141–269. Retrieved from
https://www.biodiversitylibrary.org/part/66464

Derkarabetian, S., Benavides, L. R., & Giribet, G. (2019). Sequence capture phylogenomics of
historical ethanol-preserved museum specimens: Unlocking the rest of the vault.
Molecular Ecology Resources, *19*(6), 1531–1544.
https://doi.org/https://doi.org/10.1111/1755-0998.13072

Domènech, M., Crespo, L. C., Enguídanos, A., & Arnedo, M. A. (2020). Mitochondrial
discordance in closely related Theridion spiders (Araneae , Theridiidae), with
description of a new species of the T . melanurum group, *9*(1), 1–16.
https://doi.org/10.3897/zse.9

Dunlop, J. A., Penney, D., & Jekel, D. (2017). *A summary list of fossil spiders and their
relatives version 18.0., In: World Spider Catalog*. *Natural History Museum Bern*.
Retrieved from http://wsc.nmbe.ch

Esteves, C. F., Costa, J. M., Vargas, P., Freitas, H., & Heleno, R. H. (2015). On the limited
potential of azorean fleshy fruits for oceanic dispersal. *PLoS ONE*, *10*(10), 1–11.
https://doi.org/10.1371/journal.pone.0138882

Fernández-Palacios, J. M., De Nascimento, L., Otto, R., Delgado, J. D., García-Del-Rey, E.,

Arévalo, J. R., & Whittaker, R. J. (2011). A reconstruction of Palaeo-Macaronesia, with particular reference to the long-term biogeography of the Atlantic island laurel forests. *Journal of Biogeography*, *38*(2), 226–246. https://doi.org/10.1111/j.1365-2699.2010.02427.x

Foighil, D. Ó., Jennings, R., Park, J.-K., & Merriwether, A. (2001). Phylogenetic relationships of mid-oceanic ridge and continental lineages of Lasaea (Mollusca: Bivalvia) in the Northeastern Atlantic. *Marine Ecology Progress Series*, *213*, 165–175. https://doi.org/10.3354/meps213165

Freitas, R., Romeiras, M., Silva, L., Cordeiro, R., Madeira, P., González, J. A., … Ávila, S. P. (2019). Restructuring of the 'Macaronesia' biogeographic unit: A marine multi-taxon biogeographical approach. *Scientific Reports*, *9*(1), 2006–2009. https://doi.org/10.1038/s41598-019-51786-6

García-Olivares, V., López, H., Patiño, J., Alvarez, N., Machado, A., Carracedo, J. C., … Emerson, B. C. (2017). Evidence for mega-landslides as drivers of island colonization. *Journal of Biogeography*, *44*(5), 1053–1064. https://doi.org/10.1111/jbi.12961

Gaspar, C., Gaston, K. J., Borges, P. A. V., & Cardoso, P. (2011). Selection of priority areas for arthropod conservation in the Azores archipelago. *Journal of Insect Conservation*, *15*(5), 671–684. https://doi.org/10.1007/s10841-010-9365-4

Geldmacher, J., & Hoernle, K. (2000). The 72 Ma Geochemical Evolution of the Madeira Hotspot (eastern North Atlantic): Recycling of Palaeozoic (0D Oceanic Lithosphere Appendix for EPSL - ONLINE. *Reading*, *183*, 2–4.

Gillespie, R. G., Baldwin, B. G., Waters, J. M., Fraser, C. I., Nikula, R., & Roderick, G. K. (2012). Long-distance dispersal: A framework for hypothesis testing. *Trends in Ecology and Evolution*, *27*(1), 47–55. https://doi.org/10.1016/j.tree.2011.08.009

Goloboff, P. A., & Catalano, S. A. (2016). TNT version 1.5, including a full implementation of phylogenetic morphometrics. *Cladistics*, *32*(3), 221–238. https://doi.org/https://doi.org/10.1111/cla.12160

Gunnarsson, B. (2007). Bird Predation On Spiders: Ecological Mechanisms And Evolutionary Consequences. *Journal of Arachnology - J ARACHNOL*, *35*, 509–529.

https://doi.org/10.1636/RT07-64.1

Hebert, P. D. N., Cywinska, A., Ball, S. L., & DeWaard, J. R. (2003). Biological identifications through DNA barcodes. *Proceedings of the Royal Society B: Biological Sciences*. https://doi.org/10.1098/rspb.2002.2218

Kallal, R. J., Kulkarni, S. S., Dimitrov, D., Benavides, L. R., Arnedo, M. A., Giribet, G., & Hormiga, G. (2020). Converging on the orb: denser taxon sampling elucidates spider phylogeny and new analytical methods support repeated evolution of the orb web. *Cladistics*, *n/a*(n/a). https://doi.org/https://doi.org/10.1111/cla.12439

Kalyaanamoorthy, S., Minh, B. Q., Wong, T. K. F., Von Haeseler, A., & Jermiin, L. S. (2017). ModelFinder: Fast model selection for accurate phylogenetic estimates. *Nature Methods*, *14*(6), 587–589. https://doi.org/10.1038/nmeth.4285

Katoh, K., Misawa, K., Kuma, K., & Miyata, T. (2002). MAFFT: a novel method for rapid multiple sequence alignment based on fast Fourier transform. *Nucleic Acids Research*, *30*(14), 3059–3066. https://doi.org/10.1093/nar/gkf436

Lanfear, R., Frandsen, P. B., Wright, A. M., Senfeld, T., & Calcott, B. (2017). Partitionfinder 2: New methods for selecting partitioned models of evolution for molecular and morphological phylogenetic analyses. *Molecular Biology and Evolution*, *34*(3), 772–773. https://doi.org/10.1093/molbev/msw260

MacArthur, R., & Wilson, E. (1967). *The theory of island biogeography*. Princeton, N.J.: Princeton University Press.

Macías-Hernández, N, Bidegaray-Batista, L., Emerson, B., Oromí, P., & Arnedo, M. (2013). The imprint of geologic history on within-island diversification of woodlouse-hunter spiders (Araneae, Dysderidae) in the canary islands. *Journal of Heredity*, *104*(3), 341–356. https://doi.org/10.1093/jhered/est008

Macías-Hernández, N, Bidegaray-Batista, L., Oromí, P., & Arnedo, M. (2013). The odd couple: Contrasting phylogeographic patterns in two sympatric sibling species of woodlouse-hunter spiders in the Canary Islands. *Journal of Zoological Systematics and Evolutionary Research*, *51*(1), 29–37. https://doi.org/10.1111/jzs.12008

Macías-Hernández, N, Oromí, P., & Arnedo, M. (2008). Patterns of diversification on old volcanic islands as revealed by the woodlouse-hunter spider genus Dysdera (Araneae, Dysderidae) in the eastern Canary Islands. *Biological Journal of the Linnean Society*, *94*(3), 589–615. https://doi.org/10.1111/j.1095-8312.2008.01007.x

Macías-Hernández, N, Oromí, P., & Arnedo, M. (2010). Integrative taxonomy uncovers hidden species diversity in woodlouse hunter spiders (Araneae, Dysderidae) endemic to the Macaronesian archipelagos. *Systematics and Biodiversity*, *8*(4), 531–553. https://doi.org/10.1080/14772000.2010.535865

Macías-Hernández, Nuria, López, S. de la C., Roca-Cusachs, M., Oromí, P., & Arnedo, M. A. (2016). A geographical distribution database of the genus Dysdera in the Canary Islands (Araneae, Dysderidae). *ZooKeys*, *2016*(625), 11–23. https://doi.org/10.3897/zookeys.625.9847

Magalhaes, I. L. F., Azevedo, G. H. F., Michalik, P., & Ramírez, M. J. (2020). The fossil record of spiders revisited: implications for calibrating trees and evidence for a major faunal turnover since the Mesozoic. *Biological Reviews*, *95*(1), 184–217. https://doi.org/https://doi.org/10.1111/brv.12559

Malumbres-Olarte, J., Crespo, L. C., Domènech, M., Cardoso, P., Moya-Laraño, J., Ribera, C., & Arnedo, M. A. (2020). How Iberian are we? Mediterranean climate determines structure and endemicity of spider communities in Iberian oak forests. *Biodiversity and Conservation*, *29*(14), 3973–3996. https://doi.org/10.1007/s10531-020-02058-7

Miller, M., Pfeiffer, W., & Schwartz, T. (2010). Creating the CIPRES Science Gateway for inference of large phylogenetic trees. In *Proceedings of the Gateway Computing Environments Workshop (GCE)* (p. 8).

Minh, B. Q., Schmidt, H. A., Chernomor, O., Schrempf, D., Woodhams, M. D., von Haeseler, A., & Lanfear, R. (2020). IQ-TREE 2: New Models and Efficient Methods for Phylogenetic Inference in the Genomic Era. *Molecular Biology and Evolution*, *37*(5), 1530–1534. https://doi.org/10.1093/molbev/msaa015

Müller, K. (2005). SEQSTATE – primer design and sequence statistics for phylogenetic DNA data sets. *Applied Bioinformatics*, *4*, 65–69.

Nogales, M., López, H., & Emerson, B. C. (2019). How can large flightless beetles disperse by flight? The role of the omnivorous gulls on an oceanic island. Retrieved from http://hdl.handle.net/10261/180651

Ramalho, R. S., Brum Da Silveira, A., Fonseca, P. E., Madeira, J., Cosca, M., Cachão, M., … Prada, S. N. (2015). The emergence of volcanic oceanic islands on a slow-moving plate: The example of Madeira Island, NE Atlantic. *Geochemistry, Geophysics, Geosystems*, *16*(2), 522–537. https://doi.org/10.1002/2014GC005657

Ramalho, R. S., Helffrich, G., Madeira, J., Cosca, M., Thomas, C., Quartau, R., … Ávila, S. P. (2017). Emergence and evolution of Santa Maria Island (azores)- The conundrum of uplifted islands revisited. *Bulletin of the Geological Society of America*, *129*(3–4), 372–391. https://doi.org/10.1130/B31538.1

Rambaut, A., Drummond, A. J., Xie, D., Baele, G., & Suchard, M. A. (2018). Posterior summarization in Bayesian phylogenetics using Tracer 1.7. *Systematic Biology*, *67*(5), 901–904. https://doi.org/10.1093/sysbio/syy032

Ronquist, F., Teslenko, M., Van Der Mark, P., Ayres, D. L., Darling, A., Höhna, S., … Huelsenbeck, J. P. (2012). Mrbayes 3.2: Efficient bayesian phylogenetic inference and model choice across a large model space. *Systematic Biology*, *61*(3), 539–542. https://doi.org/10.1093/sysbio/sys029

Rovner, J. S. (1986). Nests of Terrestrial Spiders Maintain a Physical Gill: Flooding and the Evolution of Silk Constructions. *The Journal of Arachnology*, *14*(3), 327–337. Retrieved from http://www.jstor.org/stable/3705673

Schwarz, S., Klügel, A., van den Bogaard, P., & Geldmacher, J. (2005). Internal structure and evolution of a volcanic rift system in the eastern North Atlantic: The Desertas rift zone, Madeira archipelago. *Journal of Volcanology and Geothermal Research*, *141*(1–2), 123–155. https://doi.org/10.1016/j.jvolgeores.2004.10.002

Simmons, M., & Ochoterena, H. (2000). Gaps as Characters in Sequence-Based Phylogenetic Analyses. *Systematic Biology*, *49*, 369–381. https://doi.org/10.1093/sysbio/49.2.369

Soto, E. M., Labarque, F. M., Ceccarelli, F. S., Arnedo, M. A., Pizarro-Araya, J., & Ramírez, M. J. (2017). The life and adventures of an eight-legged castaway: Colonization and

diversification of Philisca ghost spiders on Robinson Crusoe Island (Araneae, Anyphaenidae). *Molecular Phylogenetics and Evolution*, *107*, 132–141. https://doi.org/https://doi.org/10.1016/j.ympev.2016.10.017

Stokkan, M., Jurado-Rivera, J. A., Oromí, P., Juan, C., Jaume, D., & Pons, J. (2018). Species delimitation and mitogenome phylogenetics in the subterranean genus Pseudoniphargus (Crustacea: Amphipoda). *Molecular Phylogenetics and Evolution*, *127*, 988–999. https://doi.org/https://doi.org/10.1016/j.ympev.2018.07.002

Vaidya, G., Lohman, D. J., & Meier, R. (2011). SequenceMatrix: concatenation software for the fast assembly of multi-gene datasets with character set and codon information. *Cladistics*, *27*(2), 171–180. https://doi.org/https://doi.org/10.1111/j.1096-0031.2010.00329.x

Wheeler, W. C., Coddington, J. A., Crowley, L. M., Dimitrov, D., Goloboff, P. A., Griswold, C. E., … Zhang, J. (2017). The spider tree of life: phylogeny of Araneae based on target-gene analyses from an extensive taxon sampling. *Cladistics*, *33*(6), 574–616. https://doi.org/10.1111/cla.12182

Whittaker, R. J., Fernández-Palacios, J. M., Matthews, T. J., Borregaard, M. K., & Triantis, K. A. (2017). Island biogeography: Taking the long view of natures labor atories. *Science*, *357*(6354). https://doi.org/10.1126/science.aam8326

Whittaker, R. J., Triantis, K. A., & Ladle, R. J. (2008). A general dynamic theory of oceanic island biogeography. *Journal of Biogeography*, *35*(6), 977–994. https://doi.org/10.1111/j.1365-2699.2008.01892.x

Chapter 3

Luís C. Crespo, Isamberto Silva, Alba Enguídanos, Pedro Cardoso and Miquel A. Arnedo

(submitted)

Island hoppers: Integrative taxonomic revision of Hogna wolf spiders (Araneae: Lycosidae) endemic to the Madeira islands with description of a new species

(text presented as in the submitted manuscript)

Abstract

Because of their ability for aerial dispersal using silk and preference for open habitats, wolf spiders are formidable colonisers. Pioneering arachnologists were already aware of the existence of large and colourful wolf spiders in the Madeira archipelago, currently included in the genus *Hogna* Simon, 1885. We investigated the origins and examined species boundaries of Madeiran *Hogna* by integrating target-gene and morphological information. A multi-locus phylogenetic analyses of a thorough sampling across wolf-spider diversity, suggested a single origin of Madeiran endemics, albeit with low support. Divergence time estimation traced back their origin to the late Miocene, a time of major global cooling that drove the expansion of grasslands and the associated fauna. Morphological examination of type and newly collected material revealed a new species, hereby described as *H. isambertoi* sp. nov. Additionally, we revalidated *H. blackwalli* sp. reval. and proposed three new synonymies, namely *H. biscoitoi* Wunderlich, 1992, junior synonym of *H. insularum* Kulczynski, 1899, *H. schmitzi* Wunderlich, 1992, junior synonym of *H. maderiana* (Walckenaer, 1837) and *Arctosa maderana* Roewer, 1960 junior synonym of *H. ferox* (Lucas, 1838). Species delimitation analyses of mitochondrial and nuclear markers, provided additional support for morphological delineations. The species pair *H. insularum* and *H. maderiana*, however, constituted an exception. The lack of exclusive haplotypes in the examined markers, along with the discovery of intermediate forms pointed to hybridization between these two species, as reported in other congeneric species on islands. Finally, we discuss the conservation status of the species and identify candidates for immediate conservation efforts.

Keywords: Lycosinae, Macaronesia, morphological polymorphism, species delimitation, island radiation, endangered species

Introduction

Wolf spiders (Lycosidae) are ground-dwelling cursorial hunters. They are among the most abundant and ubiquitous spiders in open terrestrial habitats, such as grass- or shrublands. It has been suggested that lycosids underwent major global diversification

132

concomitantly with grassland expansion during the Miocene (Jocqué and Alderweireldt 2005; Piacentini and Ramírez 2019). Wolf spiders are among the families that more frequently use ballooning, a form of passive airborne transport mediated by silk (Bell et al. 2005). The ability for long-distance dispersal combined with their preference for open and disturbed habitats, makes them formidable colonisers of oceanic islands, including the world's most remote island chain, the Hawaiian Archipelago (Suman 1964). The genus *Hogna* Sundevall, 1833 includes medium to large size spiders and a has a worldwide distribution. Despite of its size, it has managed to colonize and diversify on many oceanic islands, including the Galápagos (Baert et al. 2008) in the Pacific Ocean or Saint Helena, in the South Atlantic (Tongiorgi 1977). Similarly, the Madeira archipelago also harbours several endemic species of *Hogna*. Among spiders, *Hogna* is second only to the genus *Dysdera* Latreille, 1804 in number of endemic species present in the Madeira archipelago (Crespo et al. 2020), and some of its species rank among the most emblematic organisms of the islands.

Madeira is situated in the North Atlantic Ocean, roughly 500km north of the Canary Islands, 900km west from Morocco, and 1000km southwest from the Iberian Peninsula (Fig. 1). It is composed of a small number of islands and islets aligned in a southwestern direction as a result of their sequential formation from a volcanic hotspot on the oceanic crust. Among the larger islands, Porto Santo is a small and relatively flat island (maximum altitude 516m at Pico do Facho), surrounded by several islets, in a later stage of the island ontogeny, its subaerial stage dating back to 14 million years ago (my). The emergence of the two other larger islands, Madeira and Deserta Grande, dates back to 7 and 5 my, respectively (Geldmacher and Hoernle 2000; Ramalho et al. 2015; Schwarz et al. 2005). Although both islands are in an intermediate stage of the island ontogeny, they show substantial differential geomorphology. Madeira is larger with a rugged, steep orography, especially in its northern side, reaching a maximum altitude of 1861m at Pico Ruivo. This stands at a sharp contrast with the aspect of the Deserta Grande, which together with the islets of Ilhéu Chão and Bugio constitute the Desertas islands, with a maximum altitude of only 479m (Rocha do Barbusano), yet displaying a dramatic topographic relief, also observed in Bugio. The Madeira islands exhibit a wide variety of habitats, ranging from the humid subtropical laurel forest of Madeira to the *Erica* shrublands, high-elevation and coastal grasslands, or rocky scarps across all islands and islets. Madeiran *Hogna* spiders occur throughout all the referred habitats, mostly

on montane or coastal grasslands and rocky scarps, as it is common for the family, but also in closed canopy laurel forest.
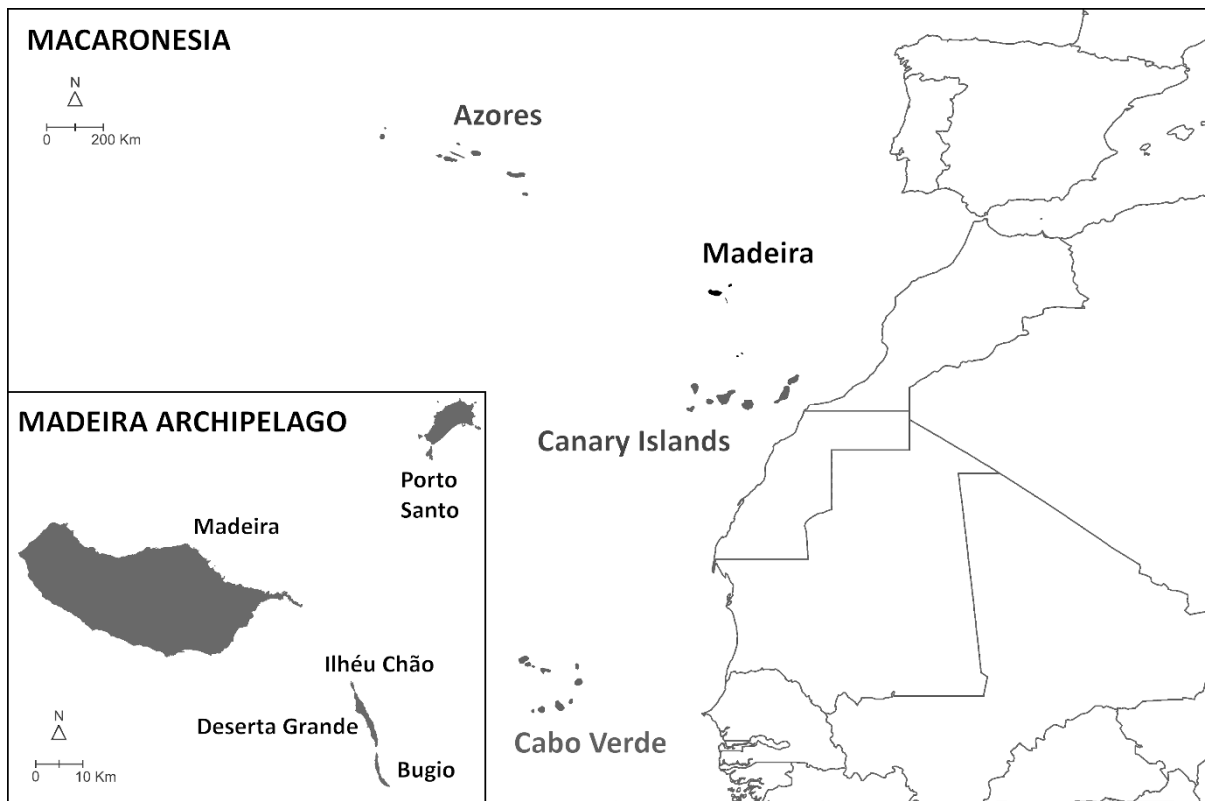
Figure 1. Map of the Macaronesia and the Madeira archipelago (adapted from Borges et al., 2008, with author's permission).

Due to their large size, restricted distribution and striking appearance of some species, either in size or distinctive leg coloration, local *Hogna* spiders were known to naturalists since the early 19th century. The largest and colourful species were the first to be described, namely *H. maderiana* (Walckenaer 1837) and *H. ingens* (Blackwall 1857). By the end of the 19th century, two smaller species, *H. heeri* (Thorell 1875) and *H. insularum* (Kulczynski 1899), were added to the checklist. The report of new endemic *Hogna* species had to wait for almost a century, until the description of *H. biscoitoi* Wunderlich, 1992, *H. schmitzi* Wunderlich, 1992 and *H. nonannulata* Wunderlich, 1995.

Although no other taxonomic work on Madeiran *Hogna* has been published for over 25 years, a number of taxonomic problems remained to be tackled, including nomenclatural issues and the interpretation of intraspecific variability in the context of intermediate forms

(Wunderlich 1992, 1995). In addition, recent studies suggest that species delimitation in wolf spiders may be hampered by either the recent origin of some species (Ivanov et al. 2021) or introgression events among close relatives (De Busschere et al. 2015). On the other hand, the genus *Hogna* is in much need of a though revision (Logunov 2020). It is ill-defined and has traditionally served as a dumping ground for large lycosids of uncertain placement in the Lycosinae. Description of the old species are usually unspecific and poorly illustrated and, in some cases, the type material has been lost. The lack of a clear circumscription of the genus poses a burden in terms of identifying the putative source of colonizers of the Madeiran species.

Some of the Madeira *Hogna* species are also of conservation concern. The Desertas giant wolf Spider, *H. ingens*, is listed as Critically Endangered on the IUCN Red List of Threatened Species due to its narrow distribution range and the fact that the native vegetation of the small valley it inhabits has been mostly displaced by an invasive grass (Crespo et al. 2014c). Conservation efforts involving an ex-situ breeding program and management control of the grasses are underway.

In the present study, we integrate morphological and natural history information with molecular data to (1) test the monophyly of the Madeiran *Hogna* to resolve the number and timeline of colonization events, (2) delimitate species boundaries and (3) conduct a taxonomic revision of these iconic endemic species.

Methods

Field work

The material studied here was made available through collections from expeditions to Madeira, Porto Santo and the Desertas in springs of 2017 and 2018. Additional specimens were provided by occasional collecting from one of us (IS). Sampling was done in a wide variety of habitats, especially in open areas surrounding native vegetation patches, by lifting stones and retrieving *Hogna* specimens manually. Each specimen was placed into a separate cryovial containing 96% molecular grade ethanol and stored in a freezer at -20°C until further study. Specimens for morphological analyses were later transferred to glass vials containing

75% ethanol. The sampling localities and coordinates are listed in Supplementary Materials 1.

Molecular lab procedures

We extracted DNA from one leg III using commercial kits (Speedtools® Tissue DNA Extraction Kit, Biotools; or DNeasy® Blood & Tissue Kit, Qiagen) following the tissue protocol suggested by the respective manufacturer. We amplified partial fragments of the mitochondrial cytochrome c oxidase subunit I (COI), i.e. the animal DNA barcode (Hebert et al., 2003), the small ribosomal subunit 12S rRNA (12S), large ribosomal subunit 16S rRNA (16S), the tRNA Leu (L1), the NADH dehydrogenase subunit 1 (nad1), and the nuclear large ribosomal subunit 28S rRNA (28S), the internal transcribed spacer 2 (ITS-2) and the histone 3 (H3) genes. The primers used for amplification and sequencing, as well as the PCR conditions for the loci are listed in Table 1. The final PCR product was sequenced by Macrogen Inc. (Seoul, South Korea). Sequences were edited and managed in GENEIOUS Prime® 2021.0.3 (https://www.geneious.com).

Phylogenetic analyses

To test the monophyly and phylogenetic structure of Madeiran *Hogna*, we combined our newly generated sequences with the data matrix of Piacentini and Ramírez (Piacentini and Ramírez 2019) designed to infer phylogenetic relationships for the family Lycosidae using a target gene approach. Additional sequences of *Hogna* species were retrieved from Genbank. We aligned sequence fragments of COI, 12S, 16S-L1, nad1, 28S and H3 individually per gene using the GENEIOUS plugin of the alignment program MAFFT v. 1.4.0 (Katoh and Standley 2013), using the G-INS-I algorithm with default options. We concatenated all genes in a super matrix for subsequent phylogenetic analyses with the help of the program SEQUENCE MATRIX (Vaidya et al. 2011).

Parsimony analysis of the matrix was conducted with the program TNT v1.5 (Goloboff and Catalano 2016). We first recoded gaps as absence/presence characters using the simple coding method proposed by Simmons & Ocheterena (Simmons and Ochoterena 2000) with

the help of the computer program SEQSTATE (Müller 2005). Search strategy for shortest trees combined sectorial searches, tree fusing, drift and ratchet. Tree searches were driven to hit independently 10 times the optimal scoring, followed by TBR branch swapping, saving up to 1000 trees (Soto et al. 2017). We estimated support values by jackknifing frequencies derived from 1000 resampled matrices using 15 random addition sequences, retaining 20 trees per replication, followed by TBR, and TBR collapsing to calculate the consensus. We inferred the best maximum likelihood trees with IQ-TREE v. 2.1.2 (Minh et al. 2020). We used MODELFINDER to first select the best-fit partitioning scheme and corresponding evolutionary models (Kalyaanamoorthy et al. 2017), and then to infer the best tree and estimate clade support by means of 1000 replicates of ultrafast bootstrapping (Hoang et al. 2018). For Bayesian analyses, the best partition scheme and evolutionary model was first selected with help of the computer program PARTITIONFINDER v2.1.1 (Lanfearet al. 2017). We implemented Bayesian inference with MRBAYES v3.2.6 (Ronquist et al. 2012). The analysis was run for 10 million generations, sampling every 1000, with eight simultaneous Markov Chain Monte Carlo (MCMC) chains, 'heating temperature' of 0.15. Support values were calculated as posterior probabilities. We assessed convergence of the chains, correct mixing and the number of burn-in generations with TRACER v. 1.7 (Rambaut et al. 2018). We ran model based analyses remotely at the CIPRES Science Gateway (Miller et al. 2010). The phylogenetic tree was edited for aesthetic purposes using FIGTREE (http://tree.bio.ed.ac.uk/software/figtree/).

Species delimitation

We used COI and ITS-2 sequences of a larger sample of Madeiran *Hogna* to explore species boundaries using single marker molecular based approaches. We investigate three alternative methods for species delineation using COI sequences, namely a distance based algorithmic method (Barcode identification number, BIN) (Ratnasingham and Hebert 2013) and two character-explicit methods, one requiring ultrametric trees (General Mixed Yule Coalescent model with single threshold, GMYC) (Fujisawa et al. 2016) and one that does not (multi-rate Poisson tree processes, mPTP) (Kapli et al. 2017). The BIN system was implemented on-line through the BOLD v4 platform (Ratnasingham and Hebert 2007). We

inferred gene trees using maximum likelihood following the same strategy specified in the previous section. In addition, we inferred an ultrametric tree using the Bayesian framework for divergence time estimation implemented in BEAST v2.6.3. We assumed a coalescent tree prior (constant population size), which has been suggested to provide a more rigorous test of delimitation since the GMYC model assumes a single species as the null option (Monaghan et al. 2009). We defined the best partition scheme and evolutionary model inferred with PARTITIONFINDER, defined a lognormal relaxed clock and used an informative prior on the ucld.mean parameter derived from the literature (mean=0.0199, sd. dev.=0.05) (Bidegaray-Batista and Arnedo 2011). Convergence and mixing of MCMC chains were assessed with TRACER v.1.7 (Rambaut et al. 2018). Independent runs were combined with LOGCOMBINER (10% burn-in), and TREEANNOTATOR was used to summarize the information from the sampled trees. The m-PTP model was implemented using a mcmc approach, which allows estimates of support values on the delimitations, on the COI matrix. The analyses were conducted on the best IQ-TREE. We ran 5 chains of 100 million generations each, removing the first 2 million as burn-in, and discarding all branches with lengths smaller or equal to 0.0012708187. We used the R package 'SPLITS' (Ezard et al. 2017) to fit the GMYC model. Additionally, we estimated haplotype/allele networks for the COI and ITS-2 matrices independently using the statistical parsimony method (Clement et al. 2000; Templeton et al. 1992), with a confidence limit of 95% implemented in the R package 'HAPLOTYPES' (Aktas 2015). The ITS-2 sequences were aligned using the phylogeny-aware algorithm implemented in WEBPRANK (Löytynoja and Goldman 2010), specially recommended for aligning closely related sequences. We determined the number of alleles in the ITS-2 matrix considering the gaps as absence/presence data. Uncorrected pairwise genetic distances were calculated in MEGA X (Kumar et al. 2018).

Divergence time estimation

In the absence of fossil evidence and to avoid using circular reasoning by using information on the island age, we estimated divergence time using published information on substitution rates in spiders (Bidegaray-Batista and Arnedo 2011). We restricted our estimates to the more exhaustively sampled COI gene. Since the COI sequences include both intra and inter-specific relationships, we used a multispecies coalescent (MSC) approach as

implemented in STARBEAST2 (Ogilvie et al. 2017), which allows combining coalescent and species (Yule) tree priors. Haplotypes were assigned to species according to the results of the molecular and morphological delimitations (see results). We included sequences of *H. radiata* and *H. ferox* as putative outgroups but did not enforce the root. We assigned unlinked evolutionary models to each codon position, as suggested by PARTITIONFINDER and defined a relaxed lognormal clock with prior rates for the ucld.mean rate as follows: mean = 0.0119 substitutions/my and Stdev = 0.5. Three independent runs of 50 million generations were performed, sampling every 5000 generations. We assessed convergence and mixing of each MCMC chain and combined them as described above.

Morphological analyses

We identified our specimens as belonging to the genus *Hogna*, by following either the generic description given by Dondale & Redner (Dondale and Redner 1990) or the identification key provided by the Araneae – Spiders of Europe portal (Nentwig et al. 2020).

Morphological observations were carried out using a stereomicroscope Leica MZ 16A equipped with a digital camera Leica DFC450. Individual raw photos were taken with the help of the software Leica Application Suite v4.4 and mounted with the software HELICON FOCUS (Helicon Soft, Ltd.). Further editions were done with PAINT SHOP PRO v21 (Corel Corporation). The epigyne was removed from female specimens with the aid of hypodermic needles and forceps. To clear the membranous tissues surrounding the spermathecae and copulatory ducts, we manually removed muscular and membranous tissue with forceps and a needle. This process accidentally led to the breakage of some copulatory ducts (usually delicate in the Lycosidae) and cracking of the median septum in some specimens (e.g., Figs 16E, 26B). SEM images of the male copulatory bulb were obtained with a Q-200 (FEI Co.) scanning electron microscope (SEM). For the SEM images, each male palp was excised at the joint between tarsus and tibia. Samples were sonicated for roughly 30 seconds with ultrasonic bath Nahita ZCC001, air dried and carbon or gold sputter-coated. In most cases, the position of the embolus of the SEM samples appears slightly altered (usually directed more anteriorly, closer to the tip of the terminal apophysis) relative to the normal resting position from specimens stored in ethanol.

We measured all adult specimens with an ocular micrometre in the stereoscope. All measurements are in millimetres (mm). Description format and nomenclature followed Baert et al. (2008).

Abbreviations

Male genitalia:

C – cymbium

E – embolus

MA – median apophysis

T – tegulum

TA – terminal apophysis

P – palea

Female genitalia:

H – hoods

MS – median septum

S – spermatheca

D – diverticulum

Collections:

BM – British Museum of Natural History, London, UK

CRBA – Centre de Recursos de Biodiversitat Animal, University of Barcelona, Barcelona, Spain

FMNH – Finnish Museum of Natural History, Helsinki, Finland

LCPC – Luís Crespo personal collection

MIZ – Museum and Institute of Zoology, Polish Academy of Sciences, Warsaw, Poland

MMUE – Manchester Museum University England, Manchester, UK

OUMNH – Oxford University Museum of Natural History, Oxford, UK

SMF – Senckenberg Research Institute, Frankfurt am Main, Germany

NHRS – Swedish Museum of Natural History, Stockholm, Sweden

Results

Phylogenetic analyses

The concatenated matrix included 2641 characters, 657 bp of the COI, 302 bp H3 and 554 bp of the nad1, and 300 and 828 aligned position for the 12S and 28S, respectively, and 173 terminals including outgroups (see Piacentini and Ramírez, 2019). Inferred relationships of the concatenated data matrix are summarized in Fig. 2 (See Supplementary Materials 2 for full trees for each inference methods). Parsimony analysis of the concatenated data matrix with gaps scored as absence/presence characters resulted in 1,000 trees (overflow) of 16,865 steps. Bayesian maximum clade credibility tree was obtained after removing 40% of the first generations as burn-in. Preferred partition schemes differed between IQTREE2 and PARTITIONFINDER in that the first joined COI and H3 second positions, while the second split by gene and codon position in all cases. Madeiran *Hogna* were recovered as two well-supported clades, one including the species *H. maderiana* and *H. insularum*, hereafter referred as the *maderiana* clade, and the other one including the remaining species, hereafter referred as the *ingens* clade. Model-based analyses inferred the two clades as sister groups, albeit with low support (Fig. 2). Conversely, parsimony inferred the *ingens* clade to be sister to the mainland species *H. radiata*. In all analyses, *H. isambertoi* sp. nov. was supported as sister to the remaining species in the *ingens* clade, while *H. nonannulata* and *H. blackwalli* sp. reval. were supported as sister in model-based analyses. All analyses agreed in supporting a surprisingly close relationship between *H. ingens* and one individual identified as *H. insularum* from Madeira. Similarly, all analyses agreed in showing the genus *Hogna* as a polyphyletic

assemblage. Remaining relationships within Lycosoidea including subfamilies, were similar to those reported in Piacentini and Ramírez (2019).
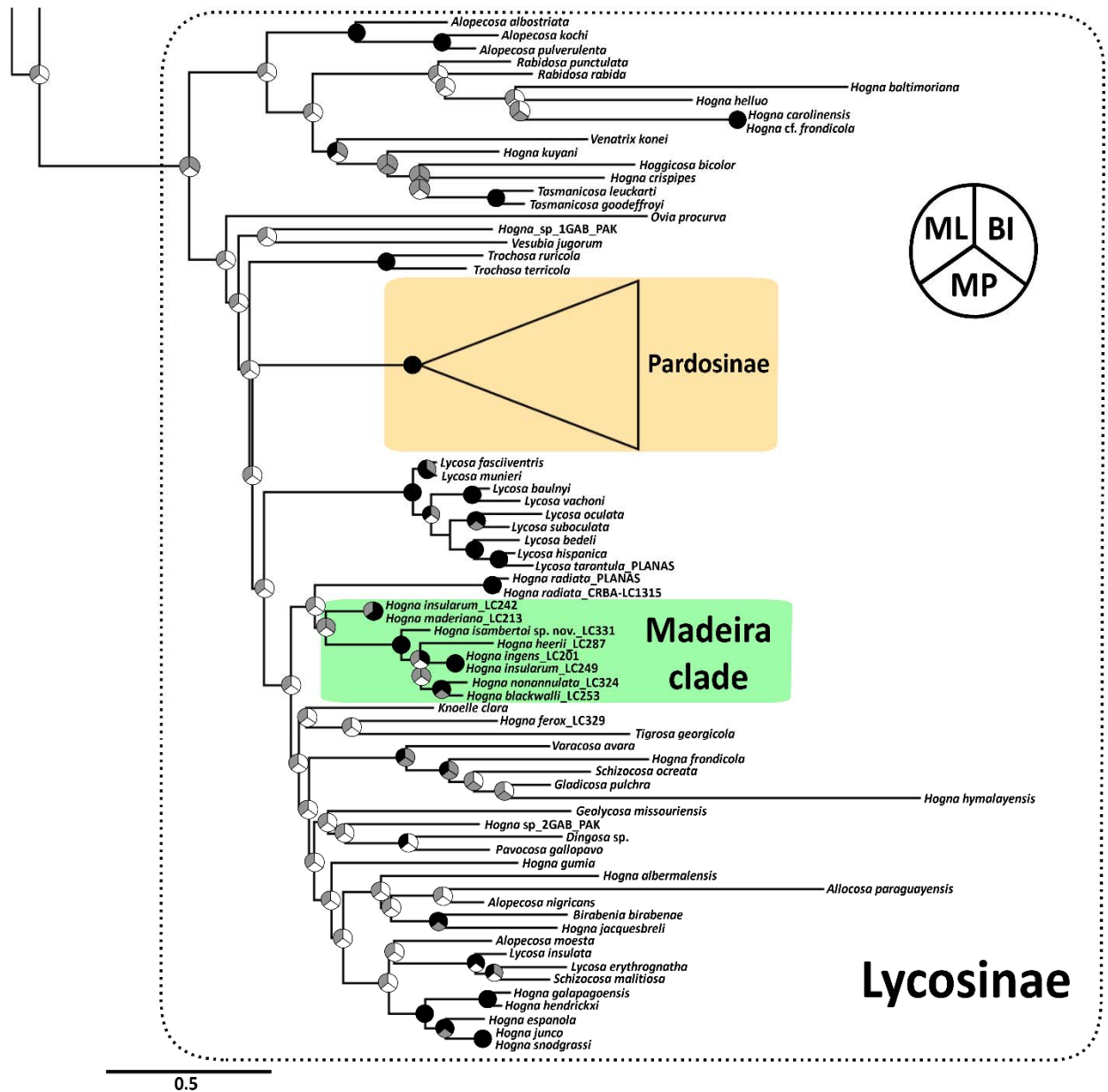
Figure 2. Best Maximum Likelihood tree of Lycosinae, inferred with IQTREE2 after selecting the best partition scheme and evolutionary models. Nodes are split in three sections, representing the different methods. Support on nodes should be read as follows: black: ML ultrafast boostrap and BI posterior probability ≥ 0.95, MP Jackknife ≥ 0.7; grey: ML Ultrafast Bootstrap and BI posterior probability < 0.95, MP Jackknife < 0.7; white: unrecovered node.

Molecular species delimitation

The COI data matrix included 134 terminals, including single sequences of the non-Madeiran *H. radiata* (Iberian Peninsula) and *H. ferox* (Gran Canaria, Canary Islands), corresponding to 64 haplotypes (2 non-Madeiran) (Fig. 3). The ITS-2 matrix included 40 terminals with 400 aligned positions and 10 additional absence/presence characters, corresponding to 17 alleles (sequence types). The clustering analysis (BIN) of the COI sequences resulted in 6 clusters, that mostly matched the morphological circumscription, except for the merging of individuals identified as *H. maderiana* and *H. insularum*. As already noted in the target multilocus phylogenetic analyses, one individual identified as *H. insularum* clustered together with individuals morphologically assigned to *H. ingens*. Uncorrected genetic distances are shown in Table 2. The genetic distance between *H. maderiana* and *H. blackwalli* sp. reval. was 1.6% similar to the values observed within *H. insularum* (1.7%). The next lower genetic distance was observed between *H. nonannulata* and *H. maderiana* (4.3%). The largest genetic distances were found between the species pair *H. insularum* and *H. maderiana* and the remaining endemic species (9.9-10.6%) and were similar to those observed with regard the mainland species *H. radiata* (9.8-11,1%).

The mPTP analysis ran on the IQ-TREE inferred tree, recovered the same groupings with high support. The GMYC model delimited 5 groups, by merging H. nonannulata and H. blackwalli sp. reval. together, but the likelihood ratio test revealed that it did not provide a significantly better fit that the null model (one single species, p=0.7764125).

The statistical parsimony analysis at 95% connection resulted in 6 independent networks that exactly matched the BIN and mPTP clusters (Fig. 4). Lowering the connection limited to 90% had no effect on the results. For the ITS alleles, a single network was obtained (both at 90 and 95%). The alleles of the species *H. maderiana* and *H. insularum* were mixed up, while the rest of alleles were exclusive to each species, except for *H. heeri*, *H. blackwalli* sp. reval. and *H. nonannulata* that shared one allele. The alleles of the putative *H. insularum* individuals bearing *H. ingens* COI haplotypes, were also observed to cluster close to the *H. ingens* alleles.
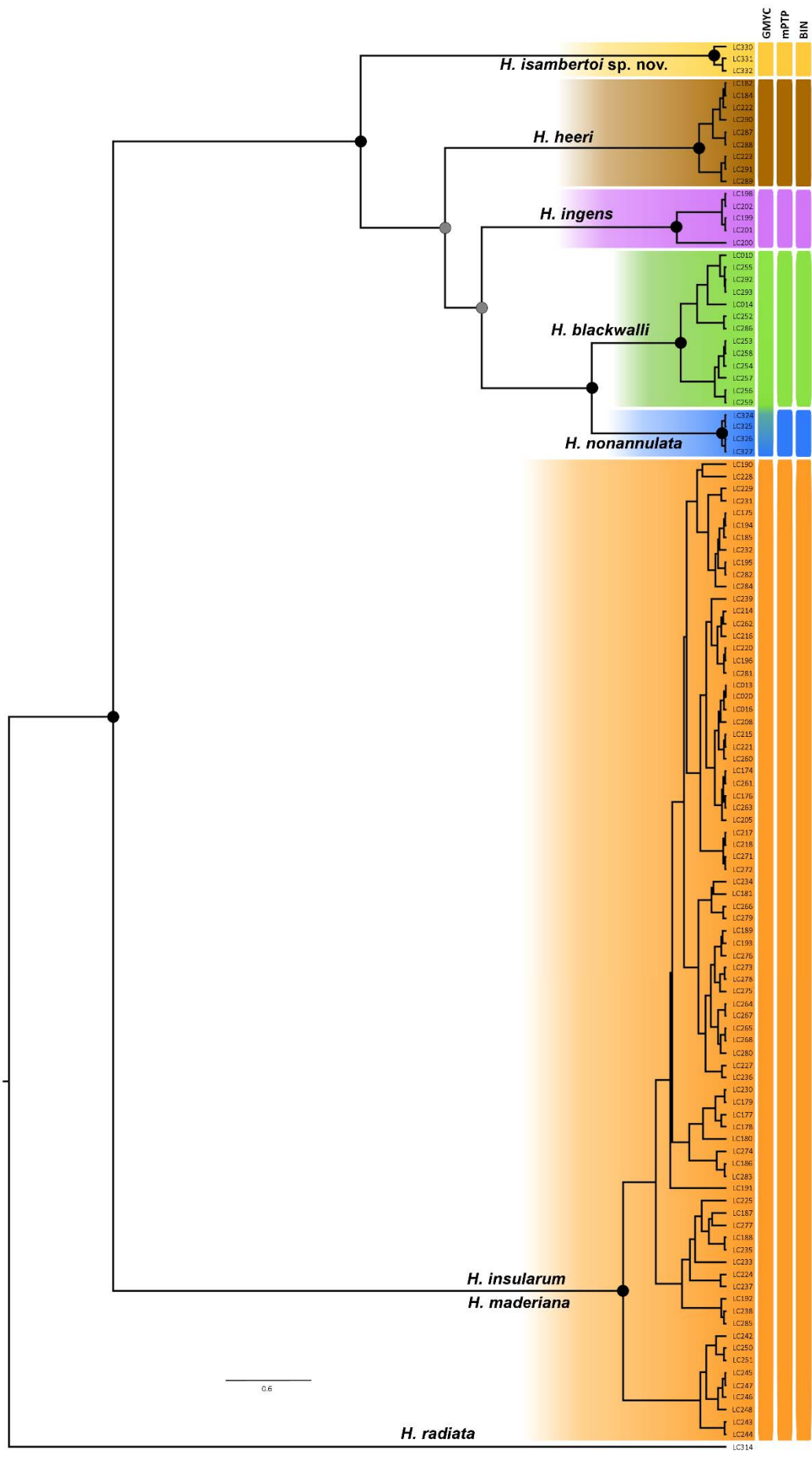
(previous page) Figure 3. Ultrametric tree for the COI obtained with BEAST using a coalescent (constant gopulation growth) prior to apply the GMYC model. Only unique sequences included. Support on nodes should be read as follows: black: BI posterior probability ≥ 0.95; grey: BI posterior probability < 0.95.
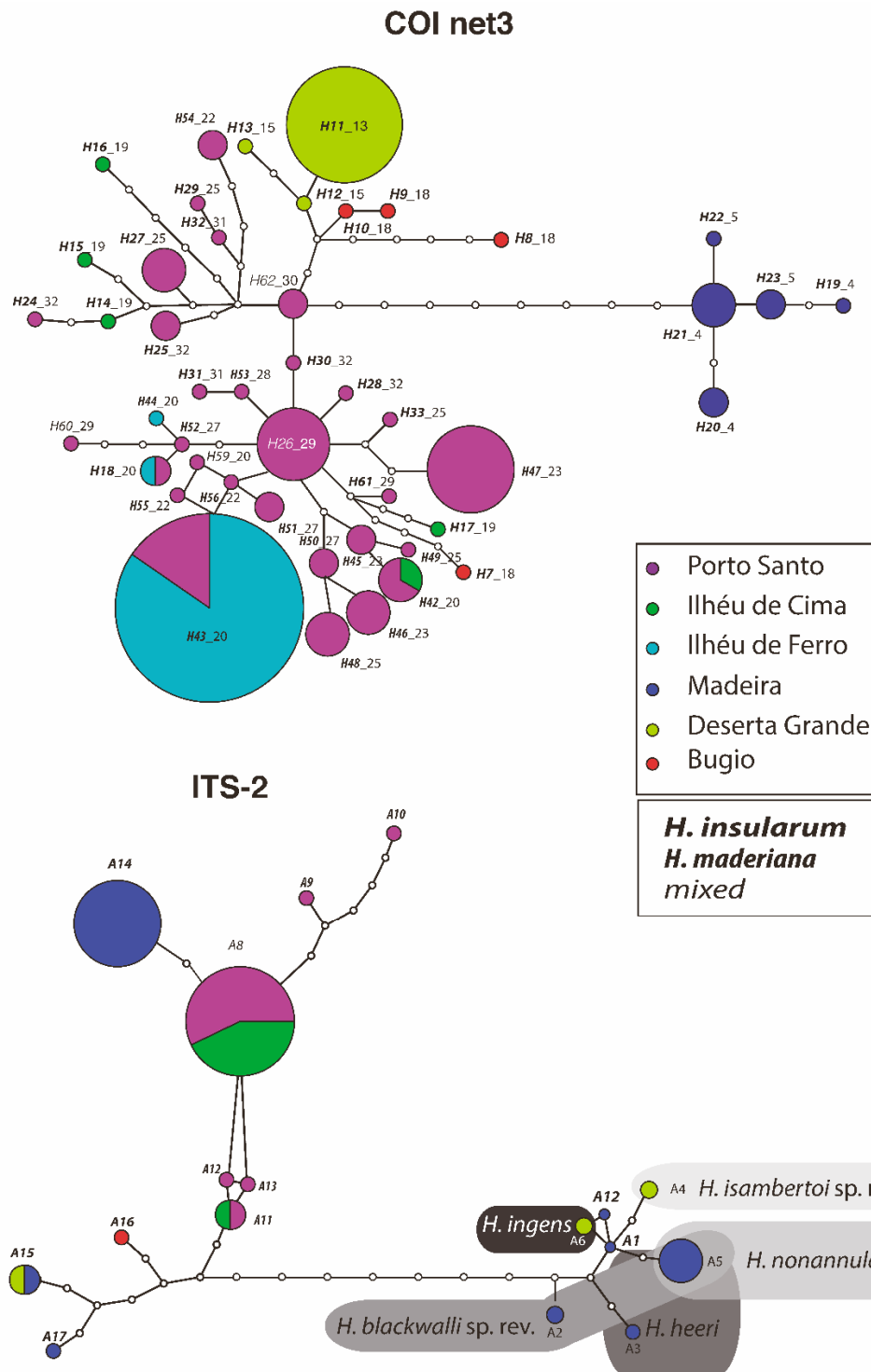
Figure 4. COI haplotype (upper) and ITS-2 allele (lower) networks inferred under statistical parsimony (0.95 probability). Pie size proportional to number of individuals

which exhibited the same haplotype/alleles. White circles represent missing haplotypes/alleles. Colours correspond to islands (colour codes in upper box). For the COI haplotypes only the network (3) including *H. insularum* / *H. maderiana* haplotypes showed (each remaining nominal species were resolved as independent networks). ITS-2 alleles boxed per species, except for *H. insularum* / *H. maderiana*. Haplotype/allele labels for *H. insularum* in bold and italics, *H. maderiana* in condensed bold and italics, not assigned in light italics (see lower box legend).

Divergence time estimation

The inferred species tree suggested non-monophyly of Madeiran *Hogna* albeit with low support (Fig. 5). Estimated time of split form their closest sister taxa was similar for the two Madeiran lineages (9.2 my, 1.9-24 my 95%HPD, and 8.8 my, 1.4-24.6 my, for the *ingens* and the *maderiana* clades, respectively). The most recent common ancestor (mrca) of the *ingens* clade was 5 my (1-13.5 my). The coalescent times inferred from the COI tree for the different species were 0.09 my for *H. isambertoi* sp. nov, 0.19 for *H. heeri*, 0.29 for *H. ingens*, 0.3 for *H. blackwalli* sp. reval. and 0.04 for *H. nonannulata*, and 0.87 for the *maderiana* clade.
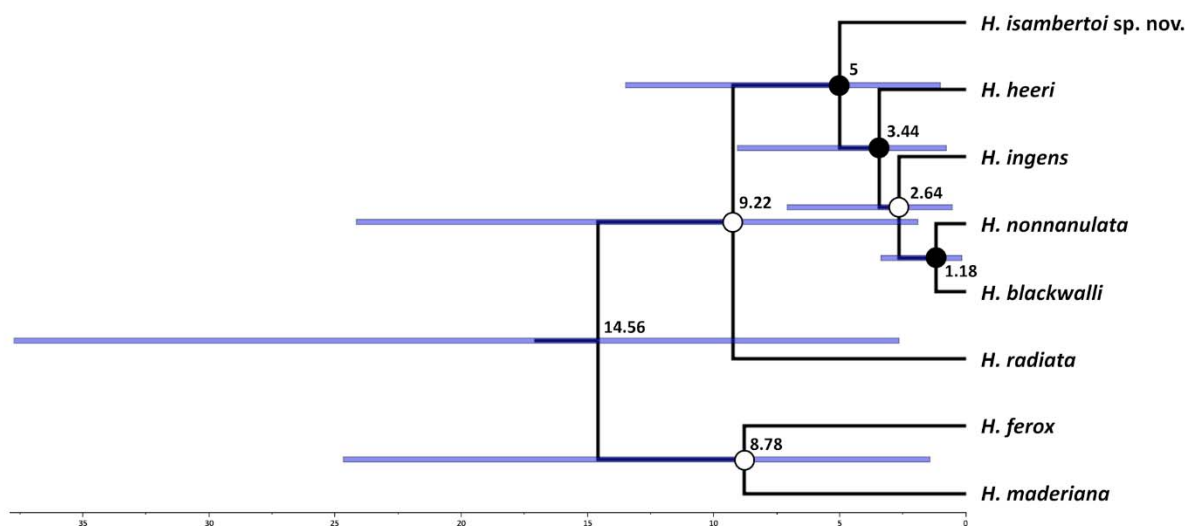
Figure 5. Species tree for the Madeiran *Hogna* including two outgroups. Values on nodes are estimated divergence times in millions of years (my). Support can read as follows: black: BI posterior probability ≥ 0.95, white: BI posterior probability < 0.95. Bars correspond to the 95%HPD of the time estimates.

Taxonomy

Family Lycosidae Sundevall, 1833

Genus *Hogna* Simon, 1885

Type species. *Hogna radiata* (Latreille, 1817).

Hogna blackwalli (Johnson, 1863) sp. reval.

(Figs 6–8)

Lycosa blackwalli Johnson, 1863: 152 (Dmf).

Trochosa maderiana Thorell, 1875: 167 (mf, misidentified).

Geolycosa blackwalli Roewer, 1955: 241.

Geolycosa blackwalli Roewer, 1960: 691, f. 387a-d (mf).

Geolycosa ingens Denis, 1962: 96, f. 78 (f). Wrong identification.

Hogna maderiana Wunderlich, 1992: 461, f. 720c-e (mf, S).

Hogna maderiana Wunderlich, 1995: 416, f. 28 (f).

Holotype: MADEIRA • 2 ♀♀; Pico Ruivo, leg. Johnson, stored at OUMNH, collection number 1617. Examined.

Additional material examined: MADEIRA • between Pico do Areeiro and Poiso, 1 ♀ (SMF65685), leg. K. Groh; Caramujo, 1 ♂ (CRBALC0010: LC010), 23.VIII.2016 (collected as subadult, reared in captivity to adult on 7.X.2016), hand collecting, leg. L. Crespo; "Funchal" [probably North of it because "600 to 2000 ft." is written in label], 1 ♀ (BM, mounted dry), V.1895, leg. O. Grant; Paúl da Serra, 1 ♀ (SMF65684), hand collecting, leg. I. Silva, 1 ♀ (CRBALC0496: LC254) and 3 juveniles (CRBALC0495: LC253, CRBALC0497: LC255, CRBALC0499: LC256), 28.III.2017, hand collecting, leg. L. Crespo & I. Silva; Paúl da Serra / Rabaçal, 5 ♀♀ (SMF65696); Pico do Areeiro, 1 ♀ (CRBALC0516: LC270), 27.III.2017, hand

collecting, leg. I. Silva; Pico do Cidrão, 1 ♀ (CRBALC0489: LC286), 27.III.2017, hand collecting, leg. L. Crespo; Rabaçal, 1 ♀ (SMF65683), 18.VIII.1991, hand collecting, leg. I. Silva; Ribeiro Bonito, 1 juvenile (CRBALC0014: LC014), 4.VIII.2016, hand collecting, leg. L. Crespo; trail from Paúl da Serra to Montado dos Pessegueiros, 1 ♀ (CRBALC0271: LC252) and 2 juveniles (CRBALC0498: LC292, CRBALC0502: LC293), 28.III.2017, hand collecting, leg. L. Crespo & I. Silva, 2 ♀♀ (CRBALC0503: LC257, CRBALC0515: LC259) and 1 juvenile (CRBALC0514: LC258), 31.III.2017, hand collecting, leg. L. Crespo, M. Arnedo & P. Oromí, 1 ♂ (CRBALC0718), 2 ♀♀ (CRBALC0601, CRBALC0605) and 2 juveniles (CRBALC0603, CRBALC0698), 4.IV.2018, hand collecting, leg. L. Crespo & A. Bellvert; 1 ♀ (SMF9910750), 1 ♂, 2 ♀♀ and 4 juveniles (NHRS-JUST-000001114), 2 ♀♀ (BM, mounted dry), [no collection data except for the data of collection of one of these females, IX.1963, which may indicate that this might come from the materials used by James Yate Johnson to describe the species].

Diagnosis: *Hogna blackwalli* sp. reval. can be diagnosed from all other Madeiran *Hogna* by the aspect of its legs, with two small patches of yellow hairs in the joints of anterior tibiae with metatarsi and of metatarsi with tarsi (Fig. 25A). In addition, by the genitalia: in males, the embolus with tip tilted retro-laterally (Fig. 6A–C). In females, the epigynal hood shows a small indentation on the lateral border (Fig. 6D–E).

Redescription – Male (CRBALC0718): (Fig. 6A–C). Total length: 18.92; carapace: 9.1 long, 6.8 wide.

Colour: carapace brown, with short black hairs except anteriorly and laterally, where short white hairs and long black hairs are present; median yellow longitudinal band present, covered with short white hairs, anteriorly broadened, with suffused greyish brown patches covered by yellow hairs; two yellow marginal bands, suffused with greyish brown patches, covered with short white hairs; four black striae well visible on each flank. Chelicerae black, covered mostly in black hairs but with sparse yellow hairs. Gnathocoxae very dark orange brown, labium blackish; sternum black, with a faint, thin longitudinal stripe extending to less than half of sternum length. Legs grey to greyish brown, with 7 to 8 patches of white hairs (anterior legs show 8, posterior legs 7) except the patches in anterior metatarsi, both yellow. Palpal femur as legs, patella, tibia and proximal cymbium with yellow hairs, apical cymbium covered in black hairs. Abdomen with a pair of anterolateral black patches, extending laterally

into grey to black flanks, interspersed with white patches; a median orange lanceolate patch is bordered by the aforementioned pattern, posteriorly also by dark chevrons; venter with a wide longitudinal black band, bordered by a mesh of white and black patches.

Eyes: MOQ: MW = 0.74 PW, MW = 1.06 LMP, MW = 1.07 AW; Cl = 0.49 DAME. Anterior eye row slightly procurved.

Legs: Measurements: Leg I: 27.32, TiI: 6.4; Leg IV: 29.7, TiIV: 6.56; TiIL/D: 5.82. Spination of Leg I: FeI: d1.1.0, p0.0.2; TiI: p0.0.1, v2l.2l.2s; MtI: p0.0.1, r0.0.1, v2l.2l.1s. MtI with very dense scopulae.

Pedipalp: cymbium with 8 dark, stout, macrosetae at tip, Fe with 2 dorsal and an apical row of 4 spines, Pa with 1 prolateral spine, Ti with 1 dorsal, 1 dorsoprolateral spine and 1 prolateral spine. Median apophysis with basal spur truncate, blunt, and with tip thin, blunt; terminal apophysis blade-shaped with sharp end; embolus short, with tip directed laterally; palea large.

Female (CRBALC0516): (Fig. 6D–E). Total length 29.88; carapace: 10.38 long, 8 wide.

Colour: overall as in male, but darker. Sternum entirely black. Yellow hairs in pedipalp restricted to the joints of tibia with tarsus and patella with tibia.

Eyes: MOQ: MW = 0.74 PW, MW = 1.23 LMP, MW = 1.1 AW; Cl = 0.7 DAME. Anterior eye row slightly procurved.

Legs: Measurements: Leg I: 27.68, TiI: 6.25; Leg IV: 31.75, TiIV: 6.8; TiIL/D: 3.77. Spination of Leg I: FeI: d1.1.0, p0.0.2; TiI: p0.0.1, v2l.2l.2s; MtI: p0.0.1, r0.0.1, v2l.2l.1s. MtI with very dense scopulae.

Epigynum: hoods almost touching, short, with lateral borders anteriorly parallel, medially slightly divergent after a small sinuosity; hood cavities deep; median septum with narrow base; spermathecae globular; copulatory ducts with small, stout diverticulum ventrally; fertilisation ducts emerging at the base of copulatory duct.

Intraspecific variation: Carapace length, males: 7.4–9.1, females: 8.9–10.38. Suffused greyish brown patches in median yellow longitudinal band not necessarily covered with yellow hairs. Epigynum can present two small depressions in the base of median septum, which can be of

variable length, position and concavity of inflexion of the lateral hood walls can also be variable, either placed near hoods or medially, median septum can be swollen medially.

Distribution: This species is known from areas in or near the laurel forest patch in Madeira, in the North half of the island (Fig. 8).

Ecology: *H. blackwalli* sp. reval. can be found in montane grasslands surrounding laurel forest areas or Erica shrubland. Surprisingly, it can also be found in closed canopy laurel forest, where, at night, specimens can be found climbing tree trunks.

Conservation status: *H. blackwalli* sp. reval. was assessed according to the IUCN Red List criteria as *H. maderiana*, with the status of Least Concern (Cardoso et al. 2018). The coastal records are probably of *H. nonannulata*.

Comments: There has been a great deal of confusion surrounding *H. blackwalli* sp. reval. and *H. maderiana*. Walckenaer's original description of *H. maderiana* (Walckenaer 1837) based on material from Madeira island indicated that legs were "(…) reddish-brown, suffused brown underneath (…)". Subsequently, Blackwall described the alleged male of Walckenaer's *H. maderiana* but mentioned a striking leg coloration: "(…) the femora, on the upper side, have a yellowish-grey hue, that of the tibia, metatarsi and tarsi being bright orange-red, and the colour of the underside of all the joints is dark brown tinged with grey; (…)" (Blackwall 1857). Additionally, he reported the locality of origin of those specimens to be Porto Santo, not Madeira. Six years later, Johnson (1863) described *H. blackwalli* from Madeira island, indicating that "(…) The metatarsus and tarsus of the two anterior pairs of legs are black, or very dark brown. At the distal extremities and on the upper sides of the femur and genua of the first two pairs of legs, as well as at the extremities of some of the joints of the two posterior pairs of legs, there is a patch of orange hairs. (…)". In the same publication, he also described an identified as *H. maderiana* specimens from Ilhéu de Ferro, near Porto Santo. It is unclear on how many specimens did Johnson based his description, but we could locate at least part of this material at the OUMNH, thus revalidating *H. blackwalli* Johnson, 1863. The next author to make a taxonomic contribution on these spiders was Thorell (1875), who redescribed *H. maderiana* based on specimens from Madeira. However, his reference to the legs colouration that reads "(…) palporum partibus pateliari et tibiali apice supra croceis, metatarsis tibiisque pedum anteriorum apice quoque croceis vel flavis (…)" suggest that his

redescription corresponds to *H. blackwalli* instead. We could locate 14 specimens labelled as *H. maderiana* in the Swedish Museum of Natural History, which most likely were the ones used by Thorell, and we confirmed their correspond to *H. blackwalli* sp. reval. Kulczynski (1899) followed Blackwall's judgement to redescribe the large specimens from Porto Santo and Ilhéu de Ferro under the name *Trochosa maderiana*. Almost one century later, Roewer provided redescriptions of three Madeiran *Hogna* (Roewer 1960), but no reference was given to the leg coloration, which is the easiest way to distinguish these larger, aforementioned species. His epigyne drawings provided little additional information and were confusing. While the epigyne of *H. ingens* allows identification of this species (Roewer 1960: Fig. 387e), the same is not true for the illustrations of *Isohogna maderiana* and *Geolycosa blackwalli* (Roewer 1960: Figs. 319a and 387a, respectively), which look rather the same. However, he reports that Thorell's *Trochosa maderiana* materials are, in fact, *H. blackwalli*, for which we assume Roewer's redescription of *Geolycosa blackwalli* to correspond to the presently revalidated *H. blackwalli*. Denis (1962) cited 2 females as *Geolycosa ingens* (Blackwall, 1857) from locations where *H. blackwalli* sp. reval. is usually found, Rabaçal and Paúl da Serra, in Madeira island. We could not find these materials, but due to the location, we confidently attribute these citations to misidentified specimens of *H. blackwalli* sp. reval. The last taxonomic works on Madeiran *Hogna* were made by Wunderlich (1992, 1995). In the first of these works (Wunderlich 1992), the species *H. maderiana* and *H. blackwalli* were wrongly synonymized and it was stated that "up to Denis (1962), most authors assumed that *H. maderiana* occurred both in Madeira and Porto Santo." This is not accurate, since Johnson discriminated between *H. blackwalli* from Madeira and *H. maderiana* from Ilhéu de Ferro. In fact, this synonymy is even stranger because while revising the materials present at the SMF, we found vial 9910750, of the Roewer collection, with an identification note by Wunderlich stating "*H. blackwalli* (Johnson)". Finally, we have located only part of the type material described by Johnson at the Oxford University Museum, because no males were accounted for, when his description mentioned males. Therefore, the whereabouts of the remaining specimens of the type series are unknown.
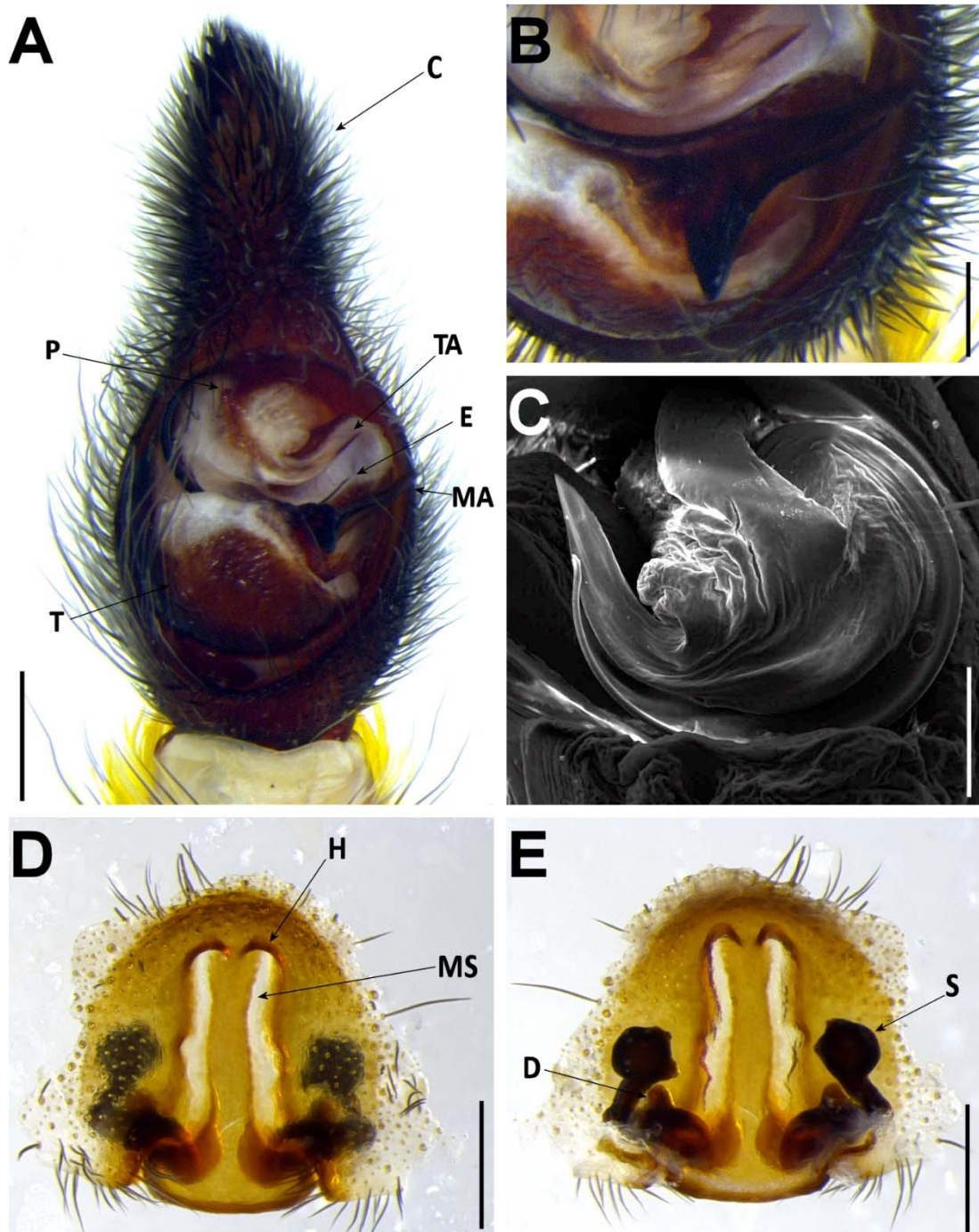
Figure 6. *H. blackwalli*. A–C, male (CRBALC0718): A, left male palp, ventral; B, detail of the median apophysis, anteroventral; C, SEM image, right male palp, ventral. D–E, female (CRBALC0516): D, epigynum, ventral; E, vulva, dorsal. Abbreviations, male palp: C – cymbium, E – embolus, MA – median apophysis, P – palea, T – tegulum, TA – terminal apophysis. Abbreviations, female genitalia: D – diverticulum, H – epigynal hoods, MS – median septum, S – spermatheca. Scale bars: A, D, E = 0.5 mm, B, C = 0.2 mm.

Figure 7. Photo of *H. blackwalli*. Female specimen, recently dead, in captivity. Photo credit: Emídio Machado, by courtesy.
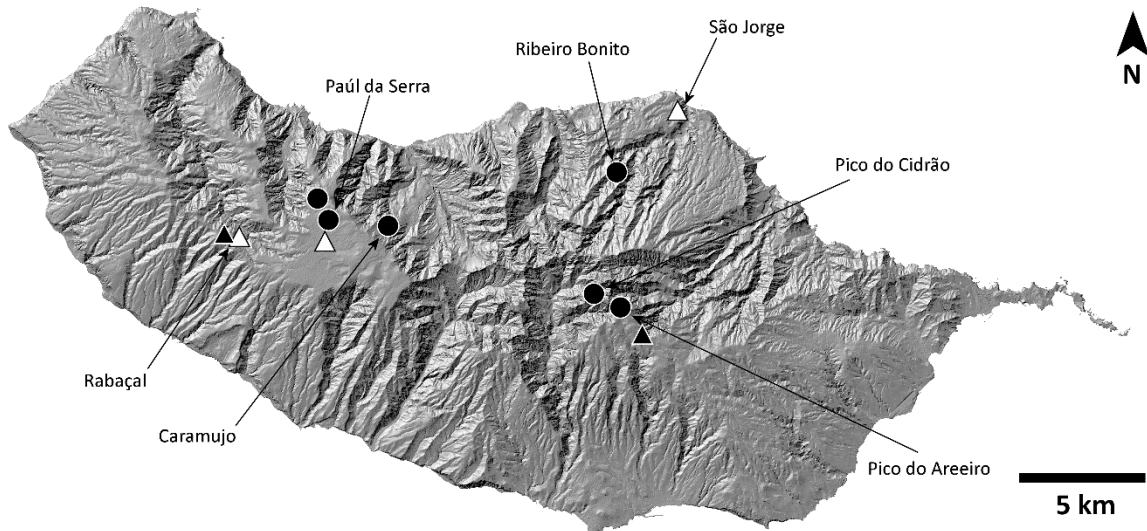
Figure 8. Distribution of *H. blackwalli*. Circles: present records; black triangles: revised records from literature; white triangles: unconfirmed records from literature.

Hogna ferox (Lucas, 1838)

Arctosa maderana Roewer, 1960: 604-605, f. 334a (f), f. 334 b (m). Type material examined. New synonymy.

(see WSC (2021) for a complete list of synonymies)

Justification of the synonymy: After its original description, the endemic species *Arctosa maderana* Roewer, 1960, was never accounted for in the archipelago of Madeira, despite extensive sampling through several biodiversity inventory projects (Boieiro et al. 2018; Crespo et al. 2014; Malumbres-Olarte et al. 2020). We had the opportunity to examine the type specimens at the SMF (vial 9903912). We identified the couple as *H. ferox* (Lucas, 1838). *H. ferox* has a widespread distribution throughout the Mediterranean, being present in the Iberian Peninsula, North Africa and the neighbouring archipelago of the Canary Islands. However, it has never been reported in Madeira, for which we propose that *A. maderana* Roewer, 1960 is a junior synonym of *H. ferox* (Lucas, 1838) and should be removed from the Madeira archipelago fauna.

Hogna heeri (Thorell, 1875)

(Figs 9–11)

Trochosa herii Thorell, 1875: 166.

Trochosa herii Kulczynski, 1899: 433, pl. 9, f. 188 (f).

Hogna heeri Roewer, 1955: 248.

Hogna herii Roewer, 1959: 411, f. 221a-d (f, Dm).

Hogna heeri Wunderlich, 1992: 459, f. 720-720a (mf).

Holotype: MADEIRA • 2 ♀♀, leg. O. Heer, stored at NHRS, collection number JUST-000001113. Examined.

Additional material examined: BUGIO • Planalto Sul, 1 ♀ (LCPC), 3.XII.2012, hand collecting, leg. I. Silva. MADEIRA • between Eira do Serrado and Curral das Freiras, 1 ♀ (SMF69107; Paúl da Serra, 2 ♀♀ (MMUE G7572.874), 25.IV.1973, leg. J. Murphy, 1 ♀ (CRBALC0492: LC289), 19.III.2017, hand collecting, leg. I. Silva, 1 ♀ (CRBALC0500: LC222) and 1 juvenile (CRBALC0494: LC291), 28.III.2017, leg. I. Silva; Pico do Cidrão, 1 ♀ (LCPC), 24.VI.2003, pitfall trapping, leg. M. Freitas, 2 ♀♀ (CRBALC0490: LC287, CRBALC0288: LC288), 27.III.2017, hand collecting, leg. L. Crespo & I. Silva; trail from Paúl da Serra to Montado dos Pessegueiros, 2 ♀♀ (CRBALC0270: LC184, CRBALC0501: LC223) and 1 juvenile (CRBALC0493: LC290), 28.III.2017, hand collecting, leg. L. Crespo & I. Silva; 1 ♀ (SMF37575).

Diagnosis: *Hogna heeri* can be diagnosed by the genitalia: in males, by a straight embolus (Wunderlich 1992: 595, Fig. 720). In females, by epigynal hoods with widely divergent lateral border and median septum with a wide base (Fig. 9).

Redescription – Male: We could not revise any male materials.

Female (CRBALC0500): (Fig. 7 corresponds to specimen CRBALC0501). Total length 13.54; carapace: 5.63 long, 4.4 wide.

Colour: carapace greyish-brown, covered with short black hairs, with a median yellow longitudinal band, anteriorly broadened, covered with short white hairs, with suffused greyish brown patches; two yellow marginal bands, with roughly round grey patches, covered with short white hairs; four black striae well visible on each flank. Chelicerae dark brown, covered in black and yellow hairs. Gnathocoxae and labium overall brown, with posterior margin blackish; sternum yellow, with a faint v-shaped grey patch and grey lateral borders. Legs yellow, with irregular grey suffused patches, except metatarsi and tarsi, brown. Pedipalps yellow except tibia, brown, tarsus, blackish brown. Abdomen with a pair of anterolateral black patches, extending laterally into grey flanks, mottled with yellowish patches covered with white hairs; a median dark lanceolate patch is bordered by two yellowish longitudinal bands interconnected in anterior half, posteriorly by means of dark chevrons; venter yellowish, with a median dark grey longitudinal band, bordered by yellowish and grey small patches.

Eyes: MOQ: MW = 0.72 PW, MW = 1.1 LMP, MW = 1.06 AW; Cl = 0.91 DAME. Anterior eye row straight.

Legs: Measurements: Leg I: 13.02, TiI: 2.75; Leg IV: 16.1, TiIV: 3.22; TiIL/D: 3.72. Spination of Leg I: FeI: d1.1.1, p0.0.1; TiI: v2l.2l.2s; MtI: p0.0.1, r0.0.1, v2l.2l.1s. MtI with sparse scopulae in basal half and dense scopulae on distal half.

Epigynum: hoods touching, short, with lateral borders widely divergent, converging solely at its posterior end; hood cavities deep; median septum with wide base; spermathecae globular; copulatory ducts basally with a laterally projected diverticulum; fertilisation ducts emerging at the base of copulatory duct.

Intraspecific variation: Carapace length, females: 5.63–5.81. In females, ventral abdominal dark band may be entirely absent; relative position of female epigynal hoods may vary from touching to almost touching.

Distribution: This species is known from two distinct regions: high altitude localities in Madeira, always above 800 m, and the island of Bugio (Fig. 11).

Ecology: *H. heeri* occurs in montane grasslands or Erica shrubland in Madeira and the steep, semi-arid summit of Bugio.

Conservation status: *H. heeri* was assessed according to the IUCN Red List criteria, with the status of Least Concern (Cardoso, P, Crespo, LC, Silva, I, Borges, P & Boieiro 2018a).

Comments: The disjunct distribution of *H. heeri*, with populations in Madeira and Bugio, is somewhat baffling. The only known specimens from Bugio previously reported (Crespo et al. 2013) were revised: while the female matches *H. heeri*, the male palp is the same as that of *H. isambertoi* sp. nov., with the tip of the embolus slightly tilted anteriorly (Fig. 16A). We would like to remark that Wunderlich (1992) reports an apophysis as a diagnostic feature to identify males of *H. heeri*. This structure is the proximal branch of the terminal apophysis, and it is present in all species, variably more or less coupled to the embolus, for which it should not be used to diagnose the species. Unfortunately, we could not gather molecular information from Bugio specimens due to their poor preservation. Lastly, while revising Thorell's type series, we identified one of the 3 adult females in the original vial as *H. insularum*.
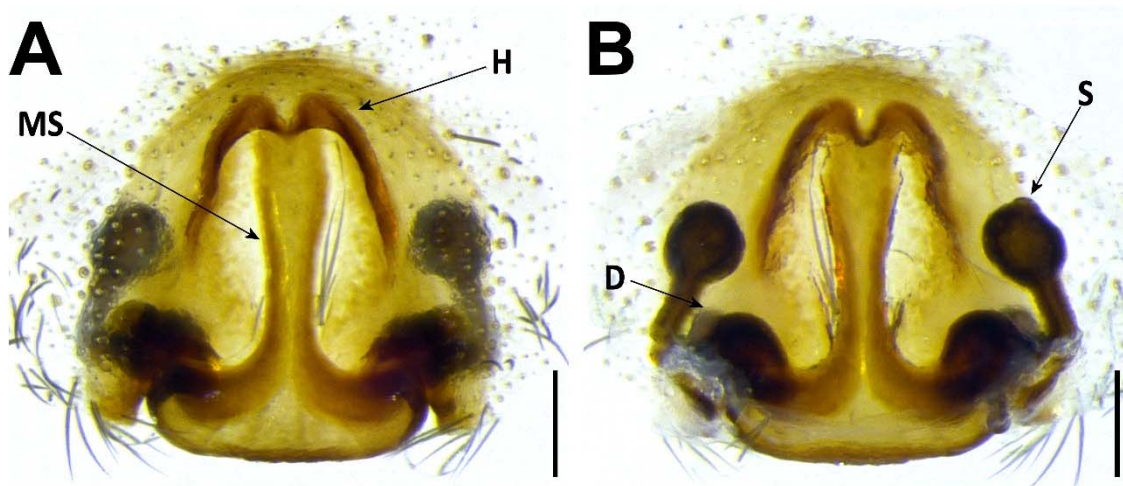
Figure 9. *H. heeri*. A–B, female (CRBALC0501): A, epigynum, ventral; B, vulva, dorsal. Abbreviations, female genitalia: D – diverticulum, H – epigynal hoods, MS – median septum, S – spermatheca. Scale bars: A, B = 0.2 mm.

Figure 10. Photo of *H. heeri*. Female specimen in captivity. Photo credit: Emídio Machado, by courtesy.
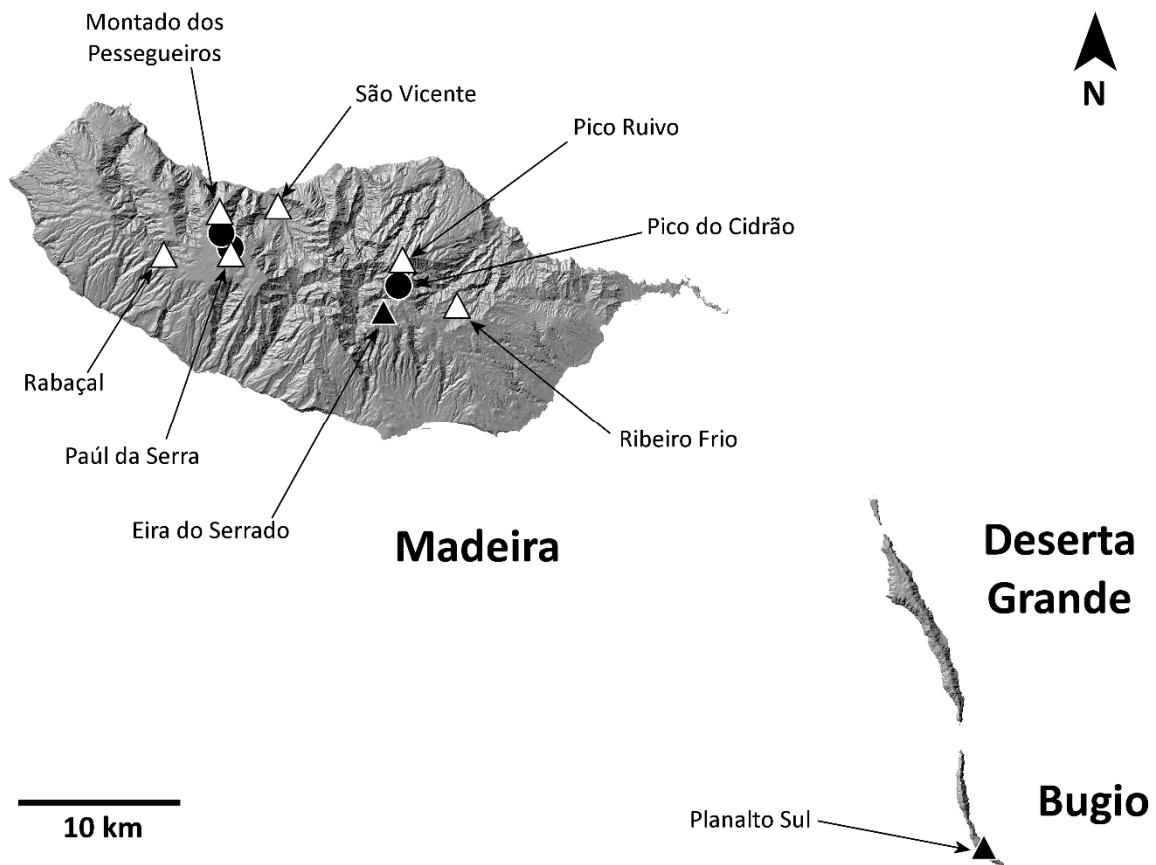
Figure 11. Distribution of *H. heeri*. Circles: present records; black triangles: revised records from literature; white triangles: unconfirmed records from literature.

Hogna ingens (Blackwall, 1857)

(Figs 12–14)

Lycosa ingens Blackwall, 1857: 284 (Df).

Lycosa ingens Blackwalli, 1867: 203 (Dm).

Trochosa ingens Kulczynski, 1899: 423, pl. 9, f. 121 (mf).

Geolycosa ingens Roewer, 1955: 241.

Geolycosa ingens Roewer, 1960: 689, f. 387e (f).

Hogna ingens Wunderlich, 1992: 459, f. 720b, f. 724a.

Holotype: no type materials from the Blackwall collection were found neither at the OUMNH nor the BM.

Additional material examined: DESERTA GRANDE • Vale da Castanheira (N), 1 ♀ (SMF21994), 26.III.1967, 1 ♀ (CRBALC0591) and 4 juveniles (CRBALC0593, CRBALC0594, CRBALC0595, CRBALC0592), 25.III.2017, hand collecting, leg. L. Crespo.

Diagnosis: Hogna ingens can be diagnosed from all other Madeiran *Hogna* by the aspect of its legs, blackish, with white patches (Fig. 23C). In addition, by its genitalia. In males, by the inclined palea shield (Wunderlich 1992: 596, Fig. 720f). In females, by short epigynal hoods, with lateral borders divergent and anteriorly swollen median septum (Fig. 12A).

Redescription – Male: We could not revise any male materials.

Female (CRBALC0591): (Fig. 12). Total length 25.08; carapace: 14.77 long, 11 wide.

Colour: carapace greyish-brown, densely covered with short black hairs, with a yellowish longitudinal band present from fovea to posterior margin of carapace; with two faint light grey marginal bands suffused with black patches, covered with white hairs; four striae well visible on each flank. Chelicerae black except apically, reddish-brown, covered in black hairs. Gnathocoxae and labium overall orange brown, densely covered with black hairs; sternum greyish brown, densely covered with black hairs. Legs greyish, with a variable number (6 to 8) of lightly colored patches covered by white hairs. Pedipalps greyish, densely covered in black hairs. Abdomen densely covered in black hairs, with only 4 very small white patches dorsally and a small anterolateral band of white hairs; venter densely covered in black hairs, with only two faint median bands of small white patches.

Eyes: MOQ: MW = 0.73 PW, MW = 1.22 LMP, MW = 1.06 AW; Cl = 0.45 DAME. Anterior eye row slightly procurved.

Legs: Measurements: Leg I: 37.7, TiI: 8.85; Leg IV: 35.93, TiIV: 8.4; TiIL/D: 2.34. Spination of Leg I: FeI: d1.1.0, p0.0.2; TiI: p0.0.0, v2s.2s.2s; MtI: p0.0.1, r0.0.1, v2s.2s.1s. MtI an TiI with dense scopulae.

Epigynum: hoods far apart, short, with lateral borders anteriorly convergent, then becoming divergent; hood cavities shallow; median septum anteriorly swollen, with wide base; spermathecae moderately swollen; copulatory ducts basally with a laterally projected bulbus; fertilisation ducts emerging at the base of copulatory duct.

Distribution: This species is known only from Vale da Castanheira, a 1 km^2 valley in the North end of Deserta Grande (Fig. 14).

Ecology: Vale da Castanheira is a semi-arid grassland area.

Conservation status: H. ingens was declared Critically Endangered in previous works (Cardoso 2014; Crespo et al. 2014). Its restricted habitat has been subject to biological invasions since humans set foot in Deserta Grande, with the introduction of herbivore vertebrates and, more recently, of the herb *Phalaris aquatica* L., which grows abundantly throughout the valley, limiting the access of *H. ingens* to shelters below rocks and fissures and displacing native flora from its habitat. An *ex-situ* breeding program is currently being conducted by the Bristol Zoo to safekeep populational levels.
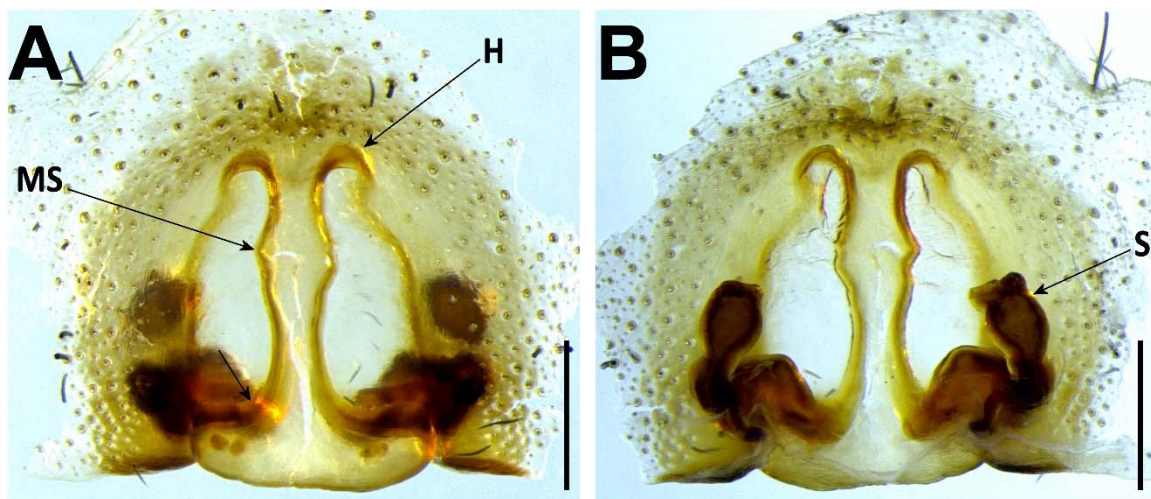
Figure 12. *H. ingens*. A–B, female (CRBALC0591): A, epigynum, ventral; B, vulva, dorsal. Abbreviations, female genitalia: H – epigynal hoods, MS – median septum, S – spermatheca. Scale bars: A, B = 0.5 mm.

Figure 13. Photo of *H. ingens*. Female specimen in the field. Photo credit: Pedro Cardoso.

Figure 14. Distribution of *H. ingens*. Black circles: present records; dotted circles: records from only leg samples; black triangles: revised records from literature; white triangles: unconfirmed records from literature.

Hogna insularum (Kulczynski, 1899)

(Figs 15–17)

Trochosa insularum Kulczynski, 1899: 429, pl. 9, f. 122, 126 (Dmf).

Hogna insularum Roewer, 1959: 517, f. 291c-d.

Hogna biscoitoi Wunderlich, 1992: pp 457, figs 708–709. Holotype ♂ without exact locality, Porto Santo; leg. Winkelmayer, stored at MMF, collection number 24551. Not examined. New synonymy.

Hogna insularum Wunderlich, 1995: 415, f. 27 (m).

Holotype: MADEIRA • 7 ♀♀, leg. Kulczynski, stored at MIZ. Examined (1 ♀).

Additional material examined: BUGIO • Planalto Sul, 1 ♂ (CRBALC0015) and 1 ♀ (CRBALC0017), 28.VI.2012, hand collecting, leg. I. Silva, 1 ♂ (CRBALC0316: LC229), 1 ♀ (CRBALC0301: LC190) and 2 juveniles (CRBALC0315: LC228, CRBALC0318: LC231), 13.IV.2017, hand collecting, leg. L. Crespo. DESERTA GRANDE • Eira, 2 juveniles (CRBALC0312: LC282), CRBALC0319: LC232), 11.IV.2017, 1 ♀ (FMNH http://id.luomus.fi/HLA.148894), 17.IV.2011, hand collecting, leg. I. Silva; North end, 1 ♂ (MMUE G7508.51), 12.VIII.1981, under stone, leg. J. Murphy; Pedregal (E), 1 ♀ (CRBALC0308: LC197) and 1 juvenile (CRBALC0306: LC195), 8.IV.2017, hand collecting, leg. L. Crespo & I. Silva, 1 juvenile (CRBALC0285: LC185), 9.IV.2017, hand collecting, leg. L. Crespo; Planalto Sul, 1 juvenile (CRBALC0413: LC284), 11.IV.2017, hand collecting, leg. L. Crespo & I. Silva; Rocha do Barbusano (S), 1 juvenile (CRBALC0262: LC175), 10.IV.2017, hand collecting, leg. L. Crespo & I. Silva; Vale da Castanheira, 1 ♂ (FMNH http://id.luomus.fi/HLA.148961), 23.IV.2011, hand collecting, leg. I. Silva *et al.*, 1 ♂ (FMNH http://id.luomus.fi/HLA.148976), 5.V.2011, pitfall trapping, leg. I. Silva *et al.*, 1 ♀ (FMNH http://id.luomus.fi/HLA.148982), 2 ♀♀ (FMNH http://id.luomus.fi/HLA.148986), 22.IV.2011, hand collecting, leg. I. Silva; Vale da Castanheira (E), 1 ♂ (CRBALC0305: LC194), 9.IV.2017, hand collecting, leg. I. Silva; Vale da Castanheira (SE), 2 ♂♂ (CRBALC0313: LC226, CRBALC0349: LC241) and 1 ♀ (CRBALC0348: LC240), 9.IV.2017, hand collecting, leg. I. Silva. ILHÉU DA CAL • 1 ♀ (SMF65693), leg. K. Groh. ILHÉU DE CIMA • top plateau, 1 ♀ (CRBALC0019), 9.IV.2012, hand collecting, leg. I. Silva, 1 ♂ (CRBALC0018), 22.V.2011, hand collecting, leg. I. Silva, 1 ♀ (CRBALC0302: LC191) and 4 juveniles (CRBALC0284: LC183, CRBALC0311: LC225, CRBALC0320: LC233, CRBALC0321: LC234), 19.IV.2017, hand collecting, leg. L. Crespo & I. Silva. ILHÉU DE FERRO • South tip, 1 ♀ (CRBALC0317: LC320) and 2 juveniles

(CRBALC0265: LC178, CRBALC0266: LC179), 18.IV.2017, hand collecting, leg. L. Crespo & I. Silva. ILHÉU DO DESEMBARCADOURO • 2 ♀♀ (MMUE G7508.50), 28.VIII.1981, under stone, leg. J. Murphy. MADEIRA • Cais do Sardinha, 5 juveniles (CRBALC0504: LC242, CRBALC0505: LC243, CRBALC0506: LC244, CRBALC0507: LC245, CRBALC0508: LC246), 30.III.2017, hand collecting, leg. I. Silva; Caniçal, 1 ♀ (MMUE G7572.859), 24.IV.1973, leg. J. Murphy; Caniço, 1 ♀ (MMUE G7508.58), 11.VIII.1981, under stone, leg. J. Murphy; Ponta de São Lourenço, 1 ♂ (MMUE G7508.54), 29.VII.1981, 1 ♀ (MMUE G7508.57), 1.VIII.1981, under stone, leg. J. Murphy, 4 ♂♂ and 5 ♀♀ (FMNH http://id.luomus.fi/HLA.156001), 15.V.2011, pitfall trapping, leg. L. Crespo *et al.,* 1 ♂ and 4 ♀♀ (FMNH http://id.luomus.fi/HLA.156012), 2.V.2011, hand collecting, leg. L. Crespo *et al.,* 2 ♀♀ (FMNH http://id.luomus.fi/HLA.156034), 26.IX.2009, hand collecting, leg. L. Crespo, 1 ♀ (CRBALC0597) and 3 juveniles (CRBALC0599, CRBALC0600, CRBALC0651), 2.IV.2018, hand collecting, leg. L. Crespo; Ponta do Rosto, 1 ♀ (CRBALC0513: LC251) and 3 juveniles (CRBALC0509: LC247, CRBALC0510: LC248, CRBALC512: LC250), 30.III.2017, hand collecting, leg. I. Silva. PORTO SANTO • Rocha de Nossa Senhora, 1 ♂ (CRBALC0290: LC187) and 1 juvenile (CRBALC0291: LC188), 21.IV.2017, hand collecting, leg. L. Crespo & I. Silva; Pedras Vermelhas, 2 ♂♂ and 1 juvenile (SMF65689), 7.VII.1983, leg. K. Groh; Pico Ana Ferreira, 1 ♂ (CRBALC0310: LC224), 1 ♀ (CRBALC0327: LC239) and 5 juveniles (CRBALC0303: LC192, CRBALC0307: LC196, CRBALC0326: LC238, CRBALC0309: LC281, CRBALC0430: LC285), 20.IV.2017, hand collecting, leg. L. Crespo & I. Silva; Pico Branco, 1 ♂ (CRBALC0304: LC193), 21.IV.2017, hand collecting, leg. L. Crespo & I. Silva, 1 ♂ (CRBALC0314: LC227), 23.IV.2017, hand collecting, leg. L. Crespo; Pico da Juliana, 1 juvenile (CRBALC0286: LC186), 24.IV.2017, hand collecting, leg. L. Crespo; Pico do Castelo, 2 ♀♀ (CRBALC0300: LC189, CRBALC0322: LC235) and 2 juveniles (CRBALC0267: LC180, CRBALC0268: 181), 17.IV.2017, hand collecting, leg. L. Crespo & I. Silva, 1 ♂ (CRBALC0692), 8.IV.2018, hand collecting, leg. L. Crespo & A. Bellvert; Pico do Concelho, 1 ♀ (SMF65695), 29.VI.1983, leg. K. Groh; Pico do Espigão, 1 ♀ (SMF65692), 1.VII.1983, leg. K. Groh; Pico do Facho, 1 ♀ (SMF65694), 28.VI.1983, leg. K. Groh; Pico do Maçarico [the label reads "Pico dos Magaricos", therefore we find it necessary to present the correct locality name], 1 ♀ (SMF65691), 10.VII.1983, leg. K. Groh; Terra-Chã (Pico Branco), 1 ♂ (CRBALC0323: LC236) and 2 juveniles (CRBALC0324: LC327, CRBALC0396:

LC283), 21.IV.2017, hand collecting, leg. L. Crespo & I. Silva, 4 juveniles (CRBALC0627, CRBALC0628, CRBALC0630, CRBALC0700), 10.IV.2018, hand collecting, leg. L. Crespo & A. Bellvert; 1 ♀ (NHRS-JUST-000001115), 1 ♂ (MMUE G7508.48), 28.VIII.1981, under stone, leg. J. Murphy, 1 ♂ 1 ♀ and 2 juveniles (SMF34577), 1983, leg. G. Schmidt, 1 ♂ and 1 ♀ (SMF65690), hand collecting, leg. I. Silva, 1 ♀ (BM 1892.7.9.12.17), leg. W.R.O. Grant.

Diagnosis: *Hogna insularum* can be diagnosed from all other Madeiran *Hogna* by a combination of the following characters: the small to medium size (prosoma length < 10 mm), the aspect of its legs, brown, with black patches (Fig. 26C), male's embolus with smoothly curved tip (Fig. 15), and female epigyne median septum roughly half as wide (at base) as long (Fig. 16 A, C, E, G).

Redescription – Male (CRBALC0310): (Fig. 15A, E, F). Total length: 7.76; carapace: 4.6 long, 3.32 wide.

Colour: carapace greyish-brown, covered with short black hairs, with a median yellow longitudinal band, anteriorly broadened, covered with short white hairs, with suffused greyish brown patches; two yellow marginal bands, with roughly round grey patches, covered with short white hairs; four black striae well visible on each flank. Chelicerae brownish orange, with blackish patches, covered in black and white hairs. Gnathocoxae greyish yellow, labium overall blackish, with anterior margin greyish yellow; sternum yellow, with a v-shaped grey patch and suffused patches at lateral borders. Legs pale yellow to orange from femora to tibia, with irregular grey suffused patches, metatarsi and tarsi brown. Pedipalps pale yellow except tarsus, brown. Abdomen with a pair of anterolateral black patches, extending laterally into grey flanks, mottled with yellowish patches covered with white hairs; a median dark lanceolate patch is bordered by two yellowish longitudinal bands interconnected in anterior half, posteriorly by means of dark chevrons; venter yellowish, with a median dark grey longitudinal band, bordered by yellowish and grey small patches.

Eyes: MOQ: MW = 0.8 PW, MW = 1.1 LMP, MW = 1.2 AW; Cl = 0.33 DAME. Anterior eye row slightly procurved.

Legs: Measurements: Leg I: 13.56, TiI: 3.06; Leg IV: 14.93, TiIV: 3.06; TiIL/D: 5.46. Spination of Leg I: FeI: d1.1.0, p0.0.1–2; TiI: p1s.0.1s, r1s.0.1s, v2l.2l.2s; MtI: p0.1.1, r0.0.1, v2l.2l.1s. MtI with sparse scopulae in basal half and dense scopulae on distal half.

Pedipalp: cymbium with 5 dark, stout, macrosetae at tip, Fe with 2 dorsal and an apical row of 4 spines, Pa with 1 prolateral spine, Ti with 1 dorsal and 1 prolateral spine. Median apophysis with basal spur truncate, blunt, and with tip wide, blunt; terminal apophysis blade-shaped with sharp end; embolus long, with tip smoothly curved anteriorly; palea small.

Female (CRBALC0308): (Fig. 16C–D). Total length 12.77; carapace: 5.44 long, 4.1 wide.

Colour: overall as in male, but darker in legs, chelicera and prosoma. Sternum with a faint v-shaped grey patch. Abdomen is lighter, with central chevrons and ventral longitudinal dark band faded.

Eyes: MOQ: MW = 0.76 PW, MW = 1.15 LMP, MW = 1.2 AW; Cl = 0.64 DAME. Anterior eye row slightly procurved.

Legs: Measurements: Leg I: 13.77, TiI: 3.05; Leg IV: 15.96, TiIV: 3.34; TiIL/D: 3.7. Spination of Leg I: FeI: d1.1.0, p0.0.2; TiI: p0.1s.0, v2l.2l.2s; MtI: p0.0.1, r0.0.1, v2l.2l.1s. MtI with sparse scopulae in basal half and dense scopulae on distal half.

Epigynum: hoods almost touching, short, with lateral borders parallel; hood cavities shallow; median septum with narrow base; spermathecae oval or piriform; copulatory ducts with small, stout diverticulum ventrally; fertilisation ducts emerging at the base of copulatory duct.

Intraspecific variation: Carapace length, males: 4.6–6.4, females: 5.13–7.4. Length of cymbium of male palp can vary from shorter to longer than the bulbus. In the single available adult female from Madeira, the hoods of the epigynum show slightly divergent lateral borders (posteriorly) (Fig. 16E), while specimens from the remaining islands show parallel lateral borders.

Distribution: This species is known from many locations in all islands of the archipelago except in Madeira island, where it is only present at the Southeast coastal regions (Fig. 17).

Ecology: H. insularum occurs in a wide variety of habitats, from grasslands, *Erica* shrubland to secondary forests (in the latter two cases, only in Porto Santo).

Conservation status: H. insularum was assessed according to the IUCN Red List criteria, with the status of Least Concern (Cardoso et al. 2018b).

Comments: H. insularum presents a remarkable genitalic variation. In males, both the length of the cymbium and the position of the sickle-shaped apophysis relative to the embolus are variable (Fig. 15). In females, the epigynum usually presents hoods with anteriorly parallel lateral borders, but a specimen from Madeira shows a posteriorly divergent lateral border. At the same time, the shape of spermathecae seem to vary from ovoid (Fig. 16, A–D), to piriform (Fig. 16, E–F), to rounded (Fig. 16, G–H). Wunderlich (1992) described *H. biscoitoi* based on specimens from Porto Santo. To diagnose it from *H. insularum* he stated that in males "the sickle-shaped apophysis points more to the tip of the cymbium" while in the former species the same structure "(…) is directed more retrolaterally". For females, although a diagnostic description was provided, the identification key directed to the same image when referring to the epigyne of both *H. insularum* and *H. biscoitoi*. We collected a thorough sample of specimens from different localities in Porto Santo (from Pico Ana Ferreira to Pico Branco) and surrounding islets. We did observe male palps with different degrees of inclination of the sickle-shaped apophysis and with cymbium shorter than the length of the copulatory bulbus (Fig. 15, A, C), but both characters were unlinked. We suspect that these traits may be affected by the time from the last moult (e.g. Fig. 15B was most likely a recently moulted individual, given its overall pale coloration). Furthermore, fixation in ethanol might sometimes cause a displacement of sclerites, even if small. Molecular data does not seem to provide any additional evidence regarding the possibility that the specimens from Porto Santo may belong to a different species that those reported form other islands. Unfortunately, we could not examine the type material of *H. biscoitoi* stored at the Funchal Municipal Museum, since it does not loan type material for study. Based on the variability in the supposedly diagnostic features and the lack of genetic divergence, we hereby consider *H. biscoitoi* as a junior synonym of *H. insularum*.
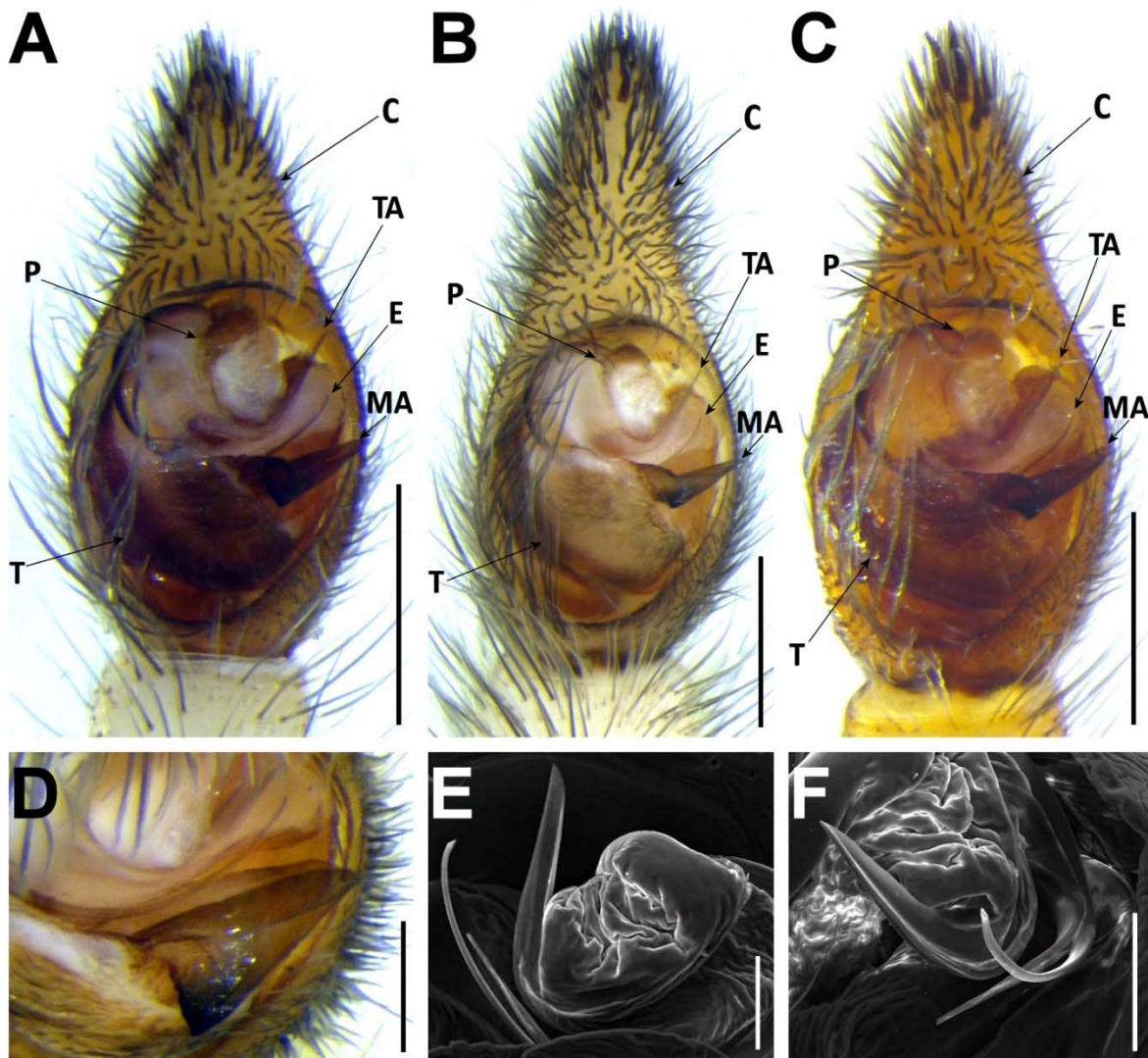
Figure 15. *H. insularum*, male palps. A, male from Porto Santo (CRBALC0310), left palp, ventral; B, male from Deserta Grande (CRBALC0305), left palp, ventral; C, male from Bugio (CRBALC0015), left palp, ventral; D, detail of the median apophysis of male from Deserta Grande (CRBALC0305), anteroventral; E, SEM image, right male palp, male from Porto Santo (CRBALC0310), ventral; F, Idem, retroventral. Abbreviations, male palp: C – cymbium, E – embolus, MA – median apophysis, P – palea, T – tegulum, TA – terminal apophysis. Scale bars: A, B, C = 0.5 mm, D = 0.2 mm.
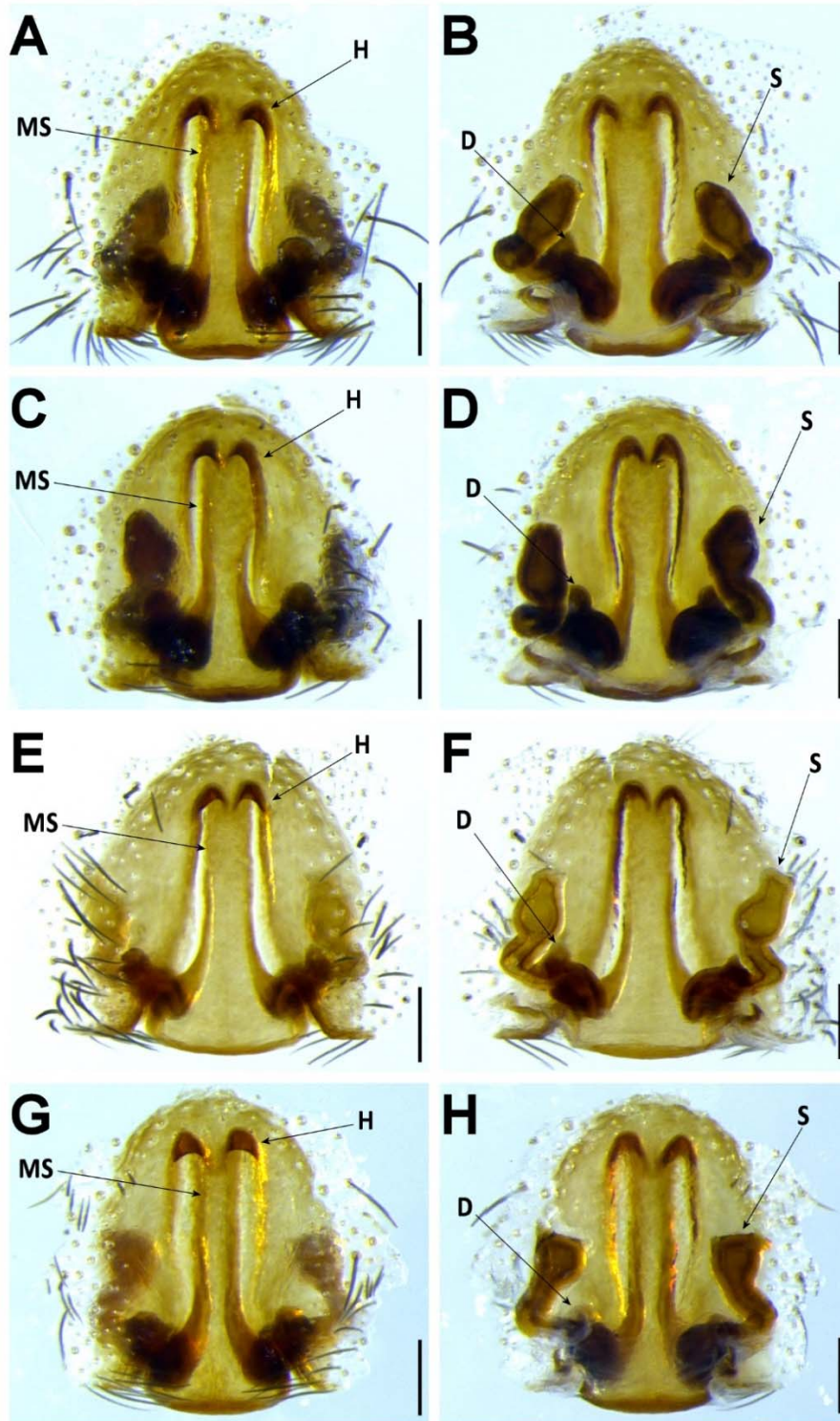
Figure 16. *H. insularum*, female genitalia. A–B, female from Bugio (CRBALC0301): A, epigynum, ventral; B, vulva, dorsal; C–D, female from Deserta Grande (CRBALC0308): C, epigynum, ventral; D, vulva, dorsal; E–F, female from Madeira (CRBALC0597): E, epigynum, ventral; F, vulva, dorsal; G–H, female from Porto Santo (CRBALC0300): G, epigynum, ventral; H, vulva, dorsal. Abbreviations, female genitalia: D – diverticulum, H – epigynal hoods, MS – median septum, S – spermatheca. Scale bars: A–H = 0.2 mm.
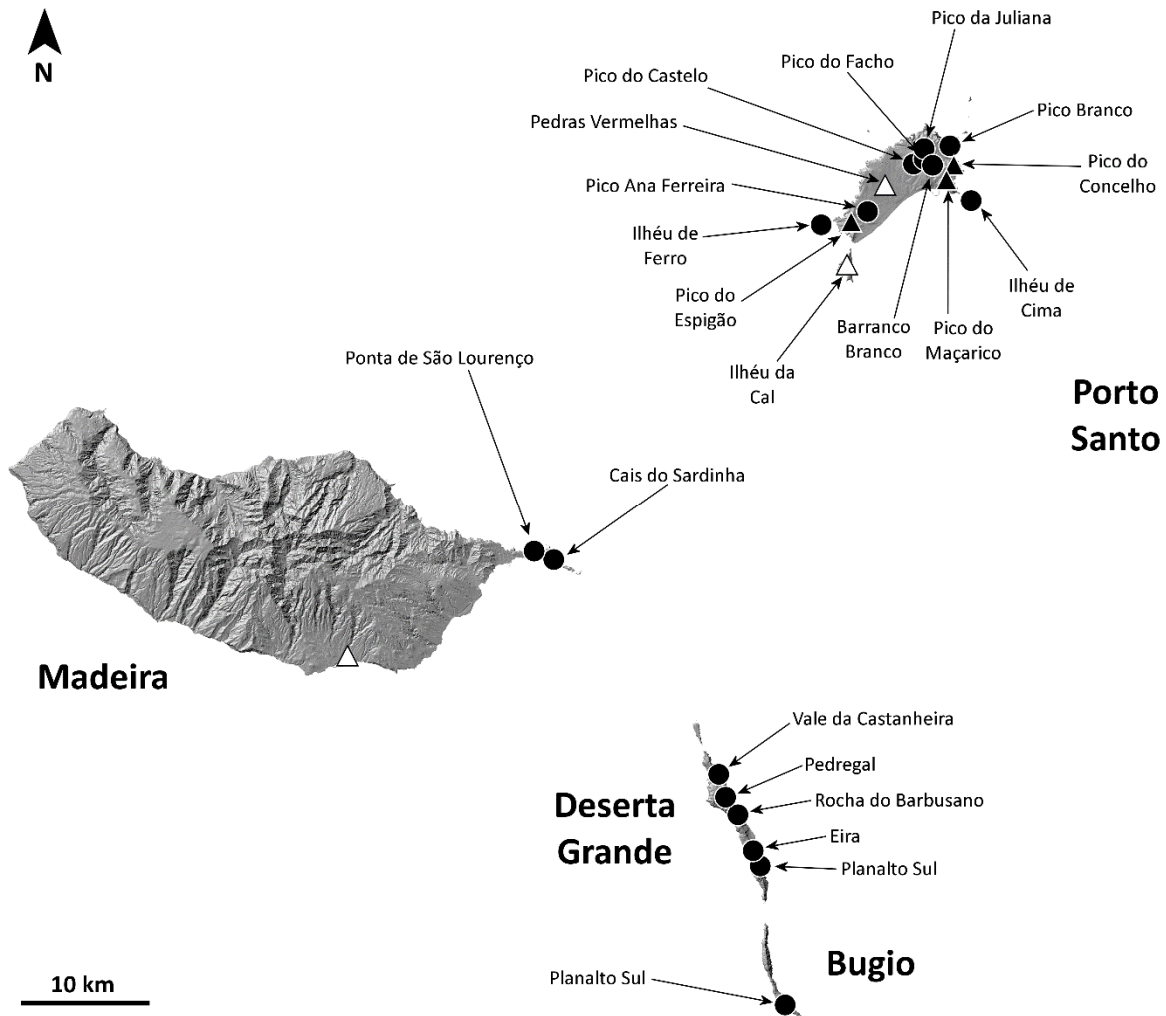
Figure 17. Distribution of *H. insularum*. Circles: present records; black triangles: revised records from literature; white triangles: unconfirmed records from literature.

Hogna isambertoi Crespo, sp. nov.

(Fig. 18–19)

Hogna heeri Crespo et al. 2013: 18. Wrong identification (m).

Holotype: DESERTA GRANDE • 1 ♂, Ponta Sul, coll. 4.XI.2017, leg. I. Silva, stored at SMF, collection number to be set after publication.

Paratypes: BUGIO • 1 ♂ (SMF), Planalto Sul, 3.XII.2012, hand collecting, leg. I. Silva. DESERTA GRANDE • Planalto Sul, 1 ♀ (SMF), 12.XI.2017, hand collecting, leg. I. Silva.

Additional material examined: DESERTA GRANDE • Planalto Sul, 1 juvenile (CRBALC0610: LC330), 12.XI.2017, hand collecting, leg. I. Silva.

Diagnosis: Hogna isambertoi sp. nov. can be distinguished from all other Madeiran *Hogna* by its genitalia. in males the tip of the embolus is tilted anteriorly (Fig. 18A, C). In females, the epigynal hoods show convergent lateral borders and the median septum has a wide base (Fig. 18D).

Description – Male holotype: (Fig. 18A–C). Total length: 7.36; carapace: 4.25 long, 3.2 wide.

Colour: carapace greyish-brown, covered with short black hairs, with a median yellow longitudinal band, anteriorly broadened, covered with short white hairs; two yellow marginal bands, suffused with grey patches, covered with short white hairs; four black striae well visible on each flank. Chelicerae yellow, with grey suffused patches, covered in black and white hairs. Gnathocoxae and labium overall pale yellow, with posterior margin with suffused grey patch; sternum pale yellow, with v-shaped grey patch. Legs pale yellow, with irregular grey suffused patches, except anterior metatarsi and tarsi, yellowish orange. Pedipalps yellow. Abdomen with a pair of anterolateral black patches, extending laterally into grey to black flanks; a median faint dark lanceolate patch is bordered by two yellowish longitudinal bands interconnected in anterior half, posteriorly by means of dark chevrons; venter yellowish, with large blackish patches near spinnerets and small patches medially.

Eyes: MOQ: MW = 0.78 PW, MW = 1.08 LMP, MW = 1.17 AW; Cl = 0.53 DAME. Anterior eye row slightly procurved.

Legs: Measurements: Leg I: 11.67, TiI: 2.63; Leg IV: 13.83, TiIV: 2.75; TiIL/D: 6.6. Spination of Leg I: FeI: d1.1.1, p0.0.1; TiI: p1.0.1, v2l.2l.2s; MtI: p0.0.1, r0.0.1, v2l.2l.1s. MtI with sparse scopulae in basal half and dense scopulae on distal half.

Pedipalp: cymbium with 1 spine along prolateral rim and 5 dark, stout, macrosetae at tip, Fe with 2 dorsal and an apical row of 4 spines. Median apophysis with basal spur truncate, blunt and tip thin, blunt; terminal apophysis with proximal branch in close apposition with terminal branch, blade-shaped with blunt end; embolus long, with tip tilted anteriorly; palea small.

Female paratype: (Fig. 18D–E). Total length 12.06; carapace: 4.7 long, 3.6 wide.

Colour: overall as in male, but darker in legs, chelicera and prosoma, where additional faint striae are present. Abdomen is lighter, with central chevrons faded, possibly due to pregnancy and correspondent tegument extension.

Eyes: MOQ: MW = 0.78 PW, MW = 1.2 LMP, MW = 1.17 AW; Cl = 0.35 DAME. Anterior eye row slightly procurved.

Legs: Measurements: Leg I: 9.93, TiI: 1.72; Leg IV: 12.99, TiIV: 2.56; TiIL/D: 3.19. Spination of Leg I: FeI: d1.1.0, p0.0.1–2; TiI: p0.0.0–1, v2l.2l.2s; MtI: p0.0.1, r0.0.1, v2l.2l.1s. MtI with sparse scopulae in basal half and dense scopulae on distal half.

Epigynum: hoods touching, short, with lateral borders parallel; hood cavities deep; median septum with wide base; spermathecae oval; copulatory ducts simple; fertilisation ducts emerging at the base of copulatory duct.

Etymology: the specific epithet is a patronym in honour of Isamberto Silva, who not only collected the only known specimens of this species,but has provided an invaluable support in field work.

Intraspecific variation: Carapace length, males: 4.1–4.25.

Distribution: This species is known only from the southernmost part of Deserta Grande and Bugio (Fig. 19).

Ecology: H. isambertoi sp. nov. occurs in arid, coastal scarps, with reduced vegetation cover.

Conservation status: the species seems to be restricted to a very small area, equivalent to an Extent of Occurrence and Area of Occupancy of 8 km^2 in two locations, both threatened by the effects of increasing aridification. The trends are unknown, but it is uncertain if the scarcity of specimens is due to rarity, or the fact that it seems to be a late autumn / early winter species, when collecting effort has been low. If the decline is confirmed the status might be Endangered, if not it might be Near Threatened.

Figure 18. *H. isambertoi* sp. nov. A–C, male (SMF): A, left male palp, ventral; B, detail of the median apophysis, anteroventral; C, SEM image, right male palp, ventral. D–E, female (SMF): D, epigynum, ventral; E, vulva, dorsal. Abbreviations, male palp: C – cymbium, E – embolus, MA – median apophysis, P – palea, T – tegulum, TA – terminal apophysis. Abbreviations, female genitalia: D – diverticulum, H – epigynal hoods, MS – median septum, S – spermatheca. Scale bars: A = 0.5 mm, B–E = 0.2 mm.

Figure 19. Distribution of *H. isambertoi* sp. nov. Circles: present records; black triangle: revised record from literature.

Hogna maderiana (Walckenaer, 1837)

(Figs 20–22)

Lycosa tarentuloides maderiana Walckenaer, 1837: 291 (Df).

Lycosa tarentuloides maderiana Blackwall, 1857a: 282 (Dm).

Tarentula maderiana Simon, 1864: 350.

Lycosa maderiana Simon, 1898: 346.

Trochosa maderiana Kulczynski, 1899: 426, pl. 9, f. 119-120 (mf).

Isohogna maderiana Roewer, 1955: 241.

Isohogna maderiana Roewer, 1960: 569, f. 319a-c (mf).

Hogna schmitzi Wunderlich, 1992: 462, f. 721-723 (Dmf).

Holotype: Not examined, supposed lost.

Additional material examined: ILHÉU DE FERRO • 1 ♂ and 1 ♀ (SMF37637), 3.VII.1983, leg. K. Groh., 1 ♂ (CRBALC0013), 6.IV.2011, hand collecting, leg. I. Silva. PORTO SANTO • Pico Branco, 1 ♂ (CRBALC0734) and 2 ♀♀ (CRBALC0704, CRBALC0717), 10.IV.2018, hand collecting, leg. L. Crespo & A. Bellvert; Pico do Facho, 1 ♂ (SMF63869), 31.X.1972; (unknown location), 2 ♀♀ and 2 juveniles (FMNH http://id.luomus.fi/KN.23945), 4.X.1959, 1 ♀ (SMF34482), VII.1983, 1 ♀ (SMF36760), 26.X.1985, leg. G. Schmidt, 1 ♂ (SMF37639), 8–
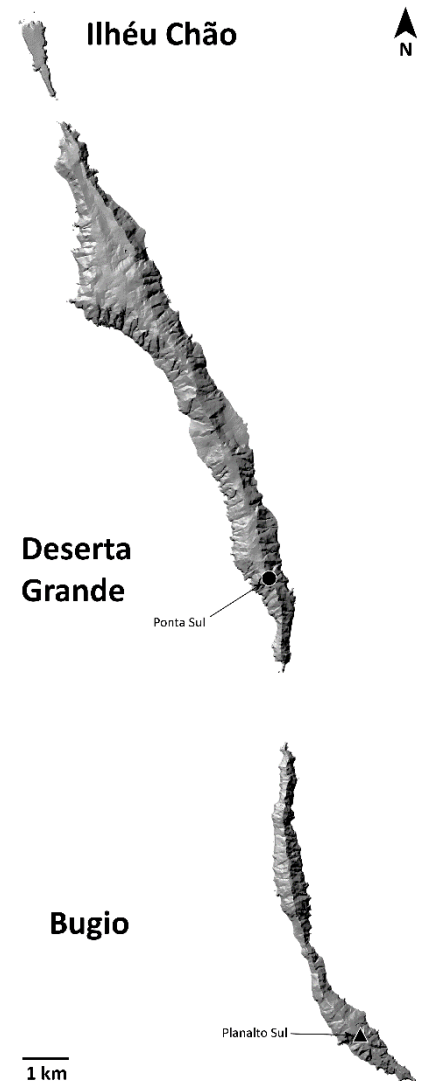
11.VII.1983, 1 ♀ (SMF37636) and 2 juveniles (SMF37638), leg. K. Groh, 8 ♂♂ and 11 ♀♀ (BM, in ethanol), VI.1962, leg. S.W. Bristowe, 1 ♀ (BM), VII.1963, leg. B.M. Cliffton, 2 ♂♂ and 2 ♀♀ (BM 1892.7.9.12.17), leg. W.R.O. Grant, 1 ♀ (BM), 12.VI.1964, 1 ♂ and 1 ♀ (BM, mounted dry).

Diagnosis: Hogna maderiana can be distinguished from all other Madeiran *Hogna* by a combination of the following characters: the large size (prosoma length > 10 mm), the aspect of its legs, with conspicuous orange hairs (Fig. 26A), and its genitalia. In males by a combination of a smoothly curved tip of the embolus and a notorious tegular concavity (Fig. 20A–D). In females by epigyne with median septum more than twice as long as wide (at base) (Fig. 20E–F).

Redescription – Male (*CRBALC0734):* (Fig. 20D–E). Total length: 19.54; carapace: 11.88 long, 8.9 wide.

Colour: carapace brown, with short black hairs covering flanks, short white hairs present posteriorly, anteriorly and laterally, long black hairs are present anteriorly or scattered around median band; median yellow longitudinal band present but faint, covered with short white hairs and scattered long black hairs, anteriorly broadened; marginal bands indistinct, made apparent only by the cover of short white hairs, long black hairs also present laterally; four darker lateral bands visible, but without striae. Chelicerae black, apically dark brown, covered in black and yellow hairs. Gnathocoxae very dark orange brown, labium blackish; sternum brown, medially lighter, but without any stripe. Legs brown, without annulations, with anterior tibiae, all metatarsi and tarsi dark brown, and covered dorsally with yellow hairs (probably orange in living or fresh specimen). Palpal femur, patella and tibia as legs, cymbium darker, yellow hairs present in all segments except femur. Abdomen with a pair of anterolateral black patches, extending laterally into grey flanks; a median yellow lanceolate patch is bordered by few whitish patches; venter greyish, darker near spinnerets.

Eyes: MOQ: MW = 0.73 PW, MW = 1.15 LMP, MW = 1.2 AW; Cl = 0.48 DAME. Anterior eye row slightly procurved.

Legs: Measurements: Leg I: 36.71, TiI: 8.75; Leg IV: 37.27, TiIV: 8.1; TiIL/D: 4.38. Spination of Leg I: FeI: d1.1.0, p0.0.2; TiI: p1.0.1, r1.0.0, v2s.2s.2s; MtI: p0.0.1, r0.0.1, v2s.2s.1s. MtI with very dense scopulae.

Pedipalp: cymbium with 1 prolateral spine and 6 dark, stout, macrosetae at tip, Fe with 2 dorsal and an apical row of 4 spines, Pa with 1 prolateral spine, Ti with 1 dorsoprolateral spine and 1 prolateral spine. Median apophysis with basal spur truncate, blunt, and with tip thin, blunt; terminal apophysis blade-shaped with sharp end; embolus long, with tip directed anterolaterally; palea small.

Female (CRBALC0717): (Fig. 20E–F). Total length 23.54; carapace: 11.25 long, 8.25 wide.

Colour: overall as in male, with the following differences: median yellow longitudinal band in prosoma clear. Cheliceral hairs black. Legs with few faint greyish patches in femora. Abdominal pattern overall greyish, darker near spinnerets, with patches unapparent.

Eyes: MOQ: MW = 0.7 PW, MW = 1.1 LMP, MW = 1.2 AW; Cl = 0.4 DAME. Anterior eye row slightly procurved.

Legs: Measurements: Leg I: 30.25, TiI: 7.16; Leg IV: 33.86, TiIV: 7.36; TiIL/D: 3.53. Spination of Leg I: FeI: d1.1.0, p0.0.2; TiI: 0.1s.0, v2s.2s.2s; MtI: p0.0.1, r0.0.1, v2l.2s.1s. MtI with very dense scopulae.

Epigynum: hoods touching, short, with lateral borders parallel; hood cavities deep; median septum with narrow base; spermathecae elongated; copulatory ducts with very small diverticulum ventrally; fertilisation ducts emerging at the base of copulatory duct.

Intraspecific variation: Carapace length, males: 11.88–14.38, females: 11–11.5.

Distribution: This species is known from the island of Porto Santo and one of its surrounding islets, Ilhéu de Ferro (Fig. 22).

Ecology: H. maderiana can be found in open habitats, such as grasslands, shrubland or sand banks.

Conservation status: H. maderiana was assessed according to the IUCN Red List criteria as *H. schmitzi* (Cardoso et al. 2018d), with the status of Least Concern.

Comments: As mentioned above (see remarks on *H. blackwalli* sp. reval.), the large specimens with striking orange coloration in legs from Porto Santo island and its neighboring islet Ilhéu de Ferro were known by pioneer arachnologists. The original, somewhat obscure, description by Walckenaer described a 2.5 cm spider ("1 pouce") with reddish-brown legs (Pattes rouges, lavées de brun en dessus (…)"), from the island of Madeira ("Ile de Madère"). After this, Blackwall was the first to provide a clear description of this taxon, while at the same time stating that it was collected in the island of Porto Santo, not Madeira. Subsequent authors reported additional materials from either Porto Santo or Ilhéu de Ferro (Johnson 1863; Kulczynski 1899). Wunderlich considered *H. blackwalli* a junior synonymy of *H. maderiana* based on the wrong assumption that previous authors repeatedly misidentified *H. maderiana* from Porto Santo, assigning *H. maderiana* to the large species with annulated legs from Madeira island. Following synonymy, Wunderlich himself named the large species from Porto Santo as *H. schmitzi*. As a matter of fact, the only indication of the presence of a large spider with reddish coloration in legs in Madeira island is Walckenaer's original description. Unfortunately, Walckenaer's type seems to be lost. However, Simon most likely examined it, because he stated that "*L. maderiana* Walck. est, en grande partie, revêtu, en dessus, de pubescence courte d'un beau rouge orange." (Simon 1898: 332). The two large species are easy to distinguish, the only misidentification between them being made by Thorell, who identified *H. blackwalli* from Madeira as *Trochosa maderiana* (Thorell 1875). We argue that the presence of *H. maderiana* in the island of Madeira reported in Walckenaer's original description was likely a labelling mistake or a misinterpretation, and probably referred to the archipelago.
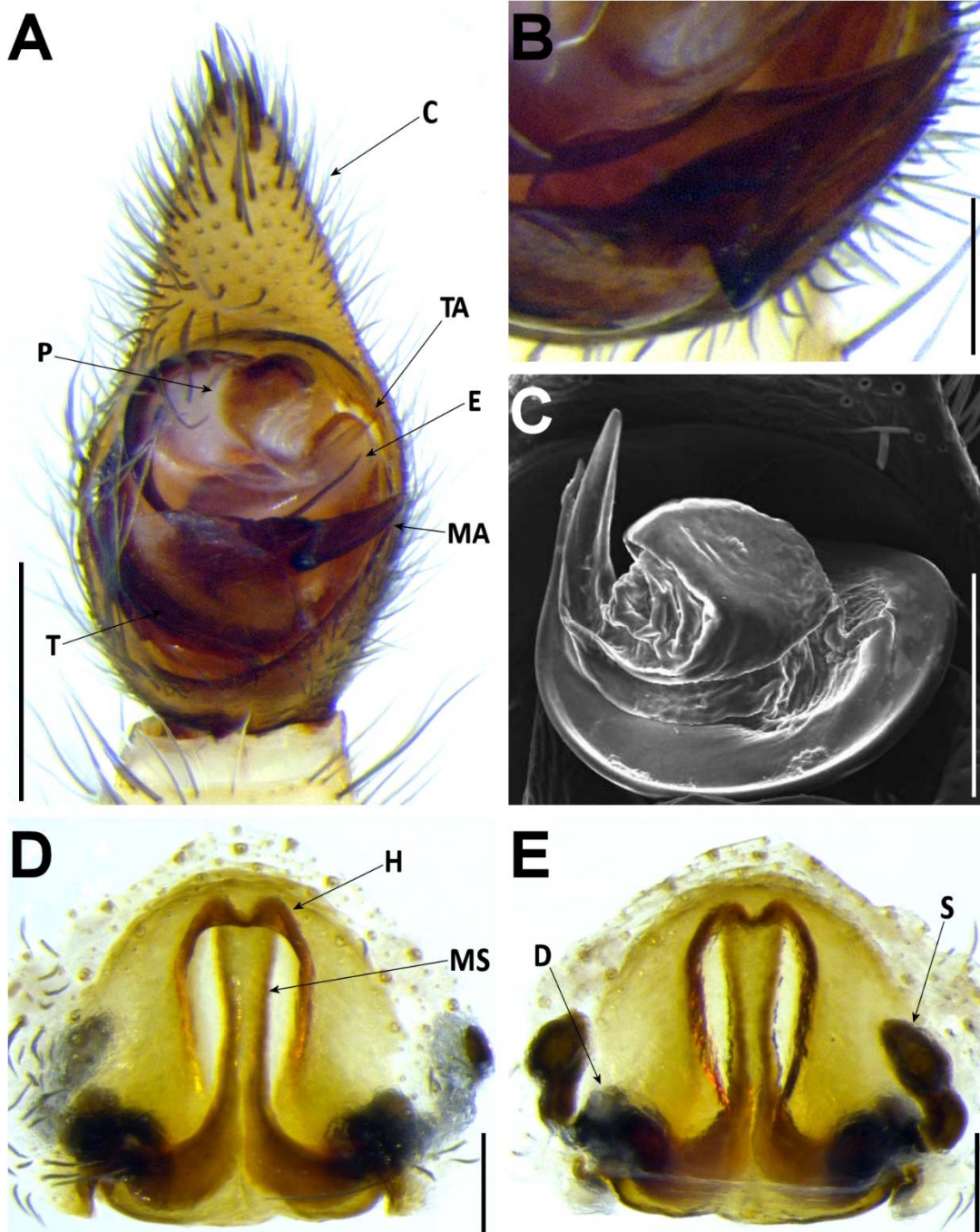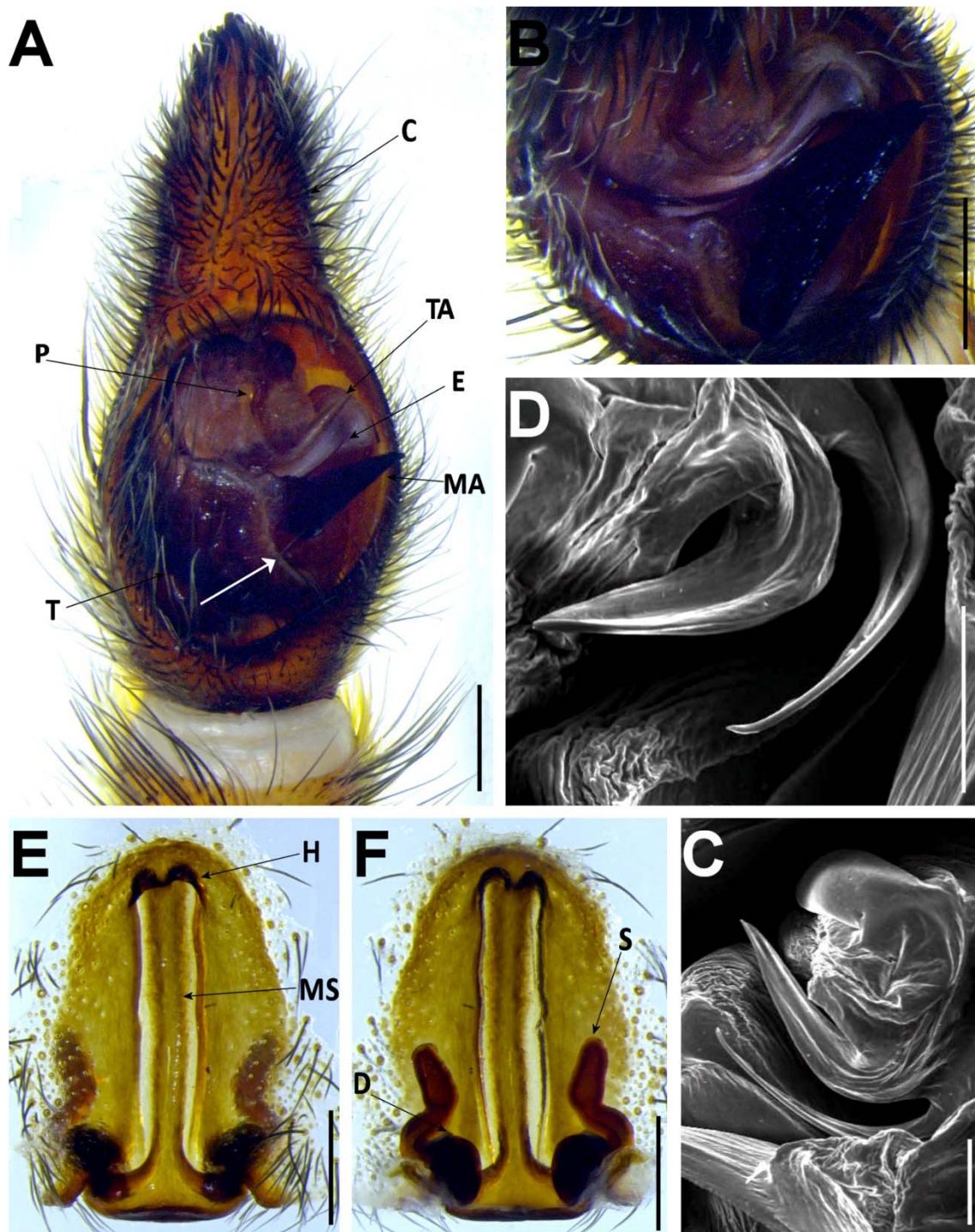
Figure 20. H. maderiana. A–C, male (CRBALC0734): A, left male palp, ventral; B, detail of the median apophysis, anteroventral; C, SEM image, right male palp, ventral; D, idem, retroventral. E–F, female (CRBALC0717): E, epigynum, ventral; F, vulva, dorsal. Abbreviations, male palp: C – cymbium, E – embolus, MA – median apophysis, P – palea, T – tegulum, TA – terminal apophysis. Abbreviations, female genitalia: D – diverticulum, H – epigynal hoods, MS – median septum, S – spermatheca. Scale bars: A–B, E–F = 0.5 mm, C–D = 0.2 mm.

Figure 21. Photo of *H. ingens*. Female specimen in the field. Photo credit: Pedro Cardoso.
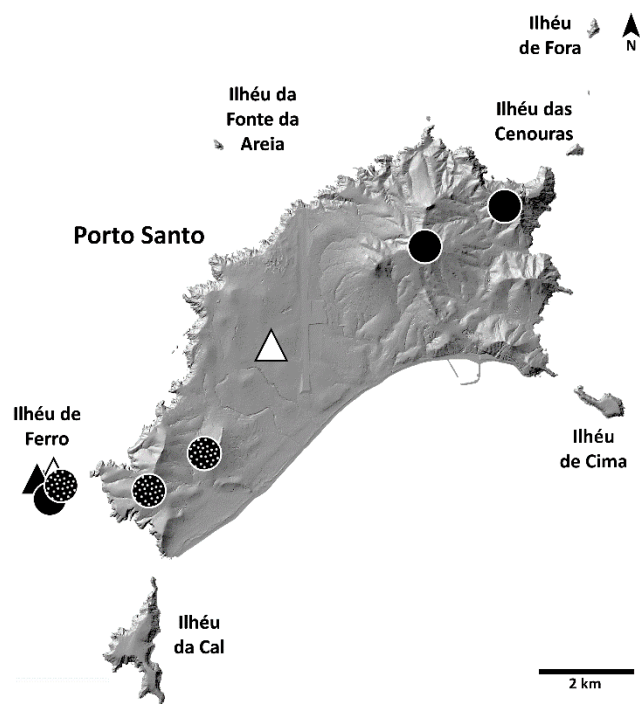
Figure 22. Distribution of *H. maderiana*. Black circles: present records; dotted circles: records from only leg samples; black triangles: revised records from literature; white triangles: unconfirmed records from literature.

Hogna nonannulata Wunderlich, 1995

(Fig. 23–24)

Holotype: MADEIRA • 1 ♂, coll. 25–30.IV.1957, leg. Roewer, stored at SMF, collection number 10754. Examined.

Additional material examined: MADEIRA • Câmara de Lobos, 1 ♂ (CRBALC0703: LC326), 27.V.2018, hand collecting, leg. É. Pereira, 1 ♂ (CRBALC0701: LC325, CRBALC0702: LC324), 29.V.2018, hand collecting, leg. I. Silva & É. Pereira, 1 ♂ (CRBALC0608: LC328), 21.VI.2017, hand collecting, leg. I. Silva, 1 ♂ (CRBALC0607: LC327), 11.VIII.2017, hand collecting, leg. I. Silva.

Diagnosis: Hogna nonannulata can be distinguished from all other Madeiran *Hogna* by the aspect of its legs, without annulations, but bearing yellow or orange patches of hairs (Fig. 23D). In addition, males have a clearly excavated terminal apophysis in the embolus (Fig. 23A, C). We could not revise any female materials, for which we propose that the leg aspect can be used to diagnose females.

Redescription – Male (CRBALC0701): (Fig. 23). Total length: 18.62; carapace: 10.31 long, 8.2 wide.

Colour: carapace greyish brown with transverse yellowish bands, generally covered with short black hairs, except anteriorly and laterally, where short white hairs and long black hairs are present; median yellow longitudinal band present, anteriorly broadened, with suffused greyish brown patches; two yellow marginal bands, suffused with greyish brown patches; ca. 7 faint blackish striae on each flank. Chelicerae blackish to dark brown, covered mostly in black and white hairs. Gnathocoxae very dark orange brown, labium blackish; sternum yellowish grey, with a faint, longitudinal yellow stripe extending to less than half of sternum length. Legs yellow to brown, without any clearly coloured patch, just scattered areas suffused with grey, grey hairs present in tibia, metatarsus and tarsus. Palpal femur, patella and tibia yellow, except cymbium, brown. Abdomen with both short and long black hairs, additionally with short greyish white hairs; with a pair of anterolateral faint blackish patches, extending laterally into grey flanks, interspersed with greyish white patches; a median greyish

lanceolate patch is bordered by two yellowish longitudinal bands interconnected in anterior half, posteriorly by means of faint dark chevrons; venter yellowish except around spinnerets, dark grey, with small blackish patches scattered laterally.

Eyes: MOQ: MW = 0.78 PW, MW = 1.18 LMP, MW = 1.3 AW; Cl = 0.65 DAME. Anterior eye row slightly procurved.

Legs: Measurements: Leg I: 40.94, TiI: 10.75; Leg IV: 42.98, TiIV: 9.8; TiIL/D: 8.77. Spination of Leg I: FeI: d1.1.0, p0.0.2; TiI: p1.0.1, v2s.2s.2s; MtI: p1.0.1, r1.0.1, v2s.2s.1s. MtI with very dense scopulae.

Pedipalp: cymbium with 2 prolateral spines, one basal, the other at rim, apically with ca. 4 dark macrosetae, Fe with 2 dorsal and an apical row of 4 spines, Pa with 1 prolateral spine, Ti with 1 dorsal, 1 dorsoprolateral spine and 1 prolateral spine. Median apophysis with basal spur truncate, blunt, and with tip stout, blunt; terminal apophysis with proximal branch separated from terminal branch due to a well-visible excavation, blade-shaped with sharp end; embolus moderately elongated, with tip directed anteriorly; palea small.

Female: We could not revise any female materials.

Intraspecific variation: Carapace length, males: 7.2–11.25. Smaller males have proportionally longer tibial spines than longer males.

Distribution: This species is known from the Southern coastal area of Camara de Lobos in the island of Madeira (Fig. 24).

Ecology: H. nonannulata can be found in coastal shrub- or grassland and rocky areas.

Conservation status: It was not previously possible to assess *H. nonannulata* according to the IUCN Red List criteria given the scarcity of past information, hence a status of Data Deficient was suggested (Cardoso et al. 2018c). Its known distribution is now limited to the area of Camara de Lobos in the Southern coast of Madeira Island, an area with no remaining natural habitat beyond the rocky areas. With an EOO and AOO of 4km^2 and a single location threatened by urban and agricultural pressure, if the trend of the species is negative its status might be Critically Endangered.
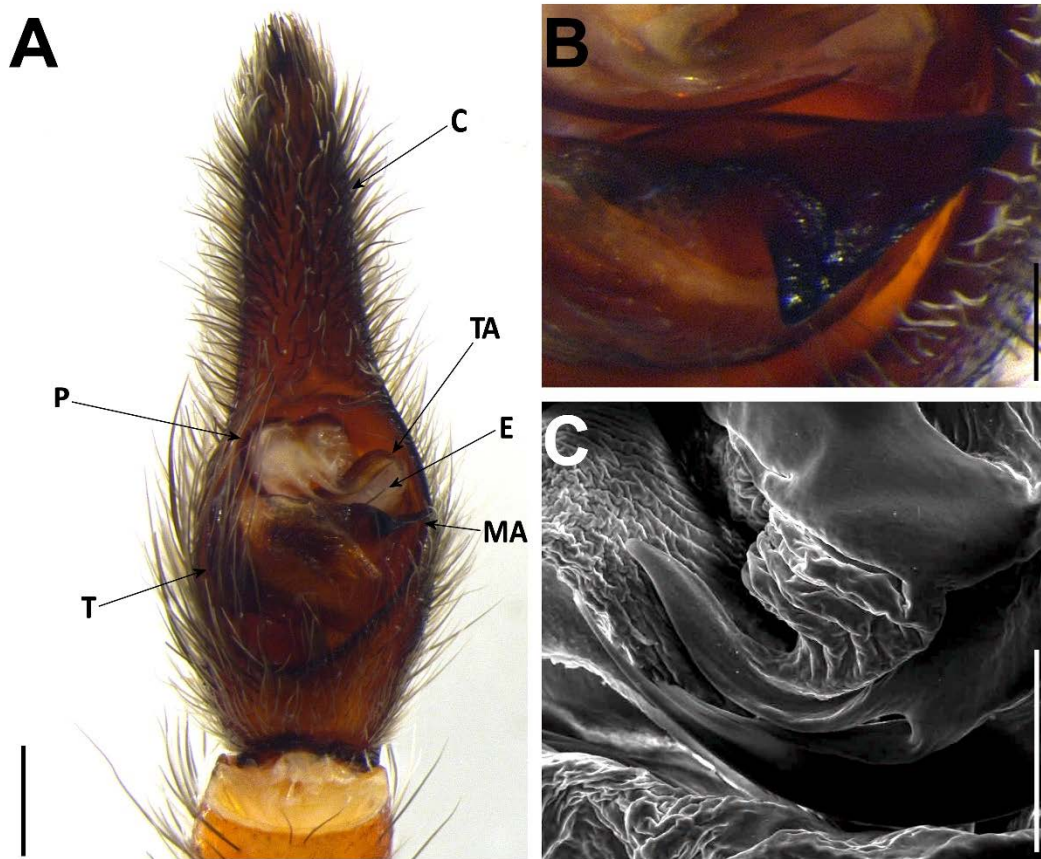
Figure 23. *H. nonannulata*. A–C, male (CRBALC0701): A, left male palp, ventral; B, detail of the median apophysis, anteroventral; C, SEM image, right male palp, ventral. Abbreviations, male palp: C – cymbium, E – embolus, MA – median apophysis, P – palea, T – tegulum, TA – terminal apophysis. Scale bars: A = 0.5 mm, B–C = 0.2 mm.
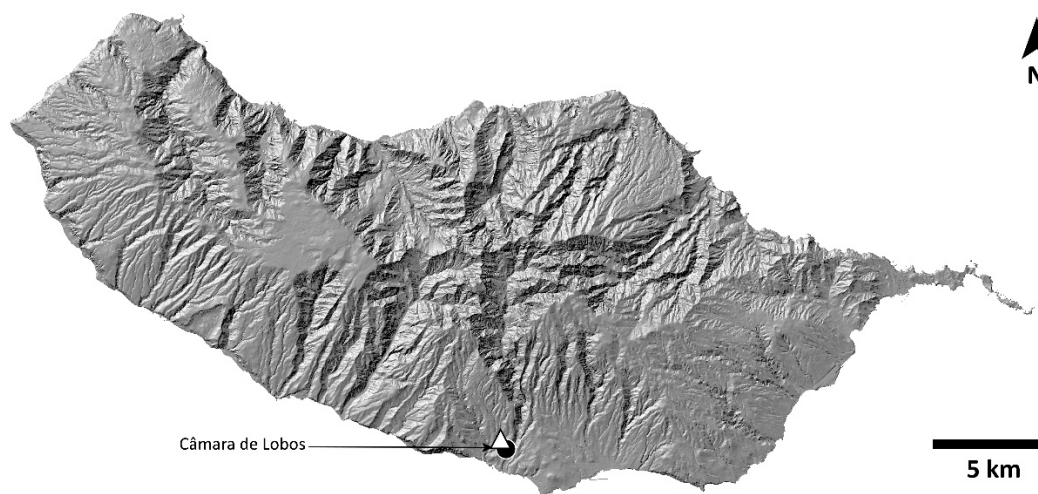
Figure 24. Distribution of *H. nonannulata*. Black circle: present record; white triangle: unconfirmed record from literature.

Key to the *Hogna* species endemic to the Madeira Archipelago

1. Species from Porto Santo.   2

   Species from Madeira.   3

   Species from Desertas.   6

2. Large species (prosoma length > 10 mm), legs furnished with orange hairs (Fig. 26A).   *H. maderiana*

   Small to medium species (prosoma length < 10 mm), legs with whitish hairs (Fig. 26C).

   H. insularum

3. Legs with a small, bright yellow patch of hairs at joints of anterior metatarsus and palp (Fig. 25A).   *H. blackwalli*

   Species without bright yellow patches of hairs in anterior legs.   4

4. Legs without any reticulated or annulated pattern (Fig. 25D).   *H. nonannulata*

   Legs with reticulated or annulated pattern.   5

5. Male with straight embolus (Wunderlich 1992: 595, Fig. 720). Female epigynal hoods with highly divergent lateral borders (Fig. 9A). Species from montane habitats.   *H. heeri*

   Male with embolus smoothly curved (Fig. 15). Female epigynal hoods with parallel lateral borders (Fig. 16C). Species from southeastern coastal grassland habitats   *H. insularum*

6. Very large species (prosoma length > 14 mm). Black legs with white patches (Fig. 25C).*H. ingens*

   Smaller species (prosoma length < 10 mm).   7

7. Male palp smoothly curved (Fig. 17). Female epigyne with median septum roughly half as wide (at base) as long (Fig. 16 A, C, E, G).   *H. insularum*

   Male palp straight or with only tilted tip. Female epigyne with median septum almost as wide (at base) as long (Figs 9A–B, 18D–E).   8

8. Male palp with embolus with tip tilted anteriorly (Fig. 18A, C). Female epigynal hoods with convergent lateral borders (Fig. 18D).   *H. isambertoi* sp. nov.

Male palp with straight embolus (Wunderlich 1992: 595, Fig. 720). Female epigynal hoods with highly divergent lateral borders (Fig. 9A). *H. heeri*
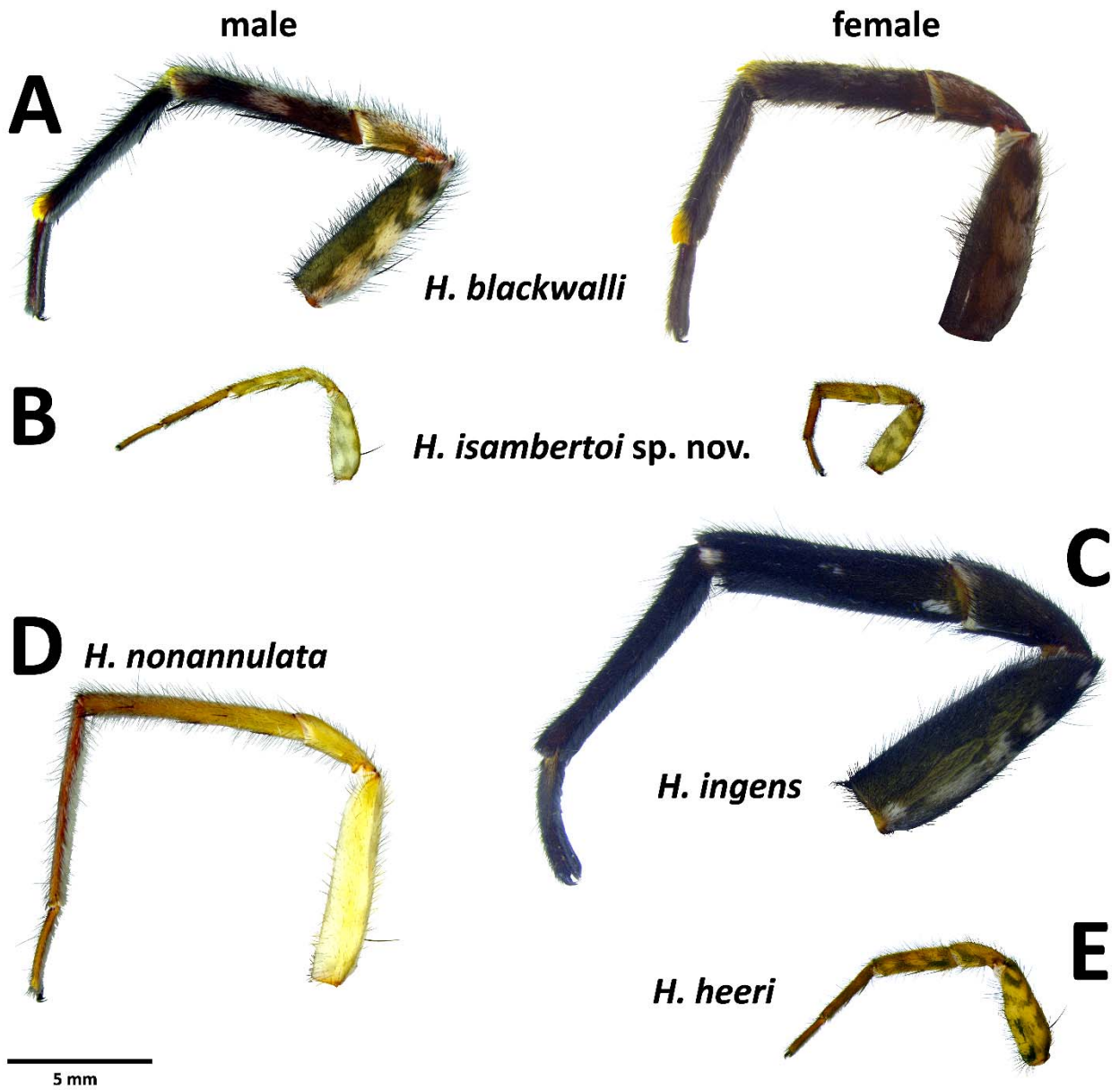
Figure 25. Plate with photographs of the lateral view of the tibia I for easily diagnosable species.

male female

A

H. maderiana

B

unidentified
specimens

C

H. insularum

5 mm
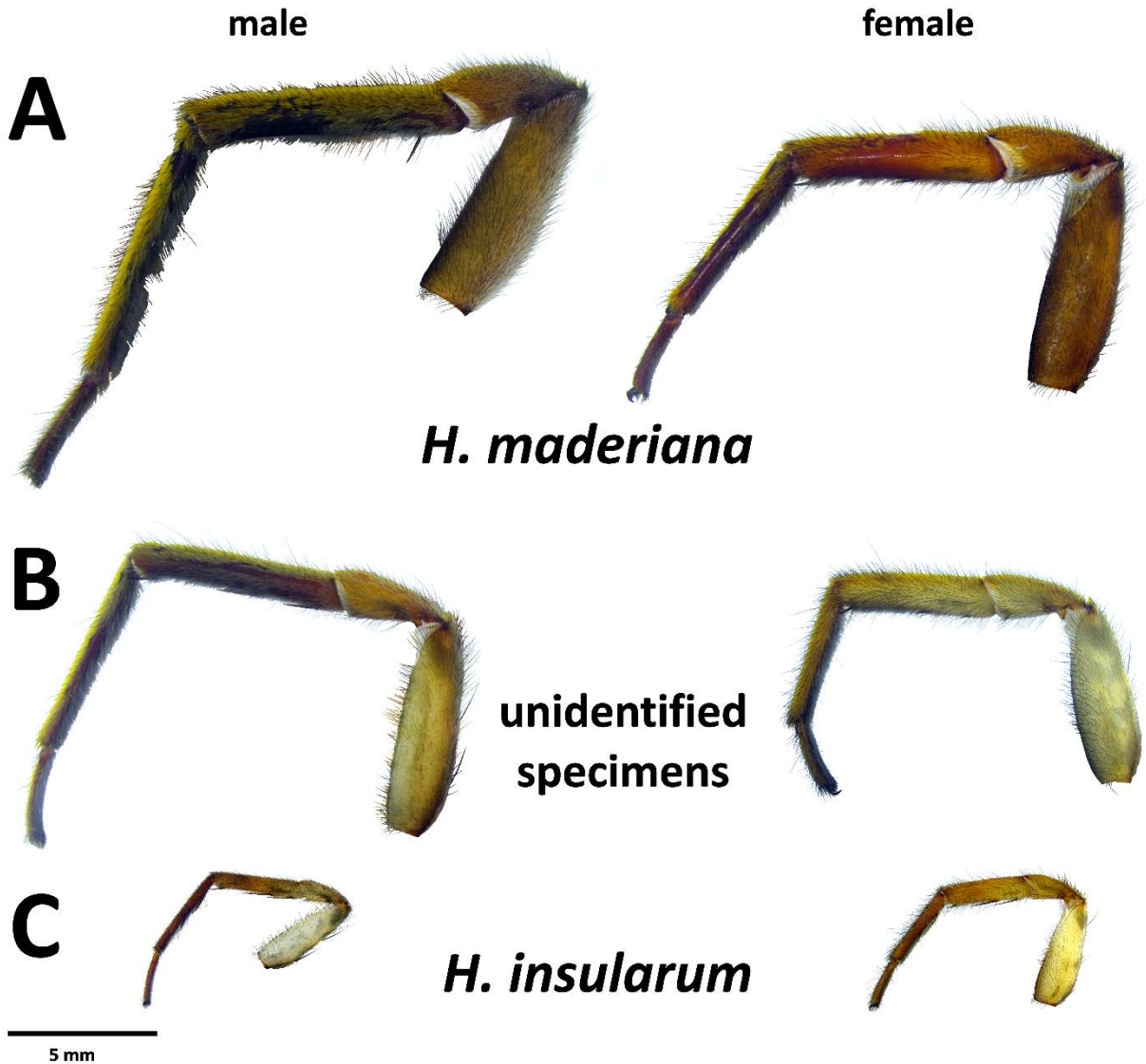
Figure 25. Plate with photographs of the lateral view of the tibia I for the complex of *H. maderiana, H. insularum* and their intermediate forms.

Discussion

Origins of Madeiran *Hogna*

Our analyses support the long-standing view that the genus *Hogna* is a paraphyletic assemblage in much need of a through taxonomic revision that establishes its limits and diagnosis. Unfortunately, only 18 species of *Hogna* were represented by at least one DNA sequence in public repositories, out of the 228 currently valid species and subspecies,

excluding Madeiran ones (World Spider Catalog 2021: accessed 26 Apr 2021). Albeit with low support, our results suggested a strong geographic component in the phylogenetic relationship of *Hogna* species, recovering mixed genera clades from the same region (e.g. North America, South America or Australia). Madeiran species were consistently recovered by all analyses as closely related to the type species of the genus, *H. radiata*, represented in the analyses by specimens form the Iberian Peninsula, yet poorly supported. Although our sampling is far from being representative of the *Hogna* diversity in the Western palearctic (only 2 species out of 45 described were included), the results are congruent with the Iberian Peninsula as a colonization source of Madeiran species. This biogeographic connexion has been recently confirmed for the endemic Madeiran species of the spide genus *Dysdera*, and was most likely favoured by the predominant aerial and marine currents in the region (Crespo et al. 2020).

Our time estimates suggest a colonization of the archipelago by the late Miocene (but note the large confidence intervals recovered). Interestingly, this sub-epoch coincides with an episode of major global cooling that brought about dramatic changes in the ecosystems, which included the expansion of grasslands and the associated fauna (see Herbert et al. 2016 and references therein). The increase in the amount of habitat type preferred by wolf spider may have facilitated the expansion and diversification of lycosids into the Mediterranean region and eventually the colonization of the Madeiran Archipelago. In this regard, it is worth to mention that the origin of the western Mediterranean species of the other genus of large wolf spiders, *Lycosa* Latreille, 1804, seems also to trace back to the late Miocene (Planas et al. 2013).

Model-based analyses recovered the monophyly of all Madeiran endemics, which would suggest a single colonization event of the archipelago. This result was disputed by parsimony analysis, which suggested at least two different events by placing the mainland *H. radiata* as sister to the *ingens*-clade. None of these alternative arrangements, however, received high support. Conversely, the existence of two well-defined lineages, the *ingens* and *maderiana*-clades, were supported in all analyses. Interestingly, our analyses also pointed out to another case of multiple colonisations of another volcanic archipelago, the Galapagos Islands. Up to seven endemics species are know from this Pacific archipelago, which include species adapted to habitats at different altitude (Baert et al. 2008). All our analyses supported

the independent colonisation of the Galapagos by at least two or even three different ancestors, one of which resulted in local diversification. Multiple island colonisation should not be unexpected in wolf spiders, given their good dispersal ability and frequent use of ballooning (Richter 1970, Greenstone 1982, Bonte and Maelfait 2001, Bonte et al. 2006).

Regardless of the actual number of colonisations, *Hogna* underwent processes of local diversification, as illustrated by the *ingens*-clade. Similarly, to what has been observed in endemic *Hogna* from the Galapagos (Busschere et al. 2010), Madeiran endemics show a certain ecological differentiation associated to elevation, some species are found in montane habitats (*H. heeri*, *H. blackwalli* sp. reval. and *H. ingens*), while other are mostly found in coastal areas (*H. isambertoi* sp. nov. and *H. nonannulata*). Body size is another functional trait with a noticeable variation across Madeiran *Hogna*, *H. ingens* and *H. maderiana* can be considered giant species for *Hogna* standards (>10 mm of carapace length), while *H. blackwalli* sp. reval. (7.3–10.4mm) and *H. nonannulata* (7.2–11.2mm) are medium-large, and *H. insularum* (4.1–4.7mm), *H. heeri* (5.2–5.8mm) and *H. isambertoi* sp. nov. (4.1–4.7mm) are small. Often sympatric species have disparate size, as is the case in Porto Santo with *H. maderiana* and *H. insularum,* or in Deserta Grande with *H. ingens* and *H. insularum*, or even in Madeira with *H. blackwalli* sp. reval. and *H. heeri.* Yet, it also occurs that in Deserta Grande (only in South end) two very similar species, *H. insularum* and *H. isambertoi* sp. nov. share the same habitat. And in Bugio island, an even smaller and steeper island than Deserta Grande, the three small species of the archipelago, *H. heeri, H. insularum* and *H. isambertoi* sp. nov., are found together. Interestingly, the few specimens available of *H. isambertoi* sp. nov. and the single specimen of *H. heeri* from Bugio were all collected in late autumn, which might indicate phenological displacement against the spring-dominant *H. insularum*.

Within the *ingens*-clade, the only well-supported sister group relationship is between *H. blackwalli* sp. reval. and *H. nonannulata*, which represents a nice example of ecological shift within the same island, from the ancestral open habitat represented by the coastal species *H. nonannulata,* to the laurel forest habitats inhabited by *H. blackwalli* sp. reval. More detailed natural history and ecological information will be required to rigorously test the role of habitat shifts in the diversification of *Hogna* in Madeira, as well as to determine instances

of parallel evolution in habitat and functional traits, as has been reported in *Hogna* in the Galapagos Is. (Busschere et al. 2010, De Busschere et al. 2012).

Hogna insularum and *H. maderiana*: one or two species?

The species pair *H. insularum* and *H. maderiana* poses a taxonomic and evolutionary conundrum. Our molecular data was unable to establish boundaries between the large specimens of *Hogna* from the island of Porto Santo showing orange pilosity, identified using traditional diagnoses as *H. maderiana*, and the smaller specimens, without the referred pilosity, identified as *H. insularum*. Re-examination of morphological data suggested the existence of a continuum of phenotypic traits between the two extremes represented by specimens univocally referred as either *H. maderiana* or *H. insularum*. Several specimens of intermediate size in Porto Santo (Figs 27–28) showed clear yellowish to orange pilosity in anterior legs (colour fades to yellow after depositing specimen in ethanol), but not as dense as in the larger specimens. Furthermore, we were able to spot the usual dark reticulate pattern on the legs of these specimens, unlike in the large specimens, which are dark, bearing no traces of reticulated patterns (Fig. 26). We considered these specimens tentatively as "unidentified" (sp.). At the other extreme, the smaller specimens from Porto Santo, putatively identified as *H. insularum*, lacked orange hairs, but showed yellowish to whitish hairs. Certainly, although a remarkable size difference stands between the smallest specimens identified as *H. insularum* and the largest specimens identified as *H. maderiana*, similar wide intraspecific variation in size has been observed in other *Hogna* species, for example the Mediterranean species *H. radiata* (Latreille, 1817), which may range in size from 10 to 25 mm (Moya-Laraño, personal communication). Regarding male genitalic characters, Wunderlich (Wunderlich 1992) proposed that the presence of a concavity in the tegulum as diagnostic trait for *H. maderiana*. This trait is readily apparent in the large specimen we photographed (Fig. 20A, white arrow), but not in the unidentified specimens of intermediate size (Fig. 27). This feature, however, could be the result of a mechanical constraint associated to the role of the tegulum in supporting the median apophysis in large specimens. Similarly, although the embolus is usually smoothly curved in both *H. maderiana* and *H. insularum*, the actual degree of curvature may also vary across specimens (e.g., specimen CRBALC0328 bears a straighter embolus compared to other specimens, Fig. 27A). On the other hand, the SEM imaging

revealed the presence in the embolic area of *H. insularum* (specimen CRBALC0310, from Porto Santo, Fig. 15E–F) of the loose membranous proximal branch of the terminal apophysis, indistinct under the microscope, which is not present in *H. maderiana* (Fig. 20D). However, caution should be taken as this might be an artifact of suboptimal drying process of the former specimen, which could have detached the branch from the embolus. Also, by looking at Fig. 20D, we can see that this branch is folded in a way that could plausibly accompany the embolus over a larger length. A similar pattern of intermediate forms can also be recognised in among female specimens. Although *H. maderiana* specimens may be diagnosed by long epigynes, the longest among Madeiran *Hogna* (Fig. 20E–F), a significant correlation exists between epigyne size (length/width at base) and body size (Pearson's R = 0.71, p < 0.05), as revealed by the unidentified specimens from Porto Santo and females identified as *H. insularum*. Regardless of the actual length, the overall shape of the hood lateral borders is very similar across both taxa, showing parallel borders. Interestingly, the single adult *H. insularum* female available from Madeira, a population with distinct and exclusive mtDNA haplotypes, showed a slightly different epigynal shape (Fig. 16C). A similar relationship with body size is also observed in the shape of the spermathecae, which are pear-shaped in larger specimens (Fig. 20F), but from ovoid, to pear-shaped and rounded in smaller *H. insularum* specimens (Fig. 16B, D, F, H). Finally, regarding habitats, the largest specimens identified as *H. maderiana* are usually found in open, grassy meadows, while smaller specimens identified as *H. insularum* can be found both in the former habitat but also in shady (secondary) forest.

With the data at hand, it may seem advisable to sink both names into the same species. However, by doing so we might have concealing some interesting biological processes. For instance, hybridization among close relatives have been uncovered between closely related *Hogna* species from the Galapagos islands (De Busschere et al. 2015). Interestingly, introgression of adaptive genes among populations on different Galapagos islands may have contributed to the parallel evolution of similar ecological preferences. The ability of *Hogna* endemic species in Madeira to disperse between islands, which could promote introgression, is evident by the surprising finding of immature specimens originally identified as *H. insularum*, but that both mitochondrial and nuclear DNA suggested they belong to *H. ingens*, supposedly endemic to Desertas. Similar conflicting signals between different sources of evidence, namely morphology and molecules, may also arise in recently

diverged species or species with large ancestral population sizes, as exemplified by wolf spiders in the genus *Pardosa* (Ivanov et al. 2021). Discerning about alternative scenarios, will require the future integration of large-scale population sampling with novel genome wide screening (e.g. ddRADSeq) methods.
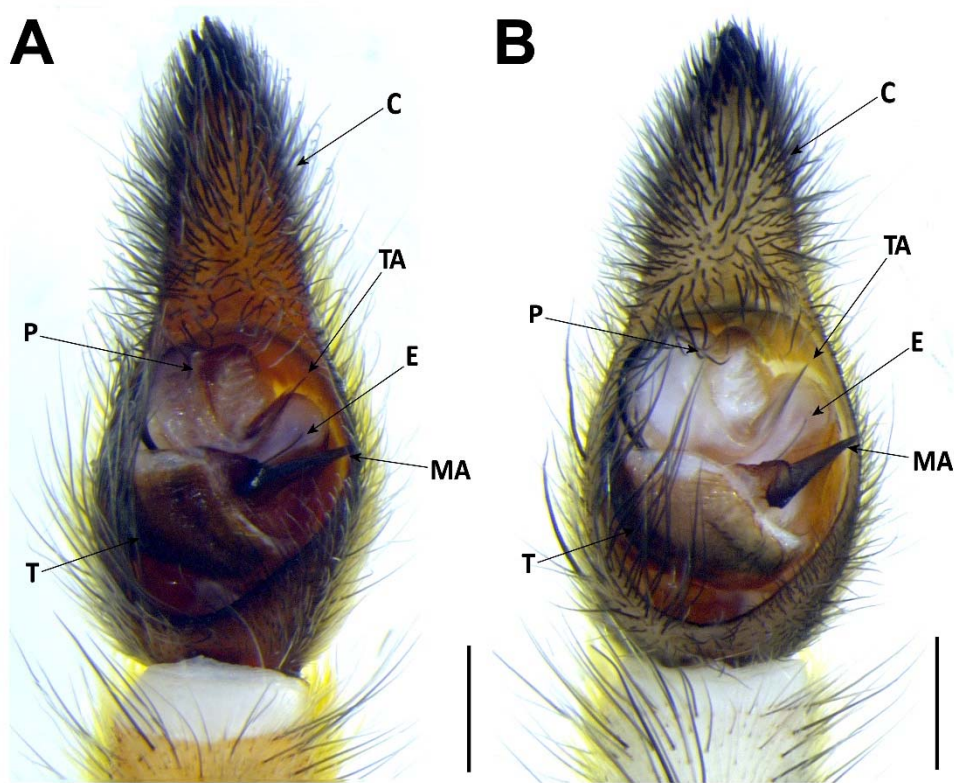
Figure 27. Unidentified male specimens belonging to the *H. maderiana-insularum* complex from Porto Santo. Left male palps, ventral. A, CRBALC0328. B, CRBALC0345. Scale bars: A = 0.5 mm.

Conservation status

As for other taxa in the archipelago (Crespo et al. 2014; Cardoso et al. 2018; Crespo et al. 2021), the combination of restricted range and degrading habitat has led several species of endemic *Hogna* to be considered as threatened. While many seem to be relatively widely distributed and abundant, three species are of concern.
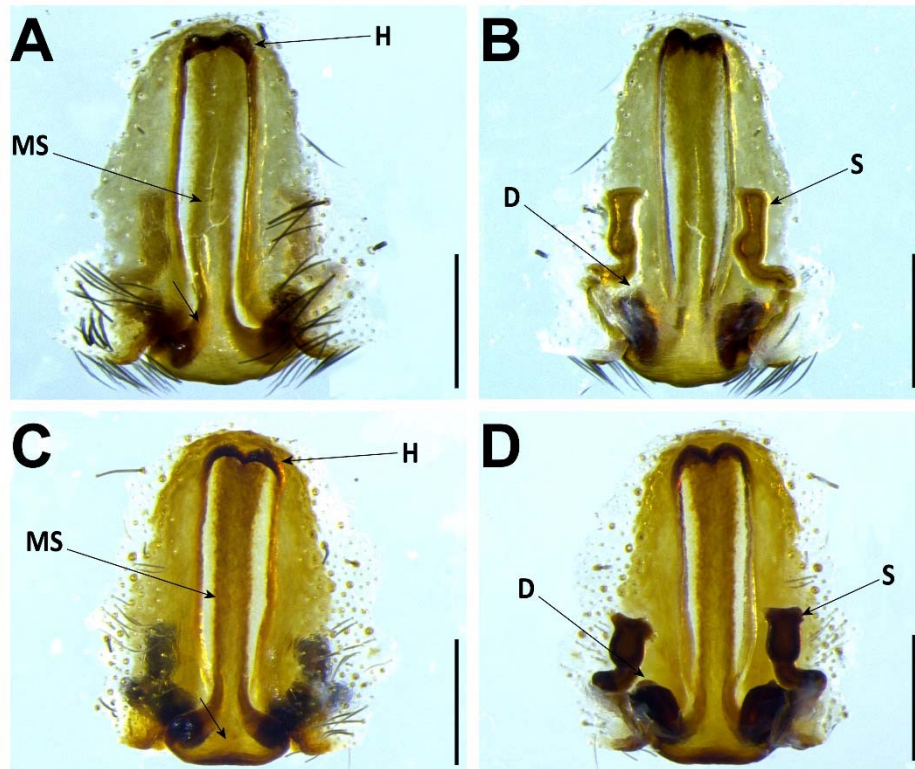
Figure 28. Unidentified female specimens belonging to the *H. maderiana-insularum* complex from Porto Santo. Female genitalia. A–B, CRBALC0329. A, epigynum, ventral; B, vulva, dorsal. C–D, CRBALC0346. C, epigynum, ventral; D, vulva, dorsal. Scale bars: A = 0.5 mm.

Hogna ingens, the Desertas wolf spider, is limited to a single valley in the Northern tip of Deserta Grande and was recently subjected to a reduction of 80% of its range in few years (Crespo et al. 2014), leading to a classification of Critically Endangered. A habitat recovery program is underway and several ex-situ populations are now guaranteeing its future survival. Recent data suggests that the habitat recovery is resulting in the recovery of the spider population to previously affected areas. If this is confirmed the status might improve and the status should be revised in the near future.

Hogna nonannulata seems to be restricted to a small range in the South coast of the island of Madeira. With increasing urban pressure, it is possible that the status of Critically Endangered is warranted for the species. More information should be collected however, as contrary to most other regions in the archipelago, the area was never subject to extensive sampling.

Hogna isambertoi is the third species of conservation concern, given its small range and possible threat from aridification of the two locations from where it is known. As few data are available due to its life cycle, with adults emerging during November and December, a monitoring program is required to confirm a possible status of Endangered.

We strongly recommend the rapid collection of data that can confirm or not the status of *H. nonannulata* and *H. isambertoi*, by focusing on monitoring programs of the Southern coast of the Island of Madeira and overwintering in the Southern tip of Deserta Grande and Bugio. If confirmed, these species would benefit from both habitat recovery programs and ex-situ conservation as is proving successful for *H. ingens*.

Conclusions

Our study underlines the importance of the integration of different lines of evidence to fully understand the origin and diversification of species endemic to oceanic islands. Madeiran *Hogna* colonised the archipelago at a time of global expansion of grasslands and subsequently diversified throughout the archipelago into a variety of forms and sizes. Yet, the boundaries of some species are ill-defined and there are cases where both morphological and molecular suggest complex underlying evolutionary processes.

We tackled nomenclatural issues by revising old types and descriptions, described a new species and provided the first molecular data of Madeiran *Hogna.* The newly collected data confirmed the localised distribution and narrow range of some species. Our study sets the stage for the urgent implementation of conservation measures for the protection of these remarkable endemic species.

Acknowledgements

References

Aktas C (2015) R Package haplotypes: Haplotype Inference and Statistical Analysis of Genetic Variation.

Baert BL, Maelfait J, Hendrickx F (2008) The Wolf Spiders (Araneae , Lycosidae) from the Galápagos Archipelago. : 5–37.

Bell JR, Bohan D, Shaw EM, Weyman G (2005) Ballooning dispersal using silk: World fauna, phylogenies, genetics and models. Bulletin of entomological research 95: 69–114. https://doi.org/10.1079/BER2004350

Bidegaray-Batista L, Arnedo M (2011) Gone with the plate: The opening of the Western Mediterranean basin drove the diversification of ground-dweller spiders. BMC Evolutionary Biology 11. https://doi.org/10.1186/1471-2148-11-317

Blackwall J (1857) Description of the male of Lycosa tarentuloides Maderiana Walck., and of three newly discovered species of the genus Lycosa. Annals and Magazine of Natural History 20: 282–287.

Boieiro M, Matthews TJ, Rego C, Crespo L, Aguiar CAS, Cardoso P, Rigal F, Silva I, Pereira F, Borges PAV, Serrano ARM (2018) A comparative analysis of terrestrial arthropod assemblages from a relict forest unveils historical extinctions and colonization differences between two oceanic islands. PLoS ONE 13: 1–22. https://doi.org/10.1371/journal.pone.0195492

Bonte D, Maelfait J (2001) Life history, habitat use and dispersal of a dune wolf spider (Pardosa monticola (Clerck, 1757) Lycosidae, Araneae) in the Flemish coastal dunes (Belgium). Belgian Journal of Zoology 131: 145–157.

Bonte D, Borre J Vanden, Lens L, Jean-Pierre Maelfait (2006) Geographical variation in wolf spider dispersal behaviour is related to landscape structure. Animal Behaviour 72: 655–662. https://doi.org/10.1016/j.anbehav.2005.11.026

De Busschere C, Van Belleghem SM, Hendrickx F (2015) Inter and intra island introgression in a wolf spider radiation from the Galápagos, and its implications for parallel evolution. Molecular Phylogenetics and Evolution 84: 73–84. https://doi.org/10.1016/j.ympev.2014.11.004

De Busschere C, Baert L, Van Belleghem SM, Dekoninck W, Hendrickx F (2012) Parallel phenotypic evolution in a wolf spider radiation on Galápagos. Biological Journal of the Linnean Society 106: 123–136. https://doi.org/10.1111/j.1095-8312.2011.01848.x

Busschere C De, Hendrickx F, Van Belleghem SM, Backeljau T, Lens L, Baert L (2010) Parallel habitat specialization within the wolf spider genus Hogna from the Galápagos. Molecular Ecology 19: 4029–4045. https://doi.org/https://doi.org/10.1111/j.1365-294X.2010.04758.x

Cardoso, P, Crespo, LC, Silva, I, Borges, P & Boieiro M (2018a) Hogna heeri. The IUCN Red List of Threatened Species 2018: 8. Available from: https://dx.doi.org/10.2305/IUCN.UK.2018-2.RLTS.T58048559A58061002.en.

Cardoso, P, Crespo, LC, Silva, I, Borges, P & Boieiro M (2018b) Hogna insularum. The IUCN Red List of Threatened Species 2018. Available from: https://dx.doi.org/10.2305/IUCN.UK.2018-2.RLTS.T58048609A58061012.en.

Cardoso, P, Crespo, LC, Silva, I, Borges, P & Boieiro M (2018c) Hogna nonannulata. The IUCN

Red List of Threatened Species 2018. Available from:
https://dx.doi.org/10.2305/IUCN.UK.2018-2.RLTS.T58048634A58061022.en.

Cardoso, P, Crespo, LC, Silva, I, Borges, P & Boieiro M (2018d) Hogna schmitzi. The IUCN Red
List of Threatened Species 2018. Available from:
https://dx.doi.org/10.2305/IUCN.UK.2018-2.RLTS.T58048645A58061027.en.

Cardoso P (2014) Hogna ingens. The IUCN Red List of Threatened Species 2014. Available
from: https://dx.doi.org/10.2305/IUCN.UK.2014-2.RLTS.T58048571A58061007.en.

Cardoso P, Crespo L, Silva I, Borges P, Boieiro M (2018) Hogna maderiana. 8235.

Clement M, Posada D, Crandall K (2000) Clement MD, Posada D, Crandall KA. TCS: a
computer program to estimate gene genealogies. Mol Ecol 9: 1657-1659. Molecular
ecology 9: 1657–1659. https://doi.org/10.1046/j.1365-294x.2000.01020.x

Colgan DJ, McLauchlan A, Wilson GDF, Livingston SP, Edgecombe GD, Macaranas J, Cassis G,
Gray MR (1998) Histone H3 and U2 snRNA DNA sequences and arthropod molecular
evolution. Australian Journal of Zoology 46: 419–437.
https://doi.org/10.1071/ZO98048

Crespo L, Boieiro M, Cardoso P, Aguiar C, Amorim I, Barrinha C, Borges P, Menezes D,
Pereira F, Rego C, Ribeiro S, Silva I, Serrano A (2014a) Spatial distribution of Madeira
Island Laurisilva endemic spiders (Arachnida: Araneae). Biodiversity Data Journal 2.
https://doi.org/10.3897/BDJ.2.e1051

Crespo L, Silva I, Borges P, Cardoso P (2013) Rapid biodiversity assessment, faunistics and
description of a new spider species (Araneae) from Desertas Islands and Madeira
(Portugal). Revista Iberica de Aracnología 23: 11–23.

Crespo L, Silva I, Borges P, Cardoso P (2014b) Assessing the conservation status of the strict
endemic Desertas wolf spider, Hogna ingens (Araneae, Lycosidae). Journal for Nature
Conservation 22: 516–524. https://doi.org/10.1016/j.jnc.2014.08.005

Crespo L, Silva I, Enguídanos A, Cardoso P, Arnedo M (2020) Integrative taxonomic revision
of the woodlouse-hunter spider genus Dysdera (Araneae :, Dysderidae) in the Madeira
archipelago with notes on its conservation status. Zoological Journal of the Linnean

Society 20: 1–60.

Crespo LC, Silva I, Borges PAV, Cardoso P (2014c) Assessing the conservation status of the strict endemic Desertas wolf spider, Hogna ingens (Araneae, Lycosidae). Journal for Nature Conservation 22: 516–524. https://doi.org/10.1016/j.jnc.2014.08.005

Denis J (1962) Les araignées de l'archipel de Madère (Mission du Professeur Vandel). Publicações do Instituto Zoologia Doutor Augusto Nobre 79: 1–118.

Dondale, C & Redner J (1990) The insects and arachnids of Canada, Part 17. The wolf spiders, nurseryweb spiders, and lynx spiders of Canada and Alaska, Araneae: Lycosidae, Pisauridae, and Oxyopidae. Research Branch Agriculture Canada Publication 1856: 383.

Ezard T, Fujisawa T, Barraclough T (2017) splits: SPecies' LImits by Threshold Statistics. Available from: https://r-forge.r-project.org/projects/splits/.

Folmer O, Black M, Hoeh W, Lutz R, Vrijenhoek R (1994) DNA primers for amplification of mitochondrial cytochrome c oxidase subunit I from diverse metazoan invertebrates. Molecular marine biology and biotechnology 3: 294–299. https://doi.org/10.1071/ZO9660275

Fujisawa T, Aswad A, Barraclough TG (2016) A Rapid and Scalable Method for Multilocus Species Delimitation Using Bayesian Model Comparison and Rooted Triplets. Systematic biology 65: 759–771. https://doi.org/10.1093/sysbio/syw028

Geldmacher J, Hoernle K (2000) The 72 Ma geochemical evolution of the Madeira hotspot (eastern North Atlantic): Recycling of Paleozoic (≤500 Ma) oceanic lithosphere. Earth and Planetary Science Letters 183: 73–92. https://doi.org/10.1016/S0012-821X(00)00266-1

Goloboff PA, Catalano SA (2016) TNT version 1.5, including a full implementation of phylogenetic morphometrics. Cladistics 32: 221–238. https://doi.org/https://doi.org/10.1111/cla.12160

Greenstone MH (1982) Ballooning Frequency and Habitat Predictability in Two Wolf Spider Species (Lycosidae: Pardosa). The Florida Entomologist 65: 83–89.

https://doi.org/10.2307/3494147

Hebert PDN, Cywinska A, Ball SL, DeWaard JR (2003) Biological identifications through DNA barcodes. Proceedings of the Royal Society B: Biological Sciences. https://doi.org/10.1098/rspb.2002.2218

Hedin MC (1997) Molecular phylogenetics at the population/species interface in cave spiders of the southern Appalachians (Araneae: Nesticidae: Nesticus). Molecular Biology and Evolution 14: 309–324. https://doi.org/10.1093/oxfordjournals.molbev.a025766

Hedin MC, Maddison WP (2001) A combined molecular approach to phylogeny of the jumping spider subfamily Dendryphantinae (Araneae: Salticidae). Molecular Phylogenetics and Evolution 18: 386–403. https://doi.org/10.1006/mpev.2000.0883

Herbert TD, Lawrence KT, Tzanova A, Peterson LC, Caballero-Gill R, Kelly CS (2016) Late Miocene global cooling and the rise of modern ecosystems. Nature Geoscience 9: 843–847. https://doi.org/10.1038/ngeo2813

Hoang DT, Chernomor O, von Haeseler A, Minh BQ, Vinh LS (2018) UFBoot2: Improving the Ultrafast Bootstrap Approximation. Molecular biology and evolution. Molecular Biology and Evolution 35: 518–522. https://doi.org/10.5281/zenodo.854445

Ivanov V, Marusik Y, Pétillon J, Mutanen M (2021) Relevance of ddRADseq method for species and population delimitation of closely related and widely distributed wolf spiders (Araneae, Lycosidae). Scientific Reports 11: 1–14. https://doi.org/10.1038/s41598-021-81788-2

Jocqué R, Alderweireldt M (2005) Lycosidae: the grassland spiders. Acta Zoologica Bulgarica 2005: 125–130. Available from: http://www.european-arachnology.org/proceedings/22nd/15_Jocque.pdf.

Johnson J (1863) Description of a new species of Lycosa living in the island of Madeira; with some remarks on the Lycosa tarentuloides maderiana Walckenaer. Annals and Magazine of Natural History 12: 152–155.

Kalyaanamoorthy S, Minh BQ, Wong TKF, Von Haeseler A, Jermiin LS (2017) ModelFinder:

Fast model selection for accurate phylogenetic estimates. Nature Methods 14: 587–589. https://doi.org/10.1038/nmeth.4285

Kambhampati S, Smith PT (1995) PCR primers for the amplification of four insect mitochondrial gene fragments. Insect Molecular Biology 4: 233–236. https://doi.org/https://doi.org/10.1111/j.1365-2583.1995.tb00028.x

Kapli P, Lutteropp S, Zhang J, Kobert K, Pavlidis P, Stamatakis A, Flouri T (2017) Multi-rate Poisson tree processes for single-locus species delimitation under maximum likelihood and Markov chain Monte Carlo. Bioinformatics 33: 1630–1638. https://doi.org/10.1093/bioinformatics/btx025

Katoh K, Standley DM (2013) MAFFT multiple sequence alignment software version 7: Improvements in performance and usability. Molecular Biology and Evolution 30: 772–780. https://doi.org/10.1093/molbev/mst010

Kulczynski W (1899) Arachnoidea opera Rev. E. Schmitz collecta in insulis Maderianis et in insulis Selvages dictis. Rozprawy i Sprawozdania z Posiedzen Wydzialu Matematyczno Przyrodniczego Akademji Umiejetnosci, Krakow 36: 319–461.

Kumar S, Stecher G, Li M, Knyaz C, Tamura K (2018) MEGA X: Molecular Evolutionary Genetics Analysis across Computing Platforms. Molecular biology and evolution 35: 1547–1549. https://doi.org/10.1093/molbev/msy096

Lanfear R, Frandsen PB, Wright AM, Senfeld T, Calcott B (2017) Partitionfinder 2: New methods for selecting partitioned models of evolution for molecular and morphological phylogenetic analyses. Molecular Biology and Evolution 34: 772–773. https://doi.org/10.1093/molbev/msw260

Logunov D V. (2020) On three species of Hogna Simon, 1885 (Aranei: Lycosidae) from the near East and Central Asia. Arthropoda Selecta 29: 349–360. https://doi.org/10.15298/arthsel.29.3.08

Löytynoja A, Goldman N (2010) webPRANK: a phylogeny-aware multiple sequence aligner with interactive alignment browser. BMC Bioinformatics 11: 579. https://doi.org/10.1186/1471-2105-11-579

Macías-Hernández N, Oromí P, Arnedo M (2008) Patterns of diversification on old volcanic islands as revealed by the woodlouse-hunter spider genus Dysdera (Araneae, Dysderidae) in the eastern Canary Islands. Biological Journal of the Linnean Society 94: 589–615. https://doi.org/10.1111/j.1095-8312.2008.01007.x

Malumbres-Olarte J, Boieiro M, Cardoso P, Carvalho R, Crespo LCF, Gabriel R, Hernández NM, Paulo OS, Pereira F, Rego C, Ros-Prieto A, Silva I, Vieira A, Rigal F, Borges PAV (2020) Standardised inventories of spiders (arachnida, araneae) of macaronesia ii: The native forests and dry habitats of madeira archipelago (Madeira and Porto Santo islands). Biodiversity Data Journal 8. https://doi.org/10.3897/BDJ.8.e47502

Miller M, Pfeiffer W, Schwartz T (2010) Creating the CIPRES Science Gateway for inference of large phylogenetic trees. In: Proceedings of the Gateway Computing Environments Workshop (GCE). , 8.

Minh BQ, Schmidt HA, Chernomor O, Schrempf D, Woodhams MD, von Haeseler A, Lanfear R (2020) IQ-TREE 2: New Models and Efficient Methods for Phylogenetic Inference in the Genomic Era. Molecular Biology and Evolution 37: 1530–1534. https://doi.org/10.1093/molbev/msaa015

Monaghan MT, Wild R, Elliot M, Fujisawa T, Balke M, Inward DJG, Lees DC, Ranaivosolo R, Eggleton P, Barraclough TG, Vogler AP (2009) Accelerated Species Inventory on Madagascar Using Coalescent-Based Models of Species Delineation. Systematic Biology 58: 298–311. https://doi.org/10.1093/sysbio/syp027

Müller K (2005) SEQSTATE – primer design and sequence statistics for phylogenetic DNA data sets. Applied bioinformatics 4: 65–69.

Nentwig W, Blick T, Bosmans R, Gloor D, Hänggi A KC (2020) Spiders of Europe. Version 11.2020. https://doi.org/https://doi.org/10.24436/1

Ogilvie HA, Bouckaert RR, Drummond AJ (2017) StarBEAST2 Brings Faster Species Tree Inference and Accurate Estimates of Substitution Rates. Molecular biology and evolution 34: 2101–2114. https://doi.org/10.1093/molbev/msx126

Palumbi S (1996) Nucleic acids II: the polymerase chain reaction. Molecular Systematics: 205–247. Available from: https://ci.nii.ac.jp/naid/10027373727/en/.

Piacentini LN, Ramírez MJ (2019) Hunting the wolf: A molecular phylogeny of the wolf spiders (Araneae, Lycosidae). Molecular Phylogenetics and Evolution 136: 227–240. https://doi.org/10.1016/j.ympev.2019.04.004

Planas E, Fernández-Montraveta C, Ribera C (2013) Molecular systematics of the wolf spider genus Lycosa (Araneae: Lycosidae) in the Western Mediterranean Basin. Molecular Phylogenetics and Evolution 67: 414–428. https://doi.org/10.1016/j.ympev.2013.02.006

Ramalho RS, Brum Da Silveira A, Fonseca PE, Madeira J, Cosca M, Cachão M, Fonseca MM, Prada SN (2015) The emergence of volcanic oceanic islands on a slow-moving plate: The example of Madeira Island, NE Atlantic. Geochemistry, Geophysics, Geosystems 16: 522–537. https://doi.org/10.1002/2014GC005657

Rambaut A, Drummond AJ, Xie D, Baele G, Suchard MA (2018) Posterior summarization in Bayesian phylogenetics using Tracer 1.7. Systematic Biology 67: 901–904. https://doi.org/10.1093/sysbio/syy032

Ratnasingham S, Hebert PDN (2007) bold: The Barcode of Life Data System (http://www.barcodinglife.org). Molecular Ecology Notes 7: 355–364. https://doi.org/https://doi.org/10.1111/j.1471-8286.2007.01678.x

Ratnasingham S, Hebert PDN (2013) A DNA-Based Registry for All Animal Species: The Barcode Index Number (BIN) System. PLOS ONE 8: e66213. Available from: https://doi.org/10.1371/journal.pone.0066213.

Richter CJJ (1970) Aerial dispersal in relation to habitat in eight wolf spider species (Pardosa, Araneae, Lycosidae). Oecologia 5: 200–214. https://doi.org/10.1007/BF00344884

Roewer C (1960) Araneae Lycosaeformia II (Lycosidae) (Fortsetzung und Schluss). Exploration du Parc National de l'Upemba, Mission G. F. de Witte 55: 519–1040.

Ronquist F, Teslenko M, Van Der Mark P, Ayres DL, Darling A, Höhna S, Larget B, Liu L, Suchard MA, Huelsenbeck JP (2012) Mrbayes 3.2: Efficient bayesian phylogenetic inference and model choice across a large model space. Systematic Biology 61: 539–542. https://doi.org/10.1093/sysbio/sys029

Schwarz S, Klügel A, van den Bogaard P, Geldmacher J (2005) Internal structure and evolution of a volcanic rift system in the eastern North Atlantic: The Desertas rift zone, Madeira archipelago. Journal of Volcanology and Geothermal Research 141: 123–155. https://doi.org/10.1016/j.jvolgeores.2004.10.002

Simmons M, Ochoterena H (2000) Gaps as Characters in Sequence-Based Phylogenetic Analyses. Systematic biology 49: 369–381. https://doi.org/10.1093/sysbio/49.2.369

Simon C, Frati F, Beckenbach A, Crespi B, Liu H, Flook P (1994) Evolution, Weighting, and Phylogenetic Utility of Mitochondrial Gene Sequences and a Compilation of Conserved Polymerase Chain Reaction Primers. Annals of the Entomological Society of America 87: 651–701. https://doi.org/10.1093/aesa/87.6.651

Simon E (1898) Histoire naturelle des araignées. Deuxième édition, tome second. Roret (Ed.). Paris, 193–380 pp.

Soto EM, Labarque FM, Ceccarelli FS, Arnedo MA, Pizarro-Araya J, Ramírez MJ (2017) The life and adventures of an eight-legged castaway: Colonization and diversification of Philisca ghost spiders on Robinson Crusoe Island (Araneae, Anyphaenidae). Molecular Phylogenetics and Evolution 107: 132–141. https://doi.org/https://doi.org/10.1016/j.ympev.2016.10.017

Suman TW (1964) Spiders of the Hawaiian Islands: catalog and bibliography. Pacific Insects 6: 665–687.

Templeton AR, Crandall KA, Sing CF (1992) A cladistic analysis of phenotypic associations with haplotypes inferred from restriction endonuclease mapping and DNA sequence data. III. Cladogram estimation. Genetics 132: 619–633.

Thorell T (1875) Descriptions of several European and North African spiders. Kongliga Svenska Vetenskaps-Akademiens Handlingar 13: 1–204.

Tongiorgi P (1977) Fam. Lycosidae. In La faune terrestre de l'île de Sainte-Hélène. IV. Annales, Musée Royal de l'Afrique Centrale, Sciences zoologiques (Zool.-Ser. 8°) 220: 105–125.

Vaidya G, Lohman DJ, Meier R (2011) SequenceMatrix: concatenation software for the fast

assembly of multi-gene datasets with character set and codon information. Cladistics 27: 171–180. https://doi.org/https://doi.org/10.1111/j.1096-0031.2010.00329.x

Walckenaer CA (1837) Histoire naturelle des insectes. Aptères. Histoire naturelle des insectes. Aptères. 682 pp. https://doi.org/10.5962/bhl.title.61095

White T, Bruns T, Lee S, Taylor J, Innis M, Gelfand D, Sninsky J (1990) Amplification and Direct Sequencing of Fungal Ribosomal RNA Genes for Phylogenetics. In: Pcr Protocols: a Guide to Methods and Applications,. , 315–322.

Whiting MF, Carpenter JC, Wheeler QD, Wheeler WC (1997) The strepsiptera problem: Phylogeny of the holometabolous insect orders inferred from 18S and 28S ribosomal DNA sequences and morphology. Systematic Biology 46: 1–68. https://doi.org/10.1093/sysbio/46.1.1

World Spider Catalog (2021) World Spider Catalog. Natural History Museum Bern, online at http://wsc.nmbe.ch, version 22.0, accessed on 21.04.2021. https://doi.org/10.24436/2

Wunderlich J (1992) Die Spinnen-Fauna der Makaronesischen Inseln: Taxonomie, Ökologie, Biogeographie und Evolution. Beiträge zur Araneologie 1: 1–619.

Wunderlich J (1995) Zu Ökologie, Biogeographie, Evolution und Taxonomie einiger Spinnen der Makaronesischen Inseln (Arachnida: Araneae). Beiträge zur Araneologie 4: 385–439.

General Discussion

General Discussion

I have investigated in detail the taxonomy, phylogeny and biogeography of the two most speciose spider genera in the Madeira archipelago. While each Chapter bears its individual detailed discussion, I hereby underline the major issues discussed in our work.

- *Biogeographic considerations*

I uncovered two independent lineages of *Dysdera* that have speciated in the Madeira archipelago, showing widely different evolutionary trajectories. The one I referred as the "Madeiran clade" (see Chapter 1), is an older lineage that has greatly diversified locally. The other, I referred as the "Azorean clade", colonized Madeira more recently than the Madeiran clade, and did not diversify, being represented by a single endemic species in the archipelago. However, it was able to colonize the remote Azores archipelago (see Chapter 2) where may have undergone diversification. The origin of these lineages could be traced to different continental sources. The Madeiran clade was found to have diverged from a cluster of lineages spread across the Iberian Peninsula (IP) and North Africa (Chapter 2, Fig. 4), although further studies are needed to identify its closest continental relative. I searched for potential continental outgroups to this clade using morphological analysis on a small set of undescribed species from the western part of the IP, but the results remain inconclusive. Conversely, I was able to pinpoint the closest relative to the Azorean clade, the continental outgroup species, *D. flavitarsis,* circumscribed to narrow stretch in the North-western corner of the IP. Although somewhat speculative, it is possible that closer relatives either remain unaccounted or maybe went recently extinct, a suspicion reinforced by the dramatic ecological shift observed in both *D. citauca* and *D.* "SPJ", which dwell in spray zones of coastal habitats, whereas *D. flavitarsis* occurs inland, in oak forests. The early colonization and subsequent diversification of the Madeiran clade could have hindered the Azorean clade from diversifying in the Madeira archipelago, maybe by competitive exclusion in habitats already occupied by the former. Alternatively, it is possible that additional species from this clade may have not been collected due to under sampling, since the habitat they occupy is uncommon among spiders, or that may have gone extinct in recent times due to competition with the exotic *D. crocata,* which favours coastal habitats over localities at higher altitudes.

Additionally, I cannot exclude a third colonization of Madeira, from the Canary Islands, as the possibly extinct *D. titanica,* for which no molecular information could be extracted, resembles some species from the Canary Islands much more than any of the conspecifics in Madeira. A close relationship between the Madeiran and Canarian fauna has been reported in other island arthropods, such as the *Calathus* carabid beetles (Emerson et al. 2000), *Rhopalomesites* weevils (Hernández-Teixidor et al. 2016) and *Tarphius* zopherid beetles (Emerson and Oromí 2005).

Because of the limited ability of *Dysdera* for long distance dispersal, as suggested by the narrow distribution of most of its near three hundred species and the absence of ballooning, I hypothesize that the ancestors of both the Madeiran and Azorean clades dispersed by means of rafting or floating islands, helped by the direction of the dominant wind and water currents in the region. Additionally, they may have benefited from a series of paleoislands, present-day seamounts created by the same volcanic hotspot which originated the Madeiran archipelago (Geldmacher et al. 2000), which may have shortened distances between current subaerial islands in the past. This possibility was already suggested for other speciose invertebrates of Madeira, such as land snails (Cook 2008).

Madeira, the largest island of the archipelago, is inhabited by solely 2 species, whereas four and five sympatric species occur respectively in the smaller and ecologically depauperated islands of Porto Santo and Deserta Grande. Past biodiversity surveys conducted in Madeira (Crespo et al. 2014a, Boieiro et al. 2018, Malumbres-Olarte et al. 2020) guarantee a reasonable sampling effort and I can discard the existence of strong sampling artifacts. Island age is also discarded as the determining factor as aerial parts of Madeira are dated older than those of Desertas (Schwarz et al. 2005, Ramalho et al. 2015), with strongly eroded Porto Santo already in the subsidence stage of the geologic cycle. The scarcity of species in Madeira island is therefore hard to explain.

Unravelling the origins of Madeiran *Hogna* wolf spiders is a completely different issue. Not only lycosids disperse through ballooning, resulting in the possibility of colonization from sources other than the nearby IP and North Africa, but data on the diversity of *Hogna* in the continent are still scarce. I did not conduct specific sampling of *Hogna* in the nearby regions, such as the Canary Islands or North Africa, except for a batch of *H. ferox* specimens collected in Gran Canaria, and I had to rely on available sequences in public data bases, which greatly

misrepresent the diversity of the genus in the mainland. Moreover, *Hogna* is taxonomically poorly defined, often serving as dumping genus for Lycosinae species of unknown placement. Incorporating the Madeiran sequences I generated to the matrix used by Piacentini & Ramírez (2019) in their family level phylogeny of wolf spiders allowed me to retrieve the Madeiran clade and identify the Mediterranean *H. radiata* (the type species for *Hogna*) as its putative sister taxa, albeit by a single inference method, and with low support. Within the Madeiran clade, the only clear pattern is that the species *H. insularum* and *H. maderiana* pair is monophyletic, and that the remaining species (*H. blackwalli, H. ingens, H. heeri, H. isambertoi* and *H. nonannulata*), which I refer as the *ingens* clade, share a common exclusive ancestor. The monophyly of the two clades, however, remains poorly supported, which prevents me suggest either one or two colonisations of the archipelago by *Hogna*. Within the *ingens* clade, *H. blackwalli* and *H. nonannulata* were consistently retrieved as sister species, and considering their known distributions, it is safe to assume that they are the result of allopatric divergence prompted by an ecological shift in the island of Madeira, since the first occurs in laurel forests or similar forested habitat, while the second occurs in coastal shrubland. It should be noted, however, that to date a single certain locality has been reported for *N. nonannulata*.

- *Overlooked species and insights into species boundaries*

For both the speciose Madeiran clade of *Dysdera* (Chapter 1) and the Madeiran *Hogna* (Chapter 3) I performed single gene (*cox1*) species delimitation analyses using *cox1*, and integrated these results along with morphological and geographical data to infer species boundaries. The results suggested uncovered some unexpected patterns worth of discussion.

In *Dysdera,* I found a clear metapopulation structure in two species, *D. coiffaiti* and *D. dissimilis*. The first is ubiquitous across humid laurel forests in Madeira, but also dwells in the arid islands of Deserta Grande and Bugio. I recovered two well supported mtDNA clades corresponding to the two main islands and habitats. Morphologically, although specimens from both sites differ in size, they are only distinguished by a subtle difference in the curvature of the male palp's external margin of the lateral sheet (eL) of the male bulb (see Chapter 1). The female genitalia is identical. Likewise, only the GMYC separated the Desertas

population as a putative species, while all other methods conservatively assigned all samples to a single group of *D. coiffaiti*. Following the species concept of De Queiroz (2007), which considers a species an independently evolving metapopulation, I opted to avoid splitting the populations of *D. coiffaiti* and consider the differences to reflect deep population structure.

Similarly, *D. dissimilis* haplotypes were highly structured across Porto Santo's mosaic landscape of small habitable patches of secondary forest at mountain tops. The relationships recovered are compatible with a westward progression, since the early divergent haplotypes to have diverged correspond to the two samples taken from the eastern Pico Branco. Two species delimitation methods have separated the samples from Pico Branco as a putative species, but I failed to find any reliable morphological differences to consider a new species. Like in the former case, I consider *D. dissimilis* a single species with deep mitochondrial divergences reflecting geographic population structure.

Within the genus *Hogna*, I uncovered a species pair that cannot be distinguished by molecular markers and that shows a gradient in morphological trait differences, namely *H. insularum* and *H. maderiana*. Both names correspond to specimens on the extremes of a continuous distribution of traits, insluding size, leg pilosity and genitalic morphology (see Discussion of Chapter 3 for detailed information). Intermediate specimens are abundant and of dubious identity. All the species delimitation methods treated the sampled specimens as one single putative species, which would support the synonymy of these species. I chose not to propose such change since it may hinder some relevant historical or ongoing biological processes that may deserve further investigation. The existence of hybridization in closely related *Hogna* species has been demonstrated in *Hogna* species from the Galapagos (De Busschere et al. 2015) and may also account for the patterns recovered in the Madeiran sister pair. However, it is unclear why specimens fitting with *H. maderiana* diagnosis are restricted to Porto Santo (Fig. 3B of Introduction), whereas *H. insularum* can be found in all semi-arid regions of the archipelago, including in sympatry with *H. maderiana*. We intend to dig deeper into this problem using genome wide screening methods (ddRADSeq).

Although not as rampant as observed in *H. insularum* and *H. maderiana,* I also detected at least one case of introgression of *H. ingens cox1* into *H. insularum,* which may add to the growing evidence of ongoing hybridization in the group, although in this case also involving long distance dispersal since the two species live in different islands. On the other

hand, I interpreted the shared ITS-2 alleles among some of the closely related species, as a case of incomplete lineage sorting, probably as a result of the recent divergence of these species as suggested by my time estimates.

- *Are Madeiran* Dysdera *a case of adaptive radiation?*

My data suggests that the Madeiran clade of *Dysdera* is an example of adaptive radiation. The members of these sympatric species-groups in Porto Santo and Deserta Grande present differences in traits involved in prey capture, namely body size and cheliceral morphology. I hypothesize those differences hint to the involvement of diversifying selection acting on morphological variation to avoid competition in small areas with limiting resources. A quantitative test to this hypothesis is already underway. I have collected all the necessary data, namely additional intron sequence data to resolve relationships using multi-coalescent approaches, morphological measurements to define the functional space and ecological information to estimate niche overlapping. Unfortunately, these analyses could not be included in the present study due to time constraints.

- *Conservation notes*

The large sampling effort made during the several collecting campaigns conducted not only in Madeira, but also in the Azores, the Canaries and in the mainland, have providedme with enough information to examine the conservation status and discuss some of the putative threats facing the endemic *Dysdera* and *Hogna* species. Madeira and Azores archipelagos, as most oceanic islands, suffer from intensive anthropogenic pressure since their colonization by humans, including changes in land use, and the consequent loss of native habitats, as well as the introduction of exotic species (Kueffer and Kaiser-Bunbury 2014). The range-restricted *Dysdera* species from Porto Santo and Desertas require urgent conservation measures including habitat recovery, econmpassing the mountain tops and, for *D. citauca*, coastal localities. Increasing levels of aridity driven by climate change might also further reduce the viability of these endemics.

The Desertas Wolf spider *H. ingens* was assessed as Critically Endangered by IUCN (Crespo et al. 2014b), as its range is restricted to the small Vale da Castanheira, with less than 1 km^2. A habitat recovery program is underway and *ex situ* breeding has been implemented by the Bristol Zoo in an attempt to safeguard the species. I suggest the same approach can be undertaken for the *Dysdera* species of Porto Santo and Desertas, as well as the inclusion of all these species, including *H. ingens*, in specific legislation targeting their protection. Finally, data are still scarce on *H. isambertoi* and *H. nonannulata*, buth both species should be candidates for targeted monitoring programs so that their status can be assessed in the near future.

- *Future perspectives for research on Madeiran spiders*

I anticipate the continuation of the research line started with this thesis through a series of studies, some of which are underway. First, we are targeting *H. insularum* and *H. maderiana* species pair for a genomics study involving ddRADSeq to reveal the role of hybridization in the evolution of their morphological and ecological diversity. Second, we are testing the hypothesis that the Madeiran clade in *Dysdera* represent a case of adaptive radiation.

Third, I think that the analyses of the patterns exhibited by different lineages with different ecological requirements and dispersal abilities will greatly help to understand the origins and colonization pathways of the Madeiran biota and identify the main drivers of diversification in the archipelago. Here I have gathered and analysed data for two speciose spider genera, *Dysdera* and *Hogna*, but other candidate lineages will include the comb-tailed spiders *Hahnia*, the ground spiders *Haplodrassus*, or the jumping spiders *Macaroeris,* all of which contain numerous, often undescribed, species.

Finally, the massive landscape transformation following human settling has taken a major toll on Madeiran original terrestrial habitats. At least two of the species investigated in the present study may have gone extinct, namely *D. cetophonorum* and *D. titanica*. In both cases the material studied was found in natural history collections, and no further individuals have been collected after 70 or more years until the present. Along with habitat destruction, the human settling also brought up the introduction of exotic species. Specifically, the

synanthropic *D. crocata* has been recorded in several localities across the archipelagos, usually associated to disturbed habitats. It would be interesting to examine in the future through experimental evidence the interaction between the exotic species and the island endemics to confirm or reject if *D. crocata* poses a threat to the local fauna or simply occupies habitats already disturbed by human activity.

Conclusions

Chapter 1: Integrative taxonomic revision of the woodlouse-hunter spider genus *Dysdera* (Araneae: Dysderidae) in the Madeira archipelago with notes on its conservation status

- A monophyletic lineage of *Dysdera* colonized the Madeira archipelago, arriving first at Porto Santo, subsequently colonizing the remaining islands;

- One of the endemic species is only known from a museum specimen in the Kulczynski collection (mid 19th to early 20th century) show morphological affinities with some endemic species form the Canary Islands and might represent an independent colonization of the archipelago;

- The large number of endemics, and the presence of co-occurring species exhibiting different body sizes and cheliceral morphology, traits associated with prey capture and trophic specialization, suggest that the Madeiran clade constitutes a case of adaptive radiation;

- The second oldest and largest island of the archipelago, Madeira, only harbours two species, while the smallest and more ecologically depauperated Porto Santo and Desertas harbour 4 and 5 species, respectively;

- The discovery of new endemic species reinforces the need to lobby for conservation efforts in the disturbed semi-natural areas of Porto Santo and Desertas. At least one of the species, which was described from museum material, may have gone extinct since it has not been collected for over 100 years.

Chapter 2: The Atlantic connection: Coastal habitat favoured long distance dispersal and colonization of Azores and Madeira by *Dysdera* spiders (Araneae: Dysderidae)

- The presence of extant endemic species of *Dysdera* in Azores, which were thought to be extinct, is confirmed;

- An additional species from Madeira, not related to the rest of endemic species and thus representing a second colonization of the archipelago, is described;

- The endemic species of Azores and the newly described endemic from Madeira form a clade and a species present in the northeastern corner of the Iberian Peninsula is identified as their sister taxa. The colonization pathway of the islands remains unclear but it was most likely by rafting favoured by the dominant water and air currents in the area;

- A time-calibrated analysis revealed that the split of the island species and their continental counterpart slightly preceded the age of the subaerial stage of the islands, which may either suggest the use of formerly emerged seamounts as stepping stones or some kind of methodological artifact;

- The taxonomic and conservation status of the Azorean endemic species *D. cetophonorum* remains obscure, molecular data could not be retrieved to compare with the coastal specimens collected and no specimens of this species has been collected in 70 years, in spite of active spider surveys conducted in the islands.

Chapter 3: Island hoppers: Integrative taxonomic revision of Hogna wolf spider (Araneae: Lycosidae) endemic to the Madeira islands with description of a new species

- The *Hogna* species of the Madeira archipelago probably are monophyletic, although support is low. The genus probably colonized the archipelago once, but a second colonization cannot be completely ruled out;

- Taxonomic treatments done summed up three synonymies, one name revalidation and one new species, proving evidence on the poor taxonomic knowledge on the group prior to the present study;

- Time estimation analysis traced back the diversification of Madeiran *Hogna* to the late Miocene, a time of major global cooling that drove the expansion of grasslands and its associated fauna;

- The species pair *H. insularum* and *H. maderiana* cannot be separated by either molecular species delimitation methods or morphological data. We hypothesize that instances of hybridization might be occurring among these species;

- We provide remarks on the conservation status of each species, and propose that the species *H. isambertoi* and *H. nonannulata* should be targeted for monitoring programs and conservation efforts, given their reduced distributions.

General Bibliography

Aguilée R, Claessen D, Lambert A (2013) Adaptive radiation driven by the interplay of eco-evolutionary and landscape dynamics. Evolution 67: 1291–1306. https://doi.org/10.1111/evo.12008

Arechavaleta M, Zurita N, Marrero MC, Martín JL (2005) Lista preliminar de especies silvestres de Cabo Verde (hongos, plantas y animales terrestres). : 155.

Arnedo M, Ribera C (1997) Radiation of the genus Dysdera (Aranea, haplogynae, dysderidae) in the Canary Islands: The island of Gran Canaria. Zoologica Scripta 26: 205–243. https://doi.org/10.1111/j.1463-6409.1997.tb00413.x

Arnedo M, Oromí P, Ribera C (1996) Radiation in the genus Dysdera (Araneae, Dysderidae) in the Canary Islands: The western islands. Zoologica Scripta 27: 604–662. Available from: http://www.jstor.org/stable/3706342%5Cnhttp://www.americanarachnology.org/JoA_free/JoA_v27_n3/arac_27_03_0604.pdf.

Arnedo M, Oromí P, Ribera C (2000) Systematics of the Genus Dysdera (Araneae, Dysderidae) in the Eastern Canary Islands. Journal of Arachnology 28: 261–292. https://doi.org/10.1636/0161-8202(2000)028[0261:sotgda]2.0.co;2

Arnedo M, Oromí P, Ribera C (2001) Radiation of the spider genus Dysdera (Araneae, Dysderidae) in the Canary Islands: Cladistic assessment based on multiple data sets. Cladistics 17: 313–353. https://doi.org/10.1006/clad.2001.0168

Arnedo M, Oromí P, Múrria C, Macías-Hernández N, Ribera C (2007) The dark side of an island radiation: Systematics and evolution of troglobitic spiders of the genus Dysdera Latreille (Araneae:Dysderidae) in the Canary Islands. Invertebrate Systematics 21: 623–660. https://doi.org/10.1071/IS07015

Arnedo M a, Ribera C (1999) Radiation of the spider genus Dysdera (Araneae, Dysderidae) in the Canary Islands: the island of Tenerife. Journal of Arachnology 27: 604–662. https://doi.org/10.2307/3706342

Baert BL, Maelfait J, Hendrickx F (2008) The Wolf Spiders (Araneae , Lycosidae) from the

Galápagos Archipelago. : 5–37.

Barraclough TG, Hughes M, Ashford-Hodges N, Fujisawa T (2009) Inferring evolutionarily significant units of bacterial diversity from broad environmental surveys of single-locus data. Biology Letters 5: 425–428. https://doi.org/10.1098/rsbl.2009.0091

Bidegaray-Batista L, Macías-Hernández N, Oromí P, Arnedo M (2007) Living on the edge: Demographic and phylogeographical patterns in the woodlouse-hunter spider Dysdera lancerotensis Simon, 1907 on the eastern volcanic ridge of the Canary Islands. Molecular Ecology 16: 3198–3214. https://doi.org/10.1111/j.1365-294X.2007.03351.x

Blair C, Bryson RW (2017) Cryptic diversity and discordance in single-locus species delimitation methods within horned lizards (Phrynosomatidae: Phrynosoma). Molecular Ecology Resources 17: 1168–1182. https://doi.org/10.1111/1755-0998.12658

Blandenier G, Fürst P a (1998) Ballooning spiders caught by a suction trap in an agricultural landscape in Switzerland. Proceedings of the 17th European Colloquium of Arachnology, Edinburgh 1997: 178–186.

Boieiro M, Matthews TJ, Rego C, Crespo L, Aguiar CAS, Cardoso P, Rigal F, Silva I, Pereira F, Borges PAV, Serrano ARM (2018) A comparative analysis of terrestrial arthropod assemblages from a relict forest unveils historical extinctions and colonization differences between two oceanic islands. PLoS ONE 13: 1–22. https://doi.org/10.1371/journal.pone.0195492

Bond JE, Garrison NL, Hamilton CA, Godwin RL, Hedin M, Agnarsson I (2014) Phylogenomics resolves a spider backbone phylogeny and rejects a prevailing paradigm for orb web evolution. Current biology : CB 24: 1765–1771. https://doi.org/10.1016/j.cub.2014.06.034

Borges P a. V., Abreu C, Aguiar AMF, Carvalho P, Jardim R, Melo I, Oliveira P, Sérgio C, Serrano ARM, Vieira P (2008a) Direcção Regional Do Ambiente Do Governo Regional Da Madeira A list of the terrestrial fungi, flora and fauna of Madeira and Selvagens archipelagos. 1–440 pp. Available from: http://scholar.google.com/scholar?hl=en&btnG=Search&q=intitle:A+list+of+the+terres

trial+fungi,+flora+and+fauna+of+Madeira+and+Selvagens+archipelagos#0.

Borges PA V., Abreu C, Aguiar AMF, Carvalho P, Jardim R, Melo I, Oliveira P, Sérgio C, Serrano ARM, Vieira P (2008b) Direcção Regional Do Ambiente Do Governo Regional Da Madeira Listagem dos fungos, flora e fauna terrestres dos arquipélagos da Madeira e Selvagens. 1–440 pp. Available from: http://scholar.google.com/scholar?hl=en&btnG=Search&q=intitle:A+list+of+the+terres trial+fungi,+flora+and+fauna+of+Madeira+and+Selvagens+archipelagos#0.

Borges PA V., Costa A, Cunha R, Gabriel R, Gonçalves V, Martins A, Melo I, Parente M, Raposeiro P, Rodrigues P, Santos RS, Silva L, Vieira P, Vieira V (2010) Biologia Listagem dos organismos terrestres e marinhos dos açores - A List of the terrestriaL and marine biota from the azores. 429 pp.

Bouckaert R, Vaughan TG, Barido-Sottani J, Duchêne S, Fourment M, Gavryushkina A, Heled J, Jones G, Kühnert D, De Maio N, Matschiner M, Mendes FK, Müller NF, Ogilvie HA, du Plessis L, Popinga A, Rambaut A, Rasmussen D, Siveroni I, Suchard MA, Wu C-H, Xie D, Zhang C, Stadler T, Drummond AJ (2019) BEAST 2.5: An advanced software platform for Bayesian evolutionary analysis. PLoS computational biology 15: e1006650. https://doi.org/10.1371/journal.pcbi.1006650

Brehm A, Jesus J, Spínola H, Alves C, Vicente L, Harris DJ (2003) Phylogeography of the Madeiran endemic lizard Lacerta dugesii inferred from mtDNA sequences. Molecular Phylogenetics and Evolution 26: 222–230. https://doi.org/10.1016/S1055-7903(02)00310-X

De Busschere C, Van Belleghem SM, Hendrickx F (2015) Inter and intra island introgression in a wolf spider radiation from the Galápagos, and its implications for parallel evolution. Molecular Phylogenetics and Evolution 84: 73–84. https://doi.org/10.1016/j.ympev.2014.11.004

De Busschere C, Baert L, Van Belleghem SM, Dekoninck W, Hendrickx F (2012) Parallel phenotypic evolution in a wolf spider radiation on Galápagos. Biological Journal of the Linnean Society 106: 123–136. https://doi.org/10.1111/j.1095-8312.2011.01848.x

Cameron RAD, Cook LM (1999) Land snail faunas of the Deserta Islands, Madeiran

archipelago, past and present. Journal of Conchology 36: 1–12.

Cardoso P (2014) Hogna ingens. The IUCN Red List of Threatened Species 2014. Available from: https://dx.doi.org/10.2305/IUCN.UK.2014-2.RLTS.T58048571A58061007.en.

Cardoso P, Arnedo M, Triantis K, Borges P (2010) Drivers of diversity in Macaronesian spiders and the role of species extinctions. Journal of Biogeography 37: 1034–1046. https://doi.org/10.1111/j.1365-2699.2009.02264.x

Cartwright J (2019) Ecological islands: conserving biodiversity hotspots in a changing climate. Frontiers in Ecology and the Environment 17: 331–340. https://doi.org/https://doi.org/10.1002/fee.2058

Cook LM (1996) Habitat, isolation and the evolution of Madeiran landsnails. Biological Journal of the Linnean Society 59: 457–470. https://doi.org/10.1006/bijl.1996.0075

Cook LM (2008) Species richness in Madeiran land snails, and its causes. Journal of Biogeography 35: 647–653. https://doi.org/10.1111/j.1365-2699.2007.01801.x

Copsey J, Black S, Groombridge J, Jones C (2018) Species Conservation: Lessons from Islands. In: , 1–16. https://doi.org/10.1017/9781139030243.003

Crespo L, Boieiro M, Cardoso P, Aguiar C, Amorim I, Barrinha C, Borges P, Menezes D, Pereira F, Rego C, Ribeiro S, Silva I, Serrano A (2014a) Spatial distribution of Madeira Island Laurisilva endemic spiders (Arachnida: Araneae). Biodiversity Data Journal 2. https://doi.org/10.3897/BDJ.2.e1051

Crespo L, Silva I, Borges P, Cardoso P (2013) Rapid biodiversity assessment, faunistics and description of a new spider species (Araneae) from Desertas Islands and Madeira (Portugal). Revista Iberica de Aracnología 23: 11–23.

Crespo LC, Silva I, Borges PAV, Cardoso P (2014b) Assessing the conservation status of the strict endemic Desertas wolf spider, Hogna ingens (Araneae, Lycosidae). Journal for Nature Conservation 22: 516–524. https://doi.org/10.1016/j.jnc.2014.08.005

Darwin C (1859) On the origin of species by means of natural selection, or preservation of favoured races in the struggle for life. London : John Murray, 1859.

Deeleman-Reinhold C, Deeleman P (1988) Revision des Dysderinae (Araneae, Dysderidae),

les especes mediterraneennes occidentales exceptees. Tijdschrift voor Entomologie 131: 141–269. Available from: https://www.biodiversitylibrary.org/part/66464.

Delsuc F, Brinkmann H, Philippe H (2005) Phylogenomics and the reconstruction of the tree of life. Nature Reviews Genetics 6: 361–375. https://doi.org/10.1038/nrg1603

Donoghue PCJ, Yang Z (2016) The evolution of methods for establishing evolutionary timescales. Philosophical Transactions of the Royal Society B: Biological Sciences 371. https://doi.org/10.1098/rstb.2016.0020

Duffey E (1956) Aerial Dispersal in a Known Spider Population. Journal of Animal Ecology 25: 85–111. https://doi.org/10.2307/1852

Emerson B, Oromí P, Hewitt G (2000) Interpreting Colonization of the Calathus (Coleoptera: Carabidae) on the Canary Islands and Madeira Through the Application of the Parametric Bootstrap. Evolution 54: 2081. https://doi.org/10.1554/0014-3820(2000)054[2081:ICOTCC]2.0.CO;2

Emerson BC, Oromí P (2005) Diversification of the forest beetle genus Tarphius on the Canary Islands, and the evolutionary origins of island endemics. Evolution 59: 586–598. https://doi.org/10.1111/j.0014-3820.2005.tb01018.x

Enghoff H (1992) Macaronesian millipedes (Diplopoda) with emphasis on endemic species swarms on Madeira and the Canary Islands. Biological Journal of The Linnean Society 46: 153–161.

Erber D (2000) Revision der Gattung Sphaericus (Col., Ptinidae) der Lauri-Makaronesischen Region (Azoren, Madeira, Selvagens, Kanaren) einschließlich Nordafiika und des europäischen Festlandes. Coleoptera 4: 153–282.

Fernández R, Kallal RJ, Dimitrov D, Ballesteros JA, Arnedo MA, Giribet G, Hormiga G (2018) Phylogenomics, Diversification Dynamics, and Comparative Transcriptomics across the Spider Tree of Life. Current Biology 28: 1489-1497.e5. https://doi.org/https://doi.org/10.1016/j.cub.2018.03.064

Figueiredo L, Krauss J, Steffan-Dewenter I, Sarmento Cabral J (2019) Understanding extinction debts: spatio–temporal scales, mechanisms and a roadmap for future

research. Ecography 42: 1973–1990. https://doi.org/10.1111/ecog.04740

Freitas R, Romeiras M, Silva L, Cordeiro R, Madeira P, González JA, Wirtz P, Falcón JM, Brito A, Floeter SR, Afonso P, Porteiro F, Viera-Rodríguez MA, Neto AI, Haroun R, Farminhão JNM, Rebelo AC, Baptista L, Melo CS, Martínez A, Núñez J, Berning B, Johnson ME, Ávila SP (2019) Restructuring of the 'Macaronesia' biogeographic unit: A marine multi-taxon biogeographical approach. Scientific Reports 9: 2006–2009. https://doi.org/10.1038/s41598-019-51786-6

Fujisawa T, Barraclough TG (2013) Delimiting species using single-locus data and the generalized mixed yule coalescent approach: A revised method and evaluation on simulated data sets. Systematic Biology 62: 707–724. https://doi.org/10.1093/sysbio/syt033

Garrison NL, Rodriguez J, Agnarsson I, Coddington JA, Griswold CE, Hamilton CA, Hedin M, Kocot KM, Ledford JM, Bond JE (2016) Spider phylogenomics: untangling the Spider Tree of Life. PeerJ 4: e1719–e1719. https://doi.org/10.7717/peerj.1719

Gascuel F, Ferrière R, Aguilée R, Lambert A (2015) How Ecology and Landscape Dynamics Shape Phylogenetic Trees. Systematic Biology 64: 590–607. https://doi.org/10.1093/sysbio/syv014

Geldmacher J, Van Den Bogaard P, Hoernle K, Schmincke HU (2000) The 40Ar/39Ar age dating of the Madeira Archipelago and hotspot track (eastern North Atlantic). Geochemistry, Geophysics, Geosystems 1. https://doi.org/10.1029/1999GC000018

Gillespie R (2004) Community Assembly Through Adaptive Radiation in Hawaiian Spiders. Science 303: 356–359. https://doi.org/10.1636/0161-8202(2002)030[0159:HSOTGT]2.0.CO;2

Goloboff PA, Catalano SA (2016) TNT version 1.5, including a full implementation of phylogenetic morphometrics. Cladistics 32: 221–238. https://doi.org/https://doi.org/10.1111/cla.12160

Griswold C, Ramirez M, Coddington J, Platnick N (2005) Atlas of phylogenetic data for entelegyne spiders (Araneae: Araneomorphae: Entelegynae) with comments on their phylogeny. Griswold, Charles E., Ramirez, Martin J., Coddington, Jonathan A., and

Platnick, Norman I. 56: 1–324.

Hamilton CA, Formanowicz DR, Bond JE (2011) Species Delimitation and Phylogeography of Aphonopelma hentzi (Araneae, Mygalomorphae, Theraphosidae): Cryptic Diversity in North American Tarantulas. PLOS ONE 6: e26207. Available from: https://doi.org/10.1371/journal.pone.0026207.

Heather JM, Chain B (2016) The sequence of sequencers: The history of sequencing DNA. Genomics 107: 1–8. https://doi.org/10.1016/j.ygeno.2015.11.003

Hebert PDN, Cywinska A, Ball SL, DeWaard JR (2003) Biological identifications through DNA barcodes. Proceedings of the Royal Society B: Biological Sciences. https://doi.org/10.1098/rspb.2002.2218

Heckman DS, Geiser DM, Eidell BR, Stauffer RL, Kardos NL, Hedges SB (2001) Molecular Evidence for the Early Colonization of Land by Fungi and Plants. Science 293: 1129 LP – 1133. https://doi.org/10.1126/science.1061457

Hedges SB, Parker PH, Sibley CG, Kumar S (1996) Continental breakup and the ordinal diversification of birds and mammals. Nature 381: 226–229. https://doi.org/10.1038/381226a0

Hernández-Teixidor D, López H, Pons J, Juan C, Oromí P (2016) Host plant associations and geographical factors in the diversification of the Macaronesian Rhopalomesites beetles (Coleoptera: Curculionidae). Journal of Biogeography 43: 1608–1619. https://doi.org/10.1111/jbi.12737

Holder M, Lewis PO (2003) Phylogeny estimation: Traditional and Bayesian approaches. Nature Reviews Genetics 4: 275–284. https://doi.org/10.1038/nrg1044

Hormiga G, Arnedo M, Gillespie RG (2003) Speciation on a Conveyor Belt: Sequential Colonization of the Hawaiian Islands by Orsonwelles Spiders (Araneae, Linyphiidae). Systematic Biology 52: 70–88. https://doi.org/10.1080/10635150309347

Hormiga G, Jäger P, Jocqué R, Platnick NI, Ramírez MJ, Raven RJ (2020) Spiders of the World Spiders of the World. Platnick NI (Ed.). Princeton University Press. https://doi.org/10.2307/j.ctvpbnqfg

Irisarri I, Singh P, Koblmüller S, Torres-Dowdall J, Henning F, Franchini P, Fischer C, Lemmon AR, Lemmon EM, Thallinger GG, Sturmbauer C, Meyer A (2018) Phylogenomics uncovers early hybridization and adaptive loci shaping the radiation of Lake Tanganyika cichlid fishes. Nature Communications 9. https://doi.org/10.1038/s41467-018-05479-9

Izquierdo I, Martín Esquivel J, Zurita N, M.Arechavaleta (2004) Lista de especies silvestres de Canarias. Hongos, plantas y animales terrestres 2004.

Kallal RJ, Kulkarni SS, Dimitrov D, Benavides LR, Arnedo MA, Giribet G, Hormiga G (2020) Converging on the orb: denser taxon sampling elucidates spider phylogeny and new analytical methods support repeated evolution of the orb web. Cladistics n/a. https://doi.org/https://doi.org/10.1111/cla.12439

Kapli P, Lutteropp S, Zhang J, Kobert K, Pavlidis P, Stamatakis A, Flouri T (2017) Multi-rate Poisson tree processes for single-locus species delimitation under maximum likelihood and Markov chain Monte Carlo. Bioinformatics 33: 1630–1638. https://doi.org/10.1093/bioinformatics/btx025

Keymer JE, Marquet PA, Velasco-Hernández JX, Levin SA (2000) Extinction Thresholds and Metapopulation Persistence in Dynamic Landscapes. The American naturalist 156: 478–494. https://doi.org/10.1086/303407

Klügel A, Schwarz S, van den Bogaard P, Hoernle KA, Wohlgemuth-Ueberwasser CC, Köster JJ (2009) Structure and evolution of the volcanic rift zone at Ponta de São Lourenço, eastern Madeira. Bulletin of Volcanology 71: 671–685. https://doi.org/10.1007/s00445-008-0253-7

Kueffer C, Kaiser-Bunbury CN (2014) Reconciling conflicting perspectives for biodiversity conservation in the Anthropocene. Frontiers in Ecology and the Environment 12: 131–137. https://doi.org/10.1890/120201

Kulkarni S, Kallal RJ, Wood H, Dimitrov D, Giribet G, Hormiga G (2021) Interrogating Genomic-Scale Data to Resolve Recalcitrant Nodes in the Spider Tree of Life. Molecular Biology and Evolution 38: 891–903. https://doi.org/10.1093/molbev/msaa251

Langlands PR, Framenau VW (2010) Systematic revision of Hoggicosa Roewer, 1960, the Australian "bicolor" group of wolf spiders (Araneae: Lycosidae). Zoological Journal of

the Linnean Society 158: 83–123. https://doi.org/10.1111/j.1096-3642.2009.00545.x

Lerner HRL, Meyer M, James HF, Hofreiter M, Fleischer RC (2011) Multilocus Resolution of
Phylogeny and Timescale in the Extant Adaptive Radiation of Hawaiian Honeycreepers.
Current Biology 21: 1838–1844.
https://doi.org/https://doi.org/10.1016/j.cub.2011.09.039

Losos JB (2009) Lizards in an Evolutionary Tree. 1st ed. University of California Press.
Available from: http://www.jstor.org.sire.ub.edu/stable/10.1525/j.ctt1pnj59.

Losos JB, Ricklefs RE (2009) Adaptation and diversification on islands. Nature 457: 830–836.
https://doi.org/10.1038/nature07893

MacArthur R, Wilson E (1967) The theory of island biogeography. Princeton University Press,
Princeton, N.J., 203 pp.

Machado A, Rodríguez-Expósito E, López M, Hernández M (2017) Phylogenetic analysis of
the genus laparocerus, with comments on colonisation and diversification in
macaronesia (coleoptera, curculionidae, entiminae). ZooKeys 2017: 1–77.
https://doi.org/10.3897/zookeys.651.10097

Macías-Hernández N, Oromí P, Arnedo M (2008) Patterns of diversification on old volcanic
islands as revealed by the woodlouse-hunter spider genus Dysdera (Araneae,
Dysderidae) in the eastern Canary Islands. Biological Journal of the Linnean Society 94:
589–615. https://doi.org/10.1111/j.1095-8312.2008.01007.x

Macías-Hernández N, Oromí P, Arnedo M (2010) Integrative taxonomy uncovers hidden
species diversity in woodlouse hunter spiders (Araneae, Dysderidae) endemic to the
Macaronesian archipelagos. Systematics and Biodiversity 8: 531–553.
https://doi.org/10.1080/14772000.2010.535865

Macías-Hernández N, Bidegaray-Batista L, Emerson B, Oromí P, Arnedo M (2013) The
imprint of geologic history on within-island diversification of woodlouse-hunter spiders
(Araneae, Dysderidae) in the canary islands. Journal of Heredity 104: 341–356.
https://doi.org/10.1093/jhered/est008

Malumbres-Olarte J, Boieiro M, Cardoso P, Carvalho R, Crespo LCF, Gabriel R, Hernández

NM, Paulo OS, Pereira F, Rego C, Ros-Prieto A, Silva I, Vieira A, Rigal F, Borges PAV (2020) Standardised inventories of spiders (arachnida, araneae) of macaronesia ii: The native forests and dry habitats of madeira archipelago (Madeira and Porto Santo islands). Biodiversity Data Journal 8. https://doi.org/10.3897/BDJ.8.e47502

Mayden R (1997) A hierarchy of species concepts : the denouement in the saga of the species problem. In: Claridge M, Dawah H, Wilson M (Eds), Species: The units of biodiversity. Chapman and Hall, London, 381–424.

Mayr E (1982) The growth of biological thought : diversity, evolution, and inheritance. Available from: http://catalog.hathitrust.org/api/volumes/oclc/7875904.html.

Michalik P, Ramírez MJ (2014) Arthropod Structure & Development Evolutionary morphology of the male reproductive system , spermatozoa and seminal fl uid of spiders (Araneae , Arachnida) e Current knowledge and future directions *. 43. https://doi.org/10.1016/j.asd.2014.05.005

Minh BQ, Schmidt HA, Chernomor O, Schrempf D, Woodhams MD, von Haeseler A, Lanfear R (2020) IQ-TREE 2: New Models and Efficient Methods for Phylogenetic Inference in the Genomic Era. Molecular Biology and Evolution 37: 1530–1534. https://doi.org/10.1093/molbev/msaa015

Monaghan MT, Wild R, Elliot M, Fujisawa T, Balke M, Inward DJG, Lees DC, Ranaivosolo R, Eggleton P, Barraclough TG, Vogler AP (2009) Accelerated Species Inventory on Madagascar Using Coalescent-Based Models of Species Delineation. Systematic Biology 58: 298–311. https://doi.org/10.1093/sysbio/syp027

Murphy NP, Framenau VW, Donnellan SC, Harvey MS, Park Y, Austin AD (2006) Phylogenetic reconstruction of the wolf spiders (Araneae : Lycosidae) using sequences from the 12S rRNA , 28S rRNA , and NADH1 genes : Implications for classification , biogeography , and the evolution of web building behavior. 38: 583–602. https://doi.org/10.1016/j.ympev.2005.09.004

Piacentini LN, Ramírez MJ (2019) Hunting the wolf: A molecular phylogeny of the wolf spiders (Araneae, Lycosidae). Molecular Phylogenetics and Evolution 136: 227–240. https://doi.org/10.1016/j.ympev.2019.04.004

Platnick NI, Coddington JA, Forster RR, Griswold CE (1991) Spinneret morphology and the phylogeny of haplogyne spiders (Araneae, Araneomorphae). American Museum novitates ; no. 3016. Available from: http://digitallibrary.amnh.org/dspace/handle/2246/5043.

Puillandre N, Lambert A, Brouillet S, Achaz G (2012) ABGD, Automatic Barcode Gap Discovery for primary species delimitation. Molecular Ecology 21: 1864–1877. https://doi.org/10.1111/j.1365-294X.2011.05239.x

de Queiroz K (2005) Ernst Mayr and the modern concept of species. Proceedings of the National Academy of Sciences of the United States of America 102 Suppl: 6600–6607. https://doi.org/10.1073/pnas.0502030102

De Queiroz K (2007) Species concepts and species delimitation. Systematic Biology 56: 879–886. https://doi.org/10.1080/10635150701701083

Ramalho RS, Brum Da Silveira A, Fonseca PE, Madeira J, Cosca M, Cachão M, Fonseca MM, Prada SN (2015) The emergence of volcanic oceanic islands on a slow-moving plate: The example of Madeira Island, NE Atlantic. Geochemistry, Geophysics, Geosystems 16: 522–537. https://doi.org/10.1002/2014GC005657

Ratnasingham S, Hebert PDN (2013) A DNA-Based Registry for All Animal Species: The Barcode Index Number (BIN) System. PLOS ONE 8: e66213. Available from: https://doi.org/10.1371/journal.pone.0066213.

Rezac M, Pekàr S, Lubin Y (2008) How oniscophagous spiders overcome woodlouse armour. Journal of Zoology 275: 64–71. https://doi.org/10.1111/j.1469-7998.2007.00408.x

Roewer C (1960) Araneae Lycosaeformia II (Lycosidae) (Fortsetzung und Schluss). Exploration du Parc National de l'Upemba, Mission G. F. de Witte 55: 519–1040.

Ronquist F, Teslenko M, Van Der Mark P, Ayres DL, Darling A, Höhna S, Larget B, Liu L, Suchard MA, Huelsenbeck JP (2012) Mrbayes 3.2: Efficient bayesian phylogenetic inference and model choice across a large model space. Systematic Biology 61: 539–542. https://doi.org/10.1093/sysbio/sys029

Rundell RJ, Price TD (2009) Adaptive radiation, nonadaptive radiation, ecological speciation

and nonecological speciation. Trends in Ecology and Evolution 24: 394–399. https://doi.org/10.1016/j.tree.2009.02.007

Rzhetsky A, Nei M (1992) Statistical properties of the ordinary least-squares, generalized least-squares, and minimum-evolution methods of phylogenetic inference. Journal of molecular evolution 35: 367–375. https://doi.org/10.1007/BF00161174

Saitou N, Nei M (1987) The neighbor-joining method: a new method for reconstructing phylogenetic trees. Molecular Biology and Evolution 4: 406–425. https://doi.org/10.1093/oxfordjournals.molbev.a040454

Satler JD, Carstens BC, Hedin M (2013) Multilocus Species Delimitation in a Complex of Morphologically Conserved Trapdoor Spiders (Mygalomorphae, Antrodiaetidae, Aliatypus). Systematic Biology 62: 805–823. https://doi.org/10.1093/sysbio/syt041

Schluter D (1988) The Evolution of Finch Communities on Islands and Continents: Kenya vs. Galapagos. Ecological Monographs 58: 229–249. https://doi.org/https://doi.org/10.2307/1942538

Schwarz S, Klügel A, van den Bogaard P, Geldmacher J (2005) Internal structure and evolution of a volcanic rift system in the eastern North Atlantic: The Desertas rift zone, Madeira archipelago. Journal of Volcanology and Geothermal Research 141: 123–155. https://doi.org/10.1016/j.jvolgeores.2004.10.002

Soulebeau A, Aubriot X, Gaudeul M, Rouhan G, Hennequin S, Haevermans T, Dubuisson JY, Jabbour F (2015) The hypothesis of adaptive radiation in evolutionary biology: hard facts about a hazy concept. Organisms Diversity and Evolution 15: 747–761. https://doi.org/10.1007/s13127-015-0220-z

Stamatakis A (2014) RAxML version 8: a tool for phylogenetic analysis and post-analysis of large phylogenies. Bioinformatics (Oxford, England) 30: 1312–1313. https://doi.org/10.1093/bioinformatics/btu033

Stratton GE (2005) EVOLUTION OF ORNAMENTATION AND COURTSHIP BEHAVIOR IN SCHIZOCOSA: INSIGHTS FROM A PHYLOGENY BASED ON MORPHOLOGY (ARANEAE, LYCOSIDAE). The Journal of Arachnology 33: 347–376. https://doi.org/10.1636/04-80.1

Talavera G, Dincă V, Vila R (2013) Factors affecting species delimitations with the GMYC model: insights from a butterfly survey. Methods in Ecology and Evolution 4: 1101–1110. https://doi.org/https://doi.org/10.1111/2041-210X.12107

Tang CQ, Humphreys AM, Fontaneto D, Barraclough TG (2014) Effects of phylogenetic reconstruction method on the robustness of species delimitation using single-locus data. Methods in Ecology and Evolution 5: 1086–1094. https://doi.org/https://doi.org/10.1111/2041-210X.12246

Telford MJ, Budd GE (2003) The place of phylogeny and cladistics in Evo-Devo research. The International journal of developmental biology 47: 479–490.

Tongiorgi P (1977) Fam. Lycosidae. In La faune terrestre de l'île de Sainte-Hélène. IV. Annales, Musée Royal de l'Afrique Centrale, Sciences zoologiques (Zool.-Ser. 8°) 220: 105–125.

Triantis KA, Borges PA V, Ladle RJ, Hortal J, Cardoso P, Gaspar C, Dinis F, Mendonça E, Silveira LMA, Gabriel R, Melo C, Santos AMC, Amorim IR, Ribeiro SP, Serrano ARM, Quartau JA, Whittaker RJ (2010) Extinction debt on oceanic islands. Ecography 33: 285–294. https://doi.org/https://doi.org/10.1111/j.1600-0587.2010.06203.x

Uetz GW, Roberts JA (2002) Multisensory cues and multimodal communication in spiders: insights from video/audio playback studies. Brain, behavior and evolution 59: 222–230. https://doi.org/10.1159/000064909

Unesco World Heritage Committee (1999) Twenty-third session: Convention concerning the protection of the cultural and natural heritage. Available from: http://whc.unesco.org/archive/1999/whc-99-conf209-22e.pdf.

Vaccaro R, Uetz G, Roberts J (2010) Courtship and mating behavior of the wolf spider Schizocosa bilineata (Araneae: Lycosidae). Journal of Arachnology 38: 452–459. https://doi.org/10.1636/Hi09-115.1

Wheeler WC, Coddington JA, Crowley LM, Dimitrov D, Goloboff PA, Griswold CE, Hormiga G, Prendini L, Ramírez MJ, Sierwald P, Almeida-Silva L, Alvarez-Padilla F, Arnedo MA, Benavides Silva LR, Benjamin SP, Bond JE, Grismado CJ, Hasan E, Hedin M, Izquierdo MA, Labarque FM, Ledford J, Lopardo L, Maddison WP, Miller JA, Piacentini LN, Platnick

NI, Polotow D, Silva-Dávila D, Scharff N, Szűts T, Ubick D, Vink CJ, Wood HM, Zhang J (2017) The spider tree of life: phylogeny of Araneae based on target-gene analyses from an extensive taxon sampling. Cladistics 33: 574–616. https://doi.org/10.1111/cla.12182

Whittaker RJ, Fernández-Palacios JM, Matthews TJ, Borregaard MK, Triantis KA (2017) Island biogeography: Taking the long view of nature's laboratories. Science 357: eaam8326. https://doi.org/10.1126/science.aam8326

Whittaker RJ, Araújo MB, Jepson P, Ladle RJ, Watson JEM, Willis KJ (2005) Conservation Biogeography: assessment and prospect. Diversity and Distributions 11: 3–23. https://doi.org/https://doi.org/10.1111/j.1366-9516.2005.00143.x

Wood JR, Alcover JA, Blackburn TM, Bover P, Duncan RP, Hume JP, Louys J, Meijer HJM, Rando JC, Wilmshurst JM (2017) Island extinctions: Processes, patterns, and potential for ecosystem restoration. Environmental Conservation 44: 348–358. https://doi.org/10.1017/S037689291700039X

World Spider Catalog (2021) World Spider Catalog. Natural History Museum Bern, online at http://wsc.nmbe.ch, version 22.0, accessed on 21.04.2021. https://doi.org/10.24436/2

Wray GA, Levinton JS, Shapiro LH (1996) Molecular Evidence for Deep Precambrian Divergences Among Metazoan Phyla. Science 274: 568 LP – 573. https://doi.org/10.1126/science.274.5287.568

Wunderlich J (1987) Die Spinnen der Kanarischen Inseln und Madeiras: Adaptive Radiation, Biogeographie, Revisionen und Neubeschreibungen. Triops, 435 pp.

Wunderlich J (1992) Die Spinnen-Fauna der Makaronesischen Inseln: Taxonomie, Ökologie, Biogeographie und Evolution. Beiträge zur Araneologie 1: 1–619.

Wunderlich J (1995) Zu Ökologie, Biogeographie, Evolution und Taxonomie einiger Spinnen der Makaronesischen Inseln (Arachnida: Araneae). Beiträge zur Araneologie 4: 385–439.

Yang Z, Rannala B (2010) Bayesian species delimitation using multilocus sequence data. Proceedings of the National Academy of Sciences 107: 9264 LP – 9269.

https://doi.org/10.1073/pnas.0913022107

Zhang J, Kapli P, Pavlidis P, Stamatakis A (2013) A general species delimitation method with
applications to phylogenetic placements. Bioinformatics (Oxford, England) 29: 2869–
2876. https://doi.org/10.1093/bioinformatics/btt499

Zuckerlandl E, Pauling L (1965) Evolutionary Divergence and Convergence in Proteins. In:
Bryson V, Vogel HJBT-EG and P (Eds), Academic Press, 97–166.
https://doi.org/https://doi.org/10.1016/B978-1-4832-2734-4.50017-6

Annex I

Supplementary Materials for Chapter 1

Table S1. List of specimens used in the molecular analysis with voucher specifications, GenBank accession numbers and collecting data. Sequences with DNA codes were newly generated in the present study. Superscript letters in COI indicate shared haplotypes. Subfamily, Genus, Species: taxonomic category; sex: life cycle stage; type: type material status of the specimen; collection code: collection number of the specimen; DNA code: DNA extraction code; COI, 16S, NAD1, 28S, H3: accession numbers for the corresponding genes; Country, Island, Locality: locality information; Additional site information: habitat characteristics; Coordinates: decimal latitude and longitude; Altitude: elevation in meters as inferred from the GPS coordinates with https://www.freemaptools.com/elevation-finder.htm.

Subfamily	Genus	Species	sex	type	collection code	DNA code	COI	16S	NAD1	28S	H3	Country	Island	Locality	Altitude	Additional site information	Coordinates
Dysderinae	*Dysdera*	*coiffaiti*	juv		CRBALC0114	lc071	MT372210	MT374368	MT374292	MT373173	MT374331	Portugal	Bugio	Planalto Sul	322 m	this is the only accessible flat area of this island	N 32.41228° W 16.47466°
Dysderinae	*Dysdera*	*coiffaiti*	♀		CRBA002500	pk100	MT372211					Portugal	Bugio	Planalto Sul	322 m	this is the only accessible flat area of this island	N 32.41228° W 16.47466°
Dysderinae	*Dysdera*	*coiffaiti*	♀		CRBA002501	pk101	MT372212					Portugal	Bugio	Planalto Sul	322 m	this is the only accessible flat area of this island	N 32.41228° W 16.47466°
Dysderinae	*Dysdera*	*coiffaiti*	♀		CRBA002562	pk678	MT372222^w					Portugal	Deserta Grande	Pedregal (E)	339 m	the easternmost flank of the barren plateau presents some hills with scarce vegetation	N 32.54613° W 16.52340°
Dysderinae	*Dysdera*	*coiffaiti*	♀		CRBA002563	pk679	MT372222^w					Portugal	Deserta Grande	Pedregal (E)	339 m	the easternmost flank of the barren plateau presents some hills with scarce vegetation	N 32.54613° W 16.52340°
Dysderinae	*Dysdera*	*coiffaiti*	♀		CRBALC0211	lc130	MT372223^i					Portugal	Deserta Grande	Pedregal (E)	339 m	the easternmost flank of the barren plateau presents some hills with scarce vegetation	N 32.54613° W 16.52340°
Dysderinae	*Dysdera*	*coiffaiti*	♀		CRBA002539	pk80	MT372214					Portugal	Deserta Grande	Planalto Sul	220 m	the largest flat area in the southern half of Deserta Grande	N 32.50596° W 16.49986°
Dysderinae	*Dysdera*	*coiffaiti*	♀		NMH001599	k525	MT372220^a					Portugal	Deserta Grande	Rocha do Barbusano	442 m	the area around the summit of Deserta Grande	N 32.53535° W 16.51782°
Dysderinae	*Dysdera*	*coiffaiti*	♀		NMH001600	k527	MT372221					Portugal	Deserta Grande	Rocha do Barbusano	442 m	the area around the summit of Deserta Grande	N 32.53535° W 16.51782°
Dysderinae	*Dysdera*	*coiffaiti*	♂		CRBALC0210	lc129	MT372220^a					Portugal	Deserta Grande	Rocha do Barbusano	442 m	the area around the summit of Deserta Grande	N 32.53535° W 16.51782°
Dysderinae	*Dysdera*	*coiffaiti*	♂		CRBA002541	pk82	MT372225					Portugal	Deserta Grande	Rocha do Barbusano	442 m	the area around the summit of Deserta Grande	N 32.53535° W 16.51782°
Dysderinae	*Dysdera*	*coiffaiti*	♂		CRBALC0076	lc048	MT372213					Portugal	Deserta Grande	Rocha do Barbusano (S)	401 m	a small valley South to Rocha do Barbusano, with a relevant cover of native vegetation	N 32.53168° W 16.51471°
Dysderinae	*Dysdera*	*coiffaiti*	juv		CRBALC0078	lc050	MT372218					Portugal	Deserta Grande	Rocha do Barbusano (S)	401 m	a small valley South to Rocha do Barbusano, with a relevant cover of native vegetation	N 32.53168° W 16.51471°
Dysderinae	*Dysdera*	*coiffaiti*	juv		CRBALC0081	lc053	MT372219^e					Portugal	Deserta Grande	Rocha do Barbusano (S)	401 m	a small valley South to Rocha do Barbusano, with a relevant cover of native vegetation	N 32.53168° W 16.51471°
Dysderinae	*Dysdera*	*coiffaiti*	juv		CRBALC0082	lc054	MT372216^f					Portugal	Deserta Grande	Rocha do Barbusano (S)	401 m	a small valley South to Rocha do Barbusano, with a relevant cover of native vegetation	N 32.53168° W 16.51471°
Dysderinae	*Dysdera*	*coiffaiti*	juv		CRBALC0084	lc056	MT372215^g					Portugal	Deserta Grande	Rocha do Barbusano (S)	401 m	a small valley South to Rocha do Barbusano, with a relevant cover of native vegetation	N 32.53168° W 16.51471°
Dysderinae	*Dysdera*	*coiffaiti*	juv		CRBALC0101	lc058	MT372217					Portugal	Deserta Grande	Rocha do Barbusano (S)	401 m	a small valley South to Rocha do Barbusano, with a relevant cover of native vegetation	N 32.53168° W 16.51471°
Dysderinae	*Dysdera*	*coiffaiti*	juv		CRBALC0105	lc062	MT372219^e					Portugal	Deserta Grande	Rocha do Barbusano (S)	401 m	a small valley South to Rocha do Barbusano, with a relevant cover of native vegetation	N 32.53168° W 16.51471°
Dysderinae	*Dysdera*	*coiffaiti*	juv		CRBALC0104	lc061	MT372216^f					Portugal	Deserta Grande	Rocha do Barbusano (S)	401 m	a small valley South to Rocha do Barbusano, with a relevant cover of native vegetation	N 32.53168° W 16.51471°
Dysderinae	*Dysdera*	*coiffaiti*	♂		CRBALC0106	lc063	MT372215^g					Portugal	Deserta Grande	Rocha do Barbusano (S)	401 m	a small valley South to Rocha do Barbusano, with a relevant cover of native vegetation	N 32.53168° W 16.51471°
Dysderinae	*Dysdera*	*coiffaiti*	♂		CRBALC0107	lc064	MT372215^g					Portugal	Deserta Grande	Rocha do Barbusano (S)	401 m	a small valley South to Rocha do Barbusano, with a relevant cover of native vegetation	N 32.53168° W 16.51471°
Dysderinae	*Dysdera*	*coiffaiti*	♂		CRBALC0108	lc065	MT372215^g					Portugal	Deserta Grande	Rocha do Barbusano (S)	401 m	a small valley South to Rocha do Barbusano, with a relevant cover of native vegetation	N 32.53168° W 16.51471°
Dysderinae	*Dysdera*	*coiffaiti*	juv		CRBALC0112	lc069	MT372223^i					Portugal	Deserta Grande	Pedregal (E)	339 m	the easternmost flank of the barren plateau presents some hills with scarce vegetation	N 32.54613° W 16.52340°
Dysderinae	*Dysdera*	*coiffaiti*	♀		CRBALC0109	lc066	MT372215^g					Portugal	Deserta Grande	Rocha do Barbusano (S)	401 m	a small valley South to Rocha do Barbusano, with a relevant cover of native vegetation	N 32.53168° W 16.51471°
Dysderinae	*Dysdera*	*coiffaiti*	juv		CRBALC0102	lc059	MT372217^h					Portugal	Deserta Grande	Rocha do Barbusano (S)	401 m	a small valley South to Rocha do Barbusano, with a relevant cover of native vegetation	N 32.53168° W 16.51471°
Dysderinae	*Dysdera*	*coiffaiti*	juv		CRBALC0113	lc070	MT372223^i					Portugal	Deserta Grande	Pedregal (E)	339 m	the easternmost flank of the barren plateau presents some hills with scarce vegetation	N 32.54613° W 16.52340°
Dysderinae	*Dysdera*	*coiffaiti*	♀		CRBALC0005	lc005	MT372182					Portugal	Madeira	Caramujo	1260 m	the area surrounding the Lagoa do Caramujo, with *Erica* spp. woodland	N 32.77161° W 17.06205°

Subfamily	Genus	Species	Stage	Voucher	Code	Accession	Country	Island	Locality	Altitude	Habitat	Coordinates
Dysderinae	*Dysdera*	*coiffaiti*	juv	CRBALC0009	lc009	MT372190	Portugal	Madeira	Caramujo	1260 m	the area surrounding the Lagoa do Caramujo, with *Erica* spp. woodland	N 32.77161° W 17.06205°
Dysderinae	*Dysdera*	*coiffaiti*	♂	MZB 2019-1961	pk88	MT372227	Portugal	Madeira	Chão da Ribeira	525 m	laurel forest patch	N 32.79349° W 17.11219°
Dysderinae	*Dysdera*	*coiffaiti*	♀	CRBA002548	pk89	MT372228	Portugal	Madeira	Chão da Ribeira	525 m	laurel forest patch	N 32.79349° W 17.11219°
Dysderinae	*Dysdera*	*coiffaiti*	♀	MZB 2019-1960	k522	MT372179	Portugal	Madeira	Chão dos Louros	827 m	laurel forest patch	N 32.75989° W 17.01727°
Dysderinae	*Dysdera*	*coiffaiti*	♂	MZB 2019-1959	k530	MT372196	Portugal	Madeira	Chão dos Louros	827 m	laurel forest patch	N 32.75989° W 17.01727°
Dysderinae	*Dysdera*	*coiffaiti*	♂	CRBA002549	pk90	MT372188	Portugal	Madeira	Chão dos Louros	827 m	laurel forest patch	N 32.75989° W 17.01727°
Dysderinae	*Dysdera*	*coiffaiti*	♂	LCPC	pk91	MT372197	Portugal	Madeira	Chão dos Louros	827 m	laurel forest patch	N 32.75989° W 17.01727°
Dysderinae	*Dysdera*	*coiffaiti*	♀	CRBALC0479	lc143	MT372200	Portugal	Madeira	Fajã da Nogueira	936 m	laurel forest patch	N 32.74053° W 16.91874°
Dysderinae	*Dysdera*	*coiffaiti*	♂	FMNH KN.17854	pk93	MT372158[b]	Portugal	Madeira	Fanal		laurel forest patch	undetermined location
Dysderinae	*Dysdera*	*coiffaiti*	♀	CRBA002504	pk222	MT372166	Portugal	Madeira	Fanal		laurel forest patch	undetermined location
Dysderinae	*Dysdera*	*coiffaiti*	♂	CRBA002508	pk225	MT372178	Portugal	Madeira	Fanal		laurel forest patch	undetermined location
Dysderinae	*Dysdera*	*coiffaiti*	♀	LCPC	pk226	MT372175	Portugal	Madeira	Fanal		laurel forest patch	undetermined location
Dysderinae	*Dysdera*	*coiffaiti*	♀	FMNH KN.17855	pk92	MT372169	Portugal	Madeira	Fanal		laurel forest patch	undetermined location
Dysderinae	*Dysdera*	*coiffaiti*	♂	CRBA002553	pk94	MT372172	Portugal	Madeira	Fanal		laurel forest patch	undetermined location
Dysderinae	*Dysdera*	*coiffaiti*	♀	MZB 2019-1962	pk95	MT372173	Portugal	Madeira	Fanal		laurel forest patch	undetermined location
Dysderinae	*Dysdera*	*coiffaiti*	♂	MMF 47910	pk96	MT372174	Portugal	Madeira	Fanal		laurel forest patch	undetermined location
Dysderinae	*Dysdera*	*coiffaiti*	♀	CRBALC0478	lc142	MT372165	Portugal	Madeira	Fanal (I)	1260 m	Erica shrubland	N 32.79213° W 17.12957°
Dysderinae	*Dysdera*	*coiffaiti*	♂	CRBALC0023	lc023	MT372159	Portugal	Madeira	Fanal (II)	795 m	laurel forest patch	N 32.82816° W 17.15780°
Dysderinae	*Dysdera*	*coiffaiti*	juv	CRBALC0024	lc024	MT372161	Portugal	Madeira	Fanal (II)	795 m	laurel forest patch	N 32.82816° W 17.15780°
Dysderinae	*Dysdera*	*coiffaiti*	juv	CRBALC0025	lc025	MT372162	Portugal	Madeira	Fanal (II)	795 m	laurel forest patch	N 32.82816° W 17.15780°
Dysderinae	*Dysdera*	*coiffaiti*	juv	CRBALC0026	lc026	MT372163	Portugal	Madeira	Fanal (II)	795 m	laurel forest patch	N 32.82816° W 17.15780°
Dysderinae	*Dysdera*	*coiffaiti*	juv	CRBALC0027	lc027	MT372168	Portugal	Madeira	Fanal (II)	795 m	laurel forest patch	N 32.82816° W 17.15780°
Dysderinae	*Dysdera*	*coiffaiti*	juv	CRBALC0028	lc028	MT372160	Portugal	Madeira	Fanal (II)	795 m	laurel forest patch	N 32.82816° W 17.15780°
Dysderinae	*Dysdera*	*coiffaiti*	juv	CRBALC0029	lc029	MT372170	Portugal	Madeira	Fanal (III)	836 m	laurel forest patch	N 32.82706° W 17.15871°
Dysderinae	*Dysdera*	*coiffaiti*	♂	CRBALC0030	lc030	MT372167	Portugal	Madeira	Fanal (IV)	904 m	laurel forest patch	N 32.82306° W 17.15336°
Dysderinae	*Dysdera*	*coiffaiti*	juv	CRBALC0031	lc031	MT372158[b]	Portugal	Madeira	Fanal (V)	760 m	laurel forest patch	N 32.83020° W 17.15850°
Dysderinae	*Dysdera*	*coiffaiti*	♂	CRBA3044	lc149	MT372206[t]	Portugal	Madeira	Funduras (I)	636 m	mixed woodland patch, with both exotic and native tree species	N 32.75618° W 16.80047°
Dysderinae	*Dysdera*	*coiffaiti*	♀	CRBA3046	lc150	MT372209	Portugal	Madeira	Funduras (I)	636 m	mixed woodland patch, with both exotic and native tree species	N 32.75618° W 16.80047°
Dysderinae	*Dysdera*	*coiffaiti*	♂	CRBA3049	lc151	MT372206[t]	Portugal	Madeira	Funduras (I)	636 m	mixed woodland patch, with both exotic and native tree species	N 32.75618° W 16.80047°
Dysderinae	*Dysdera*	*coiffaiti*	♂	CRBA3048	lc152	MT372206[t]	Portugal	Madeira	Funduras (I)	636 m	mixed woodland patch, with both exotic and native tree species	N 32.75618° W 16.80047°
Dysderinae	*Dysdera*	*coiffaiti*	♀	CRBALC0006	lc006	MT372189	Portugal	Madeira	Funduras (II)	627 m	a mixed woodland patch, with both exotic and native tree species, and some areas with the fern Woodwardia radicans	N 32.75542° W 16.79785°

Dysderinae	*Dysdera*	*coiffaiti*	♂	CRBALC0011	lc011	MT372207					Portugal	Madeira	Funduras (II)	627 m	a mixed woodland patch, with both exotic and native tree species, and some areas with the fern Woodwardia radicans	N 32.75542° W 16.79785°
Dysderinae	*Dysdera*	*coiffaiti*	♀	CRBALC0032	lc032	MT372208					Portugal	Madeira	Funduras (II)	627 m	a mixed woodland patch, with both exotic and native tree species, and some areas with the fern Woodwardia radicans	N 32.75542° W 16.79785°
Dysderinae	*Dysdera*	*coiffaiti*	♂	CRBALC0477	lc141	MT372171					Portugal	Madeira	Galhano (S)	1247 m	woodland of Erica trees in the superior eastern slope leading to Galhano	N 32.78924° W 17.17855°
Dysderinae	*Dysdera*	*coiffaiti*	♀	ZMUC	k131	AF244251					Portugal	Madeira	Levada dos Cedros (Fanal)		laurel forest patch	undetermined location
Dysderinae	*Dysdera*	*coiffaiti*	♀	MMF 47909	pk221	MT372229					Portugal	Madeira	Levada dos Tornos	648 m	laurel forest patch	N 32.77150° W 16.96550°
Dysderinae	*Dysdera*	*coiffaiti*	♀	CRBALC0222	lc138	MT372176					Portugal	Madeira	Montado dos Pessegueiros	1384 m	the contiguous areas around the trail winding into this patch of laurel forest	N 32.79333° W 17.09576°
Dysderinae	*Dysdera*	*coiffaiti*	juv	CRBALC0457	lc139	MT372184					Portugal	Madeira	Montado dos Pessegueiros	1384 m	the contiguous areas around the trail winding into this patch of laurel forest	N 32.79333° W 17.09576°
Dysderinae	*Dysdera*	*coiffaiti*	♀	CRBALC0484	lc146	MT372186					Portugal	Madeira	Montado dos Pessegueiros	1384 m	the contiguous areas around the trail winding into this patch of laurel forest	N 32.79333° W 17.09576°
Dysderinae	*Dysdera*	*coiffaiti*	♀	CRBALC0485	lc147	MT372187					Portugal	Madeira	Montado dos Pessegueiros	1384 m	the contiguous areas around the trail winding into this patch of laurel forest	N 32.79333° W 17.09576°
Dysderinae	*Dysdera*	*coiffaiti*	♀	CRBA3061	lc156	MT372183ᵘ					Portugal	Madeira	Montado dos Pessegueiros	1384 m	the contiguous areas around the trail winding into this patch of laurel forest	N 32.79333° W 17.09576°
Dysderinae	*Dysdera*	*coiffaiti*	♀	CRBALC0482	lc145	MT372199ˢ					Portugal	Madeira	Paúl da Serra	1417 m	the largest plateau of Madeira, devoid of native tree cover for a large portion of its area; specimens were found mostly in patches of Erica shrubland	N 32.78182° W 17.09978°
Dysderinae	*Dysdera*	*coiffaiti*	juv	CRBA3043	lc148	MT372199ˢ					Portugal	Madeira	Paúl da Serra	1417 m	the largest plateau of Madeira, devoid of native tree cover for a large portion of its area; specimens were found mostly in patches of Erica shrubland	N 32.78182° W 17.09978°
Dysderinae	*Dysdera*	*coiffaiti*	♀	CRBA002556	pk97	MT372177					Portugal	Madeira	Paúl da Serra	1417 m	the largest plateau of Madeira, devoid of native tree cover for a large portion of its area; specimens were found mostly in patches of Erica shrubland	N 32.78182° W 17.09978°
Dysderinae	*Dysdera*	*coiffaiti*	♀	CRBA002557	pk98	MT372164					Portugal	Madeira	Paúl da Serra	1417 m	the largest plateau of Madeira, devoid of native tree cover for a large portion of its area; specimens were found mostly in patches of Erica shrubland	N 32.78182° W 17.09978°
Dysderinae	*Dysdera*	*coiffaiti*	♂	CRBA3058	lc153	MT372183ᵘ					Portugal	Madeira	Paúl da Serra (N-trail)	1479 m	the trail from Paúl da Serra to Montado dos Pessegueiros	N 32.78837° W 17.09857°
Dysderinae	*Dysdera*	*coiffaiti*	♂	CRBA3059	lc154	MT372191					Portugal	Madeira	Paúl da Serra (N-trail)	1479 m	the trail from Paúl da Serra to Montado dos Pessegueiros	N 32.78837° W 17.09857°
Dysderinae	*Dysdera*	*coiffaiti*	♂	CRBA3060	lc155	MT372203					Portugal	Madeira	Paúl da Serra (N-trail)	1479 m	the trail from Paúl da Serra to Montado dos Pessegueiros	N 32.78837° W 17.09857°
Dysderinae	*Dysdera*	*coiffaiti*	♀	CRBA3062	lc157	MT372185					Portugal	Madeira	Paúl da Serra (N-trail)	1479 m	the trail from Paúl da Serra to Montado dos Pessegueiros	N 32.78837° W 17.09857°
Dysderinae	*Dysdera*	*coiffaiti*	♀	CRBA3063	lc158	MT372204					Portugal	Madeira	Paúl da Serra (N-trail)	1479 m	the trail from Paúl da Serra to Montado dos Pessegueiros	N 32.78837° W 17.09857°
Dysderinae	*Dysdera*	*coiffaiti*	♀	CRBALC0001	lc001	MT372192					Portugal	Madeira	Queimadas	931 m	laurel forest patch	N 32.78108° W 16.90223°
Dysderinae	*Dysdera*	*coiffaiti*	♀	CRBALC0003	lc003	MT372180					Portugal	Madeira	Queimadas	931 m	laurel forest patch	N 32.78108° W 16.90223°
Dysderinae	*Dysdera*	*coiffaiti*	♀	CRBALC0004	lc004	MT372193					Portugal	Madeira	Queimadas	931 m	laurel forest patch	N 32.78108° W 16.90223°
Dysderinae	*Dysdera*	*coiffaiti*	juv	CRBALC0008	lc008	MT372194					Portugal	Madeira	Queimadas	931 m	laurel forest patch	N 32.78108° W 16.90223°
Dysderinae	*Dysdera*	*coiffaiti*	♂	CRBALC0033	lc033	MT372201					Portugal	Madeira	Queimadas	931 m	laurel forest patch	N 32.78108° W 16.90223°
Dysderinae	*Dysdera*	*coiffaiti*	juv	CRBALC0034	lc034	MT372181					Portugal	Madeira	Queimadas	931 m	laurel forest patch	N 32.78108° W 16.90223°
Dysderinae	*Dysdera*	*coiffaiti*	juv	CRBALC0035	lc035	MT372198					Portugal	Madeira	Queimadas	931 m	laurel forest patch	N 32.78108° W 16.90223°
Dysderinae	*Dysdera*	*coiffaiti*	juv	CRBALC0036	lc036	MT372202					Portugal	Madeira	Queimadas	931 m	laurel forest patch	N 32.78108° W 16.90223°
Dysderinae	*Dysdera*	*coiffaiti*	juv	CRBALC0037	lc037	MT372195					Portugal	Madeira	Ribeiro Bonito I	567 m	laurel forest patch	N 32.79582° W 16.93710°
Dysderinae	*Dysdera*	*coiffaiti*	juv	CRBALC0038	lc038	MT372226ᶜ	MT374360	MT374277	MT373168	MT374318	Portugal	Madeira	Ribeiro Bonito II	556 m	laurel forest patch	N 32.79801° W 16.93654°
Dysderinae	*Dysdera*	*coiffaiti*	juv	CRBALC0039	lc039	MT372226ᶜ					Portugal	Madeira	Ribeiro Bonito III	582 m	laurel forest patch	N 32.80462° W 16.93470°
Dysderinae	*Dysdera*	*coiffaiti*	♀	CRBALC0002	lc002	MT372205					Portugal	Madeira	Santo da Serra	1125 m	a mixed woodland area, mainly composed of exotic Pinus, with few small Laurus trees and Erica shrubs	N 32.71942° W 16.85632°

Subfamily	Genus	Species		Type	Voucher	Code	Seq1	Seq2	Seq3	Seq4	Seq5	Country	Region	Locality	Altitude	Habitat	Coordinates
Dysderinae	*Dysdera*	*dissimilis* n. sp.	♂	Pt	FMNH KN.17861	lc085	MT372280					Portugal	Porto Santo	Pico Ana Ferreira	242 m	the area with tree cover nearest to the summit, in the North to Northwest slope	N 33.04442° W 16.36977°
Dysderinae	*Dysdera*	*dissimilis* n. sp.	♀	Pt	MZB 2019-1950	lc086	MT372285[k]					Portugal	Porto Santo	Pico Ana Ferreira	242 m	the area with tree cover nearest to the summit, in the North to Northwest slope	N 33.04442° W 16.36977°
Dysderinae	*Dysdera*	*dissimilis* n. sp.	♀		CRBALC0130	lc087	MT372281[l]					Portugal	Porto Santo	Pico Ana Ferreira	242 m	the area with tree cover nearest to the summit, in the North to Northwest slope	N 33.04442° W 16.36977°
Dysderinae	*Dysdera*	*dissimilis* n. sp.	♀	Pt	CRBALC0131	lc088	MT372217[h]					Portugal	Porto Santo	Pico Ana Ferreira	242 m	the area with tree cover nearest to the summit, in the North to Northwest slope	N 33.04442° W 16.36977°
Dysderinae	*Dysdera*	*dissimilis* n. sp.	juv		CRBALC0139	lc096	MT372286					Portugal	Porto Santo	Pico Ana Ferreira	242 m	the area with tree cover nearest to the summit, in the North to Northwest slope	N 33.04442° W 16.36977°
Dysderinae	*Dysdera*	*dissimilis* n. sp.	juv		CRBALC0140	lc097	MT372282					Portugal	Porto Santo	Pico Ana Ferreira	242 m	the area with tree cover nearest to the summit, in the North to Northwest slope	N 33.04442° W 16.36977°
Dysderinae	*Dysdera*	*dissimilis* n. sp.	juv		CRBALC0142	lc099	MT372287					Portugal	Porto Santo	Pico Ana Ferreira	242 m	the area with tree cover nearest to the summit, in the North to Northwest slope	N 33.04442° W 16.36977°
Dysderinae	*Dysdera*	*dissimilis* n. sp.	juv		CRBALC0166	lc102	MT372284					Portugal	Porto Santo	Pico Ana Ferreira	242 m	the area with tree cover nearest to the summit, in the North to Northwest slope	N 33.04442° W 16.36977°
Dysderinae	*Dysdera*	*dissimilis* n. sp.	juv		CRBALC0141	lc098	MT372285[k]					Portugal	Porto Santo	Pico Ana Ferreira	242 m	the area with tree cover nearest to the summit, in the North to Northwest slope	N 33.04442° W 16.36977°
Dysderinae	*Dysdera*	*dissimilis* n. sp.	juv		CRBALC0168	lc104	MT372285[k]					Portugal	Porto Santo	Pico Ana Ferreira	242 m	the area with tree cover nearest to the summit, in the North to Northwest slope	N 33.04442° W 16.36977°
Dysderinae	*Dysdera*	*dissimilis* n. sp.	♂		LCPC	lc089	MT372281[l]					Portugal	Porto Santo	Pico Ana Ferreira	242 m	the area with tree cover nearest to the summit, in the North to Northwest slope	N 33.04442° W 16.36977°
Dysderinae	*Dysdera*	*dissimilis* n. sp.	juv		CRBALC0138	lc095	MT372281[l]					Portugal	Porto Santo	Pico Ana Ferreira	242 m	the area with tree cover nearest to the summit, in the North to Northwest slope	N 33.04442° W 16.36977°
Dysderinae	*Dysdera*	*dissimilis* n. sp.	♀		CRBA002522	pk240	MT372277					Portugal	Porto Santo	Pico da Juliana	382 m	the area near the summit, in the North slope	N 33.09270° W 16.32186°
Dysderinae	*Dysdera*	*dissimilis* n. sp.	♀	Pt	MMF 47916	pk243	MT372267					Portugal	Porto Santo	Pico da Juliana	382 m	the area near the summit, in the North slope	N 33.09270° W 16.32186°
Dysderinae	*Dysdera*	*dissimilis* n. sp.	♂	Pt	MZB 2019-1949	lc076	MT372270					Portugal	Porto Santo	Pico do Castelo	350 m	NE slope	N 33.08196° W 16.33277°
Dysderinae	*Dysdera*	*dissimilis* n. sp.	♀	Pt	MZB 2019-1948	lc077	MT372272					Portugal	Porto Santo	Pico do Castelo	350 m	NE slope	N 33.08196° W 16.33277°
Dysderinae	*Dysdera*	*dissimilis* n. sp.	♂		CRBALC0122	lc079	MT372274					Portugal	Porto Santo	Pico do Castelo	350 m	NE slope	N 33.08196° W 16.33277°
Dysderinae	*Dysdera*	*dissimilis* n. sp.	♀		LCPC	pk308	MT372273					Portugal	Porto Santo	Pico do Castelo	350 m	NE slope	N 33.08196° W 16.33277°
Dysderinae	*Dysdera*	*dissimilis* n. sp.	♂	Pt	CRBALC0146	lc100	MT372275					Portugal	Porto Santo	Pico do Facho	473 m	the area near the summit, facing North, where a few remaining native trees can be found (Heberdenia excelsa)	N 33.08433° W 16.32174°
Dysderinae	*Dysdera*	*dissimilis* n. sp.	juv		CRBALC0184	lc119	MT372276[n]					Portugal	Porto Santo	Pico do Facho	473 m	the area near the summit, facing North, where a few remaining native trees can be found (Heberdenia excelsa)	N 33.08433° W 16.32174°
Dysderinae	*Dysdera*	*dissimilis* n. sp.	juv		CRBALC0185	lc120	MT372276[n]					Portugal	Porto Santo	Pico do Facho	473 m	the area near the summit, facing North, where a few remaining native trees can be found (Heberdenia excelsa)	N 33.08433° W 16.32174°
Dysderinae	*Dysdera*	*dissimilis* n. sp.	♀		CRBALC0145	lc165	MT372279[o]					Portugal	Porto Santo	Pico do Facho	473 m	the area near the summit, facing North, where a few remaining native trees can be found (Heberdenia excelsa)	N 33.08433° W 16.32174°
Dysderinae	*Dysdera*	*dissimilis* n. sp.	♀		CRBA002529	pk307	MT372271	MT374393	MT374312	MT373197	MT374353	Portugal	Porto Santo	Pico do Facho	473 m	the area near the summit, facing North, where a few remaining native trees can be found (Heberdenia excelsa)	N 33.08433° W 16.32174°
Dysderinae	*Dysdera*	*dissimilis* n. sp.	juv		CRBALC0186	lc121	MT372279[o]					Portugal	Porto Santo	Pico do Facho (N)	467 m	a secluded depression between two opposing slopes in the North flank of the peak, where a patch of decaying Erica bushes was found	N 33.08518° W 16.32364°
Dysderinae	*Dysdera*	*dissimilis* n. sp.	juv		CRBALC0187	lc122	MT372279[o]					Portugal	Porto Santo	Pico do Facho (N)	467 m	a secluded depression between two opposing slopes in the North flank of the peak, where a patch of decaying Erica bushes was found	N 33.08518° W 16.32364°
Dysderinae	*Dysdera*	*dissimilis* n. sp.	juv		CRBALC0189	lc124	MT372279[o]					Portugal	Porto Santo	Pico do Facho (N)	467 m	a secluded depression between two opposing slopes in the North flank of the peak, where a patch of decaying Erica bushes was found	N 33.08518° W 16.32364°
Dysderinae	*Dysdera*	*dissimilis* n. sp.	♂	Ht	MZB 2019-1947	lc134	MT372279[o]					Portugal	Porto Santo	Pico do Facho (N)	467 m	a secluded depression between two opposing slopes in the North flank of the peak, where a patch of decaying Erica bushes was found	N 33.08518° W 16.32364°
Dysderinae	*Dysdera*	*dissimilis* n. sp.	♂		CRBALC0169	lc105	MT372288					Portugal	Porto Santo	Terra-Chã (Pico Branco)	335 m	a small plateau East to Pico Branco's summit, where Pinus trees were planted in terraces	N 33.09447° W 16.29839°
Dysderinae	*Dysdera*	*dissimilis* n. sp.	♀	Pt	FMNH KN.17862	lc135	MT372289	MT374395	MT374310	MT373200	MT374351	Portugal	Porto Santo	Terra-Chã (Pico Branco)	335 m	a small plateau East to Pico Branco's summit, where Pinus trees were planted in terraces	N 33.09447° W 16.29839°
Dysderinae	*Dysdera*	*diversa*	♀		MMF 47902	pk223	MT372244	MT374379	MT374284	-	-	Portugal	Madeira	Caramujo	1260 m	the area surrounding the Lagoa do Caramujo, with woodlands of Erica spp.	N 32.77161° W 17.06205°
Dysderinae	*Dysdera*	*diversa*	♂		MMF 47903	pk224	MT372245	MT374380	MT374285	MT373195	-	Portugal	Madeira	Montado dos Pessegueiros	1384 m	the contiguous areas around the trail winding into this patch of laurel forest	N 32.79333° W 17.09576°

233

Subfamily	Genus	Species	Sex		Voucher	Code						Country	Island	Locality	Elev.	Notes	Coordinates
Dysderinae	Dysdera	exigua n. sp.	♂	Pt	MZB 2019-1939	pk675	MT372246	MT374384	MT374299	MT373203	MT374337	Portugal	Bugio	Planalto Sul	322 m	this is the only accessible flat area of this island	N 32.41228° W 16.47466°
Dysderinae	Dysdera	exigua n. sp.	♀	Pt	CRBALC0212	lc131	MT372251ᵠ	MT374385	MT374300	MT373204	MT374339	Portugal	Deserta Grande	Ponta Sul	191 m	this area is South to Planalto Sul, a small crested canyon as Deserta Grande slopes towards the sea level	N 32.49562° W 16.49562°
Dysderinae	Dysdera	exigua n. sp.	juv		CRBALC0203	lc162	MT372251ᵠ					Portugal	Deserta Grande	Ponta Sul	191 m	this area is South to Planalto Sul, a small crested canyon as Deserta Grande slopes towards the sea level	N 32.49562° W 16.49562°
Dysderinae	Dysdera	exigua n. sp.	♀	Pt	MZB 2019-1937	lc043	MT372247					Portugal	Deserta Grande	Rocha do Barbusano (S)	401 m	a small valley South to Rocha do Barbusano, with a relevant cover of native vegetation	N 32.53168° W 16.51471°
Dysderinae	Dysdera	exigua n. sp.	♀	Pt	MZB 2019-1938	lc044	MT372248ᵈ					Portugal	Deserta Grande	Rocha do Barbusano (S)	401 m	a small valley South to Rocha do Barbusano, with a relevant cover of native vegetation	N 32.53168° W 16.51471°
Dysderinae	Dysdera	exigua n. sp.	♂	Pt	FMNH KN.17856	lc045	MT372248ᵈ					Portugal	Deserta Grande	Rocha do Barbusano (S)	401 m	a small valley South to Rocha do Barbusano, with a relevant cover of native vegetation	N 32.53168° W 16.51471°
Dysderinae	Dysdera	exigua n. sp.	♀	Pt	FMNH KN.17857	lc046	MT372248ᵈ					Portugal	Deserta Grande	Rocha do Barbusano (S)	401 m	a small valley South to Rocha do Barbusano, with a relevant cover of native vegetation	N 32.53168° W 16.51471°
Dysderinae	Dysdera	exigua n. sp.	♀		LCPC	lc047	MT372248ᵈ					Portugal	Deserta Grande	Rocha do Barbusano (S)	401 m	a small valley South to Rocha do Barbusano, with a relevant cover of native vegetation	N 32.53168° W 16.51471°
Dysderinae	Dysdera	exigua n. sp.	juv		CRBALC0085	lc057	MT372249					Portugal	Deserta Grande	Rocha do Barbusano (S)	401 m	a small valley South to Rocha do Barbusano, with a relevant cover of native vegetation	N 32.53168° W 16.51471°
Dysderinae	Dysdera	exigua n. sp.	juv		CRBALC0079	lc051	MT372248ᵈ					Portugal	Deserta Grande	Rocha do Barbusano (S)	401 m	a small valley South to Rocha do Barbusano, with a relevant cover of native vegetation	N 32.53168° W 16.51471°
Dysderinae	Dysdera	exigua n. sp.	juv		CRBALC0080	lc052	MT372248ᵈ					Portugal	Deserta Grande	Rocha do Barbusano (S)	401 m	a small valley South to Rocha do Barbusano, with a relevant cover of native vegetation	N 32.53168° W 16.51471°
Dysderinae	Dysdera	exigua n. sp.	juv		CRBALC0205	lc128	MT372250					Portugal	Deserta Grande	Rocha do Barbusano (S)	401 m	a small valley South to Rocha do Barbusano, with a relevant cover of native vegetation	N 32.53168° W 16.51471°
Dysderinae	Dysdera	isambertoi n. sp.	juv		CRBALC0183	lc118	MT372295ʲ					Portugal	Porto Santo	Pico Branco	318 m	the area near the summit, in the beginning of the trail leading to Terra-Chã	N 33.09428° W 16.30137°
Dysderinae	Dysdera	isambertoi n. sp.	juv		CRBALC0190	lc125	MT372291ᵖ					Portugal	Porto Santo	Pico da Juliana	382 m	the area near the summit, in the North slope	N 33.09270° W 16.32186°
Dysderinae	Dysdera	isambertoi n. sp.	♀		MZB 2019-1952	lc126	MT372291ᵖ					Portugal	Porto Santo	Pico da Juliana	382 m	the area near the summit, in the North slope	N 33.09270° W 16.32186°
Dysderinae	Dysdera	isambertoi n. sp.	♂	Pt	MZB 2019-1953	lc073	MT372290					Portugal	Porto Santo	Pico do Castelo	350 m	NE slope	N 33.08196° W 16.33277°
Dysderinae	Dysdera	isambertoi n. sp.	♀	Pt	MZB 2019-1954	lc074	MT372293					Portugal	Porto Santo	Pico do Castelo	350 m	NE slope	N 33.08196° W 16.33277°
Dysderinae	Dysdera	isambertoi n. sp.	♂	Pt	FMNH KN.17863	lc075	MT372295ʲ					Portugal	Porto Santo	Pico do Castelo	350 m	NE slope	N 33.08196° W 16.33277°
Dysderinae	Dysdera	isambertoi n. sp.	juv		CRBALC0123	lc080	MT372294					Portugal	Porto Santo	Pico do Castelo	350 m	NE slope	N 33.08196° W 16.33277°
Dysderinae	Dysdera	isambertoi n. sp.	juv		CRBALC0124	lc081	MT372299	MT374398	MT374313	MT373189	MT374355	Portugal	Porto Santo	Pico do Castelo	350 m	NE slope	N 33.08196° W 16.33277°
Dysderinae	Dysdera	isambertoi n. sp.	juv		CRBALC0125	lc082	MT372296					Portugal	Porto Santo	Pico do Castelo	350 m	NE slope	N 33.08196° W 16.33277°
Dysderinae	Dysdera	isambertoi n. sp.	juv		CRBALC0126	lc083	MT372297					Portugal	Porto Santo	Pico do Castelo	350 m	NE slope	N 33.08196° W 16.33277°
Dysderinae	Dysdera	isambertoi n. sp.	♀		LCPC	lc116	MT372298					Portugal	Porto Santo	Pico do Facho	473 m	the area near the summit, facing North, where a few remaining native trees can be found (Heberdenia excelsa)	N 33.08433° W 16.32174°
Dysderinae	Dysdera	isambertoi n. sp.	juv		CRBALC0188	lc123	MT372292	MT374400	MT374315	MT373190	MT374357	Portugal	Porto Santo	Pico do Facho (N)	467 m	a secluded depression between two opposing slopes in the North flank of the peak, where a patch of decaying Erica bushes was found	N 33.08518° W 16.32364°
Dysderinae	Dysdera	portisancti	♂		MMF 47906	pk228	MT372301ᵐ					Portugal	Porto Santo	Pico Branco	318 m	the area near the summit, in the beginning of the trail leading to Terra-Chã	N 33.09428° W 16.30137°
Dysderinae	Dysdera	portisancti	♂		LCPC	pk233	MT372301ᵐ					Portugal	Porto Santo	Pico Branco	318 m	the area near the summit, in the beginning of the trail leading to Terra-Chã	N 33.09428° W 16.30137°
Dysderinae	Dysdera	portisancti	♂		FMNH KN.17865	pk238	MT372301ᵐ					Portugal	Porto Santo	Pico Branco	318 m	the area near the summit, in the beginning of the trail leading to Terra-Chã	N 33.09428° W 16.30137°
Dysderinae	Dysdera	portisancti	♀		MMF 47905	pk241	MT372301ᵐ					Portugal	Porto Santo	Pico Branco	318 m	the area near the summit, in the beginning of the trail leading to Terra-Chã	N 33.09428° W 16.30137°
Dysderinae	Dysdera	portisancti	♂		MMF 47904	pk235	MT372303ᵛ					Portugal	Porto Santo	Pico Branco	318 m	the area near the summit, in the beginning of the trail leading to Terra-Chã	N 33.09428° W 16.30137°
Dysderinae	Dysdera	portisancti	♀		MMF 47908	pk239	MT372303ᵛ					Portugal	Porto Santo	Pico Branco	318 m	the area near the summit, in the beginning of the trail leading to Terra-Chã	N 33.09428° W 16.30137°
Dysderinae	Dysdera	portisancti	♀		CRBA002546	pk87	MT372304					Portugal	Porto Santo	Pico Branco	318 m	the area near the summit, in the beginning of the trail leading to Terra-Chã	N 33.09428° W 16.30137°

Dysderinae	Dysdera	portisancti	juv		CRBALC0179	lc114	MT372306	-	MT374286	MT373207	MT374325	Portugal	Porto Santo	Pico do Facho	473 m	the area near the summit, facing North, where a few remaining native trees can be found (Heberdenia excelsa)	N 33.08433° W 16.32174°
Dysderinae	Dysdera	portisancti	♀		FMNH KN.17866	lc106	MT372300					Portugal	Porto Santo	Terra-Chã (Pico Branco)	335 m	a small plateau East to Pico Branco's summit, where Pinus trees were planted in terraces	N 33.09447° W 16.29839°
Dysderinae	Dysdera	portisancti	♀		MZB 2019-1958	lc107	MT372302					Portugal	Porto Santo	Terra-Chã (Pico Branco)	335 m	a small plateau East to Pico Branco's summit, where Pinus trees were planted in terraces	N 33.09447° W 16.29839°
Dysderinae	Dysdera	portisancti	♀		MZB 2019-1956	lc108	MT372301ᵐ					Portugal	Porto Santo	Terra-Chã (Pico Branco)	335 m	a small plateau East to Pico Branco's summit, where Pinus trees were planted in terraces	N 33.09447° W 16.29839°
Dysderinae	Dysdera	portisancti	♂		MZB 2019-1955	lc109	MT372305	MT374405	-	MT373206	MT374324	Portugal	Porto Santo	Terra-Chã (Pico Branco)	335 m	a small plateau East to Pico Branco's summit, where Pinus trees were planted in terraces	N 33.09447° W 16.29839°
Dysderinae	Dysdera	portisancti	♂		MZB 2019-1957	lc110	MT372301ᵐ					Portugal	Porto Santo	Terra-Chã (Pico Branco)	335 m	a small plateau East to Pico Branco's summit, where Pinus trees were planted in terraces	N 33.09447° W 16.29839°
Dysderinae	Dysdera	precaria n. sp.	♂	Pt	FMNH KN.17858	lc092	MT372257					Portugal	Porto Santo	Pico Ana Ferreira	242 m	the area with tree cover nearest to the summit, in the North to Northwest slope	N 33.04442° W 16.36977°
Dysderinae	Dysdera	precaria n. sp.	juv		CRBALC0162	lc101	MT372258					Portugal	Porto Santo	Pico Ana Ferreira	242 m	the area with tree cover nearest to the summit, in the North to Northwest slope	N 33.04442° W 16.36977°
Dysderinae	Dysdera	precaria n. sp.	♀		CRBALC0165	lc161	MT372261					Portugal	Porto Santo	Pico Ana Ferreira	242 m	the area with tree cover nearest to the summit, in the North to Northwest slope	N 33.04442° W 16.36977°
Dysderinae	Dysdera	precaria n. sp.	♀	Pt	FMNH KN.17859	lc136	MT372265	MT374402	-	MT373194	MT374343	Portugal	Porto Santo	Pico Branco	318 m	the area near the summit, in the beginning of the trail leading to Terra-Chã	N 33.09428° W 16.30137°
Dysderinae	Dysdera	precaria n. sp.	♂		CRBALC0144	lc164	MT372260					Portugal	Porto Santo	Pico Branco	318 m	the area near the summit, in the beginning of the trail leading to Terra-Chã	N 33.09428° W 16.30137°
Dysderinae	Dysdera	precaria n. sp.	juv		CRBA002513	pk231	MT372268					Portugal	Porto Santo	Pico Branco	318 m	the area near the summit, in the beginning of the trail leading to Terra-Chã	N 33.09428° W 16.30137°
Dysderinae	Dysdera	precaria n. sp.	♀		LCPC	pk242	MT372264					Portugal	Porto Santo	Pico Branco	318 m	the area near the summit, in the beginning of the trail leading to Terra-Chã	N 33.09428° W 16.30137°
Dysderinae	Dysdera	precaria n. sp.	juv		CRBALC0195	lc316	MT372266					Portugal	Porto Santo	Pico da Juliana	382 m	the area near the summit, in the North slope	N 33.09270° W 16.32186°
Dysderinae	Dysdera	precaria n. sp.	juv		CRBALC0199	lc317	MT372269					Portugal	Porto Santo	Pico da Juliana	382 m	the area near the summit, in the North slope	N 33.09270° W 16.32186°
Dysderinae	Dysdera	precaria n. sp.	♂	Pt	MMF 47919	pk244	MT372278					Portugal	Porto Santo	Pico da Juliana	382 m	the area near the summit, in the North slope	N 33.09270° W 16.32186°
Dysderinae	Dysdera	precaria n. sp.	♂	Ht	MZB 2019-1940	lc111	MT372262					Portugal	Porto Santo	Terra-Chã (Pico Branco)	335 m	a small plateau East to Pico Branco's summit, where Pinus trees were planted in terraces	N 33.09447° W 16.29839°
Dysderinae	Dysdera	precaria n. sp.	♀	Pt	MZB 2019-1941	lc112	MT372263					Portugal	Porto Santo	Terra-Chã (Pico Branco)	335 m	a small plateau East to Pico Branco's summit, where Pinus trees were planted in terraces	N 33.09447° W 16.29839°
Dysderinae	Dysdera	precaria n. sp.	juv		CRBALC0178	lc113	MT372259	MT374404	MT374302	MT373193	MT374342	Portugal	Porto Santo	Terra-Chã (Pico Branco)	335 m	a small plateau East to Pico Branco's summit, where Pinus trees were planted in terraces	N 33.09447° W 16.29839°
Dysderinae	Dysdera	recondita n. sp.	♂	Pt	MZB 2019-1946	k529	MT372241	MT374387	MT374303	MT373184	MT374344	Portugal	Deserta Grande	Rocha do Barbusano	442 m	the area around the summit of Deserta Grande	N 32.53535° W 16.51782°
Dysderinae	Dysdera	recondita n. sp.	juv		CRBA002538	pk79	MT372242					Portugal	Deserta Grande	Rocha do Barbusano	442 m	the area around the summit of Deserta Grande	N 32.53535° W 16.51782°
Dysderinae	Dysdera	recondita n. sp.	♂	Ht	MZB 2019-1944	lc144	MT372243ʳ					Portugal	Deserta Grande	Vereda do Risco (N)	321 m	the northern half of the trail	N 32.51723° W 16.50569°
Dysderinae	Dysdera	recondita n. sp.	♀	Pt	MZB 2019-1945	lc334	MT372243ʳ					Portugal	Deserta Grande	Vereda do Risco (N)	321 m	the northern half of the trail	N 32.52571° W 16.51131°
Dysderinae	Dysdera	recondita n. sp.	♂	Pt	FMNH KN.17860	pk677	MT372243ʳ	MT374389	MT374305	MT373186	MT374346	Portugal	Deserta Grande	Vereda do Risco (N)	321 m	the northern half of the trail	N 32.52571° W 16.51131°
Dysderinae	Dysdera	sandrae n. sp.	♂	Pt	MMF 47911	pk220	MT372254					Portugal	Deserta Grande	Eira	262 m	a flat area where (unsuccessful) colonists grew cereals	N 32.50993° W 16.50240°
Dysderinae	Dysdera	sandrae n. sp.	♂	Pt	MZB 2019-1930	pk72	MT372253ˣ					Portugal	Deserta Grande	Eira	262 m	a flat area where (unsuccessful) colonists grew cereals	N 32.50993° W 16.50240°
Dysderinae	Dysdera	sandrae n. sp.	♂		LCPC	pk75	MT372253ˣ					Portugal	Deserta Grande	Poço da Fajã Grande	191 m	a secluded location in a very steep slope containing one of the few springs of natural water of Deserta Grande	N 32.49562° W 16.49562°
Dysderinae	Dysdera	sandrae n. sp.	♀	Pt	FMNH KN.17851	lc335	MT372256					Portugal	Deserta Grande	Vale da Castanheira (S)	267 m	the easternmost slope leading out from Vale da Castanheira into Pedregal (E)	N 32.54861° W 16.52443°
Dysderinae	Dysdera	sandrae n. sp.	♂	Pt	NMH001593	k523	MT372252	MT374381	MT374287	MT373209	MT374326	Portugal	Deserta Grande	Vereda do Risco		undetermined location	
Dysderinae	Dysdera	sandrae n. sp.	♀	Pt	MZB 2019-1932	k528	MT372255					Portugal	Deserta Grande	Vereda do Risco		undetermined location	
Dysderinae	Dysdera	sandrae n. sp.	♀	Pt	MMF 47912	pk76	MT372253ˣ	MT374382	MT374288	MT373210	MT374327	Portugal	Deserta Grande	Vereda do Risco (S)	231 m	the southern half of the trail	N 32.51723° W 16.50569°

Subfamily	Genus	Species	Sex	Type	Voucher	Code						Country	Island	Location	Elevation	Habitat	Coordinates
Dysderinae	*Dysdera*	*sandrae* n. sp.	♂	Pt	FMNH KN.17850	pk77	MT372253ˣ					Portugal	Deserta Grande	Vereda do Risco (S)	231 m	the southern half of the trail	N 32.51723° W 16.50569°
Dysderinae	*Dysdera*	*teixeirai* n. sp.	♂	Pt	FMNH KN.17852	lc068	MT372236					Portugal	Deserta Grande	Pedregal (E)	339 m	the easternmost flank of the barren plateau presents some hills with scarce vegetation	N 32.54613° W 16.52340°
Dysderinae	*Dysdera*	*teixeirai* n. sp.	♀	Pt	FMNH KN.17853	lc301	MT372238					Portugal	Deserta Grande	Pedregal (E)	339 m	the easternmost flank of the barren plateau presents some hills with scarce vegetation	N 32.54613° W 16.52340°
Dysderinae	*Dysdera*	*teixeirai* n. sp.	♂	Pt	MZB 2019-1935	pk676	MT372240	MT374378	MT374291	MT373183	MT374330	Portugal	Deserta Grande	Pedregal (E)	339 m	the easternmost flank of the barren plateau presents some hills with scarce vegetation	N 32.54613° W 16.52340°
Dysderinae	*Dysdera*	*teixeirai* n. sp.	juv		CRBALC0110	lc067	MT372239					Portugal	Deserta Grande	Rocha do Barbusano	442 m	the area around the summit of Deserta Grande	N 32.53535° W 16.51782°
Dysderinae	*Dysdera*	*teixeirai* n. sp.	♂	Pt	MMF 47913	pk78	MT372237					Portugal	Deserta Grande	Rocha do Barbusano	442 m	the area around the summit of Deserta Grande	N 32.53535° W 16.51782°
Dysderinae	*Dysdera*	*teixeirai* n. sp.	♂	Ht	MZB 2019-1933	lc049	MT372232					Portugal	Deserta Grande	Rocha do Barbusano (S)	401 m	a small valley South to Rocha do Barbusano, with a relevant cover of native vegetation	N 32.53168° W 16.51471°
Dysderinae	*Dysdera*	*teixeirai* n. sp.	juv		CRBALC0083	lc055	MT372233					Portugal	Deserta Grande	Rocha do Barbusano (S)	401 m	a small valley South to Rocha do Barbusano, with a relevant cover of native vegetation	N 32.53168° W 16.51471°
Dysderinae	*Dysdera*	*teixeirai* n. sp.	juv		CRBALC0103	lc060	MT372231	MT374377	MT374290	MT373182	MT374329	Portugal	Deserta Grande	Rocha do Barbusano (S)	401 m	a small valley South to Rocha do Barbusano, with a relevant cover of native vegetation	N 32.53168° W 16.51471°
Dysderinae	*Dysdera*	*teixeirai* n. sp.	juv		CRBALC0198	lc132	MT372234					Portugal	Deserta Grande	Rocha do Barbusano (S)	401 m	a small valley South to Rocha do Barbusano, with a relevant cover of native vegetation	N 32.53168° W 16.51471°
Dysderinae	*Dysdera*	*teixeirai* n. sp.	juv		CRBALC0588	lc333	MT372235					Portugal	Deserta Grande	Rocha do Barbusano (S)	401 m	a small valley South to Rocha do Barbusano, with a relevant cover of native vegetation	N 32.53168° W 16.51471°
Dysderinae	*Dysdera*	*teixeirai* n. sp.	♂	Pt	NMH001596	k526	MT372230					Portugal	Deserta Grande	Vereda do Risco		undetermined location	
Dysderinae	*Cryptoparachtes*	sp.					JN689136	JN705754		JN689008	JN689178	Turkey					
Dysderinae	*Dysdera*	*adriatica*					KJ941271	EU068064		GQ285610	GQ285620	Slovenia					
Dysderinae	*Dysdera*	*alegranzaensis*					AF244257	AF244167		EU139759	EU139688	Spain	Canary Islands				
Dysderinae	*Dysdera*	*aneris*					HQ396319	HQ396277		HQ396308	HQ396298	Portugal	Salvage Islands				
Dysderinae	*Dysdera*	*arabisenen*					AF244291	AF244198		EU139786	EU139715	Spain	Canary Islands				
Dysderinae	*Dysdera*	*atlantica*					EU068029	EU068057		EU139807	EU139738	Morocco					
Dysderinae	*Dysdera*	*bandamae*					AF244286	AF244193		EU139787	EU139716	Spain	Canary Islands				
Dysderinae	*Dysdera*	*brevispina*					AF244316	AF244227		-	EU139717	Spain	Canary Islands				
Dysderinae	*Dysdera*	*calderensis*					AF244308	AF244217		EU139788	HQ396304	Spain	Canary Islands				
Dysderinae	*Dysdera*	cf. *inermis*					EF458142.2	EF458092		EU139795	EU139726	Morocco					
Dysderinae	*Dysdera*	cf. *seclusa*					EU068035	EU068071		EU139810	EU139741	Morocco					
Dysderinae	*Dysdera*	*chioensis*					AF244281	AF244188		EU139789	EU139719	Spain	Canary Islands				
Dysderinae	*Dysdera*	*crocata*					AF244237	AF244152		EU139791	EU139721	Spain					
Dysderinae	*Dysdera*	*erythrina*					AF244252	AF244162		EU139790	EU139720	Spain					
Dysderinae	*Dysdera*	*fuscipes*					EU068039	EU068073		EU139794	EU139725	Spain					
Dysderinae	*Dysdera*	*gomerensis*					HQ396326	HQ396285		EU139798	EU139729	Spain	Canary Islands				
Dysderinae	*Dysdera*	*guayota*					AF244283	AF244190		EU139792	EU139722	Spain	Canary Islands				
Dysderinae	*Dysdera*	*hungarica*					EU139633	EU139662		-	EU139723	Ukraine					
Dysderinae	*Dysdera*	*iguanensis*					AF244279	AF244185		EU139793	EU139724	Spain	Canary Islands				

Dysderinae	*Dysdera*	*inermis*	EF458141.2	EF458091		HQ407381	HQ407382	Spain	
Dysderinae	*Dysdera*	*insulana*	AF244314	AF244225		EU139796	EU139727	Spain	Canary Islands
Dysderinae	*Dysdera*	*labradaensis*	EU068040	AF244179		EU139797	-	Spain	Canary Islands
Dysderinae	*Dysdera*	*lancerotensis*	AF244238	AF244153		EU139756	EU139685	Spain	Canary Islands
Dysderinae	*Dysdera*	*lantosquensis*	GQ285628	GQ285604		GQ285612	GQ285622	Slovakia	
Dysderinae	*Dysdera*	*levipes*	AF244295	AF244202		-	EU139728	Spain	Canary Islands
Dysderinae	*Dysdera*	*liostethus*	AF244302	AF244211		EU139819	EU139750	Spain	Canary Islands
Dysderinae	*Dysdera*	*longa*	AF244254	AF244164		EU139781	EU139710	Spain	Canary Islands
Dysderinae	*Dysdera*	*lucidipes*	EU068042	EU068060		EU139799	EU139730	Morocco	
Dysderinae	*Dysdera*	*lusitanica*	GQ285629	GQ285609		GQ285614	GQ285624	Spain	
Dysderinae	*Dysdera*	*macra*	AF244300	AF244209		EU139800	EU139731	Spain	Canary Islands
Dysderinae	*Dysdera*	*mauritanica*	EF458138	EF458093		EU139801	EU139732	Morocco	
Dysderinae	*Dysdera*	*montanetensis*	AF244278	AF244183		EU139802	EU139733	Spain	Canary Islands
Dysderinae	*Dysdera*	*mucronata*	EU068044	EU068077		EU139803	EU139734	Spain	
Dysderinae	*Dysdera*	*nesiotes*	AF244261	AF244169		EU139764	EU139694	Spain	Canary Islands
Dysderinae	*Dysdera*	*ninnii*	EU068045	EU068062		EU139804	EU139735	Slovenia	
Dysderinae	*Dysdera*	*paucispinosa*	AF244306	AF244215		EU139805	EU139736	Spain	Canary Islands
Dysderinae	*Dysdera*	*rugichelis*	AF244293	AF244200		EU139816	EU139747	Spain	Canary Islands
Dysderinae	*Dysdera*	*sanborondon*	EF458135	AF244166		EU139775	EU139705	Spain	Canary Islands
Dysderinae	*Dysdera*	*scabricula*	EU068046	EU068078		EU139809	EU139740	Spain	
Dysderinae	*Dysdera*	*shardana*	GQ285634	GQ285605		GQ285613	GQ285623	Italy	Sardinia
Dysderinae	*Dysdera*	*silvatica*	AF244273.2	EU068072		EU139808	EU139739	Spain	Canary Islands
Dysderinae	*Dysdera*	sp. MA	AF244244	AF244155	EU139675	EU139811	EU139742	Morocco	
Dysderinae	*Dysdera*	sp. MB	AF244245	AF244156	EU139676	EU139812	EU139743	Morocco	
Dysderinae	*Dysdera*	sp. MC	AF244246	AF244157		EU139813	EU139744	Morocco	
Dysderinae	*Dysdera*	sp. MD	-	AF244158	EU139677	EU139814	EU139745	Morocco	
Dysderinae	*Dysdera*	sp. MF	AF244249	AF244159	EU139678	EU139815	EU139746	Morocco	
Dysderinae	*Dysdera*	*spinidorsa*	AF244268	AF244173		EU139777	EU139707	Spain	Canary Islands
Dysderinae	*Dysdera*	*tilosensis*	AF244288	AF244195		EU139817	EU139748	Spain	Canary Islands
Dysderinae	*Dysdera*	*unguimmanis*	AF244284	AF244191		EU139818	EU139749	Spain	Canary Islands
Dysderinae	*Dysdera*	*valentina*	GQ285632	GQ285608		GQ285617	GQ285627	Spain	

Dysderinae	*Dysdera*	*verneaui*	AF244319	AF244230	EU139806	EU139737	Spain	Canary Islands
Dysderinae	*Dysdera*	*yguanirae*	AF244290	AF244197	-	EU139751	Spain	Canary Islands
Dysderinae	*Dysderocrates*	*egregius*	JN689143	JN705759	JN689037	JN689181	Romania	
Dysderinae	*Harpactocrates*	*drassoides*	KM219431	KM219503	KM219361	KM219289	Italy	
Dysderinae	*Harpactocrates*	*gurdus*	KM219478	KM219549	KM219404	KM219335	Spain	
Dysderinae	*Harpactocrates*	sp.	JN689147	-	JN689041	JN689184	Turkey	
Dysderinae	*Hygrocrates*	*lycaoniae*	JN689150	JN705761	JN689039	JN689187	Greece	
Dysderinae	*Kut*	*troglophilus*	JN689148	JN705760	JN689038	JN689185	Turkey	
Dysderinae	*Parachtes*	*romandiolae*	JN689158	JN705766	JN689015	JN689195	Italy	
Dysderinae	*Parachtes*	*teruelis*	JN689163	JN705781	JN689023	JN689200	Spain	
Harpacteinae	*Harpactea*	*fageli*	JN689144	-	JN689040	JN689182	Spain	
Harpacteinae	*Harpactea*	*hombergii*	AF244233	KY015855	EU139820	EU139752	Spain	
Harpacteinae	*Holissus*	*unciger*	JN689149	-	JN689036	JN689186	France	Corsica
Rhodinae	*Rhode*	*scutiventris*	EU139636	EU139684	EU139822	EU139754	Spain	

Table S2.- Primers and amplification conditions used in the present study

Locus	Primer name	Primer Sequence	Reference
COI	C1-J-1490	GGTCAACAAATCATAAAGATATTGG	Folmer et al., 1994
	C1-N-2198	TAAACTTCAGGGTGACCAAAAAATCA	Folmer et al., 1994
	C1-N-2191	CCCGGTAAAATTAAAATATAAACTTC	Simon et al., 1994
	C1-J-1751	GGATCACCTGATATAGCATTCCC	Simon et al., 1994
16S	LR-N-13398	CGCCTGTTTATCAAAAACAT	Simon et al., 1994
	LR-J-12864	CTCCGGTTTGAACTCAGATCA	Palumbi, 1996
NAD1	LR-N-12945	CGACCTCGATGTTGAATTAA	Hedin et al., 1997
	N1-J-12373	CTTCGTATAGATCCTARTTGDCTRTATT	Macías-Hernández et al., 2008
	N1-J-12261	TCRTAAGAAATTATTTGAGC	Hedin et al., 1997
28S	28SO	GACCCGTCTTGAAACACGGA	Hedin & Maddison, 2001
	28SB	TCGGAAGGAACGAGCTAC	modified from Whiting et al., 1997
	28SC	GGTTCGATTAGTCTTTCGCC	Hedin & Maddison, 2001
H3	H3F	ATGGCTCGTACCAAGCAGACVGC	Colgan et al., 1998
	H3R	ATATCCTTRGGCATRATRGTGAC	Colgan et al., 1998

	COI	16S-NAD1	28S	H3
Denaturation	94 ºC, 5 m	94º C, 5 m	94º C, 5 m	94º C, 5 m
Cycles for annealing and initial extension*	94 ºC, 30 s	94 ºC, 30 s	94 ºC, 30 s	94 ºC, 30 s
	42 ºC, 35 s	45 ºC, 35 s	48 ºC, 35 s	40 ºC, 35 s
	72 ºC, 45 s	72 ºC, 45 s	72 ºC, 1 m	72 ºC, 45 s
Final extension	72 ºC, 5 m	72 ºC, 5 m	72 ºC, 10 m	72 ºC, 5 m

*The number of cycles used was 35 for all loci

Reference list
Colgan, D. J., McLauchlan, A., Wilson, G. D. F., Livingston, S. P., Edgecombe, G. D., Macaranas, J., . . . Gray, M. R. (1998). Histone H3 and U2 snRNA DNA sequences and arthropod molecular evolution. *Australian Journal of Zoology, 46*(5), 419-437.

Folmer, O., Black, M., Hoeh, W., Lutz, R., & Vrijenhoek, R. (1994). DNA primers for amplification of mitochondrial cytochrome c oxidase subunit I from diverse metazoan invertebrates. *Molecular Marine Biology and Biotechnology, 3*, 294-299.

Hedin, M. C. (1997). Speciational history in a Diverse clade of habitat-specialized spiders (Araneae: Nesticidae: *Nesticus*): Inferences from geographic-based sampling. *Evolution, 51*(6), 1929-1945.

Hedin, M. C., & Maddison, W. P. (2001). A combined molecular approach to phylogeny of the jumping spider subfamily Dendryphantinae (Araneae: Salticidae). *Molecular Phylogenetics and Evolution, 18*(3), 386-403.

Palumbi, S. R. (1996). Nucleic acids II, The polymerase chain reaction. In D. M. Hillis, C. Moritz, & B. K. Mable (Eds.), *Molecular Systematics* (pp. 205 - 247). Sunderland, MA.: Sinauer Associates.

Simon, C., Frati, F., Beckenbach, A., Crespi, B., Liu, H., & Flook, P. (1994). Evolution, weighting, and phylogenetic utility of mitochondrial gene sequences and a compilation of conserved polymerase chain reaction primers. *Annals of the Entomological Society of America, 87*(6), 651-701.

Whiting, M. F., Carpenter, J. C., Wheeler, Q. D., & Wheeler, W. C. (1997). The strepsiptera problem: Phylogeny of the holometabolous insect orders inferred from 18S and 28S ribosomal DNA sequences and morphology. *Systematic Biology, 46*(1), 1-68.

Annex II

Supplementary Materials for Chapter 2

Table S1. List of specimens used in the molecular analysis with voucher specifications, GenBank accession numbers and collecting data. Sequences with DNA codes were newly generated by the authors in the present or previous studies. Superscript letters in COI indicate shared haplotypes. Subfamily, Genus, Species: taxonomic category; sex: life cycle stage; type: type material status of the specimen; collection code: collection number of the specimen; DNA code: DNA extraction code; COI, 16S, NAD1, 28S, H3:

accession numbers for the corresponding genes; Country, Island, Locality: locality information; Additional site information: habitat characteristics; Coordinates: decimal latitude and longitude; Altitude: elevation in meters as inferred from the GPS coordinates with https://www.freemaptools.com/elevation-finder.htm.

Subfamily	Genus	Species	sex	type	collection code	DNA code	COI	16S	NAD1	28S	H3	Country	Island	Locality	Altitude	Additional site information	Coordinates
Dysderinae	*Dysdera*	SPG	♀	Pt	CRBA002543	pk85	TBA	TBA	TBA	TBA	TBA	Portugal	Ilhéu de Cima	erosion cave at the N-coast of islet	sea level		N 33.05698° W 16.28650°
Dysderinae	*Dysdera*	SPG	♂	Ht	CRBALC0051	lc041	TBA	TBA	TBA	TBA	TBA	Portugal	Ilhéu de Cima	erosion cave at the N-coast of islet	sea level		N 33.05698° W 16.28650°
Dysderinae	*Dysdera*	SPG	♀	Pt	CRBALC0055	lc160	TBA	TBA	TBA	TBA	TBA	Portugal	Ilhéu de Cima	erosion cave at the N-coast of islet	sea level		N 33.05698° W 16.28650°
Dysderinae	*Dysdera*	SPJ	juv		CRBALC0720	lc343	TBA	TBA	TBA	TBA	TBA	Portugal	Terceira	between São Mateus and Negrito	sea level	rocky beach	N 38.65312° W 27.27736°
Dysderinae	*Dysdera*	SPJ	juv		CRBALC0724	lc344	TBA	TBA	TBA	TBA	TBA	Portugal	Pico	Praia do Caminho de Cima	sea level	rocky beach	N 38.42813° W 28.41594°
Dysderinae	*Dysdera*	flavitarsis	♀		CRBA001023	sd3	TBA	TBA	TBA	TBA	TBA	Spain		Candín, Suarbol		*Quercus pubescens* woodland. Near river.	N 42.86545° W 6.86127°
Dysderinae	*Dysdera*	flavitarsis	♂		CRBA001683	lc294	TBA	TBA	TBA	TBA	TBA	Portugal		Ponte de São Miguel	717 m		N 41.80389° W 8.13139°
Dysderinae	*Dysdera*	coiffaiti	juv		CRBALC0114	lc071	TBA	TBA	TBA	TBA	TBA	Portugal	Bugio	Planalto Sul	322 m	this is the only accessible flat area of this island	N 32.41228° W 16.47466°
Dysderinae	*Dysdera*	coiffaiti	juv		CRBALC0038	lc038	MT372226c	MT374360	MT374277	MT373168	MT374318	Portugal	Madeira	Ribeiro Bonito II	556 m	laurel forest patch	N 32.79801° W 16.93654°
Dysderinae	*Dysdera*	dissimilis	♀		CRBA002529	pk307	MT372271	MT374393	MT374312	MT373197	MT374353	Portugal	Porto Santo	Pico do Facho	473 m	the area near the summit, facing North, where a few remaining native trees can be found (Heberdenia excelsa)	N 33.08433° W 16.32174°
Dysderinae	*Dysdera*	dissimilis	♀	Pt	FMNH KN.17862	lc135	MT372289	MT374395	MT374310	MT373200	MT374351	Portugal	Porto Santo	Terra-Chã (Pico Branco)	335 m	a small plateau East to Pico Branco's summit, where Pinus trees were planted in terraces	N 33.09447° W 16.29839°
Dysderinae	*Dysdera*	diversa	♀		MMF 47902	pk223	MT372244	MT374379	MT374284	-	-	Portugal	Madeira	Caramujo	1260 m	the area surrounding the Lagoa do Caramujo, with woodlands of Erica spp.	N 32.77161° W 17.06205°
Dysderinae	*Dysdera*	diversa	♂		MMF 47903	pk224	MT372245	MT374380	MT374285	MT373195	-	Portugal	Madeira	Montado dos Pessegueiros	1384 m	the contiguous areas around the trail winding into this patch of laurel forest	N 32.79333° W 17.09576°
Dysderinae	*Dysdera*	exigua	♂	Pt	MZB 2019-1939	pk675	MT372246	MT374384	MT374299	MT373203	MT374337	Portugal	Bugio	Planalto Sul	322 m	this is the only accessible flat area of this island	N 32.41228° W 16.47466°
Dysderinae	*Dysdera*	exigua	♀	Pt	CRBALC0212	lc131	MT372251q	MT374385	MT374300	MT373204	MT374339	Portugal	Deserta Grande	Ponta Sul	191 m	this area is South to Planalto Sul, a small crested canyon as Deserta Grande slopes towards the sea level	N 32.49562° W 16.49562°
Dysderinae	*Dysdera*	isambertoi	juv		CRBALC0124	lc081	MT372299	MT374398	MT374313	MT373189	MT374355	Portugal	Porto Santo	Pico do Castelo	350 m	NE slope	N 33.08196° W 16.33277°
Dysderinae	*Dysdera*	isambertoi	juv		CRBALC0188	lc123	MT372292	MT374400	MT374315	MT373190	MT374357	Portugal	Porto Santo	Pico do Facho (N)	467 m	a secluded depression between two opposing slopes in the North flank of the peak, where a patch of decaying Erica bushes was found	N 33.08518° W 16.32364°
Dysderinae	*Dysdera*	portisancti	juv		CRBALC0179	lc114	MT372306	-	MT374286	MT373207	MT374325	Portugal	Porto Santo	Pico do Facho	473 m	the area near the summit, facing North, where a few remaining native trees can be found (Heberdenia excelsa)	N 33.08433° W 16.32174°
Dysderinae	*Dysdera*	portisancti	♂		MZB 2019-1955	lc109	MT372305	MT374405	-	MT373206	MT374324	Portugal	Porto Santo	Terra-Chã (Pico Branco)	335 m	a small plateau East to Pico Branco's summit, where Pinus trees were planted in terraces	N 33.09447° W 16.29839°
Dysderinae	*Dysdera*	precaria	♀	Pt	FMNH KN.17859	lc136	MT372265	MT374402	-	MT373194	MT374343	Portugal	Porto Santo	Pico Branco	318 m	the area near the summit, in the beginning of the trail leading to Terra-Chã	N 33.09428° W 16.30137°
Dysderinae	*Dysdera*	precaria	juv		CRBALC0178	lc113	MT372259	MT374404	MT374302	MT373193	MT374342	Portugal	Porto Santo	Terra-Chã (Pico Branco)	335 m	a small plateau East to Pico Branco's summit, where Pinus trees were planted in terraces	N 33.09447° W 16.29839°
Dysderinae	*Dysdera*	recondita	♂	Pt	MZB 2019-1946	k529	MT372241	MT374387	MT374303	MT373184	MT374344	Portugal	Deserta Grande	Rocha do Barbusano	442 m	the area around the summit of Deserta Grande	N 32.53535° W 16.51782°
Dysderinae	*Dysdera*	recondita	♂	Pt	FMNH KN.17860	pk677	MT372243r	MT374389	MT374305	MT373186	MT374346	Portugal	Deserta Grande	Vereda do Risco (N)	321 m	the northern half of the trail	N 32.52571° W 16.51131°
Dysderinae	*Dysdera*	sandrae	♂	Pt	NMH001593	k523	MT372252	MT374381	MT374287	MT373209	MT374326	Portugal	Deserta Grande	Vereda do Risco			undetermined location
Dysderinae	*Dysdera*	sandrae	♀	Pt	MMF 47912	pk76	MT372253s	MT374382	MT374288	MT373210	MT374327	Portugal	Deserta Grande	Vereda do Risco (S)	231 m	the southern half of the trail	N 32.51723° W 16.50569°

Subfamily	Genus	Species	Sex	Code	Voucher	ID	GenBank	GenBank	GenBank	GenBank	GenBank	Country	Locality	Site	Elev.	Notes	Coordinates
Dysderinae	*Dysdera*	*teixeirai*	♂	Pt	MZB 2019-1935	pk676	MT372240	MT374378	MT374291	MT373183	MT374330	Portugal	Deserta Grande	Pedregal (E)	339 m	the easternmost flank of the barren plateau presents some hills with scarce vegetation	N 32.54613° W 16.52340°
Dysderinae	*Dysdera*	*teixeirai*	juv		CRBALC0103	lc060	MT372231	MT374377	MT374290	MT373182	MT374329	Portugal	Deserta Grande	Rocha do Barbusano (S)	401 m	a small valley South to Rocha do Barbusano, with a relevant cover of native vegetation	N 32.53168° W 16.51471°
Dysderinae	*Cryptoparachtes*	sp.					JN689136	JN705754		JN689008	JN689178	Turkey					
Dysderinae	*Dysdera*	adriatica					KJ941271	EU068064		GQ285610	GQ285620	Slovenia					
Dysderinae	*Dysdera*	alegranzaensis					AF244257	AF244167		EU139759	EU139688	Spain	Canary Islands				
Dysderinae	*Dysdera*	aneris					HQ396319	HQ396277		HQ396308	HQ396298	Portugal	Salvage Islands				
Dysderinae	*Dysdera*	arabisenen					AF244291	AF244198		EU139786	EU139715	Spain	Canary Islands				
Dysderinae	*Dysdera*	atlantica					EU068029	EU068057		EU139807	EU139738	Morocco					
Dysderinae	*Dysdera*	bandamae					AF244286	AF244193		EU139787	EU139716	Spain	Canary Islands				
Dysderinae	*Dysdera*	brevispina					AF244316	AF244227		-	EU139717	Spain	Canary Islands				
Dysderinae	*Dysdera*	calderensis					AF244308	AF244217		EU139788	HQ396304	Spain	Canary Islands				
Dysderinae	*Dysdera*	cf. inermis					EF458142.2	EF458092		EU139795	EU139726	Morocco					
Dysderinae	*Dysdera*	cf. seclusa					EU068035	EU068071		EU139810	EU139741	Morocco					
Dysderinae	*Dysdera*	chioensis					AF244281	AF244188		EU139789	EU139719	Spain	Canary Islands				
Dysderinae	*Dysdera*	crocata					AF244237	AF244152		EU139791	EU139721	Spain					
Dysderinae	*Dysdera*	erythrina					AF244252	AF244162		EU139790	EU139720	Spain					
Dysderinae	*Dysdera*	fuscipes					EU068039	EU068073		EU139794	EU139725	Spain					
Dysderinae	*Dysdera*	gomerensis					HQ396326	HQ396285		EU139798	EU139729	Spain	Canary Islands				
Dysderinae	*Dysdera*	guayota					AF244283	AF244190		EU139792	EU139722	Spain	Canary Islands				
Dysderinae	*Dysdera*	hungarica					EU139633	EU139662		-	EU139723	Ukraine					
Dysderinae	*Dysdera*	iguanensis					AF244279	AF244185		EU139793	EU139724	Spain	Canary Islands				
Dysderinae	*Dysdera*	inermis					EF458141.2	EF458091		HQ407381	HQ407382	Spain					
Dysderinae	*Dysdera*	insulana					AF244314	AF244225		EU139796	EU139727	Spain	Canary Islands				
Dysderinae	*Dysdera*	labradaensis					EU068040	AF244179		EU139797	-	Spain	Canary Islands				
Dysderinae	*Dysdera*	lancerotensis					AF244238	AF244153		EU139756	EU139685	Spain	Canary Islands				
Dysderinae	*Dysdera*	lantosquensis					GQ285628	GQ285604		GQ285612	GQ285622	Slovakia					
Dysderinae	*Dysdera*	levipes					AF244295	AF244202		-	EU139728	Spain	Canary Islands				
Dysderinae	*Dysdera*	liostethus					AF244302	AF244211		EU139819	EU139750	Spain	Canary Islands				
Dysderinae	*Dysdera*	longa					AF244254	AF244164		EU139781	EU139710	Spain	Canary Islands				

Dysderinae	*Dysdera*	lucidipes	EU068042	EU068060		EU139799	EU139730	Morocco	
Dysderinae	*Dysdera*	lusitanica	GQ285629	GQ285609		GQ285614	GQ285624	Spain	
Dysderinae	*Dysdera*	macra	AF244300	AF244209		EU139800	EU139731	Spain	Canary Islands
Dysderinae	*Dysdera*	mauritanica	EF458138	EF458093		EU139801	EU139732	Morocco	
Dysderinae	*Dysdera*	montanetensis	AF244278	AF244183		EU139802	EU139733	Spain	Canary Islands
Dysderinae	*Dysdera*	mucronata	EU068044	EU068077		EU139803	EU139734	Spain	
Dysderinae	*Dysdera*	nesiotes	AF244261	AF244169		EU139764	EU139694	Spain	Canary Islands
Dysderinae	*Dysdera*	ninnii	EU068045	EU068062		EU139804	EU139735	Slovenia	
Dysderinae	*Dysdera*	paucispinosa	AF244306	AF244215		EU139805	EU139736	Spain	Canary Islands
Dysderinae	*Dysdera*	rugichelis	AF244293	AF244200		EU139816	EU139747	Spain	Canary Islands
Dysderinae	*Dysdera*	sanborondon	EF458135	AF244166		EU139775	EU139705	Spain	Canary Islands
Dysderinae	*Dysdera*	scabricula	EU068046	EU068078		EU139809	EU139740	Spain	
Dysderinae	*Dysdera*	shardana	GQ285634	GQ285605		GQ285613	GQ285623	Italy	Sardinia
Dysderinae	*Dysdera*	silvatica	AF244273.2	EU068072		EU139808	EU139739	Spain	Canary Islands
Dysderinae	*Dysdera*	sp. MA	AF244244	AF244155	EU139675	EU139811	EU139742	Morocco	
Dysderinae	*Dysdera*	sp. MB	AF244245	AF244156	EU139676	EU139812	EU139743	Morocco	
Dysderinae	*Dysdera*	sp. MC	AF244246	AF244157		EU139813	EU139744	Morocco	
Dysderinae	*Dysdera*	sp. MD	-	AF244158	EU139677	EU139814	EU139745	Morocco	
Dysderinae	*Dysdera*	sp. MF	AF244249	AF244159	EU139678	EU139815	EU139746	Morocco	
Dysderinae	*Dysdera*	spinidorsa	AF244268	AF244173		EU139777	EU139707	Spain	Canary Islands
Dysderinae	*Dysdera*	tilosensis	AF244288	AF244195		EU139817	EU139748	Spain	Canary Islands
Dysderinae	*Dysdera*	unguimmanis	AF244284	AF244191		EU139818	EU139749	Spain	Canary Islands
Dysderinae	*Dysdera*	valentina	GQ285632	GQ285608		GQ285617	GQ285627	Spain	
Dysderinae	*Dysdera*	verneaui	AF244319	AF244230		EU139806	EU139737	Spain	Canary Islands
Dysderinae	*Dysdera*	yguanirae	AF244290	AF244197		-	EU139751	Spain	Canary Islands
Dysderinae	*Dysderocrates*	egregius	JN689143	JN705759		JN689037	JN689181	Romania	
Dysderinae	*Harpactocrates*	drassoides	KM219431	KM219503		KM219361	KM219289	Italy	
Dysderinae	*Harpactocrates*	gurdus	KM219478	KM219549		KM219404	KM219335	Spain	
Dysderinae	*Harpactocrates*	sp.	JN689147	-		JN689041	JN689184	Turkey	

Dysderinae	*Hygrocrates*	*lycaoniae*		JN689150	JN705761		JN689039	JN689187	Greece			
Dysderinae	*Kut*	*troglophilus*		JN689148	JN705760		JN689038	JN689185	Turkey			
Dysderinae	*Parachtes*	*romandiolae*		JN689158	JN705766		JN689015	JN689195	Italy			
Dysderinae	*Parachtes*	*teruelis*		JN689163	JN705781		JN689023	JN689200	Spain			
Harpacteinae	*Harpactea*	*fageli*		JN689144	-		JN689040	JN689182	Spain			
Harpacteinae	*Harpactea*	*hombergii*		AF244233	KY015855		EU139820	EU139752	Spain			
Harpacteinae	*Holissus*	*unciger*		JN689149	-		JN689036	JN689186	France	Corsica		
Rhodinae	*Rhode*	*scutiventris*		EU139636	EU139684		EU139822	EU139754	Spain			
Caponiidae	*Calponia*	sp.	CASENT9035527	KX514685	KX514518	KX514518	KX514633	KX298958			No information available, avialble from Chousou-Polydouri, N., Carmichael, A., Szűts, T., Saucedo, A., Gillespie, R., Griswold, C., & Wood, H. M. (2019). Giant Goblins above the waves at the southern end of the world: The biogeography of the spider family Orsolobidae (Araneae, Dysderoidea). Journal of Biogeography. doi:10.1111/jbi.13487	
Caponiidae	*Caponia*	sp. LBB-2011	ARASP000031	JN689215	JN689214		JN705753		South Africa		South Africa: KwaZulu-Natal, St. Lucia Game Reserve, Faines Island	
Oonopidae	*Ischnothyreus*	sp.	CASENT9035059	KX514676	KX514513	KX514513	KX514625	KX298949	Australia		Queensland, Wooroonooran NP, Tableland Section, Mt. Bartle Frere, Western side of track to summit, from Junction Camp carpark off Gourka Rd	1000
Oonopidae	*Oonops*	*procerus*	ARAMA000201	oonk314	KY015999		KY017230	oonk314	Spain		Catalonia, Bagà, Font de la Doble Ona	
Oonopidae	*Opopaea*	sp.	CASENT9024170	KX514655	KX514500	KX514500	KX514598	KX298922	South Africa		Eastern Cape, Grahmstown Municipal Caravan Park	580
Oonopidae	*Trigeris*	sp. MA176	ARAMA000176		KY016003		KY017236	KY018331	Dominican Republic		Independencia Prov., Parque Nac. Sierra de Baoruco, Rabo de Gato 18.310861,	
Orsolobidae	*Afrilobus*	sp.	CASENT9037121	KX514688	KX514521		KX514636	KX298961	South Africa		Eastern Cape, Kettlespout, 2.67 km ENE Hogsback	1333
Orsolobidae	cf. *Hickmanolobus*	sp.	CASENT9035010	KX514675			KX514623	KX298947	Australia		Western Australia, Stirling Range National Park, Toolbrunup Peak, south shaded side	975
Orsolobidae	*Osornolobus*	sp. 1	CASENT9035122	KX514681	KX514517		KX514629	KX298954	Chile		Los Ríos (Reg. XIV), Reserva Costera Valdiviana, 15.03 WSW Corral	335
Orsolobidae	*Subantarctia*	fiordensis	CASENT9035065	KX514678	KX514515		KX514626	KX298951	New Zealand		South Is., Soutland Region, Fjordlands National Park, Cascade Creek, Eglinton Valley, ~64 km NE Te Anau	499
Orsolobidae	*Tasmanoonops*	sp.2	CASENT9035008	KX514674	KX514512	KX514512	KX514622	KX298946	Australia		Western Australia, Stirling Ranges NP, Toolbrunup Peak, 72 km N Albany	975
Segestriidae	*Ariadna*	*boesenbergi*	ARAMR00076		KY016102		KY017341	KY018416	Argentina		Buenos Aires, Avellaneda, Sarandi	
Segestriidae	*Ariadna*	*insidiatrix*	ARAMA000131	KY017904	KY016103		KY017342		Spain		Murcia, Calblanque	
Segestriidae	*Segestria*	*senoculata*	ARAMA000199	KY017905	KY016104		KY017343	MN706523	France		Corsica, Foce di Vizzabona	
Segestriidae	*Segestria*	sp. LBB-2011	crba000744	JN689168	JN705789	JN705789	JN689044	JN689205	Spain		Barcelona, PN Montseny	
Trogloratoridae	*Trogloraptor*	*marchingtoni*	CASENT9040051	KY018033			KY017483	KY018527	USA		Oregon, Josephine Co., No Name Cave	

Supplementary Materials B. Full maximum clade credibility tree retrieved with time estimation analysis in a Bayesian framework using BEAST. Black indicates a supported node (Bayesian PP ≥ 0.95), grey an unsupported node (Bayesian PP < 0.95). Colored boxes signal the main groups of treated species in the genus *Dysdera*. Geological eras up to the Mesozoic are shown below and delimited with dashed lines (abbreviations: Pli – Pliocene, Q – Quaternary). Triangles denote calibration points used in the divergence time estimation (see text for details). In red fossil calibrations and in green biogeographic calibrations as follows: 1 – Harpacteinae crown (offset age), 2 – Segestriidae crown (offset age), 3 – Oonopidae stem (offset age), 4 – vicariance between the Iberian Peninsula and the western Mediterranean islands (mean age), 5 – oldest subaerial age of the western Canaries (maximum age), 6 – oldest subaerial age of the eastern Canaries (maximum age).
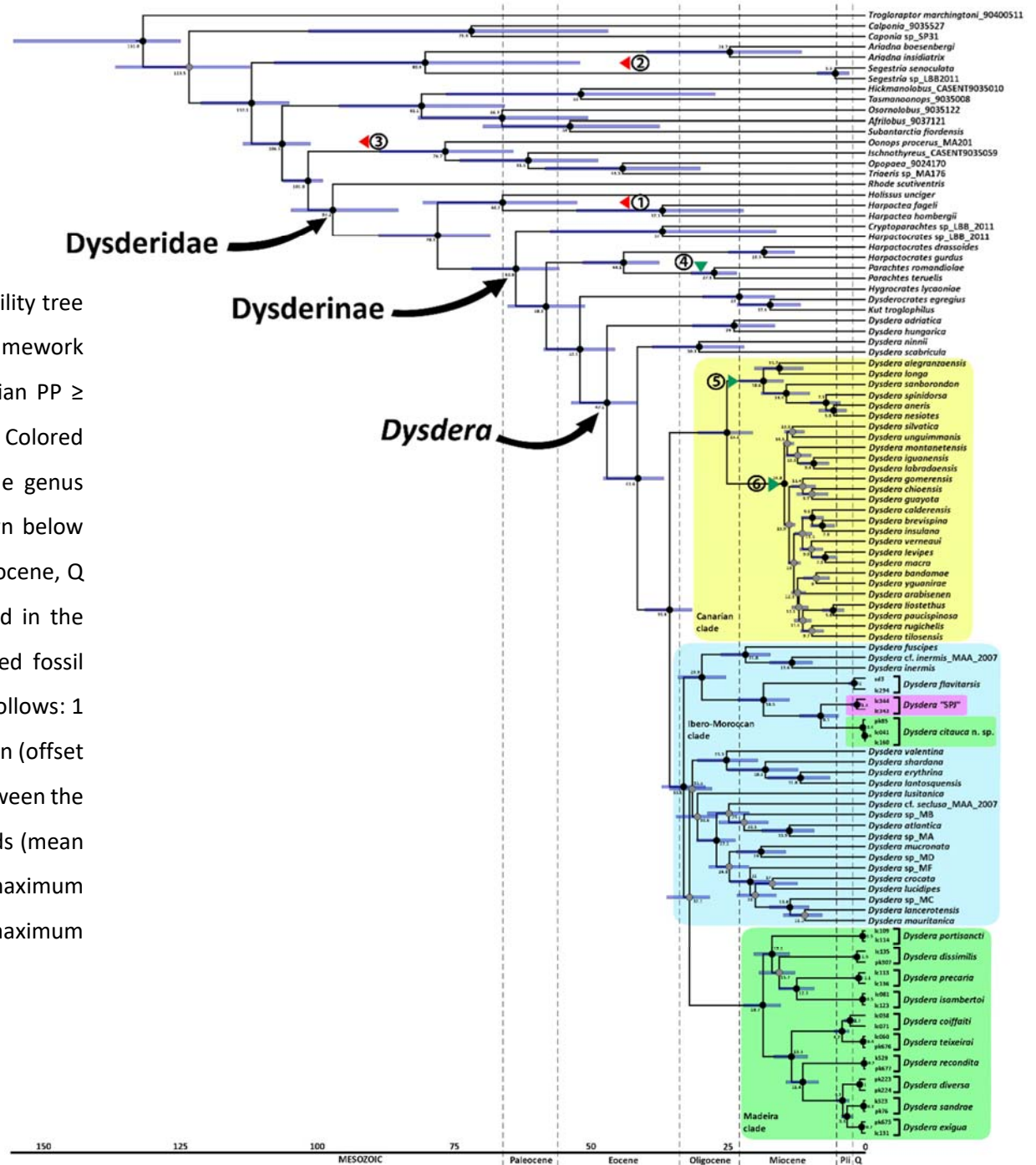
Annex III

Tables and Supplementary Materials for

Chapter 3

Table 1A: Primers used for amplification.

Locus	Primer name	Primer Sequence	Reference
COI	C1-J-1490	GGTCAACAAATCATAAAGATATTGG	(Folmer, Black, Hoeh, Lutz & Vrijenhoek, 1994)
	C1-N-2198	TAAACTTCAGGGTGACCAAAAAATCA	(Folmer et al., 1994)
	C1-N-2191	CCCGGTAAAATTAAAATATAAACTTC	(Simon et al., 1994)
	C1-J-1751	GGATCACCTGATATAGCATTCCC	(Simon et al., 1994)
16S	LR-N-13398	CGCCTGTTTATCAAAAACAT	(Simon et al., 1994)
	LR-J-12864	CTCCGGTTTGAACTCAGATCA	(Palumbi, 1996)
NAD1	LR-N-12945	CGACCTCGATGTTGAATTAA	(Hedin, 1997)
	N1-J-12373	CTTCGTATAGATCCTARTTGDCTRTATT	(Macías-Hernández, Oromí & Arnedo, 2008)
	N1-J-12261	TCRTAAGAAATTATTTGAGC	(Hedin, 1997)
28S	28SO	GACCCGTCTTGAAACACGGA	(Hedin & Maddison, 2001)
	28SB	TCGGAAGGAACGAGCTAC	(Whiting, Carpenter, Wheeler, & Wheeler, 1997)
	28SC	GGTTCGATTAGTCTTTCGCC	(Hedin & Maddison, 2001)
H3	H3F	ATGGCTCGTACCAAGCAGACVGC	(Colgan et al., 1998)
	H3R	ATATCCTTRGGCATRATRGTGAC	(Colgan et al., 1998)
ITS-2	ITS-5.8S	GGGACGATGAAGAACGGAGC	(White et al., 1990)
	ITS-28S	TCCTCCGCTTATTGATATGC	(White et al., 1990)
12S	12SR-J-14199	TACTATGTTACGACTTAT	(Kambhampati & Smith, 1995)
	12SR-N-14594	AAACTAGGATTAGATACCC	(Kambhampati & Smith, 1995)

Table 1B: PCR amplification settings for all studied loci. The number of cycles used was 35 for all loci.

	COI	16S, NAD1	28S	H3	12S	ITS-2
Denaturation	94 °C, 5 m	94 °C, 5 m	94° C, 5 m	94° C, 5 m	94° C, 5 m	94° C, 5 m
Cycles for annealing and initial extension	94 °C, 30 s	94 °C, 30 s	94 °C, 30 s	94 °C, 30 s	94 °C, 30 s	94 °C, 30 s
	42 °C, 35 s	45 °C, 35 s	48 °C, 35 s	45 °C, 35 s	42–45 °C, 35 s	50 °C, 35 s
	72 °C, 45 s	72 °C, 45 s	72 °C, 1 m	72 °C, 45 s	72 °C, 45 s	72 °C, 45 s
Final extension	72 °C, 5 m	72 °C, 5 m	72 °C, 10 m	72 °C, 5 m	72 °C, 5 m	72 °C, 5 m

BIBLIOGRAPHY

Colgan, D. J., McLauchlan, A., Wilson, G. D. F., Livingston, S. P., Edgecombe, G. D., Macaranas, J., … Gray, M. R. (1998). Histone H3 and U2 snRNA DNA sequences and arthropod molecular evolution. *Australian Journal of Zoology*, *46*(5), 419–437. https://doi.org/10.1071/ZO98048

Folmer, O., Black, M., Hoeh, W., Lutz, R., & Vrijenhoek, R. (1994). DNA primers for amplification of mitochondrial cytochrome c oxidase subunit I from diverse metazoan invertebrates. *Molecular Marine Biology and Biotechnology*, *3*(5), 294–299. https://doi.org/10.1071/ZO9660275

Hedin, M. C. (1997). Molecular phylogenetics at the population/species interface in cave spiders of the southern Appalachians (Araneae: Nesticidae: Nesticus). *Molecular Biology and Evolution*, *14*(3), 309–324. https://doi.org/10.1093/oxfordjournals.molbev.a025766

Hedin, M. C., & Maddison, W. P. (2001). A combined molecular approach to phylogeny of the jumping spider subfamily Dendryphantinae (Araneae: Salticidae). *Molecular Phylogenetics and Evolution*, *18*(3), 386–403. https://doi.org/10.1006/mpev.2000.0883

Kambhampati, S., & Smith, P. T. (1995). PCR primers for the amplification of four insect mitochondrial gene fragments. *Insect Molecular Biology*, *4*(4), 233–236. https://doi.org/https://doi.org/10.1111/j.1365-2583.1995.tb00028.x

Macías-Hernández, N., Oromí, P., & Arnedo, M. (2008). Patterns of diversification on old volcanic islands as revealed by the woodlouse-hunter spider genus Dysdera (Araneae, Dysderidae) in the eastern Canary Islands. *Biological Journal of the Linnean Society*, *94*(3), 589–615. https://doi.org/10.1111/j.1095-8312.2008.01007.x

Palumbi, S. (1996). Nucleic acids II: the polymerase chain reaction. *Molecular Systematics*, 205–247. Retrieved from https://ci.nii.ac.jp/naid/10027373727/en/

Simon, C., Frati, F., Beckenbach, A., Crespi, B., Liu, H., & Flook, P. (1994). Evolution, Weighting, and Phylogenetic Utility of Mitochondrial Gene Sequences and a Compilation of Conserved Polymerase Chain Reaction Primers. *Annals of the Entomological Society of America*, *87*(6), 651–701. https://doi.org/10.1093/aesa/87.6.651

White, T., Bruns, T., Lee, S., Taylor, J., Innis, M., Gelfand, D., & Sninsky, J. (1990). Amplification and Direct Sequencing of Fungal Ribosomal RNA Genes for Phylogenetics. In *Pcr Protocols: a Guide to Methods and Applications,* (Vol. 31, pp. 315–322).

Whiting, M. F., Carpenter, J. C., Wheeler, Q. D., & Wheeler, W. C. (1997). The strepsiptera problem: Phylogeny of the holometabolous insect orders inferred from 18S and 28S ribosomal DNA sequences and morphology. *Systematic Biology*, *46*(1), 1–68. https://doi.org/10.1093/sysbio/46.1.1

TABLE 2

	radiata	heeri	ingens	nonannulata	blackwalli	isambertoi	maderiana	insularum	hx
radiata									
heeri	0,105	**0,006**							
ingens	0,111	0,065	**0,004**						
nonannulata	0,106	0,059	0,064	**0,009**					
blackwalli	0,098	0,074	0,073	0,043	**0**				
isambertoi	0,107	0,07	0,082	0,075	0,084	**0,003**			
maderiana	0,103	0,106	0,105	0,103	0,105	0,095	**0,007**		
insularum	0,102	0,104	0,108	0,099	0,104	0,098	0,016	**0,017**	
hx	0,103	0,106	0,108	0,103	0,105	0,098	0,01	0,016	**0,01**

hins_mad_LC336_5, hins_ma_LC249_5 are included in *H. ingens*

The number of base differences per site from averaging over all sequence pairs within each group are shown. This analysis involved 133 nucleotide sequences. All ambiguous positions were removed for each sequence pair (pairwise deletion option). There were a total of 676 positions in the final dataset. Evolutionary analyses were conducted in MEGA X [1][2] The presence of n/c in the results denotes cases in which it was not possible to estimate evolutionary distances.

Supplementary Materials 1. List of sequences and accession numbers used in the phylogenetic analyses

Tree label	Species	Total length	No of genes	COI	COI_chars	H3	H3_chars	12S	12S_chars	28S	28S_chars	nad1	nad1_chars
Sosippus placidus	*Sosippus placidus*	2482 bp	5	-	600		251	DQ019808	300 (20 indels)	DQ019752	777 (85 'N', 128 indels)	DQ019702	554
Dolomedes sp ATOL	*Dolomedes sp*	2070 bp	4	-	657		285	DQ019774	300 (22 indels)	DQ019726	828 (85 'N', 125 indels)	DQ019661	-
Bradystichus crispatus	*Bradystichus crispatus*	1413 bp	3	-	-	KY018374	285	KY015524	300 (22 indels)	KY017294	828 (85 'N', 126 indels)		-
Amyciaea sp MR389	*Amyciaea* sp.	1413 bp	3	-	-	KY018475	285	KY015619	300 (22 indels)	KY017423	828 (85 'N', 127 indels)		-
Boliscus cf tuberculatus MR041	*Boliscus* cf. *tuberculatus*	1413 bp	3	-	-	KY018477	285	KY015621	300 (29 indels)	KY017425	828 (85 'N', 128 indels)		-
Hygrolycosa rubrofasciata	*Hygrolycosa rubrofasciata*	2622 bp	5	-	657	MK524712	294	DQ019812	297 (21 indels)	MK524617	820 (85 'N', 124 indels)	DQ019665	554
Aulonia albimana LNP	*Aulonia albimana*	1962 bp	4	-	-	MK524679	296	DQ019823	294 (20 indels)	MK524610	827 (85 'N', 125 indels)	MK524645	545
Tricassa deserticola	*Tricassa deserticola*	1130 bp	2	-	-	MK524704	302		-	MK524633	828 (85 'N', 125 indels)		-
hing dg LC201	*Hogna ingens*	1485 bp	2	TBU	657 (4 'N')		-		-	TBU	828 (20 'N', 39 indels)		
hins ma LC242	*Hogna insularum*	1485 bp	2	TBU	657 (4 'N')		-		-	TBU	828 (39 indels)		-
hsch if LC213	*Hogna maderiana*	1485 bp	2	TBU	657 (4 'N')		-		-	TBU	828 (40 indels)		-
hhee ma LC287	*Hogna heeri*	2039 bp	3	TBU	657 (144 'N')		-		-	TBU	828 (40 indels)	TBU	554 (160 'N')
hnon ma LC253	*Hogna blackwalli*	2039 bp	3	TBU	657 (207 'N')		-		-	TBU	828 (40 indels)	TBU	554 (160 'N')
Venatrix konei	*Venatrix konei*	1544 bp	3	-	-		-	DQ019820	278 (29 indels)	DQ019742	712 (85 'N', 125 indels)	DQ019708	554
Hippasa holmerae	*Hippasa holmerae*	1626 bp	3	-	-		-	DQ019776	295 (22 indels)	DQ019728	777 (85 'N', 133 indels)	DQ019663	554
Tetralycosa oraria	*Tetralycosa oraria*	1627 bp	3	-	-		-	DQ019811	296 (24 indels)	DQ019720	777 (85 'N', 126 indels)	DQ019703	554
Arctosa stigmosa	*Arctosa stigmosa*	848 bp	2	-	-		-	DQ019764	300 (21 indels)		-	DQ019654	548
Pardosa astrigera	*Pardosa astrigera*	848 bp	2	-	-		-	DQ019792	300 (21 indels)		-	DQ019685	548
Pardosa brevivulva	*Pardosa brevivulva*	848 bp	2	-	-		-	DQ019793	300 (21 indels)		-	DQ019686	548
Pardosa hedini	*Pardosa hedini*	848 bp	2	-	-		-	DQ019795	300 (21 indels)		-	DQ019690	548
Pardosa isago	*Pardosa isago*	848 bp	2	-	-		-	DQ019796	300 (21 indels)		-	DQ019691	548
Cupiennius salei POLOTOW	*Cupiennius salei*	2155 bp	4	-	657		-		300 (21 indels)	KM225051	740 (85 'N', 125 indels)		458
Artoria howquaensis	*Artoria howquaensis*	1631 bp	3	-	-		-	DQ019770	300 (21 indels)	DQ019724	777 (85 'N', 126 indels)	DQ019658	554
Hoggicosa bicolor	*Hoggicosa bicolor*	1629 bp	3	-	-		-	DQ019777	300 (21 indels)	DQ019713	777 (85 'N', 128 indels)	DQ019668	552
Pardosa palustris	*Pardosa palustris*	1505 bp	3	-	657		-	DQ019799	300 (22 indels)		-	DQ019694	548

Anomalosa kochi	*Anomalosa kochi*	1631 bp	3	-	-		-	DQ019761	300 (22 indels)	DQ019722	777 (85 'N', 130 indels)	DQ019649	554
Tasmanicosa leuckarti	*Tasmanicosa leuckartii*	1631 bp	3	-	-		-	DQ019810	300 (23 indels)	DQ019717	777 (85 'N', 126 indels)	DQ019672	554
Knoelle clara	*Knoelle clara*	1631 bp	3	-	-		-	DQ019818	300 (23 indels)	DQ019714	777 (85 'N', 128 indels)	DQ019667	554
Rabidosa punctulata	*Rabidosa punctulata*	2285 bp	4	-	654		-	DQ019806	300 (23 indels)	DQ019736	777 (85 'N', 128 indels)	DQ019700	554
Diahogna sp	*Diahogna pisauroides*	1631 bp	3	-	-		-	DQ019822	300 (25 indels)	DQ019743	777 (85 'N', 127 indels)	DQ019676	554
Tasmanicosa godeffroyi	*Tasmanicosa godeffroyi*	1631 bp	3	-	-		-	DQ019809	300 (30 indels)	DQ019716	777 (85 'N', 126 indels)	DQ019671	554
hins ma LC249	*Hogna insularum*	1787 bp	3	TBU	657 (4 'N')	TBU	302 (3 'N')		-	TBU	828 (15 'N', 39 indels)		-
hW dg LC331	*Hogna isambertoi* sp. nov.	2087 bp	4	TBU	657 (4 'N')	TBU	302 (3 'N')	TBU	300 (21 indels)	TBU	828 (57 'N', 39 indels)		-
radiata CRBA-LC1315	*Hogna radiata*	2341 bp	4	TBU	657 (91 'N')	TBU	302 (8 'N')		-	TBU	828 (188 'N', 33 indels)	TBU	554 (231 'N')
hmad ma LC324	*Hogna nonannulata*	1787 bp	3	TBU	657 (4 'N')	TBU	302 (8 'N')		-	TBU	828 (39 indels)		-
hfer gca LC329	*Hogna ferox*	1787 bp	3	TBU	657 (4 'N')	TBU	302 (8 'N')		-	TBU	828 (41 indels)		-

Supplementary Materials 2. Full phylogenetic tree of the Lycosidae and related families. Best Maximum Likelihood tree of Lycosinae, inferred with IQTREE2 after selecting the best partition scheme and evolutionary models. Nodes are split in three sections, representing the different methods. Support on nodes should be read as follows: black: ML ultrafast boostrap and BI posterior probability ≥ 0.95, MP Jackknife ≥ 0.7; grey: ML Ultrafast Bootstrap and BI posterior probability < 0.95, MP Jackknife < 0.7; white: unrecovered node.